

**TOBERMORITE AND TOBERMORITE-LIKE  
CALCIUM SILICATE HYDRATES:  
THEIR PROPERTIES AND RELATIONSHIPS  
TO CLAY MINERALS**

**AUG. 1963**

**NO. 24**

**Joint  
Highway  
Research  
Project**

by  
S. DIAMOND

**PURDUE UNIVERSITY  
LAFAYETTE INDIANA**



## Final Report

### TOBERMORITE AND TOBERMORITE-LIKE CALCIUM SILICATE HYDRATES:

#### THEIR PROPERTIES AND RELATIONSHIPS TO CLAY MINERALS

TO: K. B. Woods, Director  
Joint Highway Research Project

August 2, 1963

FROM: H. L. Michael, Associate Director  
Joint Highway Research Project

File: 4-6-9  
Project: C-36-47I

Attached is a Final Report by Mr. Sidney Diamond, Graduate Assistant on our staff, entitled "Tobermorite and Tobermorite-Like Calcium Silicate Hydrates: Their Properties and Relationships to Clay Minerals". This research has been performed under the direction of Professors J. L. White of the Purdue University Agronomy Department and Professor W. L. Dolch of our staff. Mr. Diamond also used the report as his dissertation for the Ph.D. Degree.

The Plan of Study for this research was approved by the Board on May 22, 1962, and it subsequently was approved by the Indiana State Highway Commission and the Bureau of Public Roads as an HPS research project. This is the final report on this project and it will be submitted to the sponsoring organization for review. Several papers from the research are anticipated and each will be submitted to the Board and the sponsors for review and approval prior to publication.

The report is submitted to the Board for information and for the record.

Respectfully submitted,

*Harold L. Michael*  
Harold L. Michael, Secretary

HLM:bc

Attachment

Copies:

F. L. Ashbaucher  
J. R. Cooper  
W. L. Dolch  
W. H. Goetz  
F. F. Havey  
F. S. Hill  
G. A. Leonards

J. F. McLaughlin  
R. D. Miles  
R. E. Mills  
M. B. Scott  
J. V. Smythe  
E. J. Yoder





Final Report

TOBERMORITE AND TOBERMORITE-LIKE CALCIUM SILICATE HYDRATES:  
THEIR PROPERTIES AND RELATIONSHIPS TO CLAY MINERALS

by

Sidney Diamond  
Graduate Assistant

Joint Highway Research Project

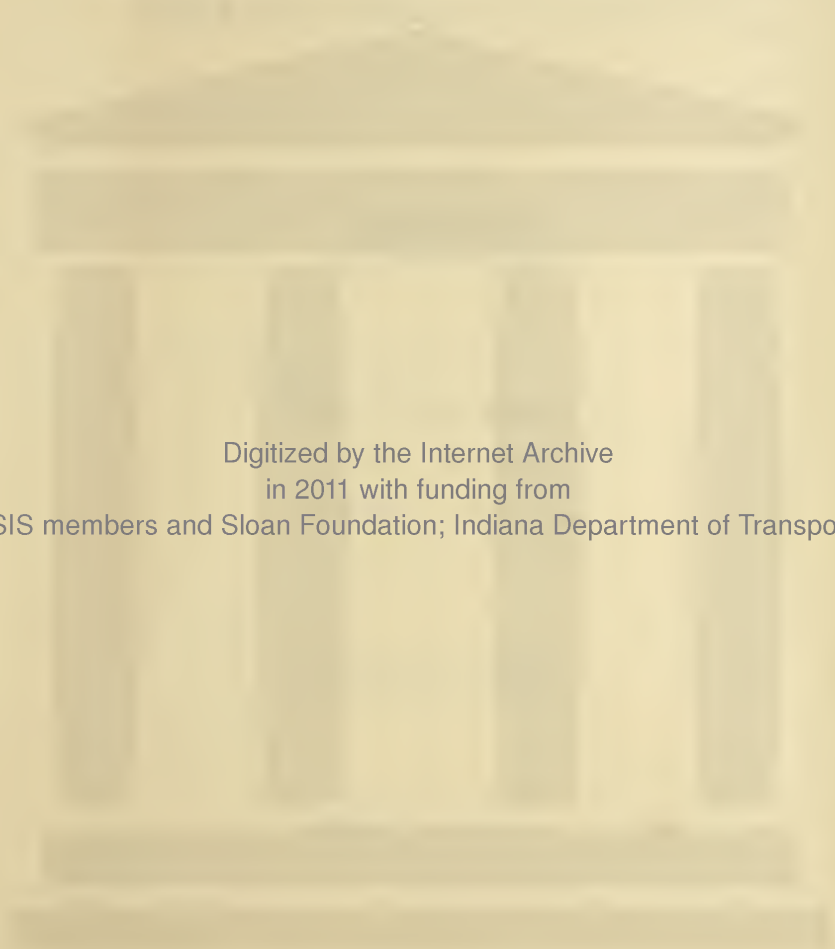
File No: 4-6-9

Project No: C-36-47I

Purdue University

Lafayette, Indiana

August 2, 1963



Digitized by the Internet Archive  
in 2011 with funding from  
LYRASIS members and Sloan Foundation; Indiana Department of Transportation

## ACKNOWLEDGMENTS

The author is deeply grateful to Dr. Joe L. White, his major professor, and to Dr. W. L. Dolch, co-chairman of his advisory committee, for their assistance, advice, and un-failing encouragement throughout his period of graduate study. Thanks are also due to Dr. Richard W. Lounsbury and Dr. James W. Richardson, who served as members of his advisory committee.

Most of the research was conducted in the laboratories of the Agronomy Department of Purdue University. The study was supported by a grant to the Joint Highway Research Project of Purdue University by the State Highway Department of Indiana and the U.S. Bureau of Public Roads. Their generous support is much appreciated. The author is further indebted to the Bureau of Public Roads for financial support of a portion of his period of graduate study as an out-service training activity.

Samples of pure calcium silicates employed in this work were generously donated by the Portland Cement Association Research and Development Laboratories, and a sample of alite was kindly supplied by Mr. Alexander Klein of the University of California. These gifts are acknowledged with thanks.

The electron micrographs presented in this report were taken by Dr. John Radovich of Micro-Met Laboratories, Inc. Mr. John Allen and Mrs. Joanne Johannsen assisted in many of



the laboratory procedures. A number of chemical analyses were performed by Mr. Larry Campbell and Mr. Lawrence Schuppert. The author is most grateful to all of these persons.

It is a pleasure to acknowledge the author's indebtedness to a number of his associates at Purdue University, both staff members and graduate students, for stimulating discussions on many occasions and for the use of research equipment. A particularly valuable discussion with Dr. G. L. Kalousek of the Universal Atlas Cement Company is also gratefully acknowledged.

Most of all, the author wishes to record his gratitude to his wife, Harriet, and to his children, whose encouragement and support were never lacking.





## TABLE OF CONTENTS

	Page
LIST OF TABLES . . . . .	1x
LIST OF ILLUSTRATIONS . . . . .	x
ABSTRACT . . . . .	xiv
INTRODUCTION . . . . .	1
REVIEW OF THE LITERATURE . . . . .	4
Introduction and Notation . . . . .	4
Tobermorite . . . . .	5
Origin, Synthesis, and Optical Properties . . . . .	5
Composition, Structure, and Morphology . . . . .	7
Chemical Composition and Extent of Variation . . . . .	7
Hydration States . . . . .	8
Crystal Structure . . . . .	10
Morphology . . . . .	13
Differential Thermal Analysis . . . . .	13
Infrared Absorption . . . . .	14
Surface Area . . . . .	15
Surface Charge . . . . .	16
Cation Exchange Properties . . . . .	17
Summary . . . . .	18
Calcium Silicate Hydrate (I) . . . . .	19
Nomenclature and Synthesis . . . . .	19
Composition, Structure and Morphology . . . . .	21
Variation in Chemical Composition . . . . .	21
Hydration States . . . . .	22
Variation in Basal Spacing Due to Composition . . . . .	22
X-ray Diffraction and Crystal Structure . . . . .	23
Morphology . . . . .	25
Differential Thermal Analysis . . . . .	26
Infrared Absorption . . . . .	27
Surface Areas and other Characteristic Properties of CSH(I) . . . . .	28
Summary . . . . .	28
Calcium Silicate Hydrate (II) . . . . .	30
Nomenclature and Synthesis . . . . .	30
Composition, Structure, and Morphology . . . . .	30
Variation in Chemical Composition . . . . .	30
X-ray Diffraction and Crystal Structure of CSH(II) . . . . .	31
Morphology . . . . .	32
Differential Thermal Analysis . . . . .	33



	Page
Infrared Absorption . . . . .	33
Surface Areas and other Characteristic Properties of CSH(II) . . . . .	33
Summary . . . . .	34
Calcium Silicate Hydrate (gel) . . . . .	35
Nomenclature and Origin . . . . .	35
Composition, Structure and Morphology . . . . .	36
Variation in Chemical Composition . . . . .	36
X-ray Diffraction and Crystal Structure . . . . .	37
Morphology . . . . .	39
Differential Thermal Analysis . . . . .	39
Infrared Absorption . . . . .	40
Surface Area and other Characteristic Properties of CSH(gel) . . . . .	41
Surface Area Measurements . . . . .	41
Surface Charge and Surface Energy of CSH(gel) . . . . .	43
Cation Exchange Properties . . . . .	44
Thermodynamic Properties . . . . .	44
Summary . . . . .	44
Hydrated Calcium Aluminates and Related Compounds . . . . .	45
Introduction to the Types of Compounds that Occur . . . . .	45
The Cubic Phase $C_3AH_6$ . . . . .	47
The Hexagonal Phases $C_4AH_{13}$ , $C_2AH_8$ , $CAH_{10}$ , and Related Phases . . . . .	48
$C_4AH_{13}$ . . . . .	48
$C_2AH_8$ . . . . .	50
$CAH_{10}$ . . . . .	50
The $^{10}$ Supposed Phase $C_3AH_{12}$ . . . . .	51
Compounds of Needle-like Habit . . . . .	51
Summary . . . . .	51
Reaction Products of $Ca(OH)_2$ with Clay Minerals . . . . .	52
MATERIALS AND PROCEDURES . . . . .	60
Preparation of Calcium Silicate Hydrates . . . . .	60
Well-Crystallized Tobermorite . . . . .	60
Unsubstituted Tobermorite . . . . .	60
Substituted Tobermorites . . . . .	61
Poorly-Crystallized Calcium Silicate Hydrates	
Synthesized at Room Temperature . . . . .	62
Samples Prepared by Double Decomposition Methods . . . . .	62
Samples Prepared by Direct Synthesis . . . . .	64
Attempted Synthesis of CSH(II) by Direct Reaction in Hot Glycerol . . . . .	65
Hydration Products of Individual Cement Minerals . . . . .	66
Cement Minerals . . . . .	66
"Paste" Hydration . . . . .	66
"Bottle" Hydration . . . . .	67
Reaction Products of $Ca(OH)_2$ with Clay Minerals and Related Silicates . . . . .	68





	Page
"Dry" Compacted Mixtures at 60°C . . . . .	68
Starting Materials . . . . .	68
Experimental Procedure . . . . .	69
Slurry Mixtures at 45°C . . . . .	70
Starting Materials . . . . .	70
Experimental Procedure . . . . .	72
Dilute Suspension at 23°C . . . . .	73
Procedures Used in Investigating the Properties	
of the Various Materials . . . . .	74
Analyses of Chemical Composition . . . . .	74
X-ray Diffraction . . . . .	74
Differential Thermal Analysis . . . . .	76
Infrared Absorption Spectroscopy . . . . .	78
Electron Microscopy and Electron Diffraction . . . . .	79
Determination of Surface Area by Water Vapor	
Adsorption . . . . .	81
Cation Exchange Capacity . . . . .	82
Determination of Zeta Potential and Sign of	
Surface Charge . . . . .	86
EXPERIMENTAL RESULTS . . . . .	90
Well-Crystallized Tobermorites Prepared by	
Hydrothermal Synthesis . . . . .	90
Unsubstituted Tobermorite . . . . .	90
Preparation . . . . .	90
Composition . . . . .	90
X-ray Diffraction . . . . .	90
Morphology . . . . .	92
Differential Thermal Analysis . . . . .	92
Infrared Absorption . . . . .	92
Water Vapor Adsorption and Surface Area . . . . .	97
Cation Exchange Capacity . . . . .	98
Zeta Potential and Sign of Surface Charge . . . . .	98
Plasticity of the Tobermorite-Water System . . . . .	100
Effect of Glycerol on Basal Spacing . . . . .	101
The Effect of Lattice Substitution on the	
Properties of Tobermorite . . . . .	102
Introduction and Notation . . . . .	102
Preparation of Substituted Tobermorites . . . . .	103
X-ray Diffraction Characteristics of	
Substituted Tobermorites . . . . .	106
Differential Thermal Analysis and Thermal	
Transformations . . . . .	112
Morphology of Substituted Tobermorites . . . . .	116
Infrared Spectra of Substituted Tobermorites . . . . .	120
The Effect of Substitution on the Surface Area	
of Tobermorite . . . . .	123
The Effect of Substitution on the Properties of	
the Tobermorite-Water Surface . . . . .	125
Cation Exchange Capacity Measurements . . . . .	131
Zeta Potential and Surface Charge of	
Substituted Tobermorites . . . . .	135



Summary of Experimental Results on Well-Crystallized Tobermorites . . . . .	135
Poorly Crystallized Calcium Silicate Hydrates	
Prepared at Room Temperature - CSH(I) . . . . .	137
Preparation and Designation of Products . . . . .	137
Composition . . . . .	138
X-ray Diffraction . . . . .	140
Morphology . . . . .	144
Differential Thermal Analysis . . . . .	147
Infrared Spectra . . . . .	148
Surface Area and Water-Vapor Adsorption . . . . .	153
Cation Exchange Capacities . . . . .	157
Zeta Potential . . . . .	159
Summary . . . . .	160
Calcium Silicate Hydrates Produced by Hydration of $\beta$ -C <sub>2</sub> S and C <sub>3</sub> S . . . . .	162
Origin and Composition . . . . .	162
X-ray Diffraction Results . . . . .	162
Morphology . . . . .	166
Differential Thermal Analysis . . . . .	169
Infrared Absorption . . . . .	172
Surface Area . . . . .	175
Cation Exchange Capacity . . . . .	175
Zeta Potential and Surface Charge . . . . .	176
Summary . . . . .	177
Products of Chemical Reaction Between Ca(OH) <sub>2</sub> and Silicate Minerals at or Near Room Temperature . .	178
Reactions of Compacted Mixtures at 60°C . . . . .	178
Starting Materials, Reaction Conditions, and Methods of Examination of Products . . . . .	178
Reaction Products of Quartz . . . . .	178
Reaction Product of Kaolinite . . . . .	182
Reaction Products of Montmorillonite . . . . .	187
Effect of Immersion on Cementation of Reacted Products . . . . .	192
Summary of Reaction Products of Compacted Mixtures at 60°C . . . . .	192
Reactions of Slurry Mixtures at 45°C . . . . .	193
Starting Materials, Reaction Conditions, Methods of Examination of Products . . . . .	193
Reaction Products of Quartz . . . . .	194
Reaction Products of Kaolinite . . . . .	196
Reaction Products of Montmorillonite . . . . .	200
Reaction Products of Pyrophyllite . . . . .	203
Reaction Products of Mica . . . . .	205
Reaction Products of Illite . . . . .	206
Failure of Talc to React . . . . .	206
Summary of Reaction Products of Slurry Mixtures at 45°C . . . . .	207
Reaction of Ca(OH) <sub>2</sub> and Kaolinite in Suspensions at 23°C . . . . .	208
The Reaction Between Ca(OH) <sub>2</sub> and Hydrous Alumina . . . .	211



	Page
DISCUSSION . . . . .	226
Classification of the Tobermorite-like	
Calcium Silicate Hydrates . . . . .	226
Structural and Cation-Exchange Properties	
of Tobermorite . . . . .	228
Effects of Lattice Substitution on the	
Properties of Tobermorite . . . . .	231
Variation in Composition of CSH(1) . . . . .	233
Surface Properties and Plasticity of	
Tobermorite and CSH(1) . . . . .	235
Reactions Between Lime and Silicates	
Near Room Temperature . . . . .	237
Characteristics of the $C_4AH_{13}$ Phase . . . . .	239
Implications of the Present <sup>13</sup>	
work on the Understanding of Cementation . . . . .	241
SUMMARY AND CONCLUSIONS . . . . .	243
Summary . . . . .	243
Conclusions . . . . .	248
BIBLIOGRAPHY . . . . .	250
APPENDIX . . . . .	259
VITA . . . . .	261





## LIST OF TABLES

Table	Page
1. Intensities of Four Strongest X-ray Lines for Tobermorite and 10% Aluminum, Iron, and Magnesium-Tobermorites . . . . .	110
2. Surface Areas and Heats of Adsorption "E <sub>1</sub> " for Tobermorite and Substituted Tobermorites . . . . .	124
3. Cation Exchange Capacities Measured for Tobermorite and Substituted Tobermorites . . . . .	133
4. Designation and Composition of Room-Temperature CSH(I) Products . . . . .	139
5. Surface Areas and Heats of Adsorption of Water Vapor for CSH(I) Preparations . . . . .	154
6. Cation Exchange Capacities of CSH(I) Samples . . . . .	158
7. Hydration Products of $C_2S$ , $C_3S$ , and Alite . . . . .	163

## APPENDIX

1. Chemical Analysis of $C_2S$ , $C_3S$ and Alite Used to Produce CSH(gel) . . . . .	259
2. Chemical Analysis of CSH(I) Products . . . . .	260



## LIST OF ILLUSTRATIONS

Figure	Page
1. Model Illustrating the Structure of Tobermorite According to Megaw and Kelsey . . . . .	12
2. Circuit Diagram for Microelectrophoresis Apparatus . . . . .	87
3. X-ray Diffractometer Traces of Unsubstituted Tobermorite and of 3, 5, 10 and 15% Substituted Al-Tobermorite . . . . .	91
4. Electron Micrograph and Electron Diffraction Pattern for Unsubstituted Tobermorite . . . . .	93
5. DTA Results for Tobermorite and 3, 5, 10 and 15% Substituted Al-Tobermorites. Heating Rate Varies from 58°C to 5°C Per Minute . . . . .	94
6. Portions of Infrared Absorption Spectra of Tobermorite and of 10% Substituted Al-, Fe-, and Mg-Tobermorites . . . . .	95
7. X-ray Diffractometer Traces of Tobermorite and of 10% Substituted Al-, Fe-, and Mg-Tobermorites . . . . .	109
8. DTA Results for Tobermorite and for 10% Substituted Al-, Fe-, and Mg-Tobermorites . . . . .	113
9. Electron Micrographs of 10%-Substituted Fe-Tobermorite. (A) Typical Field. (B) Field Selected to Show Fine Particles . . . . .	117
10. Selected Area Electron Diffraction of Fields Selected to Show Fine Particles. (A) 10% Substituted Fe-Tobermorite. (B) 10% Substituted Al-Tobermorite . . . . .	118
11. Electron Micrographs of 10% Substituted Al-Tobermorites. (A) Typical Field. (B) Field Selected to Show Fine Particles . . . . .	119
12. Shift of Tobermorite Infrared Absorption Band at Approximately 1200 cm <sup>-1</sup> With Increase in Al-Substitution. (A) Trace of	





Figure	Page
Infrared Spectra. (B) Plot of Frequency vs. % of Al-Substitution . . . . .	122
13. Reduced Water Vapor Adsorption Isotherm (21°C) For Tobermorite and Al-Substituted Tobermorites . . . . .	128
14. Experimental Water Vapor Adsorption Iso- therm for Tobermorite Compared with Iso- therms Calculated from the BDDT Equation for Adsorption Restricted to 1, 2, and 3 Molecular Layers . . . . .	130
15. X-ray Diffractometer Traces for CSH(I) Samples Synthesized at Room Temperature . . . .	141
16. Electron Micrographs of CSH(I) Preparations. (A) CSH(I) - 5. (B) CSH(I) - 7 . . . . .	145
17. Electron Micrographs of CSH(I) - 6 . . . . .	146
18. DTA of CSH(I) Preparations. Heating Rate 10°C Per Minute . . . . .	149
19. Infrared Absorption Spectra for CSH(I) Preparations . . . . .	150
20. Reduced Water Vapor Adsorption Isotherm for CSH(I) Preparations Compared with that for Tobermorite . . . . .	156
21. X-ray Diffractometer Traces for Paste and Bottle Hydration Products of $\beta$ -C <sub>2</sub> S, C <sub>3</sub> S, and Alite . . . . .	165
22. X-ray Diffractometer Trace for Moist CSH(gel) B- 2 Prepared as an Oriented Aggregate on a Porous Tile Mount . . . . .	167
23. Electron Micrographs of Paste and Bottle Hy- dration Products of C <sub>2</sub> S. (A) Paste Product, CSH(gel) P - 2. Bottle Product, CSH(gel) B - 2 . . . . .	168
24. Electron Micrographs of Bottle-Hydrated $\beta$ -C <sub>2</sub> S, CSH(gel) B - 1. . . . .	170
25. Differential Thermal Analysis of CSH(gel) Products. Heating Rate Varies from 58°C to 5°C Per Minute . . . . .	171



## Figure

## Page

26.	Infrared Absorption Spectra for CSH(gel) Products . . . . .	173
27.	X-ray Diffractometer Traces of Quartz- Ca(OH) <sub>2</sub> Mixture Before and After Reaction at 60°C . . . . .	180
28.	Differential Thermal Analysis of Products of Ca(OH) <sub>2</sub> -Silicate Reactions at 60°C. Heating Rate 10°C Per Minute . . . . .	181
29.	Electron Micrographs of Ca(OH) <sub>2</sub> -Silicate Reaction Products at 60°C. (A) Quartz. (B) Kaolinite . . . . .	183
30.	X-ray Diffractometer Traces of Ca(OH) <sub>2</sub> - Kaolinite Mixture Before and After Reaction at 60°C . . . . .	184
31.	X-ray Diffractometer Traces of Ca(OH) <sub>2</sub> - Montmorillonite Mixtures Before and After Reaction at 60°C . . . . .	188
32.	Electron Micrograph of Ca(OH) <sub>2</sub> - Montmorillonite Reaction Product at 60°C . . . . .	190
33.	Differential Thermal Analysis of Ca(OH) <sub>2</sub> - Silicate Reaction Products at 45°C. Heating Rate Varies from 58°C to 5°C Per Minute . . . . .	195
34.	Electron Micrographs of Ca(OH) <sub>2</sub> -Quartz Reaction Products at 45°C . . . . .	197
35.	Electron Micrographs of Ca(OH) <sub>2</sub> -Kaolinite Reaction Products at 45°C . . . . .	201
36.	Electron Micrographs of Ca(OH) <sub>2</sub> -Silicate Reaction Products at 45°C. (A) Mont- morillonite. (B) Mica. . . . .	204
37.	X-ray Diffractometer Traces of the Reaction Products of Ca(OH) <sub>2</sub> and Kaolinite at 23°C . . . . .	209
38.	Differential Thermal Analysis of Ca(OH) <sub>2</sub> - Kaolinite Reaction Product at 23°C. Heating Rate Varies from 58°C to 5°C Per Minute . . . . .	210
39.	Electron Micrographs of Ca(OH) <sub>2</sub> - Kaolinite Reaction Products at 23°C . . . . .	212



40. X-ray Diffractometer Traces of (A) Hydrous Alumina, (B) Dry Mixture of 4 Parts Hydrous Alumina and 1 Part  $\text{Ca}(\text{OH})_2$  By Weight, and (C) Reaction Product of this Mixture, 3 days at  $60^\circ\text{C}$  . . . . . 214
41. X-ray Diffractometer Traces of Reaction Product of 1 Part Hydrous Alumina and 3 Parts  $\text{Ca}(\text{OH})_2$  by Weight, 6 Hours at  $22^\circ\text{C}$  in Nitrogen Atmosphere. (A) Original Reaction Product. (B) Reaction Product After Washing . . . . . 216
42. Electron Micrograph of Washed Product of the Reaction Between Hydrous Alumina and  $\text{Ca}(\text{OH})_2$  . . . . . 219
43. Infrared Spectra of the Product of the Reaction Between Hydrous Alumina and  $\text{Ca}(\text{OH})_2$ . (A) Before Washing. (B) After Washing . . . . . 220
44. X-ray Diffractometer Trace and Differential Thermal Analysis (Heating Rate  $10^\circ$  Per Minute) for Hydrous Alumina- $\text{Ca}(\text{OH})_2$  Product Reacted for 15 Minutes at  $22^\circ\text{C}$  . . . . . 222
45. Relative Intensities of Peaks for  $\text{Ca}(\text{OH})_2$  and  $\text{C}_4\text{AH}_{13}$  Compared to Internal Standard as Functions of Time After Addition of Water to Dry Specimen . . . . . 224



## ABSTRACT

Diamond, Sidney. Ph.D., Purdue University, August 1963.

Tobermorite and Tobermorite-Like Calcium Silicate Hydrates:  
Their Properties and Relationships to Clay Minerals. Major

Professor: Joe L. White.

Well-crystallized tobermorite was prepared hydrothermally from  $\text{Ca}(\text{OH})_2$  and quartz, and was shown to have the characteristic x-ray and DTA patterns for this phase. The infrared spectrum was investigated using samples deposited on KBr plates; the appearance of several bands not previously reported was noted. Tobermorite disperses readily in water to primary particles, and it was observed that wetted tobermorite exhibits plastic properties similar to those of clays. The zeta potential of tobermorite in distilled water was about -30mv., but the sign of the charge was reversed in sufficiently concentrated  $\text{Ca}^{++}$  or  $\text{Al}^{+++}$  solutions.

Aluminum-, iron- and magnesium-substituted tobermorites were synthesized and the effects of the lattice substitutions studied by DTA, x-ray diffraction and infrared techniques. An intense high-temperature exotherm observed on the DTA curves of aluminum-substituted tobermorite may be due to the formation of mullite. Iron- and magnesium-substituted tobermorites appeared to suffer some c-axis disorder. Tobermorite and the aluminum substituted phase are platy; the iron-substituted phase is lath shaped. The surface area of the tobermorite measured by





water vapor adsorption was about  $80 \text{ m}^2/\text{g}$ ; those for the substituted phases slightly higher. Heats of adsorption of the first layer of water molecules calculated from the BET theory (" $E_1$ ") were about  $13,500 \text{ cal/mole}$ , suggesting strong attraction of the tobermorite surface for water. However, the isotherms were considerably flattened after the attainment of a monolayer and it appears that adsorption is restricted to two molecular layers. Cation exchange capacities were determined in alcohol solutions; the unsubstituted tobermorite had a CEC of  $34 \text{ meq/100 g}$  and it was decreased rather than increased by substitution.

CSH(I) samples of varied compositions were synthesized at room temperature. The x-ray patterns consisted of only a few lines and were generally similar; one sample was amorphous to x-rays. The DTA curves showed intense high-temperature exotherms. Electron microscopy disclosed a foil-shaped morphology. Infra-red spectra of the group were similar, but recognizably different from those of tobermorite. Measured surface areas ranged from  $150$  to  $350 \text{ m}^2/\text{g}$ , the  $E_1$  values were lower than those of tobermorite, and adsorption beyond a monolayer was not restricted. The individual primary particles were well-cemented and did not disperse in aqueous suspensions. The surface charge behavior was similar to that of tobermorite. CEC results varied but all were less than that of tobermorite.

CSH(gel) products were prepared by the paste and bottle hydration of  $\beta\text{-}2\text{CaO}\cdot\text{SiO}_2$ ,  $3\text{CaO}\cdot\text{SiO}_2$ , and "alite". The primary particles of this phase are fibrous. DTA, x-ray and infrared results for all the products studied were similar. DTA curves showed a weak but well defined high-temperature exotherm. The



infrared spectra show certain consistent differences from those of CSH(I) and tobermorite. Measured CEC values were of the order of 15 - 20 meq/100 g.

The reaction products of  $\text{Ca}(\text{OH})_2$  and a number of silicate minerals were studied. Moist, compacted mixtures of  $\text{Ca}(\text{OH})_2$  and quartz reacted at  $60^\circ\text{C}$  produced fibrous CSH(gel); similar reaction with kaolinite produced foil-shaped CSH(I), and also  $3\text{CaO}\cdot\text{Al}_2\text{O}_3\cdot 6\text{H}_2\text{O}$ . Montmorillonite produced CSH(I) but did not produce a recognizable calcium aluminate phase. All of these materials were well-cemented and retained their strength on immersion suggesting that the cementing properties of the CSH phases do not depend on the shape of the particles. A second series of reactions with  $\text{Ca}(\text{OH})_2$  was carried out in slurry mixtures shaken continuously at  $45^\circ\text{C}$ . Very extensive reactions were observed for quartz, kaolinite, montmorillonite, illite, mica, and pyrophyllite, but not for talc. The CSH product formed was CSH(gel) and a well-crystallized phase identified as  $4\text{CaO}\cdot\text{Al}_2\text{O}_3\cdot 13\text{H}_2\text{O}$  formed with all but quartz. Kaolinite reacted in dilute suspension at room temperature to produce the same products.

Well-crystallized  $4\text{CaO}\cdot\text{Al}_2\text{O}_3\cdot 13\text{H}_2\text{O}$  was shown to be produced rapidly from  $\text{Ca}(\text{OH})_2$  and synthetic hydrous alumina. Certain properties of this phase were investigated.



## INTRODUCTION

Tobermorite is a well-crystallized calcium silicate hydrate mineral occurring rarely in nature but of considerable technical interest. It is the well-crystallized member of a family of several closely-related compounds that includes also phases now generally known as calcium silicate hydrate (I), calcium silicate hydrate (II), and calcium silicate hydrate (gel), also called tobermorite (gel). Calcium silicate hydrate (gel), a poorly-crystallized colloidal substance, is responsible for the strength and cementing ability of portland cement concrete. The physical-chemical properties of this material are not well understood, and, in particular, no adequate theory exists to explain the unusual cementing properties of this substance. Only a relatively small number of investigators have concerned themselves with the tobermorite-like calcium silicate hydrates.

The clay minerals are a large group of layer-lattice and chain structure aluminum silicate and magnesium silicate hydrates that are classified together because of certain common properties. These properties include small particle size, high surface area, cation exchange capacity, marked attraction for water, and the property of becoming plastic when wet. Because of their importance in soil science, geology, engineering, and ceramics, the clay minerals have been exhaustively studied in the last three decades and their individual structures and properties



are now well understood.

Although the calcium silicate hydrates of the tobermorite-like family do not have precisely the same structure as any member of the aluminum silicate or magnesium silicate hydrate group, the known structure of tobermorite combines features of both the layer-structure and the chain structure clays. In addition to structural similarities, these calcium silicate hydrates also possess small particle size, high surface area, an attraction for water, and a number of other properties analagous to those of the clay minerals.

In addition to this resemblance in structure and in some properties, it has been determined in recent years that a genetic relationship can exist between members of the two groups; thus, it has been found that when various clay minerals are treated with calcium hydroxide under appropriate circumstances, chemical reactions occur and members of the calcium silicate hydrate group are produced as products of the reaction. This reaction has unknowingly been put to use for many years in highway construction, where calcium hydroxide has been used to "stabilize" clay soils, i.e. strengthen them and render them insensitive to water.

The present work is an attempt to investigate the various known members of the tobermorite-like group of calcium silicate hydrates, and to characterize them individually as fully as possible in the light of the insight available from studies of the clay minerals and of related layer-lattice and chain-structure silicates.





The method of procedure was to prepare a suite of calcium silicate hydrate minerals by appropriate methods; to attempt to verify or disprove certain observations concerning their properties made by previous investigators; and to characterize in as much detail as possible their individual properties as revealed by x-ray diffraction, chemical composition, electron microscopy, differential thermal analysis, infrared absorption spectroscopy, surface area properties, surface charge behavior, cation exchange activity, and various other appropriate procedures. It was hoped that this detailed study would lead to a better understanding of the differences between the different members of the calcium silicate hydrate group, as well as of the properties of the group as a whole.

A second objective of the work was to study the extent of the reaction between calcium hydroxide and clays and other silicate minerals under various circumstances, and especially to study the products of these reactions and relate them to individual members of the calcium silicate hydrate group. Since these same reactions also commonly form calcium aluminate hydrates which are not readily separated from the calcium silicate hydrates, it was found necessary also to study some of the properties of these compounds in order to interpret the data secured.

Finally, an attempt was made to relate the observed structural and other properties of the calcium silicate hydrate group materials with their known technical qualities of strength and cementing ability.



## REVIEW OF THE LITERATURE

### Introduction and Notation

The literature on calcium silicate hydrates resembling tobermorite is quite extensive, as is illustrated by the length of this review. It is also quite confusing. A major cause of the confusion is the relatively inconsistent nomenclature often employed. Since it has not been universally appreciated that the tobermorite-like materials constitute a family with individual members having distinctive properties, various authors have used the word "tobermorite" to designate both the well-crystallized phase resembling the natural mineral of that name and also one or more of the other, less-well-crystallized phases. Thus in reading the literature one must take special pains to make certain exactly which phase is being discussed.

The present review is arranged so as to minimize this confusion by treating each of the phases in a separate section. Each section contains a discussion of the nomenclature, origin or synthesis, structure and x-ray diffraction pattern, morphology, differential thermal analysis, infrared absorption spectra, surface area, and other characteristics of the individual phase. The four phases considered are tobermorite per se, calcium silicate hydrate (I), calcium silicate hydrate (II), and calcium silicate hydrate (gel).

In addition to this detailed review of the calcium silicate



hydrates, a less detailed coverage of the calcium aluminate hydrates is given in a separate section. The final portion of the review is a discussion of the relatively limited recent literature on the products of reactions between  $\text{Ca(OH)}_2$  and clay minerals at or slightly above room temperatures.

In this review, in conformity with the general practice in the literature, a number of abbreviations have been employed. These are of two types. First, the names of the phases "calcium silicate hydrate (I)", "calcium silicate hydrate (II)", and "calcium silicate hydrate (gel)" are abbreviated to "CSH(I)", "CSH(II)", and "CSH(gel)", respectively. The other type of abbreviation is actually a shortened chemical notation employed side-by-side with normal chemical terminology. The terms used are as follows:  $\text{CaO}$  is given as "C";  $\text{SiO}_2$  is given as "S";  $\text{Al}_2\text{O}_3$  is given as "A";  $\text{H}_2\text{O}$  is given as "H";  $\text{Fe}_2\text{O}_3$  is given as "F", etc. Often hybrid forms are used such as the designation for the compound monocalcium carboaluminate as  $\text{C}_3\text{A} \cdot \text{CaCO}_3 \cdot 11\text{H}_2\text{O}$  (Taylor, 1961, p. 116). Despite the objections that might well be raised to such inconsistent notation, it is felt best to conform to established practice in this regard. The shortened designation "CH" for  $\text{Ca(OH)}_2$  is not often used in the literature and the full form is employed here.

### Tobermorite

#### Origin, Synthesis, and Optical Properties

Tobermorite (approximate composition  $5\text{CaO} \cdot 6\text{SiO}_2 \cdot 5\text{H}_2\text{O}$ ) is a rare mineral of orthorhombic structure originally described



by Heddle (1880) from occurrences in Scotland. Subsequently, additional occurrences have been recorded at Ballycraigy, Northern Ireland (McConnell, 1954), and as parts of a complex intergrowth with the apatite mineral wilkeite at Crestmore, California (Eakle, 1917; McConnell, 1954). Recently it has been found in Nevada associated with alunite pseudomorphic after plagioclase phenocrysts in hydrothermally-altered dacite (Harvey and Beck, 1962).

Claringbull and Hey (1952) first examined the mineral by x-ray diffraction. It was found to be identical in crystal structure to a compound synthesized originally by Flint, McMurdie, and Wells (1938), to a product synthesized by Kalousek in the 1940's, and to a compound synthesized and studied in detail by Heller and Taylor (1951) and Taylor (1953).

The synthesis preferred by Kalousek involves the hydrothermal reaction of freshly-slaked lime with finely-divided quartz at 175°C for approximately 18 hours (personal communication). Amorphous silica can be used instead of the quartz, but in this case the time of reaction should be lengthened considerably (Kalousek, 1955). Heller and Taylor prepared the compound (in various mixtures of related phases) by reacting lime and silica gel hydrothermally at various temperatures between 100°C and 200°C for periods ranging from several days to some months. These authors also used an alternate starting material composed of a poorly-crystallized calcium silicate hydrate and additional lime.

Tobermorite has also been synthesized recently by hydrothermal reaction of lime with montmorillonite, with and without





several other admixtures (McCaleb, 1962).

The optical properties of the mineral were given by McConnell (1954), and the following description is condensed from his account:

Optical properties: biaxial positive, low 2V angle; indices of refraction  $\alpha = 1.570$ ,  $\beta = 1.571$ ,  $\gamma = 1.575$ , all  $\pm 0.002$ . Orthorhombic with  $Z = a$ ,  $Y = b$  (elongation),  $X = c$ . Cleavage, (001) perfect, (100) secondary. Weak dispersion. Density approximately 2.44 g/ml.

#### Composition, Structure, and Morphology

Chemical Composition and Extent of Variation. Most naturally occurring specimens of tobermorite seem to have Ca:Si ratios close to the theoretical value of 5:6 (Taylor, 1961). However, Harvey and Beck (1962) suggested that the tobermorite associated with alunite in Nevada has a Ca:Si ratio of approximately one. Kalousek (1955) has produced synthetic tobermorite in pure products having ratios as high as 1.00 and as low as 0.80; below this ratio unreacted silica remains, and mixtures of ratios higher than 1.00 tend to give rise to other phases, notably alpha-dicalcium silicate hydrate. Stein (1960) reported the synthesis, by Kalousek's method, of an apparently homogeneous well-crystallized tobermorite of Ca:Si ratio 1.08. In general one must conclude that the possible variation of the calcium and silica components of tobermorite is quite limited.

However, there appears to be a considerable variation in the water content of the phase: Aitken and Taylor (1960) reported  $H_2O:Ca$  ratios varying from less than 1 to as high as 1.46, as



compared to the nominal ratio of 1.00 for the natural mineral.

Isomorphous substitution in tobermorite has been studied only in one paper (Kalousek, 1957). This author has shown quite conclusively that aluminum in amounts at least up to 4 or 5% (calculated on the basis of ignited weight) can be incorporated into the lattice of synthetic tobermorite without any significant changes in the x-ray diffraction pattern of the material. Evidence was presented that the aluminum substitutes for silicon in tetrahedral coordination, rather than for the calcium in the structure.

Hydration States. There are several known discontinuous hydration states of tobermorite, each marked by a characteristic c-axis spacing. Most naturally occurring specimens and hydrothermally-synthesized specimens have c-axis unit cell thickness of approximately 22.4Å, but as each unit cell consists of two identical layers the basal spacing observed on x-ray diffraction is 11.2Å.

According to McConnell (1954) natural tobermorite from Ballycraigy with an initial 11Å basal spacing reacts readily with atmospheric moisture to produce an expanded basal spacing of 14Å, presumably by incorporating a layer of water between each pair of tobermorite layers. This is of course analagous to the well-known behavior of the clay mineral vermiculite. The mixed-intergrowth material from Crestmore, California, contains some material that has expanded in this manner. The 14Å spacing disappears on oven drying, as the water layer is removed (Taylor, 1953).



Synthetic tobermorite prepared according to Kalousek's method, and natural tobermorite from Loch Eynort, Scotland, do not expand to 14Å, even when soaked or ground in water (McConnell, 1954; Kalousek and Roy, 1957). Kalousek and Roy have synthesized a tobermorite with a 14Å spacing, but only with considerable difficulty (six month's treatment at 60°C).

On heating to sufficiently high temperature most tobermorite undergoes a rearrangement of the layers, (usually preceded or accompanied by removal of water), and the basal spacing shrinks to about 9.5Å. Ballycraigy tobermorite, Crestmore tobermorite, and synthetic tobermorite prepared by Taylor (1953) all exhibited this collapse at or below 300°C; synthetic tobermorite prepared by Kalousek's method did not similarly collapse until 650°C (Kalousek and Roy, 1957). Aitken and Taylor (1960) studied a tobermorite that retained its 11Å spacing as high as 900°C, and then converted directly to wollastonite.

Certain other basal spacings (10Å and 12Å) have been reported to occur in the Crestmore intergrowth material, but their exact significance is obscure.

The apparent parallels between the behavior of at least some of the naturally-occurring tobermorite and Taylor's synthetic material and the interlayer expansion and contraction characteristic of the so-called "expanding lattice" clay minerals (montmorillonite, vermiculite, and halloysite) were noted by both Taylor (1953) and McConnell (1954). Heller and Taylor (1956) pointed out that except for the (00 $\ell$ ) series almost all of the other strong x-ray lines (hk0 reflections with



$h$ ,  $k$ , and  $\frac{1}{2}(h + k)$  even) are common to all of the hydration states observed. However, Kalousek and Roy (1957) have pointed out that the shift in  $c$ -axis spacing was not a continuous function of the water content, as it is in expanding clays, and that at least in their material, substantial changes in the x-ray diffraction pattern (in addition to the  $(00\ell)$  reflections) occurred on collapse at  $650^{\circ}\text{C}$ .

Crystal Structure. The structure of the 11A state of tobermorite from Ballycraigy has been determined by x-ray methods by Megaw and Kelsey (1956). The following description is adapted from that given in their paper.

The structure is approximately orthorhombic, with  $a = 11.3\text{\AA}$ ,  $b = 7.33\text{\AA}$ ,  $c = 22.6\text{\AA}$ ; the cell containing four formula units. True symmetry is probably monoclinic or triclinic. Parallel to  $(00\ell)$  the cell contains two identical complex layers displaced relative to one another. Each layer has two central sheets of composition  $4\text{CaO}_2$ , arranged so that each calcium has four oxygen neighbors in its own sheet and two in the sheet at the next level. Each pair of adjacent oxygens forms one edge of a tetrahedron containing silicon. These tetrahedra are joined into chains running parallel to the "b" direction. The chains are somewhat puckered.

This arrangement, a complex layer with the composition  $4(\text{Ca}_2\text{Si}_3\text{O}_9)$ , forms the backbone of the tobermorite structure. It is rather like a piece of double-sided corrugated paper, having a strong central sheet reinforced on each surface by longitudinal ridges; the ridges themselves are somewhat toothed.





Every third tetrahedron in the chain is a "bridging" tetrahedron which does not share oxygens with the calcium sheet, but rather shares the apical oxygens of its two neighboring tetrahedra along the chain; it is thus elevated above the general level of the chain. Two complex units pack together with their ridges superimposed vertically (note that the ridges do not nest). There are grooves (channels in the "b" direction) between the ridges, and these or the interlayer spaces must hold the remaining calcium and oxygen atoms, but detailed positions of these atoms are not known. According to Megaw and Kelsey it is not certain whether hydrogens are present wholly as OH groups or partially as  $H_2O$ , but according to these authors, if the composition given is correct, some hydrogens must be attached to oxygens taking part in the silica chains.

The proposed structure accounts for both the platy and the fibrous nature of the crystals. Further, it allows an explanation of the shrinkage of the c-axis spacing on dehydration, since removal of OH or  $H_2O$  from the grooves would permit two adjacent complex units to pack together with their ridges interleaved instead of superimposed, while still leaving sufficient room to accommodate a calcium atom between them.

A model of this structure is shown in Figure 1. The balls represent the calcium atoms of the central double-sheet framework. The arrangement of the silica tetrahedra with every third tetrahedron elevated above the plane of the central sheet is displayed. The grooves or channels between the ridges run from left to right in the plane of the paper.



Figure 1. Model Illustrating the Structure of Tobermorite  
According to Megaw and Kelsey (1956).



A somewhat different structure was advanced as a hypothesis by Mamedov and Belov (1958), according to which the metasilicate chains are condensed (i.e. share single oxygens) both between adjacent layers and between adjacent chains within a layer. It is not yet known whether this hypothetical structure can be reconciled with the experimental x-ray data (Taylor, 1961).

Morphology. True, well-crystallized tobermorite always occurs as well-defined laminar crystals with a cleavage parallel to (001) and a slight tendency toward elongation parallel to the "b" axis. Noteworthy electron micrographs have been published (among others) by Kalousek (1955), Gaze and Robertson (1956), Gard, Howison, and Taylor (1959), Kalousek and Prebus (1958), and Stein (1960).

#### Differential Thermal Analysis

A differential thermal analysis (DTA) pattern for the Ballycraig tobermorite given by McConnell (1954) showed endotherms reminiscent of those of  $\text{Ca}^{++}$ -saturated vermiculite at about  $130^{\circ}\text{C}$  and  $250^{\circ}\text{C}$ , a weak endothermic break at about  $360^{\circ}\text{C}$ , and finally a weak recrystallization exotherm at about  $850^{\circ}\text{C}$ . The specimen used was a mixture of the 11.2A and 14A hydrate states.

Kalousek (1954b, 1955, 1957) has investigated the DTA behavior of hydrothermally synthesized tobermorites with 11A spacings. He indicated that samples of both 0.8 and 1.0 Ca:Si composition behaved similarly and yielded only a small dehydration endotherm at about  $260^{\circ}\text{C}$  and a very weak and indefinite high-temperature exotherm at about  $830^{\circ}\text{C}$ . Greenberg (1954) found a similar pattern, but for his material the exotherm occurred at about  $965^{\circ}\text{C}$ . Gaze and Robertson (1956), found that their exotherm



occurred at 810°C, in better agreement with Kalousek and with McConnell.

Kalousek (1957) showed that substitution of aluminum into the tobermorite lattice resulted in very much sharper and more intense exothermic peaks in the 835°-860°C region. The intensity of the peak decreased with large amounts of substitution, while the temperature of occurrence increased slightly with the increasing substitution.

### Infrared Absorption

Reported infrared studies on tobermorite are not numerous. Kalousek and Roy (1957) have examined a well-crystallized synthetic tobermorite of composition  $4\text{CaO} \cdot 5\text{SiO}_2 \cdot 5\text{H}_2\text{O}$  by means of the KBr disc technique. A broad SiO band with a maximum at about  $10\ \mu$  ( $1000\ \text{cm}^{-1}$ ) and subsidiary maxima at  $11.2\ \mu$  ( $895\ \text{cm}^{-1}$ ) and  $8.3\ \mu$  ( $1200\ \text{cm}^{-1}$ ) were present in their published patterns but not discussed by these authors. A quite pronounced band at  $6.2\ \mu$  ( $1620\ \text{cm}^{-1}$ ) was ascribed to "interlayer" water and one at  $2.9\ \mu$  ( $3450\ \text{cm}^{-1}$ ) to bonded OH groups. The difference in the relative intensities of these bands after the vacuum drying incident to the preparation of the specimens and after subsequent rehydration was essentially negligible. Drying at increasingly high temperatures did cause reductions in the intensities of both these bands, but it is noteworthy that some absorption remained at these water positions; even at 650°C when the basal spacing was reduced to 9.6Å from the original 11.3Å. The authors suggested that these results indicate the retention of interlayer molecular water, even at this high temperature.





Xonotlite, a calcium silicate hydrate resembling tobermorite in some respects, but lacking interlayer water, was shown by Kalousek and Roy to have no absorption at  $6.2\mu$  and only negligible absorption at  $2.9\mu$ ; however, xonotlite possesses definite structural hydroxyl groups and in consequence yields a sharp absorption maximum at  $2.75\mu$  ( $3640\text{ cm}^{-1}$ ), corresponding to the frequency for stretching vibration of "free" OH groups. No such band is observed in the tobermorite pattern.

A sample of 14A tobermorite synthesized hydrothermally (previously mentioned in the discussion on hydration states) was shown by these authors to possess stronger absorption at  $2.9\mu$  but weaker absorption at  $6.2\mu$  than did the 11A tobermorite, and in addition, displayed a band in the region from  $6.5\mu$  ( $1540\text{ cm}^{-1}$ ) to  $7.0\mu$  ( $1430\text{ cm}^{-1}$ ).

Hunt (1959) examined natural tobermorite from Loch Eynort, Scotland, by the same KBr pellet technique, and reported a pattern very similar to that of Kalousek and Roy for the synthetic 11A material. In particular the natural tobermorite also shows a single bonded OH vibration at  $2.9\mu$  and no "free hydroxyl" band.

#### Surface Area

Surface area (i.e. "specific surface") of fine particulate matter is commonly measured by the adsorption of nitrogen, water vapor, or some other gas, the measurements being interpreted according to the well-known multilayer adsorption theory of Brunauer, Emmett, and Teller (1938). The theory leads to an experimental value for the number of molecules of the adsorbate



that constitute a monomolecular layer on one gram of the adsorbent. The assumption of an appropriate value for the area occupied by each molecule then leads directly to the surface area per gram of the adsorbent. As will be discussed later, for calcium silicate hydrates the surface area derived from water vapor adsorption is usually higher than that derived from nitrogen adsorption, and Brunauer and Greenberg (1962) consider that the water vapor measurement gives the correct area.

No reports of water-vapor surface area measurements of pure well-crystallized tobermorite were found in the literature. Greenberg (1954) determined surface areas by nitrogen adsorption for a series of hydrothermally-synthesized tobermorite products, and found values decreasing from 90 to 25 m<sup>2</sup>/g with increasing time of hydrothermal treatment. The latter value seemed to be an equilibrium value, since increase in processing time from 4 days to 18 days only reduced the measured area by 5 m<sup>2</sup>/g. Kalousek (1954c) reported a value of 50 m<sup>2</sup>/g by nitrogen adsorption for a platy tobermorite. Gaze and Robertson (1956) calculated surface areas from dimensions of individual plates visible under the electron microscope, and for well-crystallized material arrived at a value of 67 m<sup>2</sup>/g. Kalousek (1957) noted that crystals of aluminum-substituted tobermorites were markedly smaller than those of unsubstituted material, but gave no surface area values for them.

#### Surface Charge

Pike and Hubbard (1958) examined the surface charge of a material they called CSH (B) which was prepared by autoclaving



CaO and silica gel for 50 days at 135°C. According to Kalousek's (1955) studies on hydrothermal reactions in this system, the phase formed would most likely have been platy, well-crystallized tobermorite. They measured the nature of the surface charge by treatment with  $\text{Ag}(\text{NH}_3)_2^+$  and  $\text{Br}^-$  indicator ions in full strength aqueous ammonia solution. The solution phase was found to contain a large excess of the cation, indicating a strong negative charge on the tobermorite; however, if the latter had been treated beforehand with saturated  $\text{Ca}(\text{OH})_2$  solution the apparent charge of the solid particles was found to be positive. Solid  $\text{Ca}(\text{OH})_2$  itself was indicated as having a positive surface charge.

Stein (1960) examined well-crystallized synthetic tobermorite by means of electrophoresis after dispersion in NaOH solutions containing varying amounts of  $\text{CaCl}_2$ . The minimum hydroxyl concentration of the suspensions examined was  $10^{-3}\text{M}$ . Under these conditions he found that the sign and magnitude of the charge on the particles, as determined from electrophoretic velocity, varied with the  $\text{Ca}^{++}$  concentration; in systems with  $\text{Ca}^{++}$  concentrations higher than  $4 \times 10^{-3}\text{M}$  the particles were positively charged, and their velocity toward the anode increased with increasing  $\text{Ca}^{++}$  content. For  $\text{Ca}^{++}$  contents less than this value the tobermorite particles were found to be negatively charged, again with the velocity toward the cathode increasing with decreasing  $\text{Ca}^{++}$  concentration. Stein's results thus confirm those of Pike and Hubbard.

#### Cation Exchange Properties

The thought that tobermorite might, in analogy with the



clay minerals, possess significant cation exchange capacity was entertained by McConnell (1954); Roy (1956) suggested that "The measurement of the base-exchange capacity of these phases will undoubtedly lead to the next important step in revealing the nature of the tobermorite phase". Nevertheless, apparently no investigations of the possible cation-exchange properties of tobermorite have yet been published.

The substitution of aluminum for silicon in tetrahedral coordination is commonly conceded to be the one of the main sources of the observed cation exchange capacity of the clay minerals (see for example Grim, 1953, p. 133). However, Kalousek (1957) in his study of aluminum-substituted tobermorite, did not consider this possibility in his discussion of possible mechanisms of charge compensation accompanying the substitutions.

#### Summary

Tobermorite is a platy calcium silicate hydrate of composition approximating  $5\text{CaO} \cdot 6\text{SiO}_2 \cdot 5\text{H}_2\text{O}$ , and has a structure involving a central double layer of calcium ions in sixfold coordination, coupled with chains of silica tetrahedra parallel to the "b" direction which form an overall corrugated layer structure. The corrugations themselves are "toothed" by the elevation of every third tetrahedron, which is not directly attached to the CaO framework. Tobermorite is a rare mineral but it may be synthesized readily by hydrothermal means, and a considerable proportion of aluminum may be incorporated in its structure, presumably replacing some of the silicon atoms. The mineral exists normally with a c-axis spacing of 11.2Å, but is





capable of being collapsed to a spacing of about 9.5Å on heating. A 14Å variety, presumably having an extra layer of water between the structural units, has been observed to occur naturally and been prepared synthetically. Infrared absorption studies fail to disclose the expected free hydroxyl vibration but rather suggest that the water present is in the form of H<sub>2</sub>O and H-bonded hydroxyl groups, some of which are retained against heating to temperatures as high as 650°C. DTA of the unsubstituted material reveals only a small heat effect associated with a transition to wollastonite at about 830°C (the exact temperature varying somewhat). Samples containing substituted aluminum give a pronounced exothermic effect accompanying this transition. The electrophoretic charge of dispersed particles is reported to be positive in alkaline solutions if the Ca<sup>++</sup> concentration is higher than  $4 \times 10^{-3}$  molar, otherwise the particles move as negatively charged bodies. The apparent surface area of well-crystallized synthetic samples to nitrogen is of the order of 25 to 90 m<sup>2</sup>/g. Possible cation exchange properties of tobermorite have been mentioned, but not investigated.

### Calcium Silicate Hydrate (I)

#### Nomenclature and Synthesis

The identity and designation of this phase has been a subject of much confusion in recent literature. It is intimately related to tobermorite, but, as will be pointed out later, it has a number of properties which distinguish it from the latter. However, this was not obvious in the early stages of the modern period of research on calcium silicate hydrates, and since most



workers considered it to be merely a less-well crystallized tobermorite, the names "tobermorite" and "CSH(I)" were sometimes used interchangeably. A further source of confusion is the lack of a consistent designation for the CSH(I) phase by the various workers who did make the distinction; it was called CSF(B) by Bogue (1953), the "fibrous phase" or "fibrous  $C_4S_5H_n$ " by Kalousek (1955), "C/S 0.8-1.33 hydrate" by Kalousek and Prebus (1958), etc. The designation "CSH(I)" is due to Taylor (1950) and is now most generally used.

CSH(I) is not known to occur naturally. It may be produced in any of a variety of ways, either hydrothermally or by reaction at room temperature. Common methods of preparation at room temperature are reactions of a silica sol or gel with calcium hydroxide solution and reaction of sodium silicate solution with calcium salts (Taylor, 1961). The product formed is typically a poorly crystallized substance having an x-ray diffraction pattern which displays only the strong  $hk0$  lines of tobermorite. Under hydrothermal conditions the same product is readily formed by reaction between  $Ca(OH)_2$  and silica, but it is metastable and eventually transforms to tobermorite and other phases, depending on the composition. If finely-divided quartz is employed instead of silica the transformation to tobermorite is much more rapid. A detailed study of the sequence of transformations occurring in hydrothermal systems was given by Kalousek (1955), who also discussed the difference in technically important physical properties between CSH(I) and tobermorite. Detailed criteria for distinguishing between the two phases were



given by Kalousek and Prebus (1958), and these will be discussed under the appropriate headings. In many of the hydrothermal preparations reported in the literature it appears that the products were probably mixtures of several phases (see Gard, Howison, and Taylor, 1959). This fact was often not appreciated.

### Composition, Structure and Morphology

Variation in Chemical Composition. The compositional limits for CSH(I) are considerably wider than those reported for tobermorite. The lower limit of the Ca:Si ratio has been definitely established at about 0.8 (Kalousek, 1954a). The upper limit is not so certain; Kalousek (1954b) and Kalousek and Prebus (1958) set it at 1.33, while Taylor (1950) originally considered that the upper limit was as high as 1.5. Higher values have been suggested as well, but it is likely that Kalousek's figure is at least approximately correct (Taylor, 1961, Brunauer and Greenberg, 1962). An explanation for the existence of such a wide range in possible composition is not forthcoming, and this is one of the major questions of interest in connection with this phase.

The variation in water content at a particular drying condition to the Ca:Si ratio in CSH(I) is also a matter in some dispute. Brunauer and Greenberg (1962) presented data indicating that in a series of room-temperature preparations ranging in Ca:Si ratio from 1 to 1.4, the addition of lime to the structure resulted in the concomittant addition of water, in the approximate molar proportion of 1:1 (under measured drying conditions approximately equivalent to oven-drying). On the other hand,



Taylor and Fowison (1956) found that  $H_2O:SiO_2$  ratios for their products (on oven drying) are substantially independent of the Ca:Si ratio.

The question of isomorphous substitution in CSH(I) has not been investigated in detail, although a recent report unavailable to this writer (Sudo and Mori, 1961) suggested that K can partially substitute for Ca in a room-temperature synthetic phase that is probably CSH(I).

Hydration States. The fluctuation of the basal spacing of CSH(I) with state of hydration was demonstrated in the pioneer studies of Taylor (1950). Taylor's CSH(I), synthesized at room temperature, had an initial basal spacing of 12.3A, which he interpreted as being due to mixed layers of 10.4A and 14A hydration states. On heating to 120°C the basal spacing decreased to 10.4A; (note that this is not the 11.2A spacing associated with well-crystallized tobermorite). This sample was subsequently partially rehydrated by standing over water in a desiccator for six months whereupon it expanded to 11A. Further heating of a 10.4A oven-dry CSH(I) to 240°C caused an additional collapse to 9.3A.

Variation in Basal Spacing Due to Composition. Considerable evidence exists that basal spacing varies with composition of the CSH(I) as well as with state of hydration. Taylor (1961) reported spacings ranging from 13.5A to 10.5A for "gently-dried" specimens of CSH(I), the spacing roughly decreasing with increasing Ca:Si ratio of the material. The methods of preparation of the individual samples were not cited. Taylor and Howison.





(1956) reported only a slight and uncertain tendency for this relationship for room-temperature preparations dried to  $108^{\circ}\text{C}$ . The variation was only between 11.3Å and 9.9Å, except for a single value at 9.1Å. Grudemo (1955) reported variation in basal spacing ranging from 13.8 to 10.4Å, for various room temperature CSH(I) preparations, and again the same rough relationship with respect to Ca:Si ratio seemed to hold; however the significance of this data is open to question since no attempt was made to control the state of hydration of the samples. In contrast to these results, Kalousek (1955) prepared CSH(I) hydrothermally and noted that the basal spacings were identically 11Å in preparations ranging from 1.0 to 1.33 Ca:Si ratio.

Interpretation of any variation in basal spacing with Ca:Si ratio would be on a far firmer basis if these would be determined for a suite of materials of varying ratios at each of a series of controlled relative humidities or partial pressures of water, since it appears that both factors may influence the spacing.

X-Ray Diffraction and Crystal Structure. "Typical" x-ray powder data for CSH(I) given by Taylor (1961, p. 105), and data for hydrothermal CSH(I) were given by Kalousek (1955). The patterns show essentially only the strong  $hk0$  lines of tobermorite, i.e. those indexed as  $h$ ,  $k$ , and  $\frac{1}{2}(h+k)$  even. These include the (220) at 3.04Å; (400) at 2.80Å; (040) at 1.82Å; (620) at 1.67Å; (800) at 1.40Å, etc. Normally the 3.04Å, 1.82Å, and 2.80Å lines are stronger than the rest. In addition to these lines, a c-axis (basal) spacing is sometimes present in the region 10-13Å. Taylor's compilation of a "typical" pattern lists this as



"very strong", while Kalousek in the work cited above reports it as "very weak, broad", and in one case absent entirely. It should be noted that this spacing is often not observable on diffractometer equipment, but can be observed on film camera diffraction technique, which permits long-time exposure and hence more certain recognition of peaks of weak overall intensity.

It is commonly inferred that CSH(I), being in some respects a disordered version of tobermorite, retains all the strong peaks of that substance, with the implication that peaks other than those that are present are merely too weak in the disordered phase to be seen. This is not quite correct; tobermorite has a strong peak (the 222) at 2.97Å which is not commonly present in CSH(I), as pointed out by Kalousek and Prebus (1958). It would be important to know, in a given case, whether this line is in fact present but not resolved from a broadened main 3.05Å peak adjacent, or whether it is in fact not present at all. The latter would suggest that the disorder involved is primarily in the c-axis direction, and has to do with the stacking of the unit sheets. This type of disorder is common in clays and many other substances.

Because of the paucity of reflections, the exact crystal structure of CSH(I) is not amenable to direct determination by x-ray methods. Various modifications of the basic tobermorite structure have been proposed to account for the observed variability of the Ca:Si ratio that takes place without any corresponding change in either the dimensions or the weight of the unit cell (i.e. density of the substance). Taylor and Howison



(1956) proposed a simultaneous removal of the "bridging" tetrahedra and replacement of two hydrogen atoms by a single calcium, the latter occupying an interlayer position made available by the removal of silica. Brunauer and Greenberg (1962) suggested a further modification in which the  $\text{SiO}_2$  and 2 H would be replaced not by a calcium but by a calcium plus a water molecule. However, Taylor (1961) stated that the constitution he and Howison originally proposed for lime-rich CSH(I) is "unlikely".

Brunauer (1962) cited evidence concerning the enhanced rate of dissolution of CSH(I) in molybdic acid obtained by Greenberg and Pressler as indicating that the silica chains in CSH(I) are at least partially depolymerized; the higher the Ca:Si ratio, the more nearly the actual structure is supposed to resemble an orthosilicate (i.e. a structure composed of completely independent  $\text{SiO}_4$  tetrahedra). Note that this suggestion is exactly the reverse of that put forth by Mamedov and Belov (1958) for tobermorite, which they considered to be completely polymerized.

Morphology. The morphology of CSH(I) was not at first well understood but is now seemingly established. Grudemo (1955) first studied room-temperature preparations of CSH(I) by electron microscopy; most of his samples have the common characteristic of occurring in very thin, wrinkled foils or films of almost unit cell thickness. The morphology is difficult to describe but easy to recognize after once having seen it. Some of the wrinkled sheets appeared to roll partially into fibers or tubes, particularly in the preparations higher in lime. Grudemo pointed



out a resemblance between the morphology of some of these CSH(I) preparations and several of the clay minerals, notably hectorite and montmorillonite. Kalousek (1955) described the morphology of his hydrothermal CSH(I) preparations as "fibrous"; he notes that "these fibrous crystals were exceedingly fine". In a later study (Kalousek and Prebus, 1958) this author and his associate re-examined some of the earlier preparations and some new ones, and concurred with Grudemo's findings of "crinkled foils" morphology rather than "fiber" morphology as previously defined. Gard, Howison, and Taylor (1959) reported their room-temperature preparations to be mostly crinkled foils, but autoclaved specimens appeared to be mixtures of tobermorite plates and a lime-rich fibrous phase which these authors ascribed to CSH(II), a phase which will be discussed subsequently; however, many intermediate states were observed, and according to these authors "the distinction between fibers and shredded, crumpled foils was especially indefinite".

#### Differential Thermal Analysis

Kalousek (1954b) showed that the differential thermal patterns of CSH(I) prepared at room temperature differed from those of tobermorite by the presence of a sharp and intense exothermic peak in the  $835^{\circ}$ - $900^{\circ}\text{C}$  region, the temperature of the exotherm increasing with increasing Ca:Si ratio. Kalousek (1955) later showed that hydrothermally-prepared CSH(I) compounds are identical to the room-temperature preparations in this regard. The difference in behavior of these materials as compared to that of tobermorite is sufficiently characteristic to





permit the use of the high-temperature exotherm as a definite criterion for distinguishing the two phases. However, it should be noted that if the tobermorite contains substituted aluminum one cannot use this criterion as both phases will give strong exothermic peaks in the same general region.

### Infrared Absorption

Van Bemst (1957) reported that room-temperature CSH(I) preparations examined by the KBr pellet technique gave a broad, indistinct band between  $8.2\mu$  and  $11.2\mu$  ( $1220$  and  $900\text{ cm}^{-1}$ ), with the maximum absorption at  $10\text{-}10.5\mu$  ( $1000$  to  $950\text{ cm}^{-1}$ ). Kalousek and Roy (1957) examined hydrothermally prepared CSH(I), i.e. "fibrous solids" of composition 0.8, 1.0, 1.25 and 1.5 Ca:Si ratio. The strong Si-O band found by Van Bemst and water bands previously described for tobermorite were found; but in addition a broad band at  $6.5\text{-}7.0\mu$  ( $1540$  to  $1430\text{ cm}^{-1}$ ) was present. There was increased absorption at the position of this band and decreased absorption of the water bending mode at  $6.2\mu$  ( $1615\text{ cm}^{-1}$ ) as the Ca:Si ratio increased from 0.8 to 1.5. The 0.8 Ca:Si solid had about equal absorption at the two bands. These authors speculated that it may be possible to correlate the presence of this band with either an increasing amount of structural  $\text{Ca}(\text{OH})_2$ , or with increasing proportion of water molecules coordinated around interlayer Ca ions. A similar band was observed in the 14A platy tobermorite previously mentioned as having been synthesized by these authors. Additional reference to this infrared feature will be made later.



## Surface Areas and Other Characteristic Properties of CSH(I)

Brunauer and Greenberg (1962) reported surface areas for room-temperature preparations of CSH(I) to range from 135 to 380 m<sup>2</sup>/g, when determined by water-vapor adsorption. Corresponding areas measured with nitrogen were lower, and ranged from 20% to 100% of the water values. A similar phenomenon had earlier been noted by Kalousek (1954c) in his study of autoclaved cement block containing hydrated calcium silicates. Brunauer, Kanro, and Weise (1959) demonstrated that nitrogen surface area values on tobermorite systems were unreliable; they indicated that calculations using nitrogen adsorption values frequently led to the conclusion that certain of the samples had negative surface energies, which is an impossible result. Presumably some of the surface spaces in CSH(I) and related materials are not available to nitrogen.

Neither surface charge density nor cation exchange properties seem to have been investigated for this phase.

One significant property of CSH(I) is its resistance to attack by reagents employed in tests for free lime, particularly acetoacetic ester. Kalousek (1954a) found that CSH(I) prepared with Ca:Si ratios less than 1.33 were quite stable to lime extraction by this solvent; however, preparations with Ca:Si ratios in excess of this amount (i.e. CSH(II)) were readily attacked.

### Summary

CSH(I) is a poorly crystalline substance distinct from tobermorite, which may be produced by reaction at room temperature



or as a transient phase in hydrothermal synthesis. The x-ray diffraction powder pattern displays only the strong hko lines of tobermorite plus a basal peak which is generally diffuse. The basal peak may vary from 13.8Å down to about 10Å; samples with increasing Ca:Si ratios tending to give lower values. The value also depends somewhat on the state of hydration, and on drying to sufficiently high temperatures a 9.5Å spacing is attained. The Ca:Si ratio may vary from 0.8 to 1.33, and possibly slightly higher, without significant change in the x-ray pattern or calculated density. The structure is related to that of tobermorite; but the exact structure is not known. It has been speculated that the distinction lies partially in removal of portions of some of the bridging silica tetrahedra and their replacement by Ca atoms or Ca atoms and water; also evidence is given to indicate that the silica chains are partially depolymerized. The morphology revealed by electron microscopy is usually described as one consisting of crumpled or crinkled foils, sometimes partially rolling into tubes or fibers. The individual foils are very thin, only a few unit layers in thickness at most. Infrared absorption spectra consist of a broad SiO band centered at about  $10\mu$  ( $1000\text{ cm}^{-1}$ ), bonded OH and water bending modes, and in contradistinction to tobermorite, a broad band occurs at  $6.5\text{--}7.0\mu$  ( $1540\text{--}1430\text{ cm}^{-1}$ ). The intensity of absorption at this wave length increases with increasing Ca:Si ratio. DTA of CSH(I) yields a strong sharp exotherm in the region of  $835^{\circ}\text{--}900^{\circ}\text{C}$ ; the actual temperature increases with increasing Ca:Si ratio. Reported surface area values range from 135 to  $380\text{ m}^2/\text{g}$ . Water vapor adsorption is the appropriate



technique for surface area determination for this system. CSH(I) is quite resistant to lime extraction using the aceto-acetic ester.

### Calcium Silicate Hydrate (II)

#### Nomenclature and Synthesis

This phase has also been designated " $C_2S \cdot H_2$ ", "hydrate II", "1.8 C/S hydrate", " $C_7S_4H_n$ ", etc., but CSH(II) is now the common designation (Brunauer and Greenberg, 1962; Taylor, 1961). The compound was first reported by Taylor (1950) as occurring as the result of long-time reaction of tricalcium silicate with water at room temperatures. It was not prepared by double decomposition nor by room temperature reaction of gel mixtures; nor did Heller and Taylor (1952, 1952a) find the phase in their hydrothermal preparations of appropriate Ca:Si ratio. However, Kalousek (1954b) was able to prepare it by reaction between lime and silica at room temperature, and later (1955) demonstrated its existence as a transient phase in hydrothermal systems. Toropov, Borisenko, and Shirokova (1953) reported the production of relatively well-crystallized CSH(II) by reaction of calcium glycerate solution on silica gel, but this synthesis has not been successfully repeated (Taylor, 1961).

#### Composition, Structure, and Morphology

Variation in Chemical Composition. The lower limit of the Ca:Si ratio for this phase is generally given as 1.5 (Kalousek and Prebus, 1958; Taylor, 1962). The value for the upper limit was given by Kalousek and Prebus (1956) as 2.0, a value that





was concurred with by Gard, Howison, and Taylor (1959), and Taylor (1961); however in a later paper (Taylor, 1962) suggested 1.75 as a more characteristic upper limit.

According to Gard, Howison and Taylor (1959) the  $H_2O:Si$  ratio of this phase (when oven-dried) is markedly greater than that of tobermorite, due to about 0.6 mole of extra water per mole of silica, which is lost only above  $300^{\circ}C$ .

No direct evidence of lattice substitution has yet been reported for CSH(II).

X-Ray Diffraction and Crystal Structure of CSH(II). This compound is characterized by an x-ray pattern which somewhat resembles those of other tobermorite-group phases in including at least some of the strong lines indexed as  $hk0$  reflections of tobermorite, viz. those at 3.05, 2.80, 1.82, 1.40, etc. However, the (620) line at 1.67Å, present in CSH(I) is not found in CSH(II); and the strong (222) line of tobermorite, absent in CSH(I) is also absent in CSH(II). An authoritative pattern was given by Heller and Taylor (1956, page 57). A number of previously unknown lines appear in this phase; among them one in particular at 1.56Å was suggested by these authors as a characteristic means of identifying the presence of this phase, even in mixtures.

The basal spacing of this compound appears to be comparatively strong, and fairly consistent in location at 10-10.5Å (Taylor, 1950; Heller and Taylor, 1956; Van Bemst, 1957; Kalousek and Prebus, 1958; Gard, Howison, and Taylor, 1959, etc.). In general the crystallinity of this phase appears to be inferior



to that commonly found for CSH(I) with several exceptions (Taylor, 1961). Published information appears not to indicate any particular variation of basal spacing with condition of drying or state of hydration. The crystal structure of CSH(II) has not been determined; in fact no suggestion as to the indexing of the observed powder diffraction lines has yet been made.

Gard, Howison, and Taylor (1959) have speculated that CSH(II) may be analagous to kaolin-family clay minerals in having the central sheet (in this case  $\text{CaO}_2$ ) flanked by silica tetrahedra only on one side, the opposite side being composed only of hydroxyl groups. Calcium ions and water molecules would be retained in interlayer spaces, according to this concept. The possibility that both silicates and hydroxyls might be attached randomly on both sides of the  $\text{CaO}_2$  layer is presented in a printed discussion by Schuit and Wyatt (1962) and the reply by Taylor appended to Taylor's 1962 paper.

Morphology. The morphology of CSH(II) is characteristically fibrous, as originally shown by Grudemo (1955). Kalousek and Prebus (1958) also mentioned "gel-like agglomerates" which might be fragments of fibrous products. Gard, Howison, and Taylor (1959) concurred in the description of the morphology as fibrous, and noted by electron diffraction that the fiber axis is the "b" axis and cleavage is (001). Electron micrographs of CSH(II) from so-called "bottle-hydrated"  $\text{C}_2\text{S}$  published by Copeland and Schultz (1962) revealed a particular variant of fiber morphology in which the fibers are arranged in characteristic cigar-shaped bundles. A similar morphology for CSH(II) supplied by Taylor was observed by Grudemo (1955).



## Differential Thermal Analysis

DTA curves for a number of solids classed as CSH(II) were given by Kalousek (1954b). He noted a small exothermic bulge (not sharp enough to define as a peak) in the temperature range 350-450°C, often a very small endotherm at around 800°C, and finally a relatively small exotherm in the region around 850°C. Van Bemst (1957) presented a somewhat more complicated pattern, a double set of peaks in the region 340-380°C, a slight exothermic bulge at around 600°C, and a fairly complicated combination of small exotherms and endotherms in the region 800-920°C. In their summary of the typical characteristics of the different phases, Kalousek and Prebus (1958) described the characteristic DTA of CSH(II) merely as "variable".

## Infrared Absorption

In infrared absorption studies of CSH(II) Van Bemst (1957) found that in addition to the common broad Si-O band between 8.2 and 11.2  $\mu$  (1130 and 890  $\text{cm}^{-1}$ ), some cigar-shaped samples of CSH(II) showed a pronounced band at 12.1  $\mu$  (825  $\text{cm}^{-1}$ ). Kalousek and Prebus (1958) suggested that the characteristic absorption bands for this phase are at 2.9  $\mu$  (3450  $\text{cm}^{-1}$ ), which is the bonded OH stretching frequency, and at 6.8  $\mu$  (1470  $\text{cm}^{-1}$ ), the feature usually attributed to carbonate. It is apparent that further study is needed to more definitely characterize the infrared spectrum of this phase.

## Surface Areas and Other Characteristic Properties of CSH(II)

Surface areas of CSH(II) preparations have not been measured



extensively. Copeland and Schulz (1962) reported that a bottle-hydrated  $\beta$ -C<sub>2</sub>S preparation having the typical cigar-shaped fiber bundle morphology and yielding an x-ray diffraction pattern for CSH(II), had a measured surface area of 300 m<sup>2</sup>/g, presumably to water vapor. Whether this high a surface area is characteristic for CSH(II) in general is not known.

Measurements of exchange properties, surface charge, etc. have not been reported for this phase. CSH(II) is apparently relatively unstable to the removal of lime by the acetoacetic ester, and the leached residue is somewhat different from untreated material of the corresponding Ca:S1 ratio (Kalousek, 1954b).

#### Summary

CSH(II) is a lime-rich phase of approximate Ca:S1 ratio 1.5-2.0. It appears to have a larger quantity of structural water associated with it than does CSH(I). X-ray diffraction patterns resemble CSH(I) in that many of the hk0 peaks of tobermorite are present, but several are not, and some new lines appear. The structure is unknown, but may involve hydroxyls partially replacing silica tetrahedra, either uniformly on one side of the central CaO<sub>2</sub> layer, or randomly on both sides. Morphology is typically fibrous, and sometimes involves characteristic cigar-shaped bundles of fibers. The DTA pattern is marked by an exothermic bulge at intermediate temperatures and a relatively small exotherm in the 850°C region. Infrared spectra show a distinctive band at 6.5-7.0  $\mu$ , presumably due to carbonate contamination; a 12.1  $\mu$  band is sometimes found,





but the extent to which this is characteristic is uncertain. The surface area measured (for a single specimen) is high in comparison with those reported for CSH(I). The compound is subject to significant attack by the acetoacetic ester, resulting in rapid removal of  $\text{Ca(OH)}_2$ .

### Calcium Silicate Hydrate (Gel)

#### Nomenclature and Origin

CSH (gel) was the name proposed by Taylor (1961) for the phase commonly produced by the paste hydration at room temperature of either of the two major constituents of portland cement,  $\beta$ - $\text{C}_2\text{S}$  and  $\text{C}_3\text{S}$ , or by the bottle hydration of the latter. Bottle-hydrating  $\beta$ - $\text{C}_2\text{S}$  was said to produce the CSH(II) phase with the characteristic cigar-shaped fiber bundle morphology previously discussed (Copeland and Schulz, 1962). CSH (gel) is also developed in the ball-mill hydration of  $\beta$ - $\text{C}_2\text{S}$ , but not of  $\text{C}_3\text{S}$  (Brunauer and Greenberg, 1962).

Brunauer and Greenberg (1962) and Brunauer (1962) called this phase "tobermorite-(G)" (for gel). This name is somewhat unfortunate since it implies a relatively close relationship between this phase and natural or synthetic tobermorite. As will be shown shortly, the relationship is not nearly as close as is commonly inferred. The writer is of the distinct opinion that too much credence has been placed on the supposed resemblance.

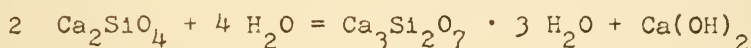
A word about hydration is in order at this point. As used in cement literature, "paste" hydration refers to mechanically mixing the anhydrous phase with a definite, limited amount of water and then permitting the mixture to "set" and harden, in



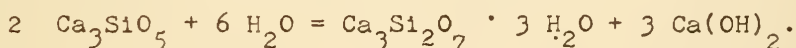
analogy with the setting and hardening process of portland cement in concrete. "Bottle hydration" refers to a treatment consisting of mixing the anhydrous phase with an excess of water (usually about 10 times its own weight) and placing it in a sealed polyethylene bottle mounted on a rotating wheel. "Ball mill" hydration is self-explanatory. Hydration of  $\beta\text{C}_2\text{S}$  and  $\text{C}_3\text{S}$  has been reviewed in detail by Brunauer and Greenberg (1962), by Brunauer (1962), and by Taylor (1961).

The stoichiometry of the hydration reactions for the two phases were given by Brunauer, Kantro and Copeland (1958) as follows:

for  $\beta\text{-C}_2\text{S}$ , regardless of hydration method:



and for  $\text{C}_3\text{S}$  by paste or bottle hydration:



#### Composition, Structure, and Morphology

Variation in Chemical Composition. CSH (gel) is a relatively high-lime phase. According to Brunauer and Greenberg (1962) CSH (gel) produced on paste or bottle hydration of  $\text{C}_3\text{S}$  has a true Ca:Si ratio of 1.5, after correction for supposedly amorphous  $\text{Ca(OH)}_2$ . Detailed evidence for this was given by Pressler, Brunauer and Kantro (1956) and by Brunauer, Kantro, and Copeland (1958). Of the three moles of lime originally present in  $\text{C}_3\text{S}$ , 1.5 were relatively firmly bound in the CSH (gel) produced, about 1.3 moles were identified as crystalline  $\text{Ca(OH)}_2$ , and the remaining 0.2 moles were characterized as amorphous  $\text{Ca(OH)}_2$ .

$\beta\text{-C}_2\text{S}$  reacts very much more slowly than  $\text{C}_3\text{S}$ ; for pastes



made from this starting material, and for long-time bottle-hydration products the Ca:Si ratio was given as 1.6-1.7, even after correction for amorphous  $\text{Ca}(\text{OH})_2$  (Brunauer and Greenberg, 1962). Presumably these high-lime forms of CSH (gel) are to be regarded as intermediate products in the overall hydration process.

The  $\text{H}_2\text{O}:\text{Si}$  ratio of CSH (gel) is particularly difficult to determine because of the colloidal nature of the phase. Reported values range from 1.0 to 1.5, depending on the method of drying used (Taylor, 1961). The stoichiometry for the hydration reactions of both starting compounds proposed by Brunauer, Kantro, and Copeland (1958) assumed that the product has 1.5 moles of  $\text{H}_2\text{O}$  per mole of silica.

X-Ray Diffraction and Crystal Structure. The crystal structure of this considerably distorted phase is unknown, although resemblance to that of tobermorite is generally postulated.

According to Brunauer (1962), x-ray diffraction yields lines at the positions of the three strongest lines of tobermorite; a large broadened reflection at about  $3.07\text{\AA}$ , and weaker ones at  $2.80\text{\AA}$  and  $1.82\text{\AA}$ . No basal spacing is observed.

Brunauer and Greenberg (1962), basing their conclusions on observed rate of solution of CSH (gel) in molybdic acid, suggested that this phase is completely depolymerized; i.e. that the chains consist of individual  $\text{SiO}_4$  tetrahedra linked by hydrogen bonds. They considered that one mole of water of the three present in their formulation of  $\text{Ca}_3\text{SiO}_2 \cdot 3\text{H}_2\text{O}$  is



interlayer water that is lost continuously on drying; the remainder was thought to be associated with the silica chains and is relatively stable to heating.

In a recent significant paper, Kantro, Brunauer, and Weise (1961) reported that an inverse linear relationship was found to hold between measured surface area and Ca:Si ratio for a large number of CSH (gel) pastes made from both  $\beta$ -C<sub>2</sub>S and C<sub>3</sub>S. Seemingly, the greater the amount of lime present in the structure the lower the surface; hence the conclusion was drawn that lime cements the individual CSH (gel) layers together within the individual particle.

These authors went on to develop a structural model of CSH (gel) in some detail. According to the picture they derived, "mature" gel consists of very thin elongated sheets two and three unit layers thick. The underlying structure is different for the two classes of particles. The "two-unit-thick" particle has a structure described on a "pseudo unit cell" basis as follows: the outermost sheets of each of the two layers contains  $0.77 \text{ CaO} + 1 \text{ SiO}_2$ ; the "central" sheet of each of the two layers contains  $2 \text{ CaO}$ ; and finally the two "inner boundary" sheets each contain an  $\text{SiO}_2$ . The overall Ca:Si ratio for this type of particle is 1.39. In contrast, in the three unit-layer thick each of the two pairs of "inner boundary" sheets contains not  $1 \text{ SiO}_2$ , but rather  $1 \text{ SiO}_2 + 0.69 \text{ CaO}$ . The calculated Ca:Si ratio for this model is 1.72. The observed Ca:Si ratio of close to 1.5 is taken as indicating a rough average of the two types of compositional units present.





These authors suggested that the 2-layer structure is unstable with respect to the 3-layer structure due to its larger surface free energy, and two-layer-thick particles spontaneously convert to the latter in time. It is difficult to see how this is accomplished without internal rearrangement, in view of the structural difference proposed.

Morphology. The morphology of CSH (gel) has been the subject of some controversy in the literature. The gel is difficult to disperse for electron-microscopic observation and ultrasonic treatment usually needs to be employed. Early studies (Bogue, 1954; Swerdlow, McMurdie and Heckman, 1957) found spherical particles 50-200A in diameter, but later work has failed to substantiate this structure. Buckle and Taylor (1959) studied a  $C_3S$  paste dispersed without solvent and found very thin irregular flakes, several hundred A across and only a few tens of A thick. On the other hand, results from the Portland Cement Association laboratories have always shown the particles as straight fibers, the fibers themselves being apparently composed of rolled-up sheets of extreme thinness. A series of excellent electron micrographs illustrating this morphology have been published by Copeland and Schulz (1962), and appear in several of Brunauer's review publications. Brunauer (1962) considered that it is the adhesion of these rolled up sheets to one another that is responsible for the strength of hardened paste of these compounds, and inferentially, of concrete.

#### Differential Thermal Analysis

Brunauer and Greenberg (1962) cited unpublished DTA results



by Gordon on paste-hydrated  $C_3S$  and  $\beta\text{-}C_2S$  as yielding a large endotherm near  $200^\circ\text{C}$ . While a number of authors have published DTA patterns of hydrated cements, published DTA patterns of CSH (gel) phases have not been found in the literature. Kurczyk and Scwiete (1962) have published a "dynamic differential calorimetry" curve of a  $C_3S$  paste; the method being similar, but not identical to DTA. A large endotherm at  $160^\circ\text{C}$  (presumably due to more or less free water) and a small endotherm at about  $260^\circ\text{C}$  were observed, in addition to the  $\text{Ca}(\text{OH})_2$  endotherm at about  $500^\circ\text{C}$ .

### Infrared Absorption

Infrared absorption characteristics of CSH (gel) have not been studied extensively until recently. However, within the last few years a number of papers have appeared (Hunt, 1959; Hunt, 1962; Lehmann and Dutz, 1959; Lehmann and Dutz, 1962; Midgley, 1962). The observations of these authors are essentially similar.

Briefly, the spectrum is dominated by a very-much broadened Si-O stretching band centered at about  $10.4\mu$  ( $960\text{ cm}^{-1}$ ), indicating at least partially linked silica tetrahedra (isolated ones vibrate at somewhat higher wave lengths). In the hydration of  $\beta\text{-}C_2S$  or  $C_3S$ , particularly the latter, a 2.75 micron ( $3640\text{ cm}^{-1}$ ) band appears, which is interpreted as a free hydroxyl stretching mode, the hydroxyl being that of the  $\text{Ca}(\text{OH})_2$  formed along with the CSH (gel). A band at  $2.9\mu$  ( $3450\text{ cm}^{-1}$ ) for H-bonded hydroxyl and a water deformation band at  $6.2\mu$  ( $1620\text{ cm}^{-1}$ ) are observed.

In addition to these, a broad, rather flat band at  $6.5\text{-}7.0\mu$  ( $1540\text{-}1430\text{ cm}^{-1}$ ) is always present. This band has previously



been mentioned in connection with the CSH(I) phase. Kalousek and Roy (1957) found that the intensity of this band in hydrothermally-prepared CSH(I) increases with Ca:Si ratio, while concomitantly the intensity of the neighboring water band at 6.2 microns decreases. The band was not found to be present for well-crystallized hydrothermal tobermorite. Hunt (1959) has observed the presence of this band in  $\text{Ca}(\text{OH})_2$  slightly contaminated with  $\text{CaCO}_3$  by reaction with atmospheric  $\text{CO}_2$ , and has ascribed it to a stretching vibration of the  $\text{CO}_3^{=}$  group. He showed that the intensity of absorption per gram of  $\text{CO}_2$  in his sample was very much greater in carbonated  $\text{Ca}(\text{OH})_2$  and in CSH (gel) than it was in  $\text{CaCO}_3$  itself. He also showed deuteration of the  $\text{Ca}(\text{OH})_2$  did not affect the position or intensity of the band. Lehmann and Dutz (1962) also ascribed this band to the effect of carbonation at least for some of their materials, but a band at almost the same position in hydrogarnet samples was ascribed by them to the deformation vibration of strongly-held water.

#### Surface Area and Other Characteristic Properties of CSH (gel)

Surface Area Measurements. Surface areas of CSH (gel) phases have been measured by various workers, notably Brunauer and his associates at the Portland Cement Association. The surface area actually determined is that of the hydration product, including the CSH (gel),  $\text{Ca}(\text{OH})_2$  produced by the hydration reaction, and any unreacted starting material. The amounts of the latter two phases and any other impurities are determined



separately and the measured areas corrected for their presence.

Brunauer, Kantro, and Weise (1959) measured the surface areas of fourteen paste, bottle, and ball-mill hydration products of  $\beta$ - $C_2S$  and  $C_3S$  both by water vapor adsorption and by nitrogen adsorption. As previously mentioned, the latter values were considered to be unreliable. CSH (gel) in pastes of both starting compounds were in the range  $135\text{--}170\text{ m}^2/\text{g}$ ; the CSH (gel) in five different bottle hydration products of  $C_3S$  varied between 190 and  $230\text{ m}^2/\text{g}$ ; and finally the CSH (gel) in four different preparations of ball-mill hydrated  $\beta$ - $C_2S$  ranged between 190 and  $220\text{ m}^2/\text{g}$ . The reasonable constancy of these values suggests that CSH (gel) has a remarkably characteristic surface area. It should be noted that the area observed is in general somewhat lower than those previously reported for at least some preparations of CSH(I).

Kantro, Brunauer, and Weise (1959) studied the product of ball-mill hydration of  $C_3S$ , an unstable phase that has properties similar to those of CSH (gel) except that it shows only a single line on x-ray diffraction, and that on continued ball-milling it spontaneously converts to moderately well-crystallized afwillite. This phase, called "hydrate III" by the authors, had measured surface areas ranging from 135 to as much as  $420\text{ m}^2/\text{g}$ .

The surface development of CSH (gel) in pastes as a function of hydration time at several temperatures has recently been studied by Kantro, Brunauer, and Weise (1961). At a relatively low temperature ( $5^\circ\text{C}$ )  $C_2S$  pastes generated CSH (gel) of surface area as high as  $500\text{ m}^2/\text{g}$  (as measured for a 14-day old paste),





but with aging the area was reduced to about  $250\text{--}300 \text{ m}^2/\text{g}$ . The higher surface area material must have consisted largely of single-unit-layer thick particles. The CSH (gel) surface of corresponding preparations of  $\text{C}_3\text{S}$  did not go above approximately  $350 \text{ m}^2/\text{g}$ . At  $25^\circ\text{C}$  neither compound produced CSH (gel) with surface much over  $350 \text{ m}^2/\text{g}$ ; pastes hydrated at  $50^\circ\text{C}$  yielded CSH (gel) products of surface areas slightly lower still. Surface areas of CSH (gel) produced by "alite", an impure form of  $\text{C}_3\text{S}$  containing alumina and magnesia in solid solution, were about the same as those for the corresponding phases generated from pure  $\text{C}_3\text{S}$ .

Surface Charge and Surface Energy of CSH (gel). Measurements of surface charge have not been made with CSH (gel) by itself, but Pike and Hubbard (1958) determined the apparent surface charge of a number of portland cement pastes after 5 days hydration, using their  $\text{AgNH}_3^+$  and  $\text{Br}^-$  indicator ion techniques; all of the pastes appeared to be charged positively. As mentioned previously, the "CSH (B)" employed by these authors to represent the gel phase in hydrating  $\text{C}_3\text{S}$  and  $\text{C}_2\text{S}$  was probably well-crystallized tobermorite.

The surface energy (actually surface enthalpy) of CSH (gel) has been determined by Brunauer, Kantro, and Weise (1959) by the method of measuring the heats of solution of preparations of varying surface area. The value secured was  $386 \pm 20$  ergs per  $\text{cm}^2$ , and refers to material dried to a stage characterized by the composition  $\text{Ca}_3\text{Si}_2\text{O}_7 \cdot 2\text{H}_2\text{O}$ . The data indicated that the surface structure of CSH (gel) products prepared from both  $\beta\text{-C}_2\text{S}$



and  $C_3S$  by paste hydration, from  $C_3S$  by bottle hydration, and from  $\beta$ - $C_2S$  by ball-mill hydration, are all essentially the same from the standpoint of surface energy. The authors also included a single preparation (D-40) of a bottle hydrated  $\beta$ - $C_2S$  in their study; this has been previously noted to yield CSH(II). The observed heats of solution and surface areas for this preparation were not significantly different from those of the others.

Cation Exchange Properties. No record of measurements of cation exchange properties of CSH (gel) has been found in the literature.

Thermodynamic Properties. Some thermodynamic properties of CSH (gel) have been estimated by Brunauer and Greenberg (1962). The heat of adsorption of water on CSH (gel) produced from  $\beta$ - $C_2S$  was estimated as 32 calories per gram of the original silicate; the corresponding values for CSH (gel) produced from  $C_3S$  was given as 26 calories per gram. The entropy of the bulk CSH (gel) phase was estimated to be 85 e. u. per mole of  $Ca_3SiO_7 \cdot 3H_2O$ , and the surface entropy of a "typical" CSH (gel) with a surface area of  $300 \text{ m}^2/\text{g}$  was estimated as 3.3 e. u. per mole.

### Summary

CSH (gel) is produced on hydration of  $C_3S$  in paste form or by bottle technique, or by hydration of  $\beta$ - $C_2S$  by paste or ball-mill technique. Bottle hydration of  $\beta$ - $C_2S$  produces CSH(II) while ball-milling  $C_3S$  yields a distorted phase that spontaneously converts to afwillite. The Ca:Si ratio of CSH (gel) is at least 1.5, and may be as high as 1.7;  $H_2O$ :Si ratio varies from 1.0 to 1.5 depending on degree of drying. X-ray diffraction shows only



three lines, at the three strongest positions of the tobermorite pattern, no basal line is observed.

It is believed by at least one noted authority that the silica chains in CSH (gel) may be completely depolymerized (i.e. consist of individual  $\text{SiO}_4$  chains linked by hydrogen bonds). CaO in excess of the structural amount needed for the lattice seems to bind individual unit layers together into two or three unit layer thick particles. Morphology of the phase is usually described as consisting of straight, long fibers, the fibers themselves being composed of rolled-up sheets. The infrared spectrum is more or less similar to that of tobermorite except that a strong band is observed at 6.5-7.0 microns which may be due to carbonation. DTA of this phase is somewhat uncertain from the literature available, mention being made of an endotherm in the 200-260°C region. Surface areas attributed to CSH (gel) in pastes and other formulations range from about 150 to over 500  $\text{m}^2/\text{g}$ ; these are interpreted as indicating the areas of rolled-up sheet-like particles one to several unit layers thick. These surface areas are measured by water-vapor adsorption; nitrogen is considered to give unreliable values. The surface of this phase is positively charged in the presence of  $\text{Ca}(\text{OH})_2$ . The surface energy of CSH (gel) has been measured to be 386 ergs per square cm; certain other thermodynamic parameters have been estimated.

### Hydrated Calcium Aluminates and Related Compounds

Introduction To the Types of Compounds That Occur

Hydrated calcium aluminates, while not the primary subjects



of the present work, are of frequent occurrence as products of the reactions between  $\text{Ca}(\text{OH})_2$  and aluminum-bearing clay minerals. Hence they are briefly reviewed here.

The literature of these phases is voluminous. No attempt is made to review the earlier work, much of which is contradictory in nature; rather the information presented here is mostly taken from recent reports by Jones (1962) and by Taylor (1961).

Calcium aluminate hydrates are relatively well-crystallized as compared with the calcium silicate hydrates; yet these phases are too complex for easy description. Jones (1962), after many years of research in the field, mentioned with regret that he could not even set out a reliable table of x-ray diffraction data for the various phases in the system.

The only phase for which the crystal structure has been determined and that is well-characterized as a stable entity is the cubic phase of composition  $\text{C}_3\text{AH}_6$ , which is structurally related to garnet (Brandenberger, 1936). A sequence of intermediate forms ("hydrogarnets") exist between the  $\text{C}_3\text{AH}_6$  and garnet.

A second set of related compounds is characterized by hexagonal or pseudo-hexagonal platy crystals. These are layer-lattice structures, and unfortunately individual specimens exhibit a high degree of stacking variation which results in differences in crystallographic unit cell size and small differences in the powder pattern from sample to sample. In addition to the stacking variations, slightly different polymorphic forms can be distinguished for some of the compounds. There are





additional difficulties; each compound has several hydration states that are easily obtained within the range of normal laboratory working conditions, and finally, solid solution occurs between at least two of the compounds. The basic compositions in this hexagonal platy group have the compositions  $C_4AH_{13}$ ,  $C_2AH_8$ , and  $CAH_{10}$ . There are several analagous carbonate and sulfate compounds isostructural with some of these.

A third set of phases is patterned after  $C_6AH_{33}$ , a needle-shaped crystal which is formed only under special conditions; this crystallization also has several important compounds incorporating other anions isostructural with it.

#### The Cubic Phase, $C_3AH_6$

This is the thermodynamically stable phase in the system at room temperature (Wells, Clark, and McMurdie, 1943). The strongest x-ray diffraction lines occur at 2.30A, 2.04A, and 5.14A, the latter being the highest spacing observed (Midgley, 1957). The common habit consists of rectangular or octahedral plates, with euهدral dodecahedra sometimes found (Majumder and Roy, 1956). A DTA curve is given by these authors, but up to only 600°C; a strong endotherm is observed at about 325°C, and a second, weaker endotherm follows at about 480°C. Infrared spectra given by these authors do not show a free water band at  $6.2\mu$  ( $1620\text{ cm}^{-1}$ ). The hydroxyl region has a complex series of bands that are not easily interpreted. In addition to the broad adsorption in the entire region beyond  $6\mu$ , there is a distinct band at about  $9.4\mu$  ( $1065\text{ cm}^{-1}$ ).



The Hexagonal Phases  $C_4AH_{13}$ ,  $C_2AH_8$ ,  $CAH_{10}$ ,  
and Related Phases

$C_4AH_{13}$ . This compound and its relatives are not thermodynamically stable at room temperature but form readily, and once formed tend to persist indefinitely. At slightly more elevated temperatures the stable phase  $C_3AH_6$  is more usually encountered.

Roberts (1957) discovered that the composition of the compound as it actually occurred in wet systems is  $C_4AH_{19}$ , and its basal spacing is 10.6Å. On washing with acetone or alcohol, or on moderate drying at room temperature the compound converts to the more well-known  $C_4AH_{13}$  phase. Two closely similar polymorphic forms of this phase occur,  $\alpha$ - $C_4AH_{13}$  having a basal spacing of 8.2Å and  $\beta$ - $C_4AH_{13}$  with a spacing of 7.9Å; most samples contain mixtures of both. Drying over  $CaCl_2$ , according to Roberts, results in further loss of water to form a phase of composition  $C_4AH_{11}$ , with a basal spacing of 7.4Å. According to this author, further drying over  $P_2O_5$  or in air at 120°C reduces the water content to that represented by  $C_4AH_7$ , but leaves the x-ray basal spacing unchanged at 7.4Å. There is some conflict in the literature at this point, since Buttler, Dent Glasser and Taylor (1959) reported that heating to about 110°C collapsed the basal spacing to about 6.5Å, and further heating to 145°C caused additional collapse to a spacing of 5.8Å; on still further heating,  $Ca(OH)_2$  crystallized out as a separate phase, which then dehydroxylated at about 420°C; a compound of composition  $C_4A_3H_3$  recrystallized, and it in turn dehydrated at about 620°C



to finally yield mainly  $C_{12}A_7$ . A DTA pattern published by Kalousek, Davis, and Schmertz (1949) does not appear to reflect all these changes; the main features recorded being a strong endotherm at around  $150^{\circ}\text{C}$  with a shoulder on the high-temperature side continuing to perhaps  $350^{\circ}\text{C}$ ; and two small endotherms at about  $500^{\circ}\text{C}$  and  $850^{\circ}\text{C}$ , respectively. A DTA curve up to about  $450^{\circ}\text{C}$  was given by Midgley and Rosamon (1962); this showed a very small endotherm at  $50^{\circ}\text{C}$ , followed by a double endotherm at about  $100^{\circ}\text{C}$ , then a large endotherm at  $290^{\circ}\text{C}$  well resolved from yet another broad endotherm at about  $300^{\circ}\text{C}$ . An infrared absorption spectrum was given for this phase by Midgley (1962).

As previously mentioned, there are several phases iso-structural with this compound in which some of the OH groups have been replaced by other anions. An important one in cement chemistry is low-sulfate sulfo-aluminate. There are two such phases known in which the anion is carbonate; they are hydrocalumite, a natural mineral with only a small carbonate content, and calcium monocarboaluminate,  $C_3A \cdot CaCO_3 \cdot 11H_2O$ . This compound is of major importance since it is said to form readily from aqueous suspensions exposed to small amounts of  $CO_2$ , such as normally exist in the atmosphere (Taylor, 1961). Its identification is difficult; the x-ray pattern resembles that of  $C_4AH_{13}$ , with a basal spacing of  $7.74\text{\AA}$  (Turriziani and Schippa, 1956). These authors also gave weight-loss and DTA data for the phase. The DTA has endotherms at  $230^{\circ}\text{C}$ ,  $300^{\circ}\text{C}$ , and  $930^{\circ}\text{C}$ ; and at about  $540^{\circ}\text{C}$  there is a feature consisting of a fairly strong exotherm followed immediately by an endotherm that perhaps can be used for identification of this phase.



$C_2AH_8$ . The second important phase in the hexagonal group is  $C_2AH_8$ , which appears to be structurally similar to the previously discussed  $C_4AH_{13}$ , and may possibly be derived from the latter by substitution of  $Al_2O_3$  in every other layer (Jones, 1962). The basal spacing given by Midgley (1957) is 10.7Å. Roberts (1957) has determined its behavior on dehydration. The basal spacing at 10.4-10.7Å is unchanged on washing with acetone or alcohol or drying very moderately at high humidity, but on heating at 100°C or drying over  $P_2O_5$  it loses about 3 molecules of water to yield an approximate composition of  $C_2AH_5$  and a spacing of 8.7Å. Further drying (at 110°C) removes another molecule of water to the stage  $C_2AH_4$  and the corresponding basal spacing is 7.4Å.

The relationships between  $C_4AH_{13}$  and  $C_2AH_8$  are complex. Jones (1962) considered that a limited degree of solid solution readily occurs between the two end-members with a  $CaO:Al_2O_3$  ratio between 2.0 and 2.4, and a water content between 8 and 10. This was not previously understood. Another complication is the lability of the  $C_4AH_{13}$  to repeated washing. Lafuma is quoted by Bessey (1938, p. 193) as having determined that when  $C_4AH_{13}$  initially present with excess lime is extracted repeatedly with water, it decomposes to  $C_2AH_8$ .

$CAH_{10}$ . This phase, with a basal spacing of 14.3Å (Midgley, 1957) occurs primarily at temperatures below room temperature. There is a transition temperature at 22°C at which this phase and  $C_2AH_8$  are unstable with respect to each other, and above which the latter phase is generally found (Jones, 1962).





The Supposed Phase  $C_3AH_{12}$ . In earlier literature a platy hexagonal phase with the composition  $C_3AH_{12}$  was thought to have been found in some preparations, and x-ray data have been attributed to it. The existence of this phase has been discredited by various workers, Jones (1962) stating definitely that it does not exist.

#### Compounds of Needle-like Habit

The "type" phase of this group,  $C_6AH_{33}$ , was prepared by Flint and Wells (1944) by employing a concentrated lime solution in which sugar had been dissolved. The analagous compound ettringite,  $C_3A \cdot 3CaSO_4 \cdot 32H_2O$ , is a naturally occurring mineral and also is formed in the hydration of portland cement containing gypsum. There is an analagous  $CO_2$  compound which has a similar x-ray diagram. (Buttler, cited by Taylor, 1961).

#### Summary

Hydrated calcium aluminates can be classed as cubic, hexagonal or pseudohexagonal platy phases, or needle-shaped phases.

The stable phase at room temperature is a well-defined cubic phase,  $C_3AH_6$ , for which considerable data is available. This phase is the end-member of the so-called hydrogarnet series of solid substitution, the other end-member being garnet.

The hexagonal or pseudohexagonal phases comprise the compound usually known as  $C_4AH_{13}$ , in its various hydration states;  $C_2AH_8$ , in its various hydration states; solid solutions between these; and a low-temperature phase,  $CAH_{10}$ . Approximately isostructural with the  $C_4AH_{13}$  phase is the mineral hydrocalumite,



containing a small content of  $\text{CO}_2$ , and the compound  $\text{C}_3\text{A} \cdot \text{CaCO}_3 \cdot 11\text{H}_2\text{O}$ , mono-calcium carboaluminate, which is said to be readily formed in the laboratory due to atmospheric carbonation. Another related phase is low-sulfate sulfoaluminate.

The needle-like phases of associated interest are built on the structure as  $\text{C}_6\text{AH}_{13}$ , which does not normally occur. These are ettringite ( $\text{C}_3\text{A} \cdot 3\text{CaSO}_4 \cdot 32\text{H}_2\text{O}$ ) and a related carbonate compound  $\text{C}_3\text{A} \cdot 3\text{CaCO}_3$ , aq.

The complexity of this system is readily apparent, and unfortunately fully reliable characterization data are not available for most of the phases.

#### Reaction Products of $\text{Ca}(\text{OH})_2$ with Clay Minerals

The chemical stabilization of plastic soils for use as improved and water-resistant bearing material under highways has been practiced for many years. One of the stabilizing agents often employed is  $\text{Ca}(\text{OH})_2$ , henceforth referred to simply as "lime". Herrin and Mitchell (1961) presented a thorough review of the technical literature relating to the practice of lime stabilization. However, knowledge of the chemical reactions taking place has not been forthcoming until recently.

Goldberg and Klein (1952) made a pioneer attempt to study the reaction between lime and montmorillonite-containing soil under room-temperature conditions. The maximum amount of lime they incorporated was only 8% by weight of the soil, and only two weeks were allowed for the reaction to occur. On examination by x-ray diffraction and DTA it was disclosed that all of the lime had reacted, but the only product that was detected was calcium carbonate.



The first work of significance in the study of the lime-clay reactions was that of Eades and Grim (1960). These authors suggested that the reactions occur in three steps: exchange of calcium ions for those originally held by the clay; formation of new minerals; and finally carbonation of the excess lime. In their studies they used prolonged curing for up to two months at  $60^{\circ}\text{C}$ , and up to 20% of lime by weight of the clay. Their results for the several clay minerals are discussed separately.

In the work of Eades and Grim, kaolinite was observed to undergo a loss of sharpness of the prism (hk0) reflections initially, and only later was there a significant alteration in the intensity of the basal peaks. The authors interpreted this as indicating an attack from the edges of the particle. New peaks appeared at 5.1A, 3.04A, 2.8A, and 1.8A. The authors suggested that the three lower peaks refer to a calcium silicate hydrate, but apparently did not appreciate the significance of the 5.1A peak, which is almost certainly due to the formation of cubic  $\text{C}_3\text{AH}_6$  at this elevated temperature.

For illites, the diffraction data observed indicated only scant formation of new crystalline phases. For montmorillonites there was an observed weakening of the peaks for the clay mineral, but the product formed seemed to be amorphous.

DTA revealed the presence of a new peak with treated kaolinite, having a strong endotherm at  $380^{\circ}\text{C}$ . A weak endotherm also occurred at  $760^{\circ}\text{C}$ , and after long curing the lime endotherm at about  $500^{\circ}\text{C}$ . had completely disappeared. DTA of montmorillonite cured for only a short time revealed a double endotherm at



110°-180°C, characteristic for  $\text{Ca}^{++}$ -saturated montmorillonite. After longer curing the entire pattern changed significantly, the major feature being a broad endothermic hump between 100° and 200°C, a sharper endotherm at 680°C, and a strong broad exotherm at about 940°C. These features were not explained.

Hilt and Davidson (1960) showed that small amounts of lime added to soils containing various clay minerals markedly increased the Atterberg plastic limit of the soil but did not result in increased strength under a standard 28-day curing regime. This was ascribed to "fixation" of the lime on the clay surfaces, and concomitant flocculation. Lime added in amounts in excess of this "fixation capacity" was shown to increase strengths of cured products remarkably, and the increase was ascribed to formation of new phases that were not studied in detail.

Later Hilt and Davidson (1961) and Hilt (1961) presented further data on the results of lime reaction with soil containing montmorillonite. They isolated crystals of a well-crystallized hexagonal reaction product and studied them by single-crystal x-ray diffraction procedures. The phase present in these large single crystals appeared to be isostructural with  $\text{C}_4\text{AH}_{13}$ , but had a basal spacing of 7.59Å. The authors spent much effort determining the dimensions of the unit cell, but as indicated by Buttler, Dent Glasser and Taylor (1959) stacking variations are so common in this system that the crystallographic unit cell has little significance and may vary from one specimen to another. However, the important point observed was that the chemical analysis





of crystals (admittedly incompletely separated from the clay) revealed a silica content of 29 per cent. Since the silica content of pure montmorillonite is only about 64% (Ross and Hendricks, 1945), one would have to suppose that either the material analyzed was about half montmorillonite, or else the phase had a very high substitution of silica for alumina. Since the reported alumina content was only 5% (by Weiss ring oven technique), the latter conclusion seems inescapable.

Hilt and Davidson also presented diffractometer charts of reacting mixtures of the lime-soil montmorillonite, cured for 30 days at 21°C and 95% relative humidity. Various moisture contents were used. The phase analyzed by single crystal methods appears in all their charts representing initial moisture contents of 50% or higher, and is accompanied by two peaks, one at 7.4Å and the other at 8.1Å. The authors interpreted the 8.1Å peak as due to an (002) reflection for montmorillonite, but this cannot be correct since no definite (001) spacing is observed. It is observed from the charts that with increasing moisture content of the mixture the peak at 7.4Å decreases and that at 8.1Å increases. It is proposed here that the two peaks represent the two appropriate hydration stages of the  $C_4AH_{13}$  phase discussed by Roberts (1957), viz, the 8.1Å peak being that for the  $\alpha$ - $C_4AH_{13}$ , the 7.4Å peak being the less hydrated state represented by  $C_4AH_{11}$ .

In addition to the peaks discussed and other ascribable to these phases, a small broad peak occurs in all samples at 3.04Å, which was ascribed by the authors to  $CaCO_3$  formed by carbonation



of  $\text{Ca}(\text{OH})_2$ . In the experience of the present writer, carbonation, when it occurs, invariably results in sharp, intense spacings at about 3.03Å; it is felt that the small peak referred to probably represents the formation of some poorly crystallizing CSH (gel) product. Thus the results of Hilt and Davidson are here reinterpreted as indicating the formation of  $\text{C}_4\text{AH}_{13}$  (or a silica-bearing compound isostructural with it);  $\text{C}_4\text{AH}_{11}$ ; and CSH (gel).

Eades, Nichols, and Grim (1962) analyzed samples taken from three field lime stabilization sites, the soils in question having diverse clay mineral suites. In all cases thin section studies have shown the presence of an iron-oxide-stained cementing material surrounding the soil grains and penetrating voids and fractures in the soil minerals. The outlines of individual quartz grains and other particles have become frosted and indistinct, which is indicative of strong chemical attack. It was determined that about half of the 5%  $\text{Ca}(\text{OH})_2$  added had been converted to  $\text{CaCO}_3$ , but the remainder had reacted with the soil minerals. X-ray studies showed new crystalline phases appeared in addition to calcium carbonate, and that the calcium hydroxide had all reacted. It was suggested by these authors that the new minerals are calcium silicate hydrates; the possibility of aluminum compounds was apparently overlooked. No detailed analysis of the x-ray tracings was presented.

A recent paper by Glenn and Handy (1963) gave detailed x-ray and DTA results of a laboratory experiment in which clay minerals were reacted with lime and cured at 21°C for two years. Several types of lime were used, including dolomitic and semi-dolomitic



forms. Kaolinite samples yielded a 7.6A product with  $\text{Ca}(\text{OH})_2$ . A vermiculite-hydrobiotite clay did not react much, but gave rise to compounds having spacings at 8.1 and 4.6A. Muscovite reacted with  $\text{Ca}(\text{OH})_2$  to yield a 7.6A product; but it did not react with dolomitic lime. Quartz did not react. Montmorillonite reaction yielded a complex series of spacings; many of which were thought to be characteristic of 10A tobermorite; other constituents presumed to be present are  $\alpha$  and  $\beta$ - $\text{C}_4\text{AH}_{13}$ , and the compound giving a 7.6A spacing found by Hilt and Davidson. Single crystal work on what was thought to be the 10A product indicated that a micaceous contaminant was giving rise to the 10A peak. Examination of the published x-ray diffraction trace suggests to the present writer that the calcium silicate hydrate phase, if present, is probably a variant of CSH (gel); it is not well crystallized. In fact there is no peak in the 2.80-2.82A region and the strong relatively sharp line at 3.05 appears to be largely  $\text{CaCO}_3$ .

Benton (1959) studied so-called "pozzolanic" reactions between calcined clays (and other phases) and  $\text{Ca}(\text{OH})_2$ . While not directly applicable to reactions of uncalcined clays, his results are of some interest here. Reactions were carried out at  $38^\circ\text{C}$  for up to 6 months. The main product appeared to be a hydrous calcium silicate identified by a single broad line at 3.05A. With uncalcined gibbsite as the "pozzolan" the main product was  $\text{C}_3\text{AH}_6$  (cubic phase). With calcined kaolinite hydrogarnet intermediate between  $\text{C}_4\text{AH}_{13}$  and garnet was obtained. All the mixtures containing aluminum yielded as one product a phase whose x-ray



peaks were very similar to  $C_4AH_{13}$ , but whose basal spacing was 7.6Å instead of the accepted 7.9Å, 8.1Å, or the dehydrated spacing of 7.4Å. This phase contained some carbonate, perhaps partially derived from a 5%  $CaCO_3$  impurity in the lime used. All the specimens had endothermic reactions near 200°C; characteristic for the carbonated compound. The overall interpretation was that this component was a solid-solution compound intermediate between  $C_4AH_{13}$  and calcium monocarboaluminate, despite the fact that it was noted by the author that Carlson (1958) had failed to find any evidence for the existence of such intermediate phases. With calcined kaolinite only, Benton found an additional reaction product which he interpreted by x-ray diffraction as Stratling's compound,  $C_2ASH_x$ . The identification in this case seemed rather uncertain when compared to the original pattern of Stratling reproduced in Benton's paper, but Schmitt (1962) later presented a more detailed pattern for 'Stratling's compound' ( $C_2ASH_8$ , called "gehlenite hydrate\*") which perfectly matched the pattern for the compound found by Benton. Also, zurStrassen (1962) has shown that Stratling's compound is essentially iso-structural with  $C_4AH_{13}$ .

Herzog and Mitchell (1962, 1963) studied the reactions occurring on the hydration of cement when mixed with soil (a technique in common use for the stabilization of soil for highway purposes), and concluded that  $Ca(OH)_2$  arising from the hydration of the  $C_2S$  and  $C_3S$  cement minerals in turn reacted with the clay present to yield secondary cementitious products of the same kinds as evolved separately in lime-clay interaction.





In summary, evidence from current studies clearly indicates that  $\text{Ca(OH)}_2$  reacts with at least certain clay minerals at normal or slightly elevated temperatures; that the phases produced bear at least some relation to the known calcium silicate hydrates and calcium aluminate hydrates; but that their detailed composition and structure is imperfectly understood and that even correct identification of the phases is difficult.



## MATERIALS AND PROCEDURES

### Preparation of Calcium Silicate Hydrates

#### Well-Crystallized Tobermorite

Unsubstituted Tobermorite. Preparation of a sample of pure, well-crystallized tobermorite of Ca:Si ratio 0.83, was undertaken according to a method recommended by Kalousek (personal communication). The silica employed was in the form of "special silica" a pure quartz product of the Ottawa Silica Company, having all particles passing 325 mesh. The calcium source was reagent grade  $\text{CaCO}_3$ , calcined at  $1050^\circ\text{C}$  for four hours. Exactly 8 grams of the resulting CaO were weighed out, suspended in 32 ml. of distilled water at  $65^\circ\text{C}$ , and stirred for about three minutes. Considerable heat was evolved as the lime slaked. The newly-formed  $\text{Ca(OH)}_2$  was then transferred to a malted milk machine cup, and approximately 40 ml. of boiled distilled water added. Then exactly 10.3 grams of the quartz (previously weighed out) was added to the suspension and the resulting mix stirred at high speed for 5 minutes by the malted milk stirrer. The material, now of the consistency of heavy cream, was then poured equally into two hydrothermal bombs of a type to be described, which were then sealed and placed in a Fisher "Isotemp" oven preset at  $175^\circ\text{C}$ . The system was allowed to react for 19 hours; then the bombs were removed from the oven, cooled, opened, the



sample removed and immediately bottled without further treatment. A portion of the material was subsequently oven dried at  $110^{\circ}\text{C}$ .

The hydrothermal bombs were stainless steel devices adapted from the containers manufactured for the A.S.T.M. chemical test for potential reactivity of aggregates in concrete (designation : C 289). The rubber gasket supplied with each device was discarded and a bead of molten lead was formed in the annular groove in the lid of the device, to provide a tight seal against the raised rim of the main portion of the container. A clamping device consisting of two  $3/8$ th-inch stainless steel plates bolted together by four  $3/8$ th-inch diameter bolts was fabricated to replace the clamping bar supplied with the equipment, which was inadequate for hydrothermal work. It was found in trials that the lead bead deformed just enough to give a tight seal with relatively moderate tightening of the bolts, and no water was lost on overnight trials at  $200^{\circ}\text{C}$ . The hydrothermal devices so prepared worked perfectly in all of the runs in which they were used.

Substituted Tobermorites. Substituted tobermorites of varying composition were synthesized hydrothermally by essentially the same technique as outlined above. The only modifications involved were that the admixture to be used in each case was weighed out beforehand and thoroughly mixed with the quartz before the addition of the latter to the freshly-slaked lime, and that for each of the substituted products only half the quantities of materials stated above and only a single bomb were used.



## Poorly Crystallized Calcium Silicate Hydrates

### Synthesized at Room Temperature

A number of preparations of this type were undertaken by various procedures as described below.

Samples Prepared by Double Decomposition Methods. Four samples were prepared by double decomposition of sodium silicate and a calcium salt. A 0.5 M. solution of sodium silicate was employed in each case. 100 ml. of this solution were mixed with an appropriate quantity of either 0.5N  $\text{CaCl}_2$  or 0.5N  $\text{Ca}(\text{NO}_3)_2$  to give the compositions listed below. The procedure was to pour proportional quantities of the two solutions carefully into a third container, the contents of which were vigorously stirred. The reaction took place at room temperature, which was  $33^\circ\text{C}$  at the time. The calcium silicate hydrate immediately precipitated in large white flocs. The suspension was then diluted with distilled water, filtered over suction, washed a number of times with water, then with acetone, and then with ether, and then dried at  $110^\circ\text{C}$  overnight. No particular attempt was made to avoid carbonation, except that the relatively small amounts of sample prepared were dried rapidly in the preheated oven. The individual calculated mole ratios of the reactants employed were as follows:

<u>Source of Calcium</u>	<u>Ca:Si Mole Ratio Employed</u>
$\text{CaCl}_2$	1:1
$\text{Ca}(\text{NO}_3)_2$	1:1
$\text{Ca}(\text{NO}_3)_2$	1.5:1
$\text{Ca}(\text{NO}_3)_2$	2:1





A somewhat more elaborate procedure was later employed for a double decomposition preparation in an effort to insure that the product produced would be as homogeneous as possible. Two 10-ml. Luer-lock syringes were mounted obliquely to each other so that their tips were almost but not quite touching. The arrangement was so designed that on simultaneously depressing the syringes the two very fine streams produced would be intimately mixed on contact and the combined droplets would fall into a flask mounted on a magnetic stirring device just below the intersection of the syringe tips. Separate reservoirs were provided and connected to each syringe so that both could be refilled repeatedly without disturbing the arrangement. A sodium silicate solution was loaded into one reservoir and a calcium nitrate solution into the other. The syringes were evenly and simultaneously depressed so that the rate of emptying of both syringes was the same, the mixed droplets produced being collected in the flask below and constantly stirred. The syringes were then refilled and the procedure repeated until about the desired amount of material (about 200 ml. of each solution) had been reacted. In an effort to obtain a calcium silicate hydrate rich in calcium, the molar concentration of the  $\text{Ca}(\text{NO}_3)_2$  was 3.5 times that of the sodium silicate.

On completion of the reaction the flask was shaken vigorously and the resulting precipitated material filtered on a Buchner funnel. The precipitate was washed repeatedly using saturated  $\text{Ca}(\text{OH})_2$  solution, as recommended by Midgley and Chopra (1960), then was washed exhaustively with a water-acetone mixture, then



with acetone, and finally with ether. The material was dried under vacuum at  $110^{\circ}\text{C}$ , powdered, and bottled.

Samples Prepared by Direct Synthesis. For these products a concentrated silica sol known by the trade name of "NalcoAg10-22" (National Aluminate Co.). was reacted with appropriate weighed amounts of reagent grade solid  $\text{Ca}(\text{OH})_2$ . The resulting suspensions were diluted with distilled water, placed in polyethylene bottles, and the bottles rotated on a roller mill for 2 days, then allowed to stand undisturbed for three weeks. A single sample was prepared in this manner, using a calculated Ca:Si ratio of 1:1. After aging, the sample was filtered on a Buchner funnel. The cloudy filtrate initially observed was recycled several times until the solution passing through was clear. The pH of the filtrate was only 10.6, suggesting that essentially all of the  $\text{Ca}(\text{OH})_2$  had reacted; consequently, the material was washed once and then sealed in a polyethylene bottle.

A second sample was prepared in the same manner, except that the molar Ca:Si ratio of the reactants was 2:1 instead of 1:1. The initial filtrate was again cloudy, and was recycled several times until a clear filtrate was produced. The pH of this filtrate was 12.5, suggesting that unreacted  $\text{Ca}(\text{OH})_2$  was present in the sample; this was confirmed by x-ray diffraction. The product was washed with water until the pH of the filtrate dropped below 12.3. X-ray examination of the material at this point disclosed the absence of crystalline  $\text{Ca}(\text{OH})_2$ , and the sample was then bottled and stored without further treatment. Portions of both samples were later oven-dried prior to various analytical determinations.



## Attempted Synthesis of CSH(II) by

### Direct Reaction in Hot Glycerol

A synthesis of pure, relatively well-crystallized CSH(II) by reaction of CaO with dehydrated silica in hot glycerol suspension followed by precipitation of the hydrate on transfer to a water system has been reported by Toropov, Borisenko, and Shirapova (1953); but according to Taylor (1961) this synthesis has never been repeated. Several attempts were made early in the course of this research to produce this product using slight modifications of the procedure of Toropov, et al., but were unsuccessful. Finally it was decided to attempt to duplicate the reported synthesis by following the stated procedures of these authors as strictly as possible.

Reagent-grade  $\text{CaCO}_3$  was calcined for 1 hour at  $1000^\circ\text{C}$ , and a chromatography-grade silica gel (shown to be amorphous by x-ray diffraction) was dehydrated at  $500^\circ\text{C}$  for six hours. Reagent grade glycerol was dried at  $160^\circ\text{C}$ . Appropriate amounts of the CaO and the dried silica to give a Ca:Si mole ratio of 2:1 (2.604 g CaO and 1.396 g  $\text{SiO}_2$ ) were rapidly weighed out, mixed dry on weighing paper, and then ground in a mortar and pestle after the addition of several drops of glycerol. The grinding (or rather "working", since the material was so stiff that little particle size commutation could have been occurring) was carried out for one-half hour. The material was then transferred to a 250 ml. Erlenmeyer flask, about 35 ml. of hot dried glycerol was added, and the flask was placed on a hot plate and stirred. Toropov et al. reported that their mixture began to froth at  $180\text{--}185^\circ\text{C}$ , and



that frothing continued for 3-3½ hours at this temperature, at the conclusion of which the liquid became clear. No such action occurred with our material. After a considerable waiting period at 185°C, the temperature was allowed to rise to approximately 200°C, and kept there for a further period, but no evidence of frothing was forthcoming and the suspension remained turbid. Finally the attempted synthesis was abandoned.

#### Hydration Products of Individual Cement Minerals

Cement Minerals. Through the courtesy of Dr. D. L. Kantro and Dr. L. E. Copeland of the Portland Cement Association, several samples of pure, well-characterized cement minerals were made available for this study. These included a sample of  $\beta$ -C<sub>2</sub>S, two samples of C<sub>3</sub>S, and a sample of "alite". Alite is a purposely impure C<sub>3</sub>S product with aluminum and magnesium substituted in the lattice of the mineral; such a phase more closely simulates the actual constitution of the C<sub>3</sub>S phase found in portland cement. Chemical analysis of these materials were kindly supplied by the Portland Cement Association laboratories, and are given in the Appendix. An additional sample of alite of a somewhat different type was made available through the courtesy of Mr. Alexander Klein of the University of California, along with Mr. Klein's analysis of the material, which is also given in the Appendix.

X-ray diffraction examination of the several phases verified their identities and no crystalline impurities were detected.

"Paste" Hydration. Hydration of the single sample of  $\beta$ -C<sub>2</sub>S and of one of the samples of C<sub>3</sub>S in paste form was carried out





using a water-cement ratio of 0.7. The samples were simply mixed with an appropriate amount of previously boiled, distilled water (which had been cooled to  $10^{\circ}\text{C}$ ), stirred until homogeneous, poured into a plastic container, sealed, and allowed to hydrate in a constant temperature room at  $23^{\circ}\text{C}$ . Approximately 3 ml. of additional water were added to the top of the "set"  $\text{C}_2\text{S}$  sample after approximately nine hours. The samples were hydrated for a period of seven months before examination of the products was undertaken.

"Bottle" Hydration. Bottle-hydration procedures employed in this study are patterned after those in use at the Portland Cement Association laboratories (see for example Brunauer, Kantro, and Copeland, 1958). A suitable motor and mounting were obtained such that a 22" diameter wooden wheel could be rotated continuously at a constant speed. The sample to be hydrated was mixed with nine times its own weight of water, transferred to a polyethylene bottle, sealed with tape and then paraffin, and mounted on the wheel, which was then rotated at 30 r.p.m. in a room kept at  $23^{\circ}\text{C}$ .

In the initial trial, samples of the two  $\text{C}_3\text{S}$  materials and the  $\beta\text{-C}_2\text{S}$  were hydrated for a period of six months. Previous results reported by Brunauer, Kantro, and Copeland (1958) suggest that hydration of  $\text{C}_3\text{S}$  on a wheel of this type is essentially complete in about six weeks; whereas  $\text{C}_2\text{S}$  is only about 70% hydrated after  $5\frac{1}{2}$  months. Presumably, one would expect approximately similar results for the specimens prepared here. In a second trial the two samples of  $\text{C}_3\text{S}$  were again hydrated along with the two "alite" samples. Length of hydration for the second run was approximately 4 months.



Reaction Products of  $\text{Ca}(\text{OH})_2$  with Clay Minerals  
and Related Silicate

"Dry" Compacted Mixtures at  $60^\circ\text{C}$

Starting Materials. The  $\text{Ca}(\text{OH})_2$  used was freshly-opened Mallinckrodt AR grade. Four silicates were employed, as follows:

- a) Kaolinite in the form of "Hydrite - 10" grade supplied by the Georgia Kaolin Co. No crystalline impurities were determined to be present. The average particle diameter of this material is  $0.5\mu$  and 97% is said to be less than  $2\mu$  in size.
- b) Montmorillonite in the form of the well-known "Volclay" brand Wyoming bentonite supplied by the American Colloid Co. The material was used as supplied, and passed at least the 270 mesh sieve. Impurities are small contents of quartz, feldspar, and probably some amorphous glass shards.
- c) Quartz in the form of #29C Ground Silica supplied by the Ottawa Silica Co. The material is essentially pure quartz, and all of it passes the 270 mesh sieve. Essentially all of the small content of clay-sized particles in the sample used here was removed by centrifugation to be used in another experiment.
- d) Pyrophyllite from Hemp, Moore Co., North Carolina, supplied by Ward's Natural Science Establishment. This material was received in massive form, ground carefully in small portions with frequent removal of



undersized material until all of the sample passed a  $\frac{1}{2}$  mm. sieve, and then dispersed for 40 minutes in a malted milk stirrer in a suspension containing 2% sodium hexametaphosphate (Calgon). The material passing 2 microns was removed by centrifugation and saved for another experiment. The remainder was dried and lightly ground as required to pass through a 270 mesh sieve. Impurities observed in the x-ray diffraction pattern included a small content of quartz and some mica.

Experimental Procedure. 25 g of the air-dried mineral were mixed in the dry state with 10 g of  $\text{Ca(OH)}_2$ . The mixture was then placed in a porcelain dish and 20 ml. of previously boiled distilled water were added. Water and solids were mixed thoroughly and then the mixture was compacted with hand pressure into a rigid plastic container. A plastic disc of diameter just sufficient to permit being forced inside the container was then inserted and forced into position just above the compacted mass and in close contact with it. Sufficient water was then added over the plastic seal to fill the container (about 10 ml) and the top of the plastic container was then put on and carefully sealed with plastic electrical tape. It was felt that these precautions would be sufficient to prevent carbonation and little or no evidence of carbonation was observed in the reaction products.

The compacted mineral-lime-water mixes varied somewhat in consistency at the time of initiation of the experiment. It was judged that the kaolinite sample was approximately at the



consistency characterized by the Atterburg plastic limit; the montmorillonite sample at somewhat below its plastic limit, the pyrophyllite in a consistency that would characterize a plastic sample at the liquid limit and the quartz mixture was in a state difficult to characterize in these terms but extremely dilatent, i.e. free water would appear if the sample were squeezed, otherwise it appeared comparatively dry.

The sealed samples were then placed in a steam cabinet at a temperature of about  $60^{\circ}\text{C}$ , for a period of 55 days.

#### Slurry Mixtures at $45^{\circ}\text{C}$

Starting Materials. A series of 7 relatively pure, well-characterized minerals were selected for this experiment as follows:

- a) Kaolinite: Sample No. H-5 from the American Petroleum Institute Project 49 reference collection, all samples of which were supplied through Ward's Natural Science Establishment.
- b) Illite: Beavers Bend, Oklahoma. Reference sample was supplied by the Oklahoma Geological Survey and characterized by Mankin and Dodd (1963).
- c) Montmorillonite: Otay, California, Sample No. H-24 of the American Petroleum Institute Collection.
- d) Mica: "Delamica", a finely divided mica separated from Cornish china clay and supplied by English Clays Lovering Pochin and Co., Ltd. This material has been characterized by White (1956, p. 135).





- e) Quartz: the less than 2 micron size fraction of the Ottawa silica previously described.
- f) Pyrophyllite: the less than 2 micron fraction of the Hemp, North Carolina, pyrophyllite previously described.
- g) Talc: U.S.P. material supplied by the Purdue University Pharmacy. Origin unknown.

The  $\text{Ca}(\text{OH})_2$  used in this experiment was the same as that previously mentioned.

All samples except the quartz and pyrophyllite were dispersed in a malted milk stirrer using a small concentration of "Calgon" (sodium hexametaphosphate) as a dispersing agent. Fractions less than two microns equivalent spherical diameter were separated by standard centrifugation methods. Each of the separated clay-size fractions was then characterized as to purity by x-ray diffraction using oriented aggregate mounts prepared from suspensions dried on glass slides. Impurities noted were as follows: Kaolinite - none; illite - some chlorite; montmorillonite - none; mica - trace of kaolinite; quartz - none, however it should be noted that the intensity of the quartz lines was unexpectedly weak; pyrophyllite - some mica and kaolinite; talc - none.

All samples were calcium-saturated according to the following procedure: a large excess of  $\text{CaCl}_2$  was added to the suspensions, resulting in immediate flocculation in all cases. The suspensions were allowed to stand overnight, then centrifuged and the supernatant solution decanted. Each sample was then treated



with an excess of 1N  $\text{CaCl}_2$  solution, stirred vigorously, allowed to stand for approximately one-half hour, centrifuged, and the supernatant liquid was again discarded. This procedure was followed three additional times to insure complete calcium saturation. The samples were then repeatedly dispersed with distilled water, centrifuged at high speed (15,000 rpm) and the supernatant suspension decanted and discarded. This procedure was repeated until the supernatant suspension was free of chloride ions, as indicated by the silver nitrate test. This required six to eight repeated treatments, depending on the sample.

The resulting  $\text{Ca}^{++}$  saturated clays were dried at  $110^\circ\text{C}$  and gently powdered; x-ray diffraction powder mounts were prepared and the patterns again checked for any impurities that were not evident on the oriented aggregate patterns previously obtained. The only additional contaminants observed were traces of quartz in the pyrophyllite, a trace of talc in the quartz, and a trace of kaolinite in the talc. In the powder mount the quartz appeared to give its normally strong x-ray pattern with no sign of disorder or weakness of peaks; and the illite was noteworthy for its  $2\text{M}_1$ -type pattern.

Experimental Procedure. A one-gram portion of each of the calcium-saturated clay-size minerals was mixed with 4 grams of  $\text{Ca}(\text{OH})_2$  and transferred to a 50 ml. polyethylene centrifuge tube. A sufficient volume of freshly boiled, distilled water was added to completely fill the tube (about 45 ml.). The tubes were then sealed with tight-fitting polystyrene closures, and



then taped securely with plastic electrical tape. After hand shaking, the samples were mounted in a specially prepared rack on a reciprocating shaking device; the device was designed in such a way that the tubes were positioned horizontally with the direction of motion along the axis of the tubes. The entire assemblage was placed inside a thermostated air bath regulated to maintain a temperature of  $45^{\circ}\text{C} \pm 1^{\circ}\text{C}$ . The shaking device was connected to a time control unit programmed to stop the shaking for a period of  $1\frac{1}{2}$  hours every eight hours, to help avoid the possibility of overheating the shaking device motor. It was determined in trial runs that no significant temperature variations occurred during either the active part of the cycle or the rest period. The samples were allowed to react under these conditions for a period of 60 days.

#### Dilute Suspension at $23^{\circ}\text{C}$

A single sample consisting of a portion of the calcium saturated, less than 2 micron-fraction of the kaolinite described above, was reacted with  $\text{Ca}(\text{OH})_2$  at  $23^{\circ}\text{C}$  in a manner analogous to the "bottle" hydration procedure of the cement minerals. Five grams of the clay mineral were mixed with an equal amount of stock  $\text{Ca}(\text{OH})_2$ , suspended in 250 ml. of boiled distilled water, and placed in a polyethylene bottle, which was then sealed and mounted on the rotating wheel apparatus in the same manner as the cement mineral samples discussed previously. The reaction was allowed to proceed for 6 months at  $23^{\circ}\text{C}$ .



Procedures Used in Investigating the Properties  
of the Various Materials

Analysis of Chemical Composition

Calcium was determined by the versenate titration procedure of Chang, Kurtz, and Bray (1952). Silica was determined gravimetrically after carbonate fusion (Washington, 1930). Water was determined by ignition after oven-drying at 110°C. All procedures were carried out at least in duplicate. Analyses of the several preparations are given in the Appendix.

X-ray Diffraction

All x-ray diffraction results in this work were obtained on a General Electric XRD - 5 diffractometer using Cu-K $\alpha$  radiation and a nickel filter. The x-ray tube was operated at 16 ma. and 40 kvp; a 1° beam slit and an 0.2° detector slit were employed. The goniometer speed was 2° per minute, the chart speed 30 inches per hour, the time constant 4 seconds and the linear mode of intensity display was employed throughout.

Sample preparation was of several different types. For certain purposes, notably examination of the clay minerals as previously discussed, oriented aggregate specimens were prepared by the common expedient of air-drying suspensions of the samples on glass microscope slides. However this type of specimen preparation was not employed extensively with the calcium silicate hydrates because of the obvious danger of carbonation.

The sample preparation considered standard for this investigation was a randomly-oriented powder mount technique adapted





from that of McCreery (1949). The procedure is as follows: a 1/8" thick aluminum frame with a 5/8" diameter circular hole is covered with a piece of mimeograph paper cut to the outline of the frame; this is in turn covered with a glass slide which is taped in place and the mount is then inverted. The dry, powdered sample (usually ground to pass the 200 mesh sieve) is then sifted into the exposed well through a screen. The powder mass is then compacted lightly with the thin edge of a spatula and trimmed. A slight excess of powder is then added to the surface, and a second glass slide is applied with a slight compactive effort. The second slide is then taped to the aluminum frame, the sample again inverted and the original slide and mimeograph paper are carefully removed with the aid of a razor blade, leaving the plane face of randomly-oriented compacted powder for exposure to the x-ray beam. Somewhat greater compactive effort is required for use with the General Electric diffractometer than with certain other instruments since the mount is positioned vertically on the x-ray instrument; the powdered must be compacted tightly enough to avoid spilling.

A third expedient used occasionally in this study was a modification of the powder mount technique described above, used in situations where it was desired to determine the x-ray lines of a slurry or very wet sample without drying it. The aluminum frame was backed with about 8 thicknesses of filter paper (instead of a single thickness of mimeograph paper), covered with a glass slide and taped, as before. Then the slurry is transferred to the sample well. Water from the wet sample is rapidly absorbed



by the filter paper and as the slurry is de-watered and its volume shrinks, additional slurry is added. Finally after several minutes the sample becomes moderately rigid. The surface is lightly smoothed with a spatula and the wet sample immediately x-rayed. If the procedure is properly done, a reasonably satisfactory geometry can be maintained by the surface of the sample for the period required to run through the angular range of interest, generally about 30 minutes. In all cases in which this procedure was used, supplementary "standard" powder diffraction mounts were always subsequently made of dried material.

In some of the x-ray diffraction work the samples were examined in a dry-nitrogen atmosphere, to avoid possible carbonation of the surface by atmospheric  $\text{CO}_2$  during the diffraction run.

Early in the study a number of trials of adaptations of the porous tile mount method of Kinter and Diamond (1956) were attempted. However, it rapidly became obvious that any form of sample preparation of poorly-crystalline calcium silicate hydrates involving a wet, thin film of sample is exceedingly prone to carbonation; this difficulty, coupled with extreme difficulty of dispersing the calcium silicate hydrates into any sort of uniform suspension led to early abandonment of the effort, except for special purposes.

#### Differential Thermal Analysis

Most of the DTA results in this study were obtained using a slightly modified Eberbach portable DTA apparatus, which uses



a nickel sample block and chromel-alumel thermocouples. The instrument is discussed briefly by MacKenzie and Mitchell (1957). The instrument is manually recording: an amplitude corresponding to the difference in temperature between the sample and the reference wells is read on a galvanometer at intervals delineated with respect to the temperature of the block, which is displayed on a second meter.

The present instrument was modified by substituting a 1-inch thick sleeve of commercial pipe-insulation (fitted closely over the heating unit) for the partitioned transite insulation assembly supplied with the instrument. For additional insulation a close-fitting transite disc was cemented to the top of the furnace assembly. With these modifications a temperature of  $1000^{\circ}\text{C}$  could readily be attained, and more important, a more reasonable rate of temperature increase in the range  $800\text{--}1000^{\circ}\text{C}$  was provided. The measured rate of increase of temperature is linear (after a short initiation period) at the high rate of  $58^{\circ}\text{C}$  per minute until a temperature of  $600^{\circ}\text{C}$  is attained; thereafter rate of increase falls monotonically to  $5.4^{\circ}\text{C}$  per minute at  $1000^{\circ}\text{C}$ . The latter temperature is reached about 40 minutes from the beginning of the run.

A small number of samples were run on the equipment in use at the Soils Branch of the Bureau of Public Roads, Washington, D.C. This equipment uses a Leeds and Northrup variac controller to maintain a very steady and reproducible rate of temperature increase, which, for the samples discussed here, was set at  $10^{\circ}\text{C}$  per minute. DTA patterns secured in these runs are so designated



and due allowance should be made in comparing such patterns with those secured on the modified portable instrument.

### Infrared Absorption Spectroscopy

Most of the infrared absorption spectra were secured on a Perkin-Elmer Model 421 dual grating instrument which was operated between 2.5 and 16 microns. The conventional specimen preparation technique for inorganic solids involves mixing a very small amount of the sample with potassium bromide powder, and forming a disc or pellet under pressure in an evacuated die. Unfortunately KBr is somewhat hygroscopic and it is very difficult to be absolutely certain whether observed bands relating to hydroxyl and water are due to the sample or due to interaction of the finely divided sample intimately mixed with the KBr. Considerable preliminary experimental work was done in an effort to fine a more suitable technique. Attenuated total reflectance spectroscopy using AgCl plates was tried, but it proved quite difficult to get satisfactory contact between the powdered sample material and the plate. Deposition of a film of sample onto windows made of IR-tran-2 (supplied by the Eastman Kodak Co.) was reasonably satisfactory, except that the IR-tran material has several small absorption bands of its own in the region of interest, and also its transmission falls off rapidly below about 12 microns.

The technique finally adopted for most of the work involved merely the deposition of a thin film of the sample on a polished KBr plate. The plates were dried in an oven prior to sample preparation and left there; a small quantity of the sample, also





oven-dried, was mulled briefly in a small agate mortar with several drops of spectral-grade carbon tetrachloride. Several drops of the resulting suspension were deposited directly on the surface of the plate in the oven. The solvent evaporated within a minute or so, leaving a deposit of sample on the surface of the KBr window. The deposit, while not a smooth homogeneous film, was still sufficiently thin and well-distributed on the plate to provide excellent spectra. The window bearing the mounted film was conveyed directly to the infrared spectrometer from the oven, and the spectrum was run immediately. With a little practice it was relatively easy to gauge the appropriate amount of suspension to use; if the amount actually deposited on the plate proved to be too much or too little the sample could easily be removed from the plate with carbon tetrachloride and another sample immediately prepared.

Since no direct control was exercised over the weight of sample deposited on the plate it would be relatively difficult to adapt this procedure for quantitative analysis, but it does provide a useful technique for the purpose of characterizing the infrared spectra of the various calcium silicate hydrates.

#### Electron Microscopy and Electron Diffraction

The electron microscopic investigation of these materials was performed through special arrangement by Dr. John Radavich, of Micro-Met Laboratories, Inc. The instrument used was an R.C.A. EMU-3, operated at 50 kv. The sample preparation procedure employed by Dr. Radavich is still experimental in nature, although very good results seem to have been obtained. The method does



not employ ultrasonic vibration to assist in dispersion, hence is free from the possibility of the formation of artifacts due to the violent disruption of particles that may occur with ultrasonic treatment. The procedure was as follows:

- 1) A brief mulling of the sample in a mortar with a specially-formulated dispersing grease compound.
- 2) Addition of a solvent for the grease.
- 3) Casting of a drop of the resulting suspension containing the desired particles onto a carbon-coated substrate.
- 4) Brief immersion of the substrate in amyl acetate to remove the grease solution, and then evaporation of the amyl acetate.
- 5) Examination by electron microscopy or selected area electron diffraction.

The method has apparently resulted in very good dispersion of the various samples. Generally the individual particles can be seen spread out evenly across the field, and are not collected into agglomerates. This facilitates recognition of the morphology of the individual particles, and the very large number of particles available for individual examination permits a representative picture of the morphology of the sample to be obtained. However, if the sample consists of particles of widely-varying size, a certain degree of sorting by sedimentation in the solvent suspension may occur, so that the coarsest particles may not be observed unless special effort is made to sample the bottom of the suspension.

The electron micrographs of the tobermorite and substituted



tobermorite samples (Figures 3, 9 and 11) were made at a magnification of 3200X, which was doubled by photographic enlargement; in these figures one micron is approximately a sixteenth of the length or width of the field displayed. For all of the remaining materials the direct magnification used was 4400X, again doubled by photographic enlargement; and a micron in the remaining plates occupies about a twelfth of the length or width of the field.

#### Determination of Surface Area by Water Vapor Adsorption

Samples weighing approximately 0.5 grams after preliminary drying were placed in small weighing bottles and initially dried for four days over  $P_2O_5$  at room temperature. The desiccators used to contain the weighing bottles were continuously evacuated by connection to a laboratory vacuum line, which gave a residual pressure of about 50 mm Hg. The samples were then weighed and placed in vacuum desiccators over concentrated sulfuric acid solutions. The desiccators were evacuated for at least an hour, and then the samples were allowed to equilibrate for at least four days in a constant temperature room held at  $21^{\circ}C (\pm \frac{1}{2}^{\circ})$ . The desiccators were then opened, the samples weighed immediately, and the procedure repeated with acid of lower concentration. The molality of the acid was determined by titrating weighed amounts of acid against standard sodium hydroxide solution.

The partial pressure of water vapor was determined from the molality of the acid solution by reference to unpublished data of D. M. Anderson and P. F. Low, who determined the activity



of water in sulfuric acid solution by graphical integration of the Gibbs-Duhem equation, using mean activity coefficients for sulfuric acid as given by Harned and Hamer (1935).

For some of the samples a number of additional points were secured beyond the usual range of partial pressures employed for surface area estimation, so that a representation of the adsorption isotherm up to partial pressures of 0.8 were secured.

For surface area determination, the adsorption data were plotted according to the well-known "BET" procedure (Brunauer, Emmett, and Teller, 1938), and the slopes and intercepts of the resulting straight lines were determined using the least squares method. The data gave good straight lines in all cases except a few, which are not reported here. The parameters " $V_m$ " and " $c$ " of the BET equation were computed, and the surface area was calculated, using an assigned area per water molecule of  $11.4 \text{ \AA}^2$  (Brunauer and Greenberg, 1962). The estimated heat of adsorption of the first layer of water molecules (" $E_1$ ") was also calculated for each sample.

#### Cation Exchange Capacity

A measurement of the possible cation exchange capacity of the various calcium silicate hydrates was desired, but since most of these compounds tend to dissolve and decompose on repeated leaching with water or aqueous solutions, the methods usually employed for the determination of cation exchange capacity could not be used. After a good deal of experimentation an appropriate method was developed, using potassium as the measuring cation and using absolute ethyl alcohol (specific gravity 0.785)





as the solvent and washing medium. The potassium was added to the sample in the form of a solution of potassium acetate in alcohol, the exchange was allowed to take place in alcohol, and the excess potassium acetate and the cations removed from the samples, presumably Ca, were washed out with alcohol. The potassium was in turn replaced by ammonium or sodium cations (also added as the acetate) and the amount of potassium replaced was determined by flame photometry. The details of the method are given below.

Duplicate small samples (0.5 g or less, depending on the amount of material available) were dried and weighed analytically and transferred into dry 50 ml. polyethylene centrifuge tubes. Twenty-five ml. of a 1N solution of potassium acetate in absolute alcohol were added to each, and the tubes capped with tight-fitting closures and shaken in a mechanical reciprocating shaking device for 30 minutes. They were then set aside overnight (at least 16 hours). At the conclusion of that period the samples were centrifuged (1500 rpm for at least 10 minutes) and the clear supernatant solution was carefully decanted and discarded. A second 25 ml. portion of the solution of potassium acetate in alcohol was then added, the samples again shaken for 30 minutes by machine, and the centrifuging and decantation again repeated. Two additional treatments with the potassium acetate solution were performed in the same manner, a total of four such treatments in all. Following the last decantation, 35 ml. of absolute alcohol were added and the samples shaken for ten minutes, centrifuged and the clear supernatant containing excess potassium acetate



decanted and discarded. This alcohol washing procedure was repeated four additional times. After the fifth wash, 25 ml. of a 1N ammonium acetate solution (in absolute alcohol) were added to the sample. They were then shaken for 30 minutes using the mechanical shaker, then set aside for at least four hours. The samples were then again shaken for ten minutes, then centrifuged. The supernatant liquid from each sample was decanted into a 100 ml. volumetric flask. Another 25 ml. portion of the ammonium acetate solution was added, the samples shaken for 30 minutes and again centrifuged, the supernatant solution being added to that previously obtained for each sample. This was repeated one additional time; then the volumetric flasks were made up to volume with distilled water.

A twenty ml. aliquot of the resulting solution was pipetted into a second 100 ml. volumetric flask (a fivefold dilution). Five ml. of a 5000 ppm  $\text{LiNO}_3$  solution were then added as an internal standard, and the contents of the flask made up to volume with distilled water. The potassium content was then determined with a Perkin-Elmer model 52C flame photometer, using the conventional internal standard procedure. The standard solutions for the determinations were prepared using 0 to 10 ppm of potassium derived from a standard potassium acid phthalate solution by appropriate dilution. The standards were prepared so as to have the same concentration of the same alcoholic solution of ammonium acetate as that present in the diluted samples, to compensate for effects of both the alcohol and the salt on the flame. The amount of potassium determined and the initial weight



of the original sample were used to calculate the cation exchange capacity in milliequivalents per 100 grams.

There were two difficulties found with this procedure. First, it became apparent after several trials that potassium was being adsorbed onto the walls of the polyethylene container. This was retained by the container against washing with alcohol, but was released to the solution on treatment with the ammonium salt, and thus measured along with the potassium exchanged by the sample. An appropriate blank correction was determined experimentally and used throughout. Its magnitude was small but not negligible compared to the amount of potassium exchanged from most of the samples.

A second difficulty occurred only with the relatively poorly crystallized calcium silicate hydrates prepared at room temperature, or those containing free calcium hydroxide. For these samples, gelation occurred after the addition of the sodium acetate solution to the washed, potassium-saturated specimens. Although the gel could be partially broken up mechanically, it was felt that it would interfere with complete removal of the exchangeable potassium from the sample. For samples subject to this effect, a nearly saturated solution of sodium acetate in absolute alcohol (about 0.2N) was substituted for the ammonium acetate solution. No gel was formed with the sodium salt, and thus the difficulty was satisfactorily resolved. A separate set of flame photometer standards incorporating the sodium acetate solution was used in the determination of potassium for samples in which this substitution was used.



It is recognized that in this method, as in any cation exchange capacity method, there is an essential element of arbitrariness in that the time allowed for the exchange reactions to occur is limited. Some substances such as vermiculite and various zeolites have very slow rates of exchange and for systems of this type only a portion of the ultimate capacity of the exchange reaction is usually measured by conventional techniques. The present system may well have additional "slow" exchange capacity beyond that measured here, but the time available did not permit this to be investigated.

#### Determination of Zeta Potential and Sign of Surface Charge

Zeta potential determinations were carried out by the micro-electrophoresis method using a flat cell of rectangular cross-section such as recommended by Abramson, Moyer, and Gorin (1942, p. 44). The apparatus employed was the standard Mudd-type equipment, as supplied by the Arthur H. Thomas Company.

The electrophoretic velocity of the particles of the sample was determined by direct microscopic observation of particles streaming at the level corresponding to 21% of the total height of the cell, in accord with the theory of Smoluchowski (1921) as described by Abramson, Moyer, and Gorin (1942, p. 50). The particular cell used had a depth of  $6.55 \times 10^{-2}$  cm and a width of 1.23 cm. The electrodes consisted of plaster of paris plugs which were immersed in a saturated solution of zinc sulfate. The circuit employed is shown in Figure 2. A reversing switch was





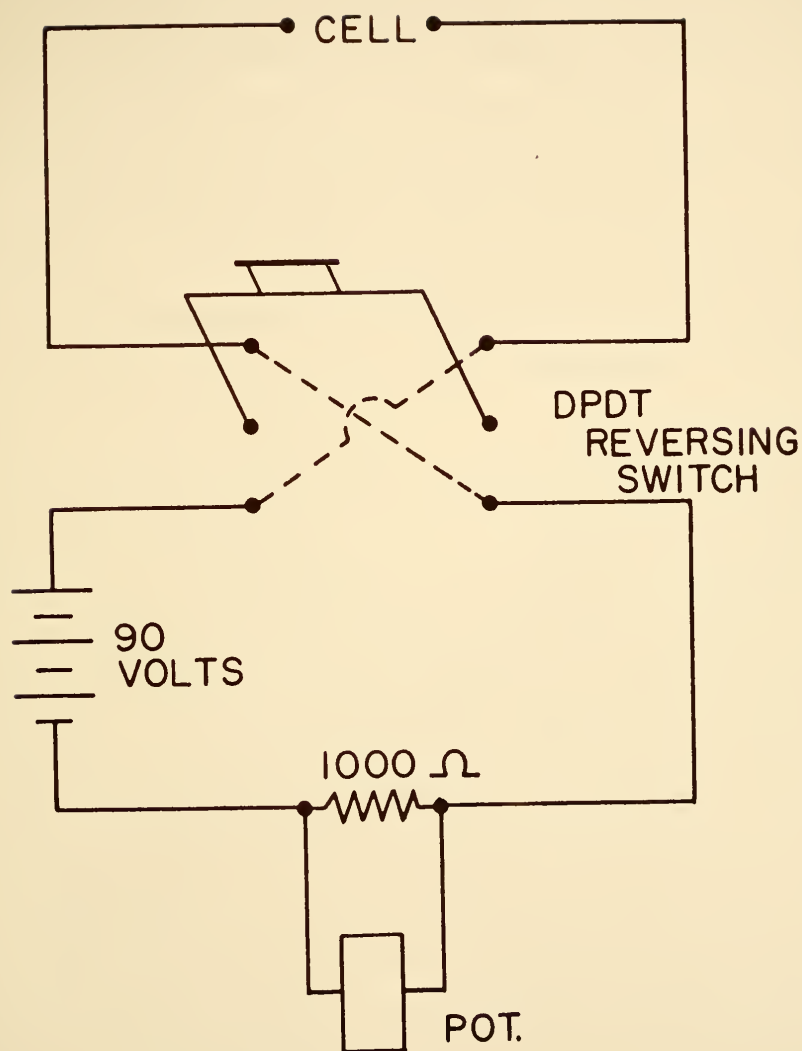


Figure 2. Circuit Diagram for Microelectrophoresis Apparatus.



used to change the direction of the current flow at will without the necessity of switching the connections to the potentiometer.

Very dilute suspensions were employed, the concentration of the sample being less than 0.01% in all cases. The concentrations and kind of salt used were varied and will be discussed later in connection with the individual results.

The sign of the surface charge on the particles was readily noted by determining whether the particles travel to the anode or to the cathode under the influence of the applied electric current.

Determination of the zeta potential requires the measurement of the particle velocity at a known field strength or potential gradient. After the microscope was focused at the correct height above the bottom of the cell, the current was turned on and the velocity of the particles was calculated by timing the movement of individual particles observed with reference to a grid of known size incorporated in the eyepiece of the microscope. Particles were measured moving in both directions and the transit times of six to eight particles in each direction were averaged to give the estimate of velocity used. The particles were observed only with considerable difficulty, and no great accuracy can be claimed for the measurements of their velocity, although the results obtained seemed to be reasonably reproducible.

The field strength existing at the time of each measurement was calculated from the relation  $H = I/KA$ , where  $H$  is the desired field strength,  $I$  is the amount of current flowing in the circuit at the time of the measurement,  $K$  is the conductivity



of the suspension, and  $A$  is the cross-sectional area of the cell, in this case  $0.0805 \text{ cm}^2$  (Abramson, Moyer, and Gorin, 1942, p. 47). The current was determined from the potential measured across a standard resistance box in series with the cell as shown in the circuit diagram, the resistance used being generally 500 or 1000 ohms. The potentiometer used for this purpose was a Leeds and Northrup portable precision Potentiometer, Type 8662. The conductivity of each suspension was determined in a separate conductivity apparatus at the same time as the measurements of particle velocity were made. The conductivity apparatus consisted of a Leeds and Northrup Model 4911 conductivity cell in a Wheatstone bridge circuit employing Leeds and Northrup instruments as follows: a Kohlrausch slide wire (Model 4528), an AC-DC resistance box (Model 4756), an AC Null detector (Model 9844), and a 1000-cycle oscillator (Model 9856).

The zeta potential was calculated from the well-known equation:

$$\zeta = \frac{4\pi\eta v}{DE}$$

where  $\zeta$  is the zeta potential,  $\eta$  is the viscosity of the suspension,  $v$  is the velocity of the particles,  $D$  is the dielectric constant of the suspension, and  $E$  is the field strength. The viscosity and dielectric constant of the various suspensions were assumed to be those of water at the same temperature ( $22^\circ\text{C}$ ).



## EXPERIMENTAL RESULTS

### Well-Crystallized Tobermorites Prepared by Hydrothermal Synthesis

#### Unsubstituted Tobermorite

Preparation. Details of the preparation of this material have been given in the previous section.

Composition. The mole ratio of reagents employed in the preparation of this material was 0.83 Ca:Si. The previous results of Kalousek (1957) revealed that a negligible amount of free silica remained in a similarly-prepared product made with Ca:Si ratio 0.80; it was considered that the slightly increased Ca content would result in complete conversion of all of the silica present. The various characterization methods employed revealed no indication of any incompletely reacted starting materials or of any impurities. No chemical analysis was performed, but the loss on ignition was determined to be 13%. If it is assumed that all of the initial material reacted and all of the ignition loss is due to water, the calculated molecular composition for the compound is then  $\text{Ca}_{0.83}\text{Si}_{1.00}\text{H}_{0.78}$ .

X-ray Diffraction. The x-ray diffraction pattern for this preparation is given in Figure 3. Virtually exact agreement is observed between this pattern and the corresponding diffractometer trace of Kalousek and Roy (1957, Fig. 2). Agreement with the





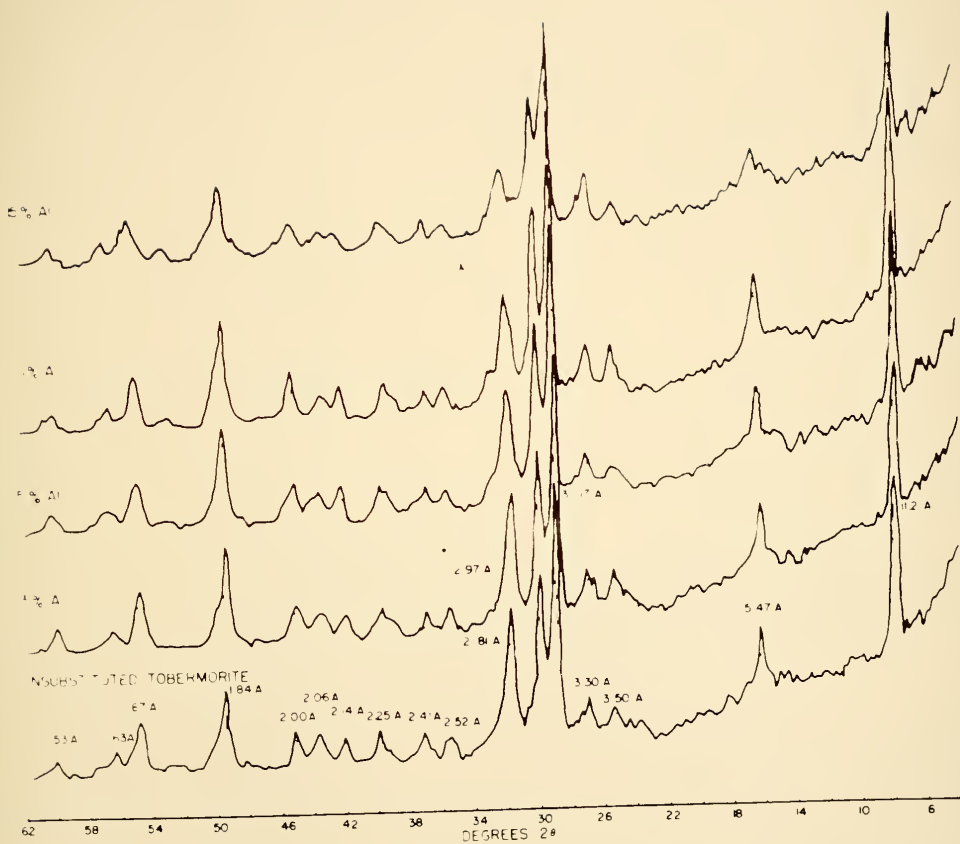


Figure 3. X-ray Diffractometer Traces of Unsubstituted Tobermorite and of 3, 5, 10 and 15% Substituted Al-Tobermorites.



powder pattern for tobermorite listed by Heller and Taylor (1956) is also excellent. The observed basal spacing is 11.2A.

Morphology. The appearance of the unsubstituted tobermorite under the electron microscope is shown in Figure 4. The material occurs in thin plates with only a slight tendency toward elongation. This morphology is essentially identical to that found by previous investigators for synthetic tobermorite. An electron diffraction pattern from a typical field is also given in Figure 4. The electron diffraction pattern is consistent with the x-ray diffraction results given above.

Differential Thermal Analysis. The DTA diagram for this pattern secured on the Eberbach portable DTA unit is given in Figure 5. A distinct endothermic reaction is observed at 275°C due to dehydration and partial collapse of the structure to a 9.5A phase; a barely noticeable exothermic reaction takes place at about 820°C. Similar features were displayed in a corresponding pattern by Kalousek (1957, Fig. 5a).

It was observed that the unsubstituted tobermorite did not undergo any particular shrinkage in the sample well as the result of thermal transformations. After the conclusion of the run the sample material was removed and x-rayed. As expected, the pattern observed was that for wollastonite, and no other phases were observed.

Infrared Absorption. The infrared spectrum obtained for unsubstituted tobermorite is given in Figure 6. A 5X scale expansion was used, and the resulting resolution and definitiveness of the pattern is noticeably better than those so far published in the literature.



(A)



(B)

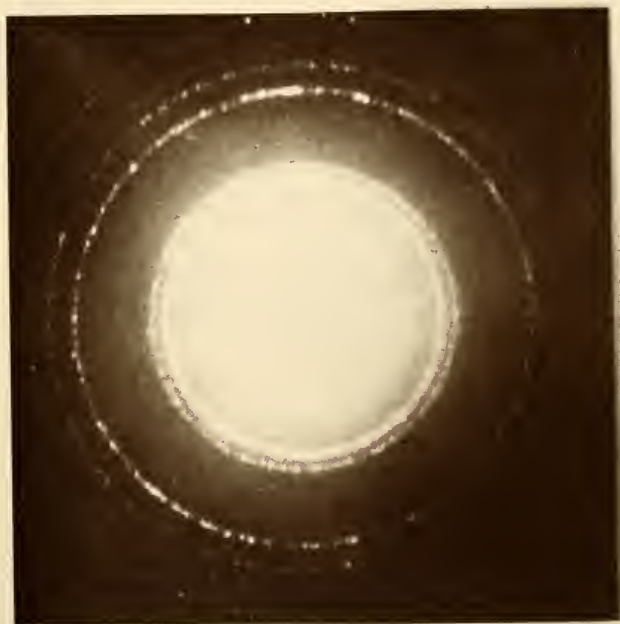


Figure 4. Electron Micrograph and Electron Diffraction Pattern for Unsubstituted Tobermorite.



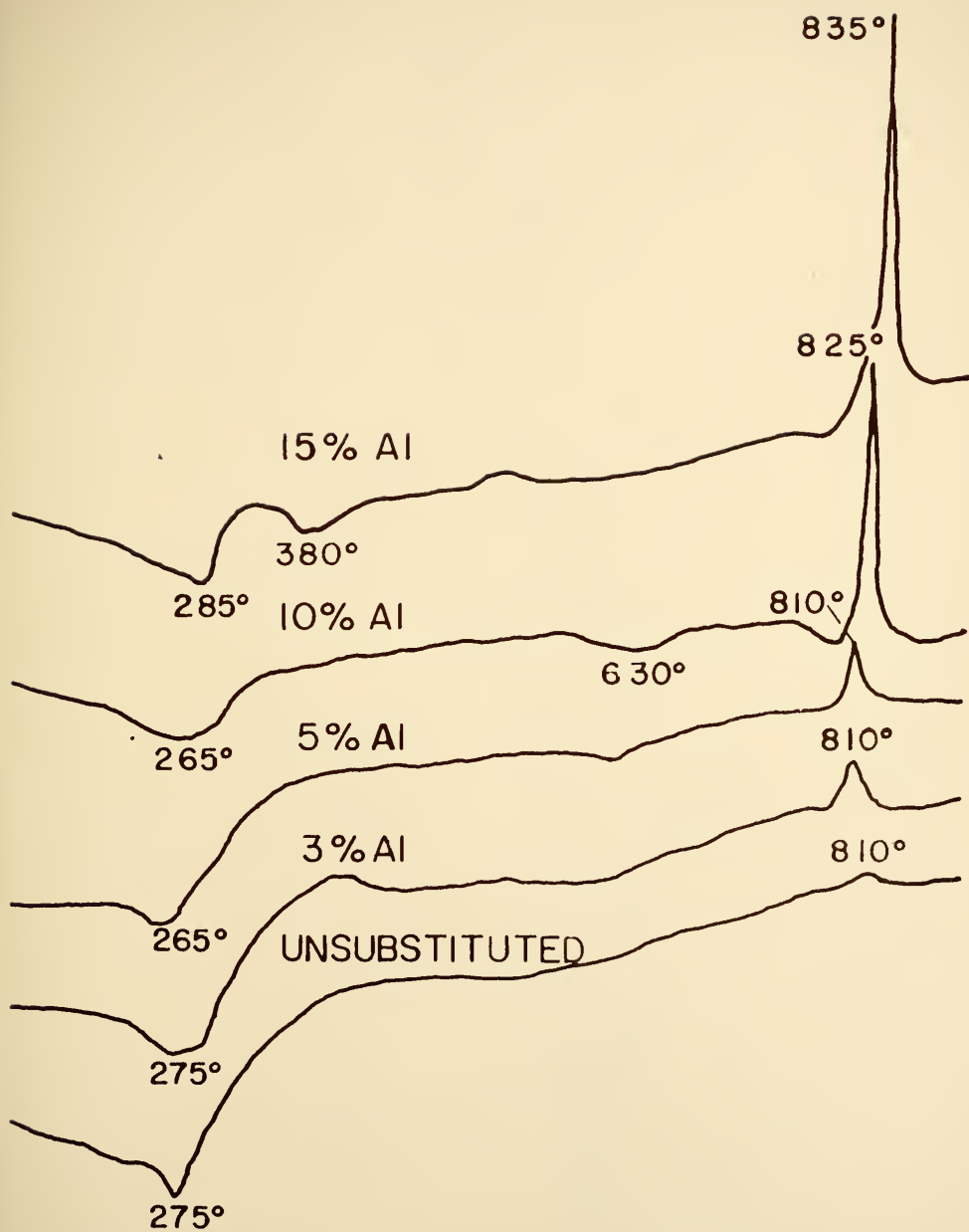


Figure 5. DTA Results for Tobermorite and 3, 5, 10 and 15% Substituted Al-Tobermorites. Heating Rate Varies From 58°C to 5°C Per Minute.





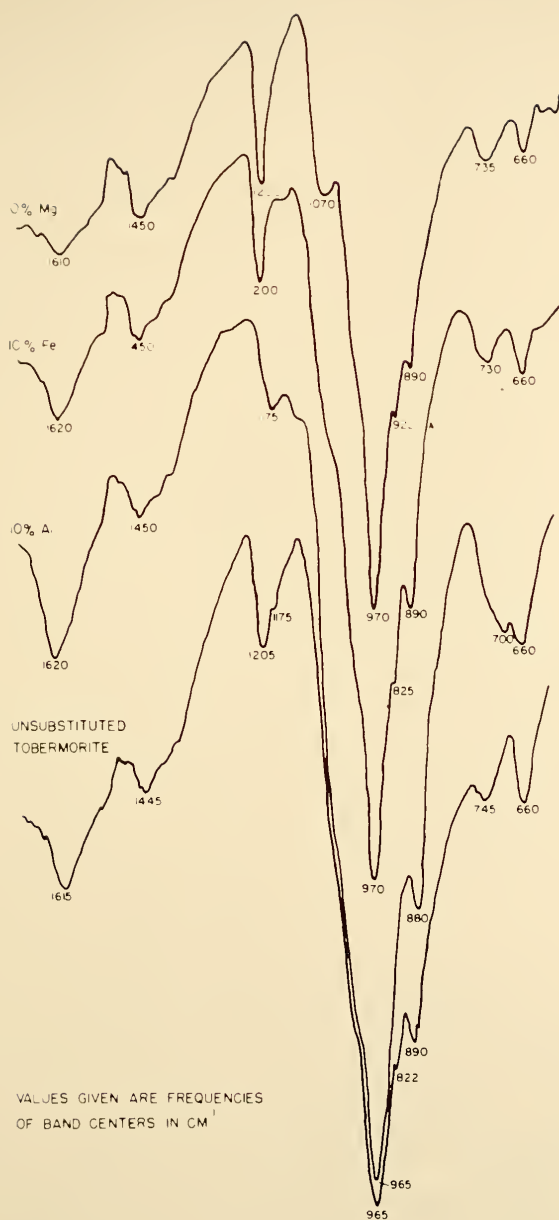


Figure 6. Portions of Infrared Absorption Spectra of Tobermorite and of 10% Substituted Al-, Fe- and Mg-Tobermorites.



The major feature observed is a strong, comparatively sharp band centered at  $970\text{ cm}^{-1}$  ( $10.3\text{ }\mu$ ), attributable to Si-O lattice stretching vibrations. A small subsidiary maximum on the shoulder of this band is noted at  $890\text{ cm}^{-1}$  ( $11.25\text{ }\mu$ ), probably due to a trace of  $\text{CaCO}_3$  produced by carbonation. A very small but reproducible absorption feature occurs at  $922\text{ cm}^{-1}$  ( $10.85\text{ }\mu$ ). The water deformation vibration is observed at about  $1620\text{ cm}^{-1}$  ( $6.18\text{ }\mu$ ). However, the only feature observable in the hydroxyl region is a very broad, weak band between  $3400$  and  $3000\text{ cm}^{-1}$  (about  $2.95$  to  $3.35\text{ }\mu$ ); apparently bonded OH groups of various strengths of bonding are present in the sample. Another feature noted is a fairly weak but broad band centered at about  $1440\text{ cm}^{-1}$  ( $6.95\text{ }\mu$ ); presumably this is the band attributed to carbonate and discussed at some length in the literature review. Other features not previously encountered are visible in the low-frequency end of the spectrum. These include a relatively sharp band at about  $1200\text{ cm}^{-1}$  ( $8.35\text{ }\mu$ ), with a shoulder at about  $1170\text{ cm}^{-1}$  ( $8.55\text{ }\mu$ ); and a pair of bands at  $740$  and  $660\text{ cm}^{-1}$  ( $13.5\text{ }\mu$  and  $15.1\text{ }\mu$ ) respectively.

The interpretation of the infrared spectra of complex silicates of this type is not far advanced and no explanation can be offered for most of these observed features. Several of them appear to change somewhat with isomorphous replacement in the lattice, and these shifts will be discussed later.

The amplitude of the adsorption in the OH stretching region is unexpectedly small, being only about 10% of that of the main Si-O band. Published spectra of synthetic tobermorite by



Kalousek and Roy (1957) and of Loch Eynort natural tobermorite by Hunt (1962) show OH stretching bands that appear to have intensities in the range of 50-75% of that of the Si-O band. Both these workers used the KBr pellet technique in which the sample was mixed with KBr powder and subsequently formed into a transparent window under pressure. One wonders whether these workers were completely successful in eliminating adsorbed water from the KBr powder, despite their efforts to do so.

It was suggested to the writer by W. F. Bradley that lack of more definite OH stretching vibrations might possibly be due to orientation of the OH groups in a direction perpendicular to the plate; in dioctahedral micas such an orientation prevents activation of OH stretching vibrations unless the plate is oriented at an angle to the direction of the beam other than  $90^\circ$  (Serratosa and Bradley, 1958). However, experiments in which the plate was oriented at  $30^\circ$  and at  $60^\circ$  to the incident beam produced no significant change in the spectrum in this region except a slight decrease in intensity, thus eliminating this possibility.

Water Vapor Adsorption and Surface Area. The surface area of this preparation was measured in duplicate using water vapor adsorption at  $21^\circ\text{C}$ . Adsorption data plotted according to the standard BET equation gave a good straight line fit; however, the partial pressures limits of the region of fit were lower than those commonly observed, being at least as low as 0.03 at the lower limit and about 0.22 at the upper limit. The slope and intercept of the line were evaluated by least squares,



and using an area of 11.4Å per H<sub>2</sub>O molecule, the surface area was determined to be 78 m<sup>2</sup>/g. The precision between duplicates was reasonably good, the individual estimates being 76.0 and 80.6 m<sup>2</sup>/g. The heat of adsorption of the homogeneous part of the first layer ("E<sub>1</sub>") was quite high, 13,640 cal/mole. It should be noted that this heat of adsorption value includes the heat of condensation of liquid water which at the temperature employed is 10,550 cal/mole.

The isotherm itself was essentially a type II according to Brunauer's classification (Brunauer, 1943, p. 150). Certain features observed on this and similar isotherms for substituted tobermorites are worthy of further note and are discussed in the section on substituted tobermorites.

Cation Exchange Capacity. The cation exchange capacity of this phase, as determined by the procedure described in the section on methods, was 34 milli-equivalents per 100 grams. This is about the range normally reported for the clay mineral illite (Grim, 1953, p. 129). Possible causes of this observed capacity are discussed later.

Zeta Potential and Sign of Surface Charge. Attempts were made to measure the zeta potential of this tobermorite in a very dilute suspension (0.005%) in distilled water. The pH of the resulting suspension was approximately 9.0; the particles were observed to be negatively charged (i.e. moving toward the anode) at a velocity consistent with a moderately high zeta potential. However measurements of the field strength in such a system were practically impossible to duplicate because of the erratic





nature of the current flow across the cell, and no value of zeta potential can be reported.

A similar suspension was prepared in  $10^{-3}$  M NaCl solution (pH 8.0) and this appeared to give reliable results. The zeta potential determined for this system was -33 mv., a reasonable figure.

Stein (1960) reported that the electrophoretic velocity of tobermorite in strongly basic systems decreased continuously as the  $\text{Ca}^{++}$  concentration increased, and the particles became positive at a  $\text{Ca}^{++}$  concentration higher than  $4 \times 10^{-3}$  M. To confirm this effect, portions of the present sample were suspended in two  $\text{Ca}(\text{OH})_2$  solutions: a) a tenfold dilution of saturated  $\text{Ca}(\text{OH})_2$  in distilled water (approximately  $2 \times 10^{-3}$  M., pH 11.0), and b) the undiluted saturated solution (approximately  $2 \times 10^{-2}$  M., pH 12.4). Suspension in the diluted solution reduced the negative zeta potential of the tobermorite particles to 11.6 mv.; in the saturated  $\text{Ca}(\text{OH})_2$  the zeta potential could not be accurately determined owing to flocculation but it was apparent that the particles were moving toward the cathode, i.e. had become positively charged. Thus the results of Stein are confirmed with this tobermorite.

The effect of calcium in lowering and eventually reversing the negative charge of tobermorite particles is not restricted to strongly basic suspensions. Tobermorite suspended in a  $10^{-3}$  M  $\text{CaCl}_2$  solution (pH 8.6) had a measured zeta potential of only -16 mv., compared to the -33 mv. found in the NaCl solution of the same concentration of cations. Furthermore, the phenomenon



is not restricted to calcium ions; the same tobermorite suspended in a  $10^{-3}$  M solution of  $\text{AlCl}_3$  was examined, and although the zeta potential was not measured, the particles were seen to be strongly positive.

These observations suggest that the phenomenon involved is the well-known ability of certain inherently negatively-charged surfaces to irreversibly adsorb certain kinds of polyvalent cations from solution and thus lower their negative charge; if the solution is sufficiently concentrated, a large enough number of cations may be adsorbed to reverse the sign of the surface charge and make it strongly positive. Such phenomena have been reported for glass (Rutgers and deSmet, 1945), for montmorillonite (Hemwall and Low, 1956) and for many other kinds of material.

Plasticity of the Tobermorite-Water System. It is apparent that tobermorite resembles the clay minerals in many of its properties, including platy shape, high surface area, cation exchange capacity and negative charge (at least in the absence of high concentrations of polyvalent cations). One of the outstanding characteristics of clays is their ability to form plastic systems when wetted with appropriate amounts of water. An attempt was made to see if tobermorite has analagous properties.

A portion of the undried hydrothermally-prepared material was removed from the bottle and worked between the fingers for some minutes. The initially gritty texture of the mass was gradually replaced by a smooth plastic "feel" akin to that used by soil surveyors and field geologists as an indication of the presence of clay. It was found that a fine "wire" of tobermorite



could be formed easily and the mechanical behavior of the tobermorite-water system seemed to be completely analagous to that expected of a wet, plastic clay.

In an attempt to quantify this observation the standard Atterberg limit tests (ASTM designations: D-423 and D-424) were performed. The material appeared to behave in a reasonably satisfactory manner in both tests and the observed liquid and plastic limits were 375% and 270%, respectively. The high water holding capacity of the material in the plastic state is noteworthy.

Effect of Glycerol on Basal Spacing. A characteristic property of expanding lattice clay minerals is their ability to imbibe polyalcohols, notably glycerol and ethylene glycol, between the individual unit layers of the clay structure. This normally results in an increased basal spacing for the substance, and is the basis for the common methods of identification of montmorillonite and halloysite (see for example Grim, 1953, p. 271).

To see if similar behavior could be demonstrated for tobermorite, glycerol was added to a portion of the undried material, mullied well, and the preparation x-rayed immediately and again several days later. The basal spacing remained at 11.2Å in both cases, suggesting that polyalcohols are not intercalated between the unit layers.



## The Effect of Lattice Substitution on the Properties of Tobermorite

Introduction and Notation. As previously discussed, Kalousek (1957) prepared a set of well-crystallized tobermorites incorporating various amounts of aluminum (from kaolinite) into the tobermorite lattice; he characterized the resulting products by x-ray diffraction and DTA. The present phase of this study had three objectives: to reproduce the work of Kalousek and further characterize the phases produced; to determine if aluminum could be introduced into the tobermorite lattice from other sources; and to explore the possible substitution of other atoms, notably iron and magnesium into the tobermorite lattice.

In discussing substitution of one element for another in a crystal lattice it is desirable to have a pertinent measure for the amount of substitution attempted or achieved. Kalousek expressed the percentage of aluminum in tobermorite in terms of percent of  $\text{Al}_2\text{O}_3$  based on the ignited weight of the sample. He presented considerable evidence to show that the substitution occurred as replacement of silicon atoms in tetrahedral coordination (in the silica chains). In the light of this result, in the present work the convention is adopted of expressing the amount of aluminum added as the mole fraction (expressed in percent) of the silica that is presumed to be replaced by alumina. The common convention with calcium silicate hydrates is to write the chemical composition in terms of mole fractions of other constituents relative to silica, as for example,  $\text{C}_{0.83}\text{S}_{1.00}\text{H}_{1.00}$ . One can readily express the composition of a substituted phase





in a similar manner. For example, consider a tobermorite of an ideal Ca:Si ratio of 0.83 and water stoichiometrically equivalent to the amount of silica, which then has a 3% replacement of Al for Si. Its formula would be written  $C_{0.83} [S_{0.97}Al_{0.03}] H_{1.00}$ .

The equivalent of 1%  $Al_2O_3$  based on the ignited weight of the sample, as used in Kalousek's paper, is almost 2% substitution of Si by Al in the present notation.

Preparation of Substituted Tobermorites. A set of aluminum-substituted tobermorites having their aluminum derived from additions of kaolinite (Georgia Kaolin Co. "Hydrite 10" grade) were synthesized hydrothermally in accordance with the methods previously described. Kaolinite was added to the mix in amounts calculated to supply aluminum to substitute for 3, 5, 10 and 15% of the silica in tobermorite. The quartz used in the starting mix was reduced by the calculated amount of  $SiO_2$  introduced in the kaolinite.

Two samples of tobermorite were prepared having aluminum substitution derived from gibbsite (Mallinckrodt U.S.P. grade  $Al(OH)_3$ ) instead of from kaolinite, the percentages of replacement being calculated as 10 and 15%, respectively.

The results for these samples, discussed in detail below, were at first interpreted as indicating that essentially complete incorporation of the aluminum was obtained in both sets and that the phases present after synthesis consisted only of tobermorite; except that materials having 15% substitution of Al for Si were thought to contain a small content of hydrogarnet. These results would be in accord with the conclusions of Kalousek (1957) on



similar preparations. However, electron microscopy and electron diffraction results, which are discussed subsequently, suggest that one of the alumina-bearing samples contains in addition to the tobermorite a fraction of material that is identifiable as CSH(I) and some of the aluminum added may possibly be found in this second phase.

Substitution of other atoms into the tobermorite lattice was also attempted. Samples were prepared incorporating iron in the form of hematite in amounts calculated to yield 5% and 10% replacement of Si by Fe. However, x-ray diffraction of the resulting products suggested that not all the iron had entered the tobermorite lattice, but that some residual hematite remained. This was also attested to by the red color of the hydrothermal products. On firing to wollastonite (a phase whose x-ray lines do not seriously overlap the main lines of hematite), this conclusion was confirmed. A set of standards were prepared by mixing hematite with a wollastonite produced by firing pure unsubstituted tobermorite. Detailed comparison of the peak height of the main hematite peak for the fired substituted tobermorites with those for the standards suggested that only a very slight degree of lattice substitution had been accomplished, and that most of the added hematite remained as such.

A second trial was made, using goethite instead of hematite as the iron-bearing phase; this procedure appeared to be more successful. Goethite added in an amount calculated to replace 10% of the silica in the resulting tobermorite produced a product that was almost white; a faint tan tinge could be seen on



careful examination. X-ray diffraction of the product showed no trace of goethite (main peak at 4.16A completely absent), nor was there any indication for hematite. However, on firing, the sample turned a faint pink, and examination of the material formed disclosed a pattern for wollastonite with a small but definite peak for hematite. Comparison of the size of the peak with those of the standards previously prepared suggested that about 8% of the desired 10% replacement had been accomplished, free hematite equivalent to about 2% replacement being observed.

The incorporation of magnesium into the tobermorite lattice was also attempted, the magnesium being supplied as periclase (reagent grade  $\text{MgO}$ ). The amount added was calculated as that sufficient to effect a 10% replacement of Si by Mg. The product was white in color and gave a tobermorite x-ray pattern with no evidence of residual periclase. A small peak occurred at 2.35A that might be due to brucite ( $\text{Mg}(\text{OH})_2$ ). The fired product gave a wollastonite x-ray diagram with no evidence of  $\text{MgO}$ . However, a small endothermic reaction was observed at about  $435^\circ\text{C}$  on DTA, and this is attributed to a small content of Mg that did not enter the tobermorite lattice but was converted to brucite instead. A series of standards was prepared from mixtures of brucite and unsubstituted tobermorite and DTA patterns were run. A comparison of the intensities of the  $435^\circ\text{C}$  endothermic peaks suggested that the equivalent of about 7% of the silica had been replaced by Mg, an amount equivalent to about 3% being found as brucite.

It should be stated at this point that the assignment of



substitution of iron and magnesium as replacing the silica of tobermorite is at present only "conventional"; there is no definite proof at hand that these elements actually substitute in the silica chains although it is thought that this is probable.

Thus, the evidence summarized here indicates that not only aluminum but also iron (when added as goethite) and magnesium (when added as periclase) can be incorporated into the lattice of hydrothermally-synthesized tobermorite. The effect of these substitutions on some of the characteristics of the tobermorite phase are discussed.

X-Ray Diffraction Characteristics of Substituted Tobermorites. X-ray diffractometer chart tracings of the series of Al-substituted tobermorites prepared with kaolinite as the source of aluminum are given in Figure 3. All of the materials give almost identical patterns indicative of well-crystallized tobermorite. There are, however, some slight but systematic differences that are worthy of note.

First, there is a slight increase in the basal spacing with aluminum substitution, the shift being from about 11.2Å in the unsubstituted tobermorite to about 11.5Å in the sample having 15% nominal Al-substitution. Such an effect was noted previously by Kalousek (1957).

Kalousek also reported a gradual increase in the intensity of the strong peak at 2.81Å with increasing content of aluminum in his aluminum-substituted tobermorites. For the present samples, the relative intensities of this line (as a percentage of the





intensity of the strongest line at 3.07A in each case) decreases approximately linearly with aluminum content, being 55%, 52%, 44%, 39%, and 33% for samples containing zero, 3, 5, 10, and 15% nominal aluminum substitution, respectively. Thus this observation of Kalousek's is confirmed with the present materials.

It is pertinent to note here that the x-ray diffractometer traces of the two Al-substituted tobermorites prepared with gibbsite as the aluminum source are almost completely identical to those of the corresponding samples prepared with kaolinite, with the exception noted below.

Kalousek reported the appearance of a hydrogarnet phase ( $C_3ASH_4$ ) in his compositions prepared with more than 5.7%  $Al_2O_3$ ; this corresponds in the present notation to products having nominal substitution greater than 11%. Thus one would expect to find evidence of the hydrogarnet phase in the nominally 15% substituted sample. The strongest line for the hydrogarnet is at 2.76A; Kalousek used this line as the criterion for the presence of the phase, but since it overlaps the strong tobermorite line at 2.81A, he used the 5.07A line of the hydrogarnet to estimate the amount present. Inspection of the present pattern for the 15% phase shows no line at 5.7A, but there is a definite shift downward in the position of the 2.81A tobermorite line for this phase, the actual peak being 2.79A. Also, the general sharpness of the tobermorite pattern for this phase is somewhat reduced. Thus the presence of a small amount of perhaps poorly-crystallized hydrogarnet in this nominally 15% Al-substituted phase is a possibility. Examination of the corresponding product prepared



using gibbsite rather than kaolinite reveals a definite, though small, peak at 5.07Å, confirming the formation of the hydrogarnet. It is not known whether the apparent difference in the amount or crystallinity of the hydrogarnet is accidental, or if the kaolinite restricts the formation of the hydrogarnet phase.

Having explored the effects of substitution of increasing amounts of Al on the tobermorite x-ray pattern, we turn our attention next to a comparison of the differing effects produced by nominally the same amount of substitution of the elements, aluminum, iron, and magnesium. Figure 7 gives the x-ray diffractometer traces of the unsubstituted tobermorite again, for reference, and those of three samples each containing a nominal 10% of its silica replaced by aluminum, iron, and magnesium, derived from gibbsite, goethite, and periclase, respectively.

Perhaps the major difference observed is the change in relative intensities of some of the strongest peaks. These differences are difficult to see in the figure, but Table 1 presents the intensities of the four main peaks as scaled from the charts, along with those of the sample with 10% Al-substitution from kaolinite. It is clear from the table that Al-substitution has only a very moderate effect on the intensities of these peaks, but the effect of Fe and Mg substitution is qualitatively different. For both the latter, the basal intensities of the (002) and the (222) peaks are approximately halved, while the strong peaks due to reflecting planes entirely within the unit layer, viz the (220) and the (400), are essentially unchanged in intensity. It appears that the substitution of



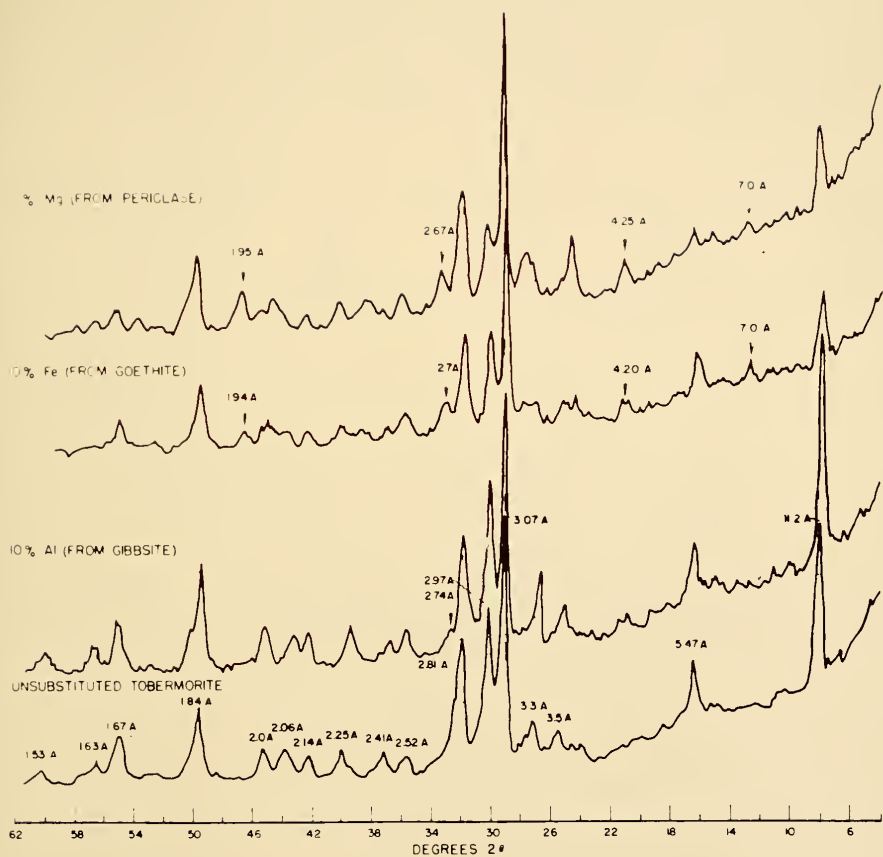


Figure 7. X-ray Diffractometer Traces of Tobermorite and of 10% Substituted Al-, Fe-, and Mg-Tobermorites.



Table 1. Intensities\* of Four Strongest X-ray Lines for Tobermorite and 10%-substituted Aluminum- Iron- and Magnesium- Tobermorites

	11A (002)	3.07A (220)	2.97A (222)	2.81A (400)
Tobermorite	61	90	58	49
Al-Tobermorite (from kaolinite)	71	98	64	38
Al-Tobermorite (from gibbsite)	72	91	60	42
Fe-Tobermorite	33	92	32	43
Mg-Tobermorite	30	102	31	44

\* Intensity values are net peak heights, CPS, scaled from chart.





iron and magnesium (both of which have ionic radii substantially larger than aluminum) results in some disorder in the c-axis direction, i.e. perpendicular to the plane of the layers.

Another marked difference between the pattern for unsubstituted tobermorite and those obtained for the substituted phases is the appearance of new peaks marked by arrows on the chart. The new peaks appearing and the kind of substitution for which they are observed are as follows:

1.94 - 1.95A	(Fe, Mg)
2.67 - 2.74A	(Al, Fe, Mg)
4.20 - 4.25A	(Al, Fe, Mg)
7.0A (weak)	(Fe, Mg)

A third difference involved marked intensity increases for lines at 3.35A and 3.60A in the Al and Mg tobermorites, respectively. These are presumably (h0l) lines according to Heller and Taylor (1956, p. 36).

To summarize these results, the observations of Kalousek (1957) with regard to small changes in the x-ray pattern of tobermorite with increasing aluminum substitution have been confirmed in detail. Aluminum substitution does not seriously affect the intensities of the major peaks, but corresponding iron and magnesium substitutions approximately halve the intensities for the (002) and (222) peaks, indicating disorder in the "c" axis direction. Certain new peaks (2.7A, 4.2A) appear with all of the substituents while others (1.95A, 7.0A) appear only with substitution of the larger ions, iron and magnesium. Two other lines previously observed become prominent; one at 3.35A with aluminum substitution and the other at about 3.6A with



aluminum or magnesium substitution.

Differential Thermal Analysis and Thermal Transformations.

According to Kalousek (1957) the major characteristic observed for Al-substituted tobermorite on DTA was a strong, sharp exotherm at about  $860^{\circ}\text{C}$ ; the exact temperature was said to increase slightly with increasing Al content. With very high contents of aluminum added to the charge (and concomitant formation of noticeable amounts of the hydrogarnet phase) the intensity of the reaction was observed to decrease.

DTA diagrams of Al-substituted phases containing 3, 5, 10, and 15% substitution were given in Figure 5. The analyses were made using the Eberbach portable DTA unit and in view of the varying but reproducible heating rate the temperature of the exotherm is not directly comparable to that obtained by Kalousek. It is immediately obvious that within this range of substitution, increasing the amount of aluminum leads to increasing sharpness and intensity of the exothermic effect, and to an increase in the temperature at which this effect occurs. The small exotherm observed at  $380^{\circ}\text{C}$  is apparently due to the small content of hydrogarnet formed in the sample with the highest aluminum content.

The DTA patterns of unsubstituted tobermorite and those of nominally 10% Al, Fe, and Mg-substituted tobermorites are compared in Figure 8. The aluminum-bearing phase shown here is that derived from gibbsite; its DTA is similar to the corresponding pattern in Figure 5, for the corresponding phase with



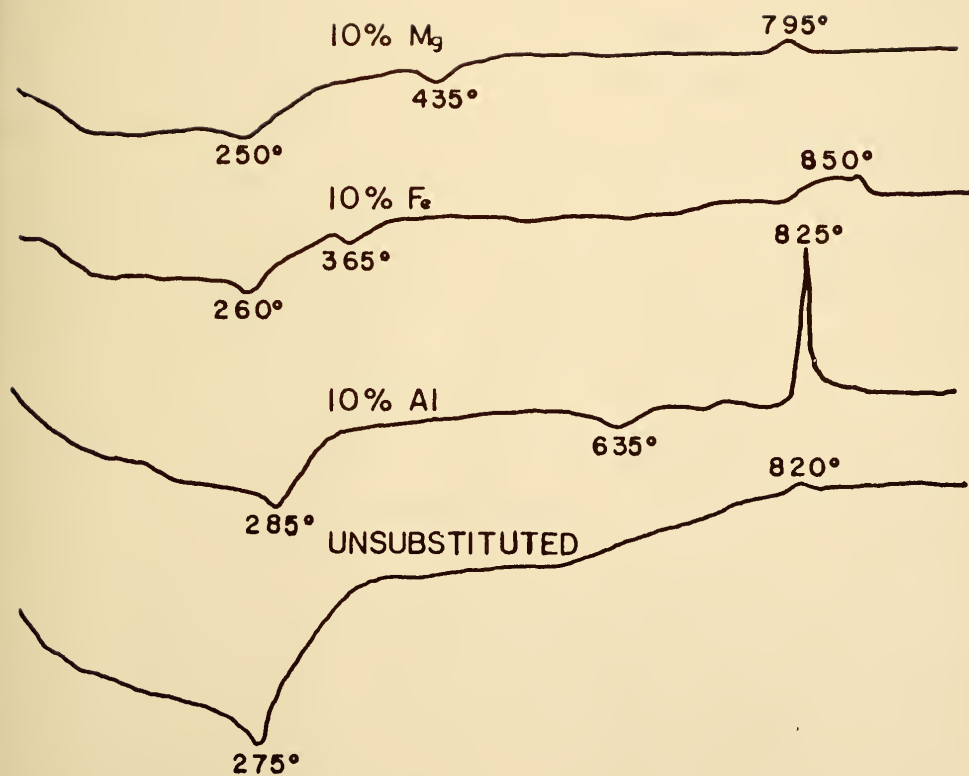


Figure 8. DTA Results for Tobermorite and for 10% Substituted Al-, Fe-, and Mg-Tobermorites.



aluminum derived from kaolinite. The cause of the endotherm at  $635^{\circ}\text{C}$  is not known. The endothermic response at  $475^{\circ}\text{C}$  in the Mg-substituted sample is attributed to a small content of brucite and similarly the slight response at  $365^{\circ}\text{C}$  is due to a trace of unreacted goethite in the Fe-substituted sample.

The most prominent feature of Figure 8 is the absence in Fe- and Mg-substituted tobermorites of the strong exothermic reaction observed for the Al-substituted phases. It was observed that Al-substituted tobermorite undergoes a very remarkable volume shrinkage in the course of the differential thermal analysis, the sample at the conclusion of the run being a very hard white product seemingly fused to the thermocouple bead. Its volume is only about half the initial volume of the packed tobermorite powder. The iron and magnesium-substituted tobermorites do not undergo any such change, nor does the unsubstituted tobermorite. Yet all four materials yield apparently identical x-ray diffraction patterns for wollastonite at the conclusion of the run.

To determine whether the exothermic response of the aluminum-bearing tobermorites is in fact associated with the shrinkage phenomenon, a sample of the aluminum-bearing phase with 10% nominal substitution, derived from kaolinite, was packed into a DTA sample well and a DTA run was started. The run was interrupted at  $25^{\circ}$  intervals to observe whether the shrinkage had yet occurred. No change had occurred at  $750^{\circ}\text{C}$ , but at  $775^{\circ}\text{C}$  partial shrinkage was observed, and by  $800^{\circ}\text{C}$  the shrinkage was complete. The temperature of the exothermic response for





this sample in Figure 5 is  $825^{\circ}\text{C}$ , but its initiation is preceded by a small dip at just below  $800^{\circ}\text{C}$ . Thus the two phenomena appear to be manifestations of the same reaction, the shrinkage apparently just preceding the exothermic response.

According to literature reviewed earlier in this report, tobermorites generally undergo a transition to a 9.5A collapsed, partially dehydrated state at some temperature below  $650^{\circ}\text{C}$ , and the latter transforms to wollastonite at about  $800^{\circ}\text{C}$ . At least one report has been published about a 11A tobermorite which is transformed directly to wollastonite (Gard and Taylor, 1957). To check on whether such differences in the course of thermal rearrangement might possibly explain the differing behavior of the Al-substituted tobermorite from the others, samples of the four tobermorites whose DTA patterns are given in Figure 8 were heated in a muffle furnace at  $350^{\circ}\text{C}$  for one-half hour, cooled, and x-rayed. In all cases the 11A basal spacing had disappeared. Small but distinct peaks at 9.8A and 9.3A appeared for the unsubstituted and the Al-substituted tobermorites, respectively, while less definite peaks at about 9.5A appeared for the other two materials. Further heating at  $650^{\circ}\text{C}$  for 30 minutes had no significant effect on diffraction spacings and intensities. Thus it appears that collapse of all of the materials to the 9.5A state occurs by  $350^{\circ}\text{C}$ , and the results offer no indication of why the Al-substituted tobermorite transforms to wollastonite accompanied by shrinkage and a strong exothermic peak and the others do not.



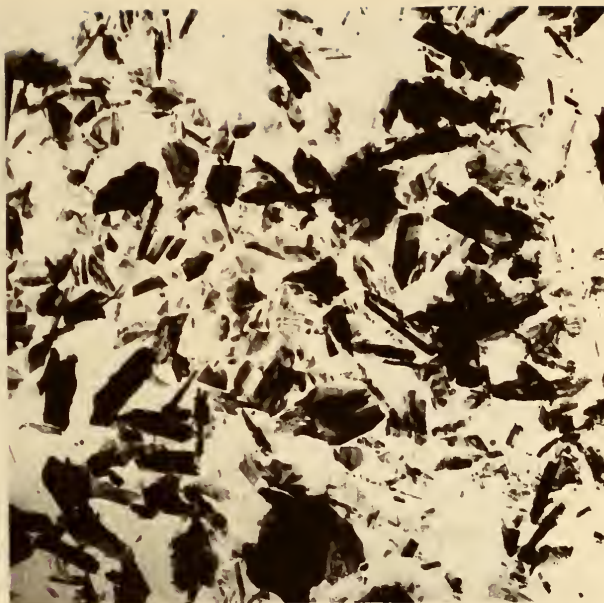
Morphology of Substituted Tobermorites. Samples with 10% nominal substitution of aluminum from kaolinite and of iron from goethite were examined under the electron microscope. The morphology of the iron-substituted material was similar to that of the unsubstituted tobermorite (Figure 9A) except that there was a considerably more pronounced tendency to elongation of the plates, many of the particles approaching a lath-like morphology. It is interesting that iron-rich montmorillonite (i.e. nontronite) also exhibits elongate, lath-shaped units (Grim, 1953, p. 116).

The electron diffraction diagram from a field corresponding to that shown in Figure 9A gives "spotty" rings similar to those of Figure 4 for unsubstituted tobermorite except that additional lines occur corresponding to the additional lines found on x-ray diffraction. The sample also contains some material of finer particle size, and a field of such material was isolated and is shown in Figure 9B. The morphology is similar to that of the coarser particles; and electron diffraction of the field (Figure 10A) shows that the fine material is also very well crystallized tobermorite with an electron diffraction pattern identical to that of the coarser particles, except that the rings are noticeably less spotty.

However, a different situation arises with the aluminum-substituted sample. The morphology of this product is shown in Figure 11A. The particles are flat sheets, many of which have sharp angled corners. There is no particular tendency toward elongation. In a few of the fields examined, including this one, some very fine platy or foil-like material is also observed.



(A)



(B)

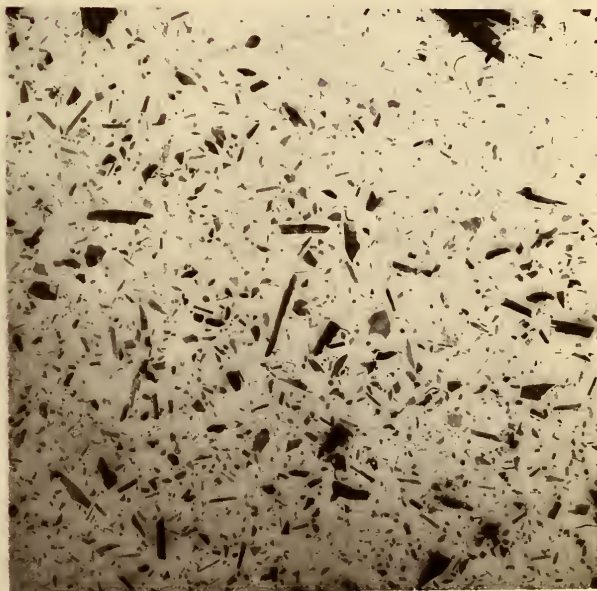


Figure 9. Electron Micrographs of 10%-Substituted Fe-Tobermorite. (A) Typical Field. (B) Field Selected to Show Fine Particles.





(A)



(B)

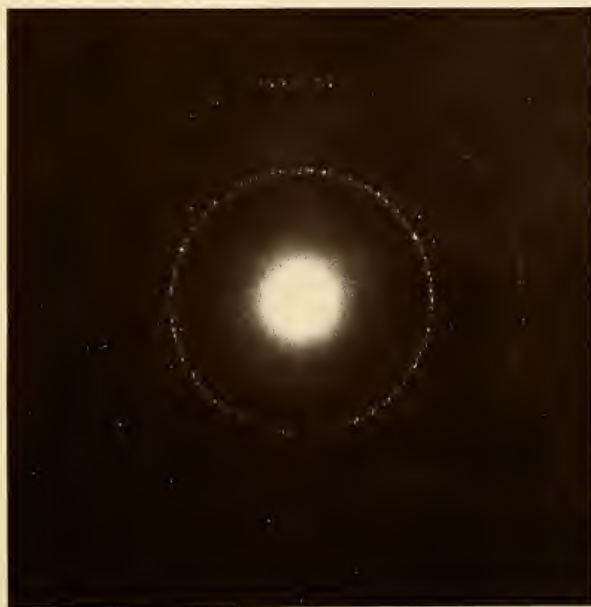
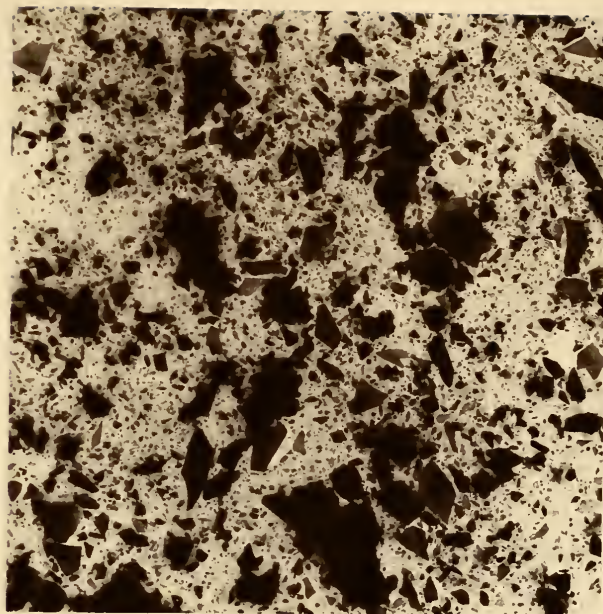


Figure 10. Selected Area Electron Diffraction of Fields Selected to Show Fine Particles. (A) 10% Substituted Fe-Tobermorite. (B) 10% Substituted Al-Tobermorite.





(A)



(B)

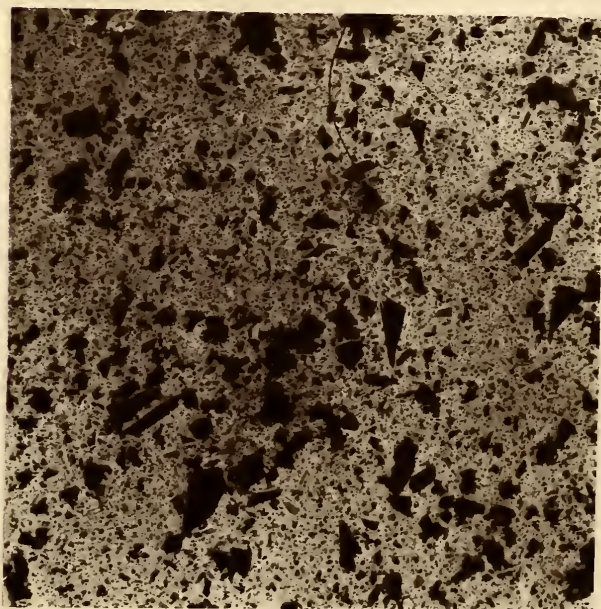


Figure 11. Electron Micrographs of 10% Substituted Al-Tobermorites. (A) Typical Field. (B) Field Selected to Show Fine Particles.



This material appears to resemble the CSH(I) preparations to be discussed later. It was difficult to find a field in which the larger particles were absent, but one was located in which only a few of the coarse particles were present (Figure 11B) and a selected area electron diffraction diagram secured. This diagram, Figure 10B, shows primarily the three rings corresponding to the three spacings of tobermorite that are carried over into the CSH(I) crystallization. There are additional spots for a few lines at smaller "d" values than these, but they are too faint to show up in the photographic reproduction and are presumably due to the few large crystals that are present in the field.

Careful examination of the outermost ring which corresponds to a "d" value of about 1.8Å indicates that there are two spacings present; an inner ring with a definitely coarse spotty character, and an outer ring a slight distance away, which is smooth in character. The x-ray diffraction line for this peak of tobermorite occurs at 1.84Å; that for the corresponding line of CSH(I), as will be indicated later, is at 1.82Å. Thus the electron diffraction data are interpreted as indicating that at least this particular member of the aluminum-substituted samples is composed of two phases; most of the material is well-crystallized, aluminum-substituted tobermorite, but some fine material is also present which is foil-like CSH(I) and not tobermorite.

Infrared Spectra of Substituted Tobermorites. The infrared spectra of the Al-substituted tobermorites are similar to the



pattern for the unsubstituted phase. The strongest feature was the Si-O band at about  $970\text{ cm}^{-1}$  and again the very weak, broad OH-stretching band at about  $3400\text{ cm}^{-1}$ , the water bending vibration at about  $1615\text{ cm}^{-1}$  and the band attributed to carbonate at about  $1440\text{ cm}^{-1}$  were observed. Certain subtle, but distinct differences between the spectra of the tobermorite and Al-substituted tobermorites were observed. First, the small but reproducible absorption feature at  $922\text{ cm}^{-1}$  in tobermorite was not present in the Al-substituted samples. Second, the band at  $890\text{ cm}^{-1}$  in tobermorite, presumably the out of plane bending mode of  $\text{CO}_3^{=}$  appeared at about  $878\text{ cm}^{-1}$  in the Al-substituted tobermorites. Third, the sharp band at about  $1200\text{ cm}^{-1}$  in tobermorite shifted to lower frequencies with increasing Al-substitution, the lowest position being approximately  $1170\text{ cm}^{-1}$  with the 15% Al-substituted sample. Finally, the band at  $745\text{ cm}^{-1}$  in tobermorite shifted markedly to about  $720\text{ cm}^{-1}$  in the 3% Al-substituted sample and then shifted further toward the low frequency end with additional aluminum substitution. The regular shift of the  $1200\text{ cm}^{-1}$  band with amounts of Al-substitution is shown in Figure 12. These tracings are for the set of samples with the aluminum derived from kaolinite; the two samples prepared using gibbsite gave virtually identical patterns to the corresponding members of the above series.

Figures 7 and 8 show a portion of the patterns for the unsubstituted tobermorite and for the nominally 10% substituted tobermorites with Al, Fe, and Mg replacement, respectively. In general, the latter two patterns resembled that for the unsubstituted material even more closely than did the Al-substituted





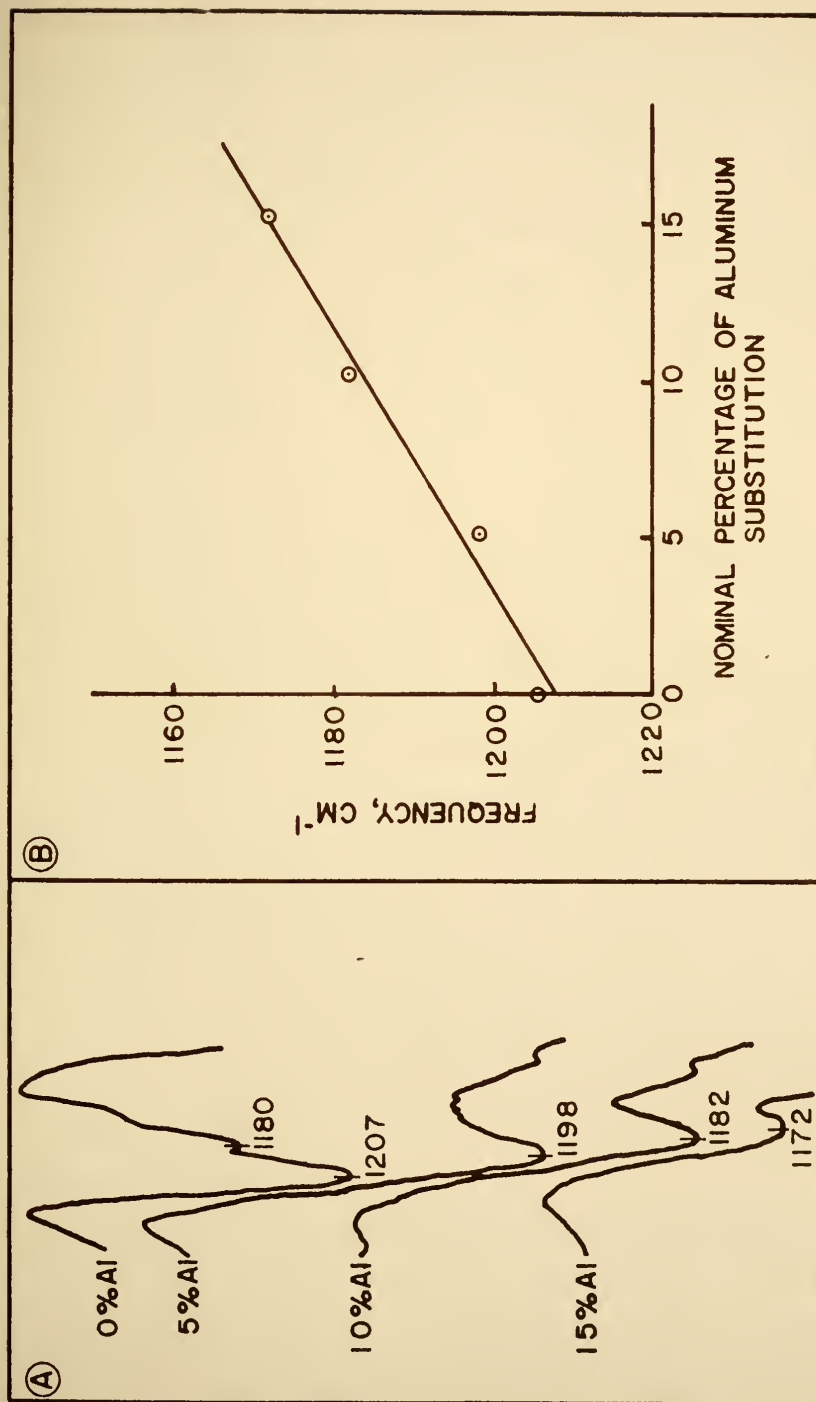


Figure 12. Shift of Tobermorite Infrared Absorption Band at Approximately  $1200 \text{ cm}^{-1}$  With Increase in Al-Substitution. (A) Trace of Infrared Spectra. (B) Plot of Frequency vs. % of Al-Substitution





samples discussed above. The small feature at  $922\text{ cm}^{-1}$  in tobermorite, absent in the Al-substituted materials, was present in both Fe- and Mg-tobermorites; Fe and Mg substitution did not cause a shift in the bands at  $890\text{ cm}^{-1}$  and  $1200\text{ cm}^{-1}$ . The feature at about  $1175\text{ cm}^{-1}$  in unsubstituted tobermorite shifted to about  $1150\text{ cm}^{-1}$  in the Fe-bearing sample and disappeared entirely in the Mg-bearing material. The band at  $745\text{ cm}^{-1}$  in unsubstituted tobermorite shifted slightly to about  $735\text{ cm}^{-1}$  in the Mg-substituted sample and to  $730\text{ cm}^{-1}$  in the Fe-tobermorite.

Assignment of various bands to particular vibrational modes in complicated silica structures is still strictly empirical. Stubican and Roy (1961, 1961a) have allocated various bands in the hydrated aluminosilicates and magnesium silicates on the basis of a program of synthesizing known phases and observing their spectra. Roy (1962) tabulated these assignments for the specific purpose of possible assistance in interpreting corresponding spectra of tobermorite-like calcium silicate hydrates. Unfortunately, the features observed in the present study, aside from the main Si-O band itself, do not appear to have any obvious correspondence to those noted in Roy's table. In view of this, no attempt will be made to interpret the observed spectral features.

The Effect of Substitution on the Surface Area of Tobermorite. The surface areas of the substituted tobermorites were determined from water vapor adsorption experiments at  $21^{\circ}\text{C}$  by the standard BET procedure. The results are given in Table 2.



Table 2. Surface Areas and Heats of Adsorption "E<sub>1</sub>" for Tobermorite and Substituted Tobermorites.

Kind of Substitution	Nominal Percentage	Source	Surface Area, m <sup>2</sup> /g	E <sub>1</sub> , cal/mole
Unsubstituted	--	--	78	13,640
Aluminum	3%	kaolinite	74	13,700
"	5%	"	117	13,300
"	10%	"	107	13,690
"	15%	"	103	13,280
Aluminum	10%	gibbsite	97	13,650
Iron	10%	goethite	81	13,210
Magnesium	10%	periclase	86	12,750



Kalousek (1957) noted by electron microscopic observation that the crystal size of aluminum-substituted tobermorite "decreased markedly" with increasing aluminum content; thus, one would expect a more or less regular increase in surface area with Al-substitution. These expectations were not borne out. The range in surface area observed is only from 74 to 117  $\text{m}^2/\text{g}$ . The two extreme values were for samples with 3% and 5% Al-substitution, respectively. In general, the data suggest that substituted tobermorites have slightly greater surface areas than the unsubstituted material, and that the iron- and magnesium-bearing preparations have slightly less surface area than the corresponding aluminum-bearing phases. The general order of magnitude of surface is about that normally associated with the clay mineral illite, which occurs in platy crystals of about the same size range as the tobermorite particles. There is no need to postulate any "internal surface" to account for the observed magnitude of the surface area.

The Effects of Substitution on Properties of the Tobermorite-Water Surface. Adsorption isotherm data can yield considerable information with regard to the interaction of a surface with the adsorbate used; for this reason several additional isotherm points were taken beyond the 0.05-0.35 partial pressure range normally required for BET surface area analysis for some of the samples.

The BET treatment yields a parameter "c", which is related to the heat of adsorption of water on the supposedly energetically uniform portion of the first layer of adsorbed



molecules; that is to say, the heat of adsorption onto the surface remaining after initial sorption has resulted in occupation of the more energetic adsorption sites or "hot spots". The "c" parameters determined for the tobermorite and substituted tobermorites in the present study were used to calculate values of heats of adsorption " $E_1$ " by the relation given by Brunauer, Emmet, and Teller (1938),

$$c = \exp (E_1 - E_L)/RT$$

where  $E_1$  is the heat of adsorption of the uniform portion of the first layer

$E_L$  is the heat of condensation of water vapor

R is the gas constant

T is the absolute temperature.

As may be seen in Table 2 the heats of adsorption for the unsubstituted tobermorite and for the Al-substituted samples range from about 13,300 to 13,700 cal/mole. The corresponding values for the iron- and magnesium-bearing phases are distinctly lower. Relatively high heats of adsorption suggest a comparatively strong attraction of the surface for the adsorbate, and vice versa.

If the surface area of a sample is calculated, it is possible to plot its adsorption isotherm on a reduced scale, that is to say, using as the ordinate the amount of water adsorbed per square meter of surface rather than per gram of adsorbent. If adsorption isotherms for a series of samples of differing surface areas but of identical surface properties are so plotted, all the points should fall on the same adsorption





curve, within experimental error. Such a situation was demonstrated by Wade, et al. (1961) in their study of the water vapor sorption properties of fused quartz.

A plot prepared in this manner for unsubstituted tobermorite and for the several Al-substituted tobermorites is given in Figure 13. It appears that one may conclude from the concordance demonstrated that aluminum substitution in the lattice does not significantly affect the water-vapor sorption properties of the tobermorite surface.

Similar data were calculated for the iron and magnesium-substituted tobermorites. These show the same shaped isotherm, but the amounts adsorbed per unit of surface at a given value of the partial pressure are slightly less than those shown in the figure. This may be interpreted as reflecting a slightly less hydrophilic surface, which is in accord with the lower heats of adsorption calculated for these samples by the BET theory.

All of the adsorption isotherms appear to be of the "Type II" classification of Brunauer (1943, p. 150). However, the relative height and sharpness of the "knee" of the isotherm suggest that adsorption in excess of a monolayer was limited, at least until relatively high partial pressures were attained. Brunauer, Deming, Deming, and Teller (1938) developed a generalized theory of adsorption which includes the cases in which adsorption is restricted to a specific number of molecular layers of adsorbate on the surface of the adsorbent. This theory resulted in an equation for the isotherm (the BDDT equation) in which there is a specific parameter  $n$ , that represents



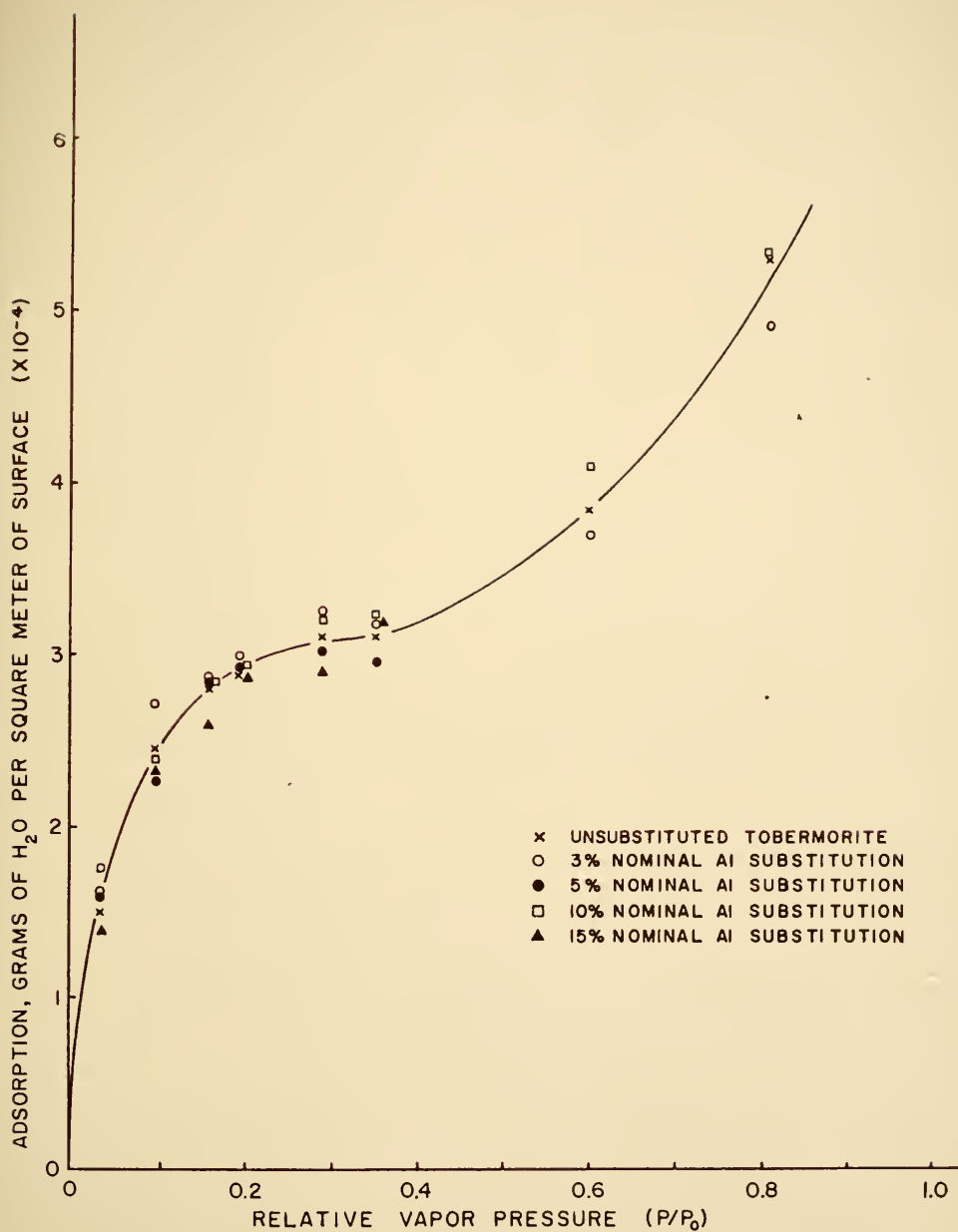


Figure 13. Reduced Water Vapor Adsorption Isotherm ( $21^{\circ}\text{C}$ )  
For Tobermorite and Al-Substituted Tobermorites.



this number of layers directly. The equation reduces to the more commonly-used BET equation when  $n$  becomes large.

In accordance with the procedure outlined by Brunauer (1943, p. 154), the monolayer volume  $V_m$  and the  $c$  parameter derived from the BET treatment of the water adsorption data for the unsubstituted tobermorite were used to calculate BDDT adsorption isotherms for several values of  $n$ . The resulting calculated isotherms are shown in Figure 14, which presents the calculations for  $n$  values of 1, 2, and 3 layers and the experimental adsorption points. Although the experimental points deviate at higher partial pressures, (presumably due to the effect of capillary condensation), they fit the BDDT equation quite well for  $n$  equal to 2 layers. It should be noted that this two-layer figure is a limiting value; the actual adsorption, even at the highest partial pressure used, is distinctly less than two molecular layers.

Restriction of adsorption to a certain number of layers is usually explained as the effect of steric limitation set by the configuration of the adsorption surface; a common example is adsorption in material containing most of its surface as very fine capillaries, such as charcoal. Tobermorite has a structure in which relatively narrow channels occur between the ridges formed by the silica chains. If these channels provided the major portion of the surface being measured, the restriction of adsorption to two molecular layers might be readily understood. However the surface area measured by water vapor sorption, about  $80 \text{ m}^2/\text{g}$  for the tobermorite and slightly higher for the various substituted tobermorites,



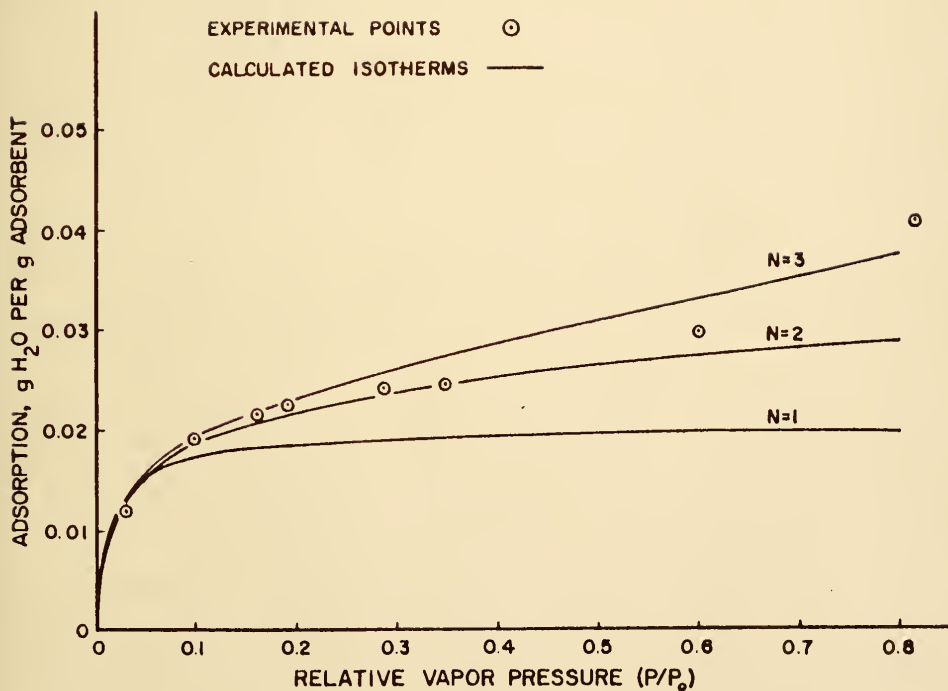


Figure 14. Experimental Water Vapor Adsorption Isotherm for Tobermorite Compared with Isotherm Calculated from the BDDT Equation for Adsorption Restricted to 1, 2, and 3 Molecular Layers.





is only of the order of magnitude attributable to the external particle surfaces, considering the dimensions of the particles seen in electron micrographs. Hence the internal channels are presumably not active in adsorption of water vapor in the BET partial pressure region, and little adsorption occurs beyond it. Perhaps the failure of the channels to appreciably adsorb water vapor is due to their being plugged near the ends, possibly with hydrated calcium ions.

An alternate explanation of the observed restricted adsorption feature of tobermorite must then be sought. It appears to the author that the only remaining possibility is that the energetics of adsorption on tobermorite are such that adsorption beyond the first layer on the planar surface is possible but not energetically favorable, i.e. the heat of adsorption of the second and succeeding layers is very small (Brunauer, 1943, p. 168).

Cation Exchange Capacity Measurements. The substitution of trivalent and divalent cations into the tobermorite lattice, presumably for tetravalent silicon, suggests the strong possibility that cation exchange sites should be generated as a result of such isomorphous substitution. Basically a cation exchange determination as conventionally performed involves a process of saturating the exchange complex with a large excess of a particular cation, washing out the excess, and then either determining the amount retained in situ, or more commonly, replacing the measuring cation with a large excess of another variety and determining the amount so dislodged. The difficulty of applying this simple scheme to the calcium silicate hydrates



is their relative instability to the washing treatments. By definition, "ion exchange is the reversible exchange of ions between a solid and a liquid in which there is no substantial change in the structure of the solid" (Trooper and Worth, 1956). If the procedure involved in the determination breaks down the solid to any extent the validity of the exchange capacity value so measured becomes questionable.

The use of absolute alcohol as the solvent medium for the exchange reaction has the advantage that the tobermorites are at least reasonably insoluble in this medium and even  $\text{Ca}(\text{OH})_2$  has only a slight solubility. When the excess  $\text{K}^+$  ions are removed from the tobermorite suspension by washing, undesired replacement of the remaining  $\text{K}^+$  ions adsorbed on the tobermorite exchange sites by  $\text{Ca}^{++}$  ions generated by partial dissolution of the sample, is minimized by use of the alcohol.

Several experiments were performed to fix the conditions of the cation exchange determination used, particularly the conditions of the saturation and washing procedure. These will not be reported here, but the procedure as evolved appears to give reproducible and satisfactory results. A sample of Wyoming bentonite ("Volclay" brand, American Colloid Co.) gave a cation exchange capacity (CEC) of 85 meq/100 g by this method; this is essentially the same value as is commonly secured for this material with conventional cation exchange capacity methods.

The CEC measurements for the various tobermorite products by the procedure outlined previously are given in Table 3. The values reported are averages of duplicate determinations;



Table 3. Cation Exchange Capacities Measured for Tobermorite and Substituted Tobermorites.

Kind of Substitution	Nominal Percentage	Source	Cation Exchange Capacity, meq/100g
Unsubstituted	--	--	34
-----			
Aluminum	3%	kaolinite	29
"	5%	"	27
"	10%	"	33
"	15%	"	20
Aluminum	10%	gibbsite	23
"	15%	"	24
Iron	10%	goethite	21
Magnesium	10%	periclase	13



the average variation between duplicates was  $\pm 1.3$  meq/100 g. The values range downward from the 34 meq/100 g reported for the unsubstituted tobermorite to 13 meq/100 g for the Mg-substituted material.

The variation in exchange capacity with substitution is opposite to that predicted. Unsubstituted tobermorite has the highest exchange capacity reported. Within the series of substituted Al-tobermorites there seems to be a trend of decreasing CEC with increasing substitution. For Mg-substitution, one would have predicted an even greater increase in exchange capacity since it is believed that divalent ions are replacing tetravalent ones; instead the reverse was found. It is evident that substitution in the tobermorite lattice does not have the same effect as it does in hydrated aluminosilicates and magnesium silicates.

For certain clays, notably kaolinite, a definite correlation is often observed between CEC and surface area; the exchange capacity being generally attributed to the effects of "broken bonds" on the particle edges (see for example Ormsby and Shartsis, 1960). In this study essentially no correlation was found between surface area and CEC for the various samples. This does not necessarily imply that one would not find such a correlation if one examined a collection of tobermorites of the same kind and degree of substitution that differed only in particle size.

These CEC results are discussed further in a later section in this report. Despite the apparently anomalous effect of





substitution, it is felt that the phenomenon of cation exchange in these systems has been demonstrated in a valid manner, and that the results obtained are of significance.

#### Zeta Potential and Surface Charge of Substituted Tobermorites.

The zeta potentials of several of the substituted tobermorites suspended in  $10^{-3}$  M NaCl solution were examined by the method previously outlined. Under these conditions, all the samples examined were negatively charged. The observed zeta potentials were quite similar to that of unsubstituted tobermorite; the individual values being -32 mv. for the 10% Al-substituted material derived from kaolinite, -30 mv. for the nominally 10% Mg-substituted tobermorite, and -38 mv. for the corresponding Fe-substituted specimen. In view of the approximate nature of the determination, no significance is attached to these differences.

#### Summary of Experimental Results on

##### Well-crystallized Tobermorites

A well-crystallized tobermorite of composition  $C_{0.83}S_{1.00}H_{0.78}$  was synthesized hydrothermally from lime and quartz. It gave a complete and detailed x-ray diffraction pattern for tobermorite and was observed to have a dominantly platy morphology. DTA features included an endotherm at  $275^{\circ}C$  associated with a collapse of the 11.2Å basal spacing to 9.5Å spacing and a very small exotherm at  $820^{\circ}C$  on conversion to wollastonite. Infrared spectroscopy revealed bands for Si-O bonds, a very weak "bonded OH" stretching band, a water deformation band, a band commonly



attributed to the carbonate asymmetrical in-plane stretching mode, and a number of less prominent features. The surface area to water vapor was  $78 \text{ m}^2/\text{g}$ ; the apparent heat of adsorption of the first layer of water was about  $13,600 \text{ cal/mole}$ . Adsorption of water vapor is apparently limited to two molecular layers, with the second probably being held much less energetically than the first. Tobermorite particles were shown to exert a negative surface charge and a zeta potential of about  $-30 \text{ mv.}$  in systems dominated by  $\text{Na}^+$  cations, but the charge is reduced in the presence of  $\text{Ca}^{++}$  ions and becomes positive in solutions with high concentrations of  $\text{Ca}^{++}$ ,  $\text{Al}^{+++}$ , and probably other polyvalent cations. The cation exchange capacity of unsubstituted tobermorite was determined to be  $34 \text{ meq/100 g.}$  Tobermorite-water systems are plastic in nature and behave in a manner similar to that of wet clays.

A series of substituted tobermorites was prepared hydrothermally by incorporating aluminum derived from kaolinite and from gibbsite, iron derived from goethite, and magnesium derived from periclase. The morphology of these products was in general platy, except that the iron-substituted phase had a tendency toward elongated, lath-shaped particles. It was discovered that the aluminum-substituted materials contain fine, foil-shaped particles in addition to the tobermorite plates, and these were shown by electron diffraction to be CSH(I). Slight modifications of the x-ray pattern of tobermorite were obtained on substitution, notably a weakening of (002) and (222) peaks with iron and magnesium substitution,



suggesting c-axis disorder. Several peaks not previously observed appeared as a result of substitution. The differential thermal analysis of aluminum-bearing phases was distinctive in displaying a very sharp, intense exothermic response on conversion to wollastonite. This response was accompanied by a very marked shrinkage and cementation of the sample. Neither the unsubstituted tobermorite nor the iron- or magnesium-bearing phases exhibited these responses. Slight modifications of the infrared spectra were described for the substituted phases. Substitution was found to increase the surface area slightly but no relation was found between the extent of aluminum substitution and the surface area of the product. The surface areas of the iron- and magnesium-bearing phases were less than those of the corresponding aluminum phases. Substitution did not appear to affect the water vapor sorption properties of tobermorite to any marked extent. The cation exchange capacities measured for substituted tobermorites were significantly less than, rather than greater than, that of the unsubstituted tobermorite; this is opposite to the effect predicted. The zeta potentials of the substituted phases are similar to that of unsubstituted tobermorite.

Poorly Crystallized Calcium Silicate Hydrates Prepared  
at Room Temperature - CSH(I)

Preparation and Designation of Products

The preparation of these materials has been described in the section on Materials and Experimental Methods. Seven products have been characterized: four samples produced by double



decomposition at room temperature with immediate precipitation and no aging period; a single preparation by a more elaborate double decomposition procedure involving simultaneous manipulation of two syringes, where again no aging was involved and two preparations made by direct action of lime on a special dispersion product of silica, in which the product was allowed to age for several weeks in contact with its mother liquor before being washed and dried.

For purposes of brevity these preparations will be designated CSH(I) - 1 to CSH(I) - 7. Table 4 presents a list of the products, the starting materials used for each, and the chemical formula as derived from the analyses for each given in Table 2 of the Appendix.

#### Composition

The similarity in composition displayed by the samples CSH(I) - 1 to CSH(I) - 4 is remarkable, considering the range in the Ca:Si ratios of the starting solutions used. These preparations represent the immediate precipitation product which perhaps is the first stage of crystallization prior to rearrangement and improved crystallinity characteristic of aged products. As such, it seems clear that the typical composition of such a stage is about  $C_{1.0}S_{1.0}H_{1.6}$ , regardless of the relative amounts of starting materials present.

CSH(I) - 5 represents an effort to get a higher lime CSH(II) phase to form; as such it was unsuccessful. There was only a slight increase in the Ca:Si ratio of the product over that







Table 4. Designation and Composition of Room Temperature CSH(I) Products.

Designation	Starting Materials	Type of Reaction	Ca:Si Ratio of Starting Materials	Composition of Product
CSH(I) - 1	$\text{Na}_2\text{SiO}_3$ and $\text{CaCl}_2$	double decomp.	1:1	$\text{C}_{0.97}\text{S}_{1.00}\text{H}_{2.74}$
CSH(I) - 2	$\text{Na}_2\text{SiO}_3$ and $\text{Ca}(\text{NO}_3)_2$	double decomp.	1:1	$\text{C}_{0.96}\text{S}_{1.00}\text{H}_{1.59}$
CSH(I) - 3	" "	double decomp.	1.5:1	$\text{C}_{0.99}\text{S}_{1.00}\text{H}_{1.62}$
CSH(I) - 4	" "	double decomp.	2:1	$\text{C}_{1.01}\text{S}_{1.00}\text{H}_{1.64}$
CSH(I) - 5	$\text{Na}_2\text{SiO}_3$ and $\text{Ca}(\text{NO}_3)_2$	double decomp.	3.5:1	$\text{C}_{1.16}\text{S}_{1.00}\text{H}_{1.00}$
CSH(I) - 6	$\text{SiO}_2$ and $\text{Ca}(\text{OH})_2$	direct synthesis	1:1	$\text{C}_{0.91}\text{S}_{1.00}\text{H}_{1.08}$
CSH(I) - 7	" "	direct synthesis	2:1	$\text{C}_{1.58}\text{S}_{1.00}\text{H}_{1.80}$



of the preceding specimens. The relatively smaller amount of water found to be associated with this phase is of some significance and will be discussed later.

CSH(I) - 6 contains slightly less lime and a little more water but is otherwise similar to the CSH(I) - 5 product produced in a vastly more lime-rich environment. It should be noted that the water content is far below that of the "initial" room temperature products, as represented by CSH(I) - 1 to - 4.

CSH(I) - 7, despite its high calcium content is a true CSH(I) phase and clearly not CSH(II) as will be shown later.

#### X-ray Diffraction

Figure 15 gives x-ray diffractometer traces for all seven of the CSH(I) materials. The charts fall into three groups which will be discussed separately.

CSH(I) - 3 through CSH(I) - 7, despite their diverse conditions of preparation are remarkably alike so far as x-ray diffraction is concerned. All have the strong main peak at about 3.02 - 3.08A which is characteristic of tobermorite-like calcium silicate hydrates. All have definite peaks at about 2.78A and 1.81A. These are the characteristic peaks of CSH(I) or CSH(II) phases. In addition, all have a faint peak at about 1.66A and all except CSH(I) - 5 have a peak at 3.25A; none has a peak at or near 1.56A which would characterize CSH(II), according to the criterion of Heller and Taylor (1956, p. 57). In the patterns for tobermorite and aluminum-substituted tobermorite (Figure 2) the intensity



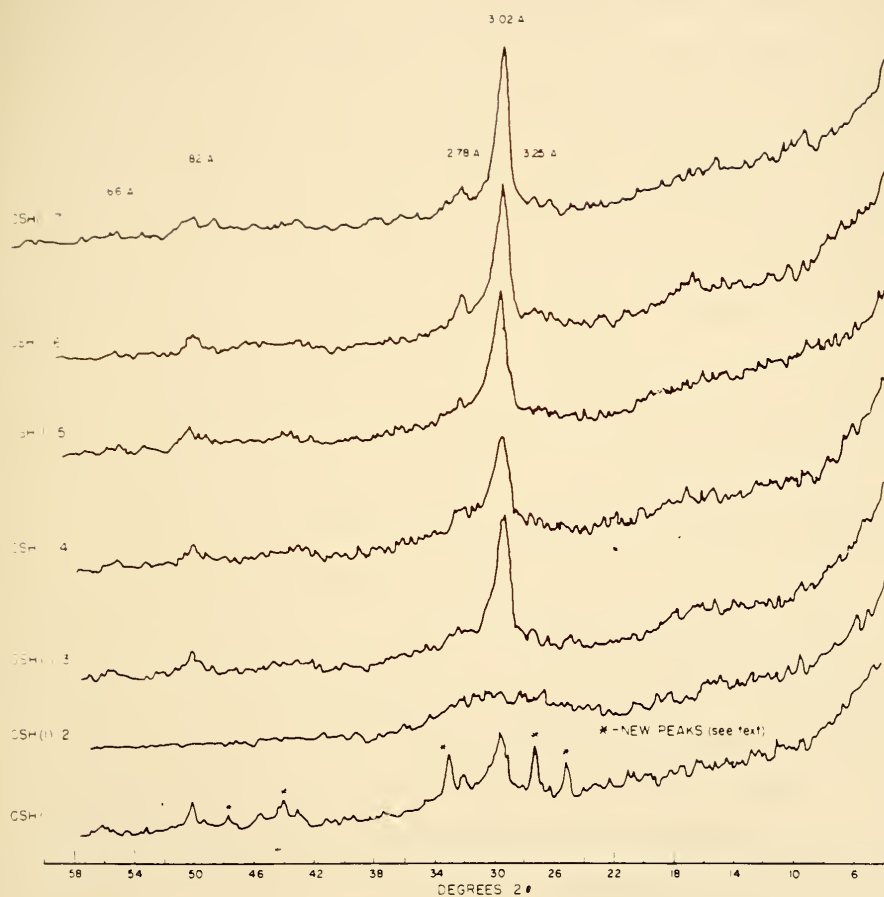


Figure 15. X-ray Diffractometer Traces for CSH(I) Samples Synthesized at Room Temperature.



of the (222) peak at 2.97A was always distinctly greater than that of the (400) peak at 2.82A and much greater than that of the (040) peak at 1.84A. In the present patterns there is little evidence of any peak at a position corresponding to that of the (222) peak at 2.97A. While the main peak at about 3.02A in these patterns overlaps the position somewhat, if the peak at 2.97A were present but not resolved, one would expect a noticeable bulge on the high-angle side of the 3.02A peak. There seems to be a hint of such an effect only with CSH(I) - 3; the other peaks are apparently symmetrical. In view of this and the lack of any basal spacing, it appears that there must be almost total disorder in the c direction for these phases, all available peaks being reflections from planes of atoms entirely within the unit layer.

CSH(I) - 2 appears to be essentially amorphous. No definite peaks were obtained by x-ray diffraction techniques regardless of sample preparation. There is however a "bulge" in the scattering indicative of some short-range order in the vicinity of the main peak for the other specimens.

CSH(I) - 1 presents a problem of interpretation. X-ray diffraction patterns made shortly after the preparation of the product showed a pattern very similar to those of CSH(I) - 3 or - 4, etc. However, on re-examination of the material after storage for approximately a year, the pattern shown in Figure 2 was obtained. A second portion of the material stored in another laboratory in a different building also showed a changed pattern similar to the one shown. The new





peaks present are starred on the chart, and occur at 3.56A, 3.27A, 2.72A, 2.05A, and 1.91A. The present pattern resembles that of xonotlite, which has strong lines at 3.65A, 3.23A, 3.07A, 2.04A, and 1.95A (Heller and Taylor, 1956, p. 47).

No information relative to the basal spacing could be obtained from the powder mount x-ray results of Figure 15. An attempt was made to secure such information by preparing oriented x-ray specimens. Samples of all of the CSH(I) specimens were dispersed in water by the use of ultrasonic apparatus, and portions of the suspension were allowed to dry overnight on ordinary glass microscope slides. The drying was carried out in vacuum desiccators over ascarite, with continuous pumping during the drying period. The results of x-ray diffraction examination were disappointing. Broad, shallow and irregular peaks were observed in the region of 10-14A, but their peak positions were indefinite, and the reproducibility between duplicate specimens was poor. All that could be concluded was that the basal spacings were somewhere in this range. Oven-drying the specimens did not improve the patterns; this suggests that the irregularity observed was not due to a random collection of mixed layer hydration states. Effective dispersion to primary particles (which are only a few unit layers thick) was definitely not achieved; the specimens deposited on the glass slides were not well-oriented. In contrast with these results, tobermorite disperses readily to primary particles and a specimen of tobermorite made in the manner described above show only a



large, sharp basal spacing peak at 11.2A due to the high degree of preferred orientation of the primary particles.

### Morphology

Samples CSH(I) - 1 through CSH(I) - 4 were not observed by electron microscopy; electron micrographs for CSH(I) - 5 and CSH(I) - 7 are shown in Figure 16, and for CSH(I) - 6 in Figure 17.

CSH(I) - 5 occurs primarily in extremely thin "foils" which were readily dispersed by the preparative procedure and resemble "snowflakes" spread out on the field (Figure 13A). A few fields show a greater population of thicker, irregularly-shaped aggregates, the margins of which are toothed as if they were composed of fibrous particles, but no individual fibers can be observed. The product gives a distinct, strong, polycrystalline electron diffraction diagram consisting of three perfectly smooth rings corresponding to the three main peaks recorded on x-ray diffraction.

CSH(I) - 6 (Figure 17) occurs in much thicker particles having a more definite appearance than the previous material. The individual particles that are visible appear to be aggregates composed of twisted platy material. A few rather large aggregates such as that depicted in the bottom photograph of Figure 17 is almost identical in appearance to Figure 1 of Kalousek and Prebus (1958), which these authors cite as an example of "crinkled foil" morphology.

CSH(I) - 7 (Figure 16) has a general morphology similar to that of CSH(I) - 6 except that a much larger portion of the



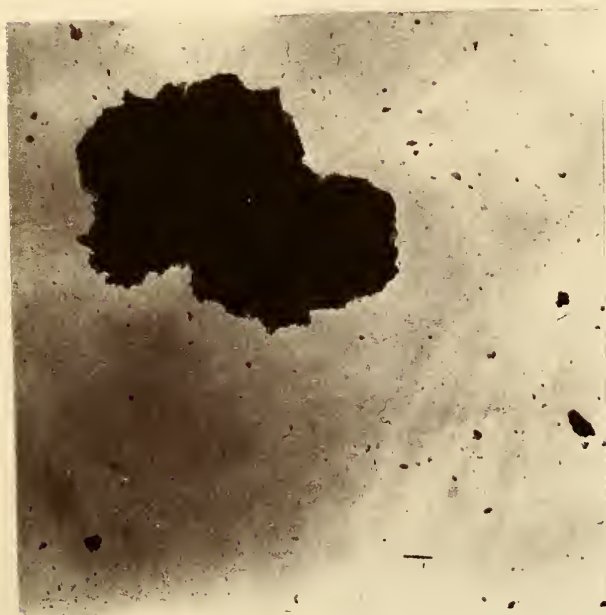
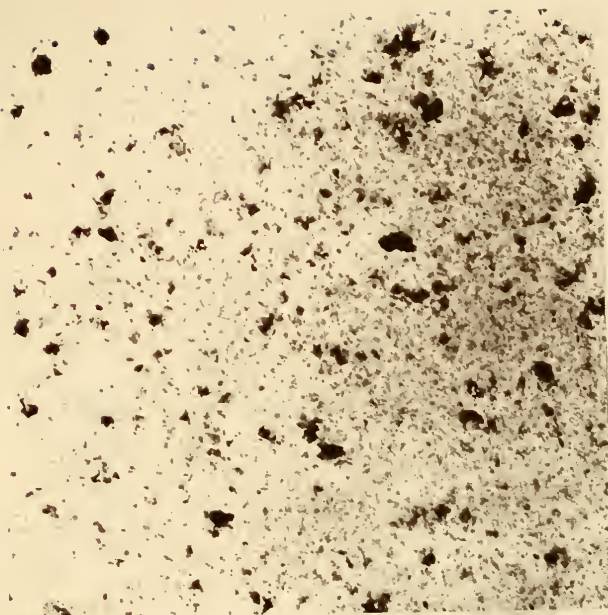


Figure 16. Electron Micrographs of CSH(I) Preparations.

(A) CSH(I) - 5. (B) CSH(I) - 7.



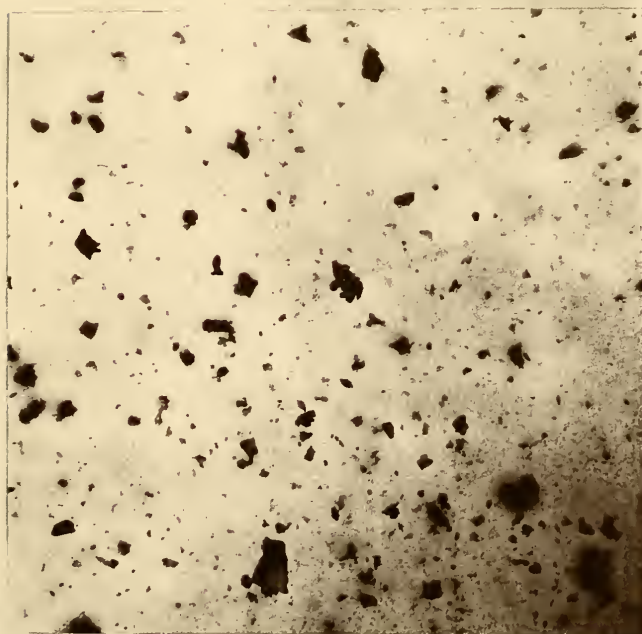
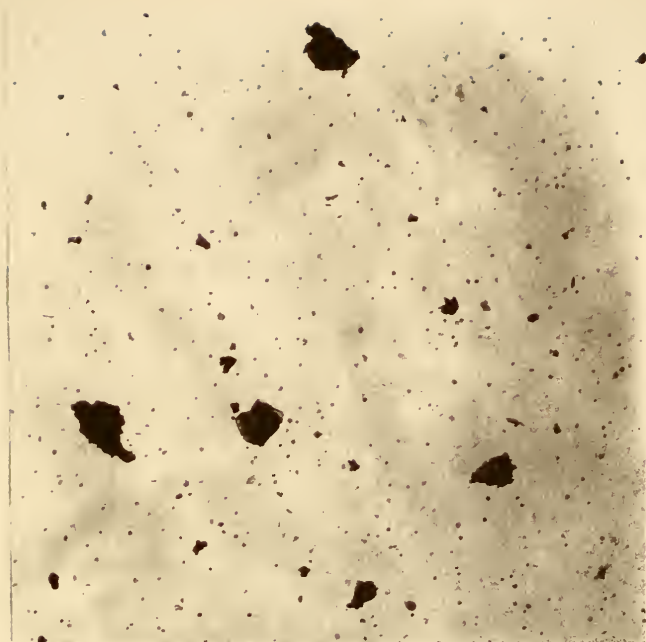


Figure 17. Electron Micrographs of CSH(I) - 6.





material is in the fine foil state and the coarser particles seem to be more definitely platy. There is no indication of any lath-like or fibrous material in this preparation. The definite absence of elongated particles in this phase confirms its assignment as a CSH(I) material rather than a CSH(II), despite the apparent high-lime content.

It may be recalled from the literature review that most workers now are in agreement that the morphology of CSH(I) is foil-like rather than fibrous; the present work confirms this interpretation.

#### Differential Thermal Analysis

DTA diagrams of CSH(I) - 5, - 6, and - 7 are given in Figure 18. The major feature is the expected sharp exothermic reaction noted on the transformation to wollastonite at  $825^{\circ}\text{C}$  for the first two specimens and  $860^{\circ}\text{C}$  for the last. All specimens show a distinct endothermic response at about  $790^{\circ}\text{C}$ , just prior to this transition and all show a very faint endothermic deflection at about  $665^{\circ}\text{C}$ . These features closely resemble those displayed by the aluminum-substituted hydrothermal tobermorites in Figure 4, especially that for the 10% replacement sample. The latter was shown to contain particles of CSH(I).

The strong exothermic peak for these materials is accompanied by a shrinkage reaction similar to that noted for the aluminum-substituted tobermorites. However the shrinkage is not as great and the product is soft and crumbly instead of very hard and fused.

The other prominent feature of these patterns is the initial



water loss endothermic responses; it is observed that the one for CSH(I) - 7 is less strong than those for the other two samples, even though the formula derived from the chemical analysis of this material suggests a much higher water content (Table 4).

These DTA patterns were run at the Laboratories of the Materials Research Division, Bureau of Public Roads, MacLean, Virginia, on DTA equipment capable of maintaining a  $10^{\circ}$  linear rate of temperature increase. For comparative purposes, sample CSH(I) - 6 was also run on the Eberbach portable DTA instrument. The result of this run is similar to that shown in Figure 18, the major differences being that the bottom of the initial endotherm is at  $200^{\circ}\text{C}$  instead of  $160^{\circ}\text{C}$ , and the peak of the final exotherm is at  $795^{\circ}\text{C}$  instead of  $825^{\circ}\text{C}$ , due to the very high heating rate in the early part of the run and the low heating rate in the latter part of the run with the portable unit.

#### Infrared Spectra

As expected, the infrared spectra of these CSH(I) materials bear close resemblances to those of the tobermorite and substituted tobermorite materials previously discussed.

The OH stretching vibrations in these phases (not shown) are similar to those of the tobermorites; in each case consisting of a broad, comparatively shallow trough centered at about  $3400\text{ cm}^{-1}$  ( $2.94\text{ }\mu$ ); and in no case was there a band assignable to the "free" OH stretching mode near  $3700\text{ cm}^{-1}$  ( $2.7\text{ }\mu$ ).

The remaining details of the spectra are shown in Figure 19



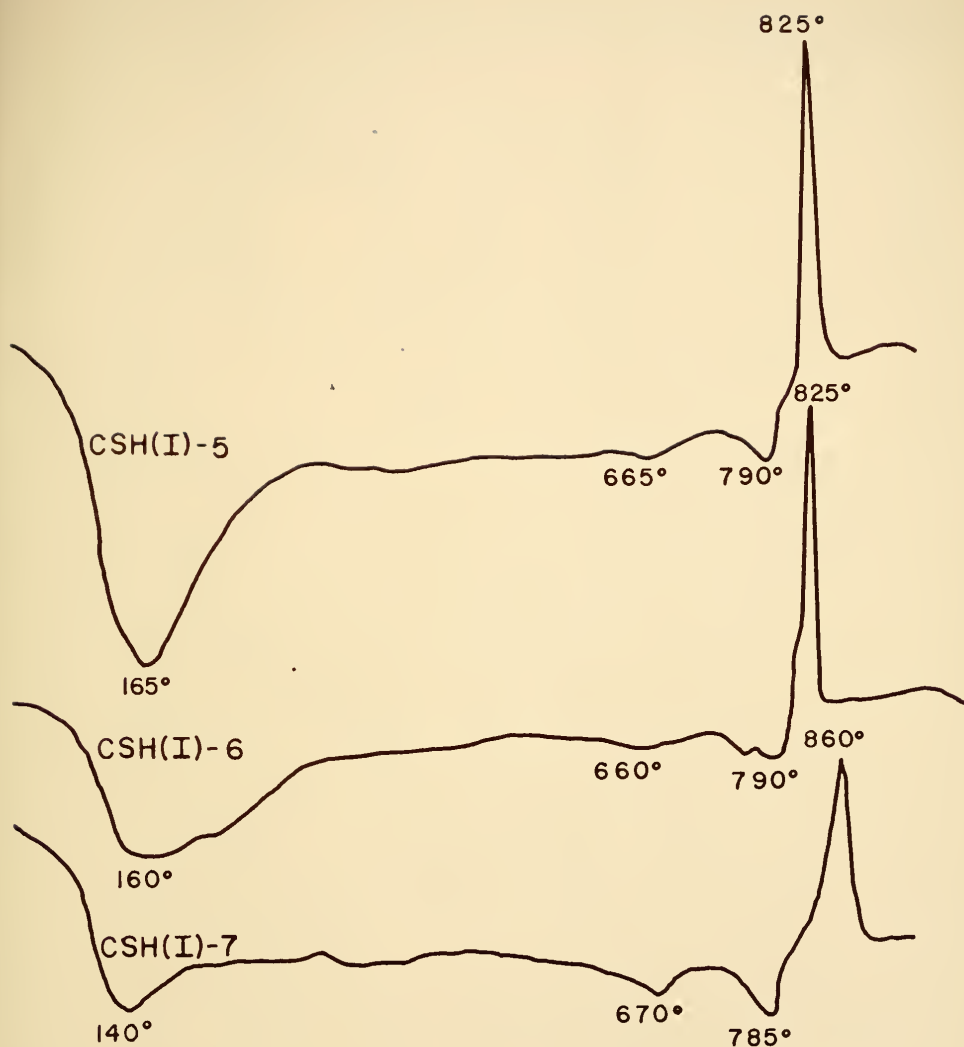


Figure 18. DTA of CSH(I) Preparations. Heating Rate 10°C Per Minute.



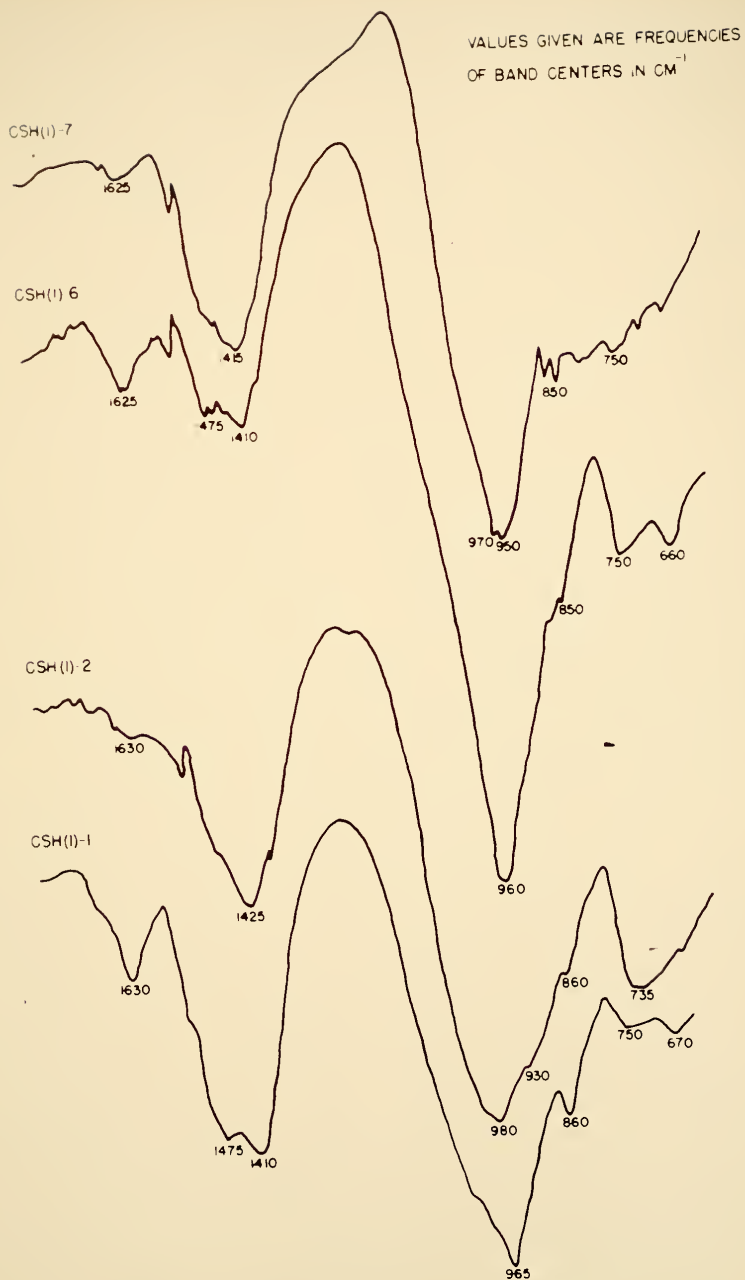


Figure 19. Infrared Absorption Spectra for CSH(I)  
Preparations.





for CSH(I) - 1, 2, 6, and 7, respectively. In general, the same major bands previously reported for tobermorite are visible here as well; the water bending vibration at about  $1630\text{ cm}^{-1}$  ( $6.15\text{ }\mu$ ), the  $\text{CO}_3^{=}$  asymmetrical stretching band at about  $1440\text{ cm}^{-1}$  ( $6.95\text{ }\mu$ ), the main Si-O lattice vibration at about  $970\text{ cm}^{-1}$  ( $10.3\text{ }\mu$ ), and bands at about  $750\text{ cm}^{-1}$  and  $660\text{ cm}^{-1}$  ( $13.3$  and  $15.1\text{ }\mu$ ). However, one obvious feature of the present patterns is the increased intensity of the band at about  $1440\text{ cm}^{-1}$  and the fact that in some cases it appears to be split into two vibrations, one at about  $1410\text{ cm}^{-1}$  and the other at about  $1475\text{ cm}^{-1}$ . This may be due to a removal of degeneracy usually associated with this mode of vibration of  $\text{CO}_3^{=}$  as suggested by Hunt (1959). Another noticeable feature is the obvious weakness of the  $1630\text{ cm}^{-1}$  band attributed to the water bending vibration; in both CSH(I) - 2 and CSH(I) - 7 it is almost negligible in intensity despite the high compositional water content of both these samples. The exact position of the Si-O maximum varies somewhat, being as low as  $950\text{ cm}^{-1}$  for CSH(I) - 7 and as high as  $980\text{ cm}^{-1}$  for CSH(I) - 2. These differences may indicate differences in degree of polymerization of the  $\text{SiO}_2$  chains as suggested for CSH(gel) by Lehmann and Dutz (1959). Other general differences from the tobermorite spectra include the complete lack of any band in the  $1100\text{-}1200\text{ cm}^{-1}$  region. Also the position of the band which is probably the  $\text{CO}_3^{=}$  out of plane bending vibration which occurs at  $890\text{ cm}^{-1}$  in the tobermorites occurs at about  $850\text{-}860\text{ cm}^{-1}$  in these materials. Finally, for the tobermorites, especially the substituted ones, the general level of absorption



of the infrared radiation is almost the same on both sides of the Si-O band; in the present samples this is not the case; rather, absorption at frequencies lower than that of the main band is intense to the low frequency end of the pattern. It is clear that despite the similarities in gross features one should readily be able to distinguish the infrared absorption spectra of true tobermorite from those of CSH(I).

The patterns for the individual CSH(I) samples have interesting variations among themselves. CSH(I) - 1 seems to be similar to the other CSH(I) materials despite the deviant x-ray diffraction pattern. The pattern for xonotlite (Kalousek and Roy, 1957) shows a strong band at about  $1200\text{ cm}^{-1}$ , which is absent here. The relatively strong water vibration band and the strong, split  $\text{CO}_3^{=}$  asymmetrical stretching bands are prominent, otherwise the pattern is typical. CSH(I) - 2, despite the apparent lack of crystallinity of this material, has about the same sort of spectrum as the others; the major distinctive feature seems to be the enlarged band at  $735\text{ cm}^{-1}$ . The spectra for CSH(I) - 3, 4, and 5, not shown, are similar to that shown for CSH(I) - 6, which, accordingly, may be considered typical of the group as a whole. CSH(I) - 7, the high-lime member, has a remarkably small water band as mentioned previously and strong general absorption below the main Si-O band. It appears that the large water content of this phase must consist almost entirely of OH water rather than any form of interlayer water molecules. Also, the association of the general absorption level at frequencies below that of the Si-O band with calcium



content appears to be manifest; CSH(I) - 7 has a significantly higher calcium content than the remainder of the group, these in turn have a generally higher calcium content than the tobermorites.

#### Surface Area and Water Vapor Adsorption

The surface areas of these products are given in Table 5, along with corresponding values of the heat of adsorption of the "uniform" portion of the first molecular layer, " $E_1$ ", from the BET theory. The first four samples, prepared without any aging procedure, have distinctly higher areas than the remainder. All of the products have higher surface areas than the well-crystallized hydrothermal products previously discussed. However, there is no direct correlation between area and degree of crystallinity. Some of the well-crystallized hydrothermal substituted tobermorites have areas approaching the minimum value for this distinctly less-well crystallized group and within this group the sample totally amorphous to x-rays (CSH(I) - 2) occupies only the median position with regard to surface area.

The surface area values themselves ranged from about 150 to about  $350 \text{ m}^2/\text{g}$ ; these limits are consistent with earlier values discussed by Brunauer (1962) which ranged from 135 to  $380 \text{ m}^2/\text{g}$ .

With respect to the heats of adsorption, only one sample, CSH(I) - 6, has an  $E_1$  as large as that of the tobermorites. The others have somewhat lower values and that of the x-amorphous sample, CSH(I) - 2, is distinctly lower yet, being only about



Table 5. Surface Areas and Heats of Adsorption of Water Vapor for CSH(I) Preparations.

Sample No.	Surface Area ( $\text{m}^2/\text{g}$ )	" $E_1$ ", (cal/mole)
CSH(I) - 1	(355)	(12,700)
CSH(I) - 2	(245)	(11,700)
CSH(I) - 3	278	(12,800)
CSH(I) - 4	300*	12,510*
CSH(I) - 5	167	13,090
CSH(I) - 6	175	13,660
CSH(I) - 7	157	12,720

Note: Brackets around surface area values denote averages of two determinations which were greater than  $\pm 5\%$  apart. Brackets around " $E_1$ " values denote rounded averages of duplicate values which were greater than  $\pm 100$  cal/mole apart. Starred values denote a single determination.





1150 cal/mole greater than the heat of condensation of liquid water.

The accuracy and reproducibility of the determinations for the first four samples appear to leave something to be desired. This was surprising, since these materials, having high surface areas, adsorb more water vapor at a given increment of vapor pressure, and hence the weighing errors should have been proportionately less. Nevertheless the results were fairly erratic. The problem may be partially due to the difficulty of arriving at a uniform initial condition of dryness, and partially to non-uniform dissipation of heat released on adsorption of the water. Adsorption of significant quantities of water vapor liberates enough heat to raise the temperature of the sample several degrees. The system used is evacuated, and the glass weighing bottles, the ceramic plates on which they rest, and the glass desiccators themselves are all relatively nonconducting; hence heat dissipation must be slow and perhaps erratic.

The adsorption isotherm data representing six of the seven CSH(I) samples are given in reduced isotherm form in Figure 20. Adjacent data points for two pairs of samples were given a single symbol to avoid crowding the figure. The adsorption isotherm thought to be characteristic for all these samples is indicated in the heavy solid line. The corresponding isotherm for the tobermorite and substituted tobermorites previously shown in Figure 9 is represented by the dashed line. The difference is obvious. The CSH(I) isotherm is clearly a "standard" Brunauer type II isotherm, and presumably would fit a BDDT



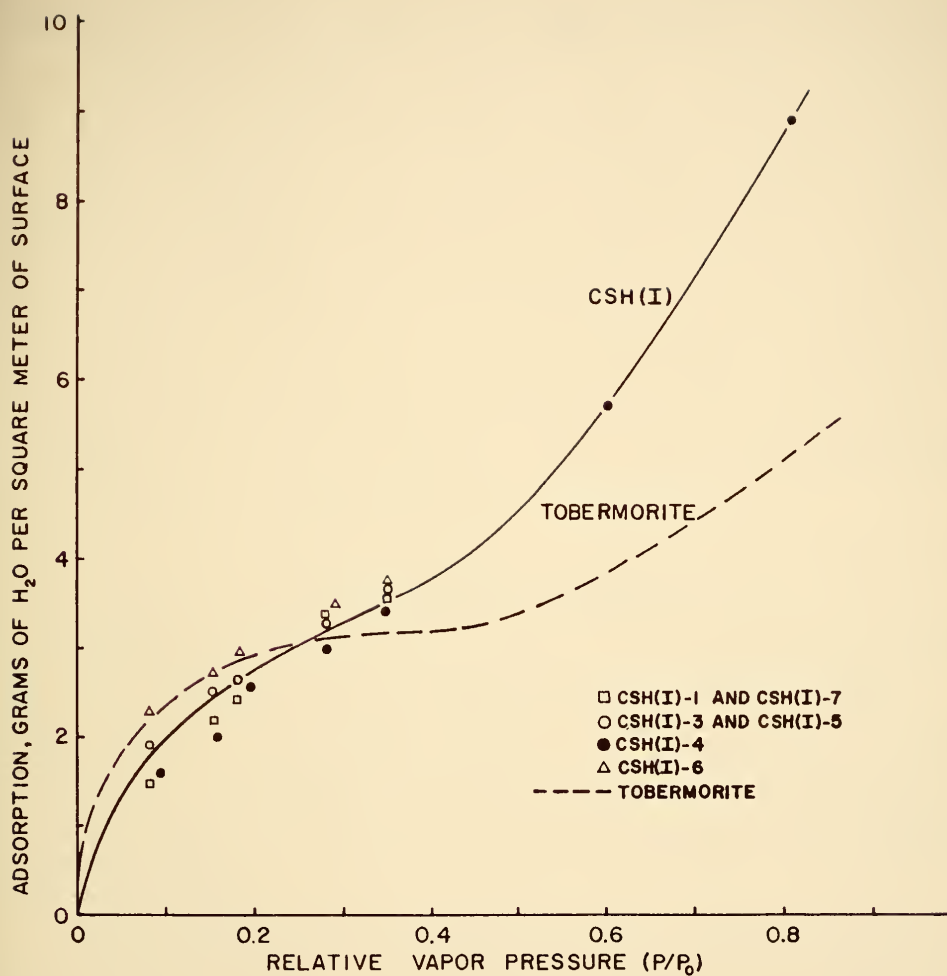


Figure 20. Reduced Water Vapor Adsorption Isotherm for CSH(I) Preparations Compared with that for Tobermorite.



equation for  $n = \text{infinity}$ ; i.e. there seems to be no restriction in the number of layers of adsorbate that can form. This points to a distinctly different kind of surface for the CSH(I) phase.

The data given are for the six crystalline CSH(I) samples. Corresponding data for the amorphous sample, CSH(I) - 2, not plotted in the figure, fall far below the characteristic trend line. This is in agreement with the much lower  $E_1$  calculated for this phase and the two strongly suggest that rather surprisingly, the surface of the amorphous phase has a relatively weak attraction for water vapor.

#### Cation Exchange Capacities

Cation exchange capacities of 5 of the 7 preparations were measured according to the method outlined earlier. Sodium acetate solution in alcohol was used for the removal of potassium exchanged on the samples in this portion of the work, to avoid the gel formation that occurs with these samples when ammonium acetate is used.

The results of these determinations are given in Table 6. The observed exchange capacities are somewhat lower than those of the tobermorites. The exchange capacity does not appear to be correlated with the surface area or other characteristic property of the samples as determined in this study.

The accuracy of some of the results for the very low exchange capacities is uncertain. For these samples the blank correction applied for the effect of potassium held by the polyethylene centrifuge tubes was an appreciable part of the



Table 6. Cation Exchange Capacities of CSH(I) Samples.

Sample	Cation Exchange Capacity in Milli-equivalents per 100 Grams
CSH(I) - 2	(10)?
CSH(I) - 3	19.7
CSH(I) - 5	3.6
CSH(I) - 6	23.9
CSH(I) - 7	8.9





total potassium found. Indeed, for CSH(I) - 5 the blank was actually greater than the potassium exchanged by the relatively small samples used which weighed about 0.15 grams each. Unfortunately, a shortage of material prevented redetermination of this value. The duplication determinations for this sample and for all others except one, agreed with each other within  $\pm 0.3$  of a milli-equivalent per 100 grams. The CSH(I) - 2 samples gave erratic values and the figure cited should be considered an indication of order of magnitude only.

#### Zeta Potential

Attempts to measure the zeta potential of the CSH(I) specimens were not successful due to failure to achieve a satisfactory degree of dispersion. Even after the use of ultrasonic treatment for long periods of time the particles existing in suspension were aggregates that settled to the bottom of the thin microelectrophoresis cell so rapidly that measurement of particle velocity under the influence of an applied electric current was impossible.

However, it was not difficult to determine the direction of travel of the particles, i.e. whether they have a net positive or negative surface charge. Examination of CSH(I) particles dispersed in distilled water indicated that they were negatively charged. When the particles were dispersed in saturated  $\text{Ca(OH)}_2$  solution they were found to be positively charged. Thus, CSH(I) has essentially the same surface charge behavior as tobermorite except for the important distinction that tobermorite particles spontaneously disperse in aqueous suspension



while CSH(I) is apparently effectively cemented into micro-aggregates that resist such dispersion.

### Summary

CSH(I) samples were prepared in a variety of ways at room-temperatures. Four preparations made by double decomposition had Ca:Si ratios very close to 1 and three had  $H_2O:Si$  ratios near 1.6 regardless of initial proportions of reagents used. One preparation made by different means had a similar Ca:Si ratio, but much less water ( $H_2O:Si$  about 1); while one preparation made from a high-lime mixture had both a high calcium content (Ca:Si about 1.6) and high water content ( $H_2O:Si = 1.8$ ); despite the high Ca:Si ratio, this latter preparation is definitely CSH(I).

X-ray diffraction patterns of all but 2 of the specimens were practically identical, showing peaks at 3.02A, 2.78A, 1.82A, and 1.66A, with one or two other very small peaks sometimes observed. One sample was amorphous; another sample initially similar to the others apparently changed on extended storage showed new peaks similar to those reported for xonotlite. Efforts to determine basal spacings were fruitless; well-oriented specimens could not be prepared, presumably due to inability to disperse the CSH(I) samples into primary particles.

The morphology of several samples was observed by electron microscopy. One sample consisted of very thin "snowflakes" or foils and others displayed characteristic spherical "crinkled foil aggregates" and some distinctly thicker platy material. Essentially no individual lath-like or fibrous particles were



present in the samples observed.

DTA revealed a fairly large broad endotherm associated with water removal at low temperatures; a weak endothermic break at about  $660^{\circ}\text{C}$ , a third endotherm at about  $790^{\circ}\text{C}$ , shortly followed by a strong, sharp exotherm. The product shrank as a result of the transition marked by the exotherm. Infrared spectra were similar to those of tobermorite with the following exceptions: the  $1440\text{ cm}^{-1}$  ( $6.95\text{ }\mu$ ) band attributed to carbonate is much stronger and the water deformation band is weaker or almost absent; there is no band in the  $1100\text{-}1200\text{ cm}^{-1}$  ( $8.3\text{-}9.0\text{ }\mu$ ) range, and general absorption on the low frequency side of the main Si-O band is noticeably greater, especially for the samples with higher calcium content.

Some specific differences in spectra were found among the CSH(I) samples.

The surface areas found ranged from 150 to  $350\text{ m}^2/\text{g}$ , somewhat greater than the values for tobermorite. Surface area is not correlated with crystallinity. Heats of adsorption of water vapor from the BET determination were slightly less than the corresponding values for tobermorite, and the isotherms did not show any indication of adsorption being restricted to a definite number of layers. The amorphous sample had a distinctly lower heat of adsorption for water, and the amount of water adsorbed per unit area of surface at a given partial pressure was also distinctly less. Measured cation exchange capacities ranged from 4 to 24 milli-equivalents per 100 grams and did not appear to correlate with other properties in any recognizable



manner. Zeta potential could not be determined but it was shown that, like tobermorite, the particles of CSH(I) are charged negatively in distilled water and positively in saturated solutions of  $\text{Ca}(\text{OH})_2$ .

### Calcium Silicate Hydrates Produced by Hydration of $\beta\text{-C}_2\text{S}$ and $\text{C}_3\text{S}$

#### Origin and Composition

The common methods in use for hydrating these phases have been discussed in detail in the literature review and details of the methods used in the present study have already been given. Table 7 gives the pertinent information on the designation, origin and mode of treatment of the samples prepared in the present study.

No attempt was made to establish the chemical composition of the CSH(gel) materials themselves, since existing techniques for the removal of "excess" lime produced as a by-product of the reaction are difficult and tedious and the validity of the separation is open to question. Chemical analysis of the starting phases are given in the Appendix.

In addition to the samples listed, bottle hydration products were prepared for a second sample of  $\text{C}_3\text{S}$  and a second sample of alite donated by the Portland Cement Association; however, results were essentially identical to those cited for similar samples recorded in the table.





Table 7. Hydration Products of  $\beta$ -C<sub>2</sub>S, C<sub>3</sub>S, and Alite.

Starting Material	Source and Code Designation	Method of Hydration	Time of Hydration	Water-Cement Ratio
$\beta$ -C <sub>2</sub> S	P.C.A. Sample B-91	Paste	7 months	0.4
C <sub>3</sub> S	P.C.A. Sample B-101	Paste	7 months	0.4
$\beta$ -C <sub>2</sub> S	P.C.A. Sample B-91	Bottle	6 months	9.0
C <sub>3</sub> S	P.C.A. Sample B-101	Bottle	6 months	9.0
Alite	P.C.A. Sample B-93	Bottle	4 months	9.0
Alite	A. Klein, U. of Calif., "Sept."	Bottle	4 months	9.0



### X-Ray Diffraction Results

Figure 21 presents x-ray diffractometer traces of the products of hydration of  $\beta$ - $C_2S$ ,  $C_3S$ , and alite, as listed in Table 7. The peaks for the CSH(gel) phase are shaded; those for  $Ca(OH)_2$  formed in the hydration reaction are marked with a "C"; those for the residual starting compound are marked with an "A" for  $C_3S$  or alite, and with a "B" for  $C_2S$ . In general the calcium silicate hydrate formed gives only a weak pattern, broader and even less well-crystallized than that of CSH(I).

The pattern for CSH(gel) P - 1 showed a definite portion of unreacted  $\beta$ - $C_2S$  remaining in the paste; the amount of crystalline  $Ca(OH)_2$  formed is apparently small. The corresponding pattern for CSH(gel) P - 2, made from  $C_3S$ , showed much more  $Ca(OH)_2$ , as expected; almost all of the  $C_3S$  starting material seems to have reacted.

In all of the bottle-hydrated products  $Ca(OH)_2$  is present in well-formed platy crystals, some of which are large. Despite the effort to maintain random orientation in the x-ray powder mount these crystals seem to have been exceedingly well-oriented, the (001) spacing of the  $Ca(OH)_2$  at 4.92A being greatly enhanced.  $\beta$ - $C_2S$  hydrates very slowly even under the bottle-hydration conditions; a considerable pattern still remained for this phase in CSH(gel) B - 1. Again,  $C_3S$  and one of the two alites reacted almost completely, and produced a larger proportion of lime, in line with the stoichiometry of the hydration reactions; the other alite product has not reacted so completely.



A  $C_3S$  or ALITE

B  $\beta C_2S$

C  $-Ca(OH)_2$

SHADED PEAKS CSH (GEL)

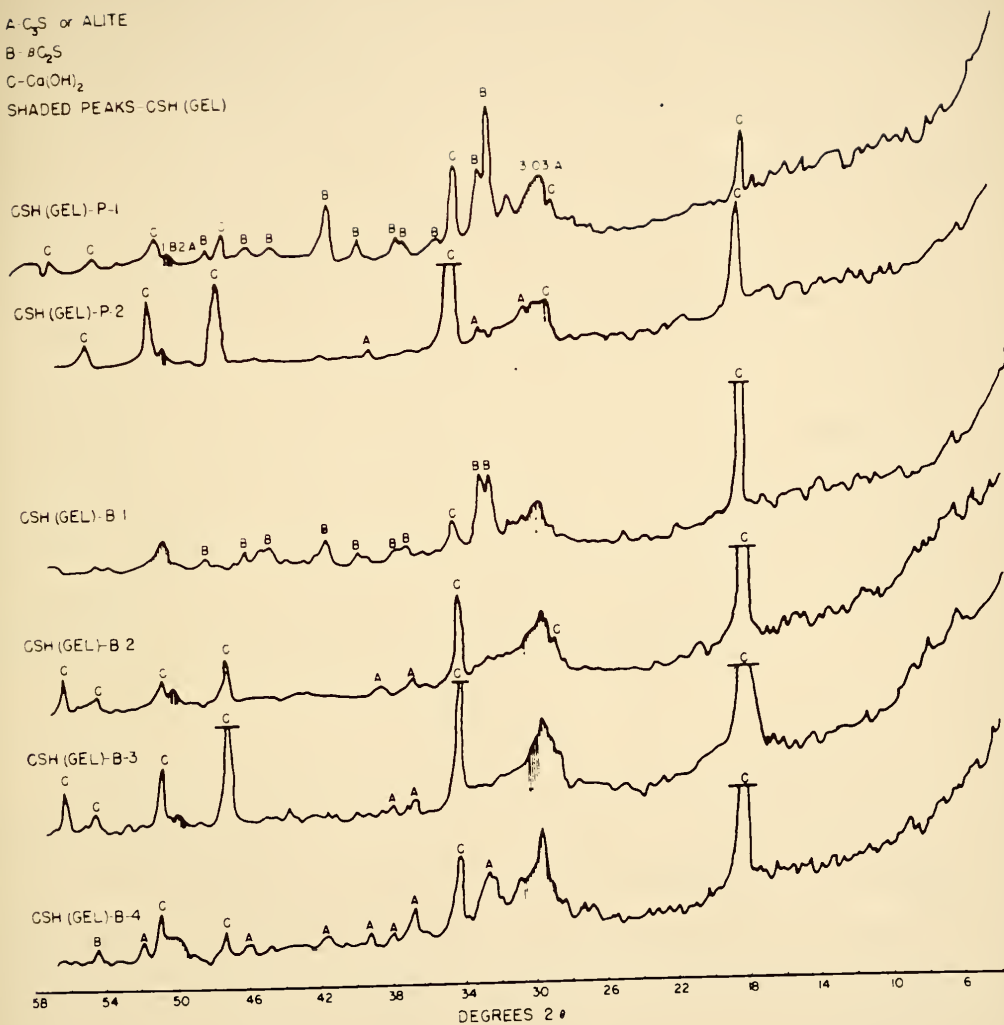


Figure 21. X-ray Diffractometer Traces for Paste and Bottle Hydration Products of  $\beta C_2S$ ,  $C_3S$  and Alite.



The basal spacings of CSH(gel) are very difficult to obtain. Brunauer and Greenberg (1962) reported only a single instance of an (001) spacing being recorded in their laboratory, an 11A spacing on a dried product which was never reproduced. Several attempts at finding these peaks for the present CSH(gel) products were made by using the porous tile mount procedure of Kinter and Diamond (1955). All processing was done under nitrogen insofar as possible. Figure 22 presents the only successful result obtained; this was for the bottle-hydrated  $C_3S$  product, CSH(gel) B - 2. Most of the lime has apparently been left behind in the water dispersion process. The sample shows a strong 14A basal spacing and an apparent higher order reflection at 7A. Similar attempts to demonstrate a basal spacing for the other samples were not successful.

### Morphology

Paste-hydrated  $\beta$ - $C_2S$  and  $C_3S$  usually show a distinctly fibrous morphology in electron microscopic examination after the usual dispersion technique involving ultrasonic treatment; the fibers are apparently composed of thin rolled up sheets (Copeland and Schulz, 1962). Figure 23A is a representation of a typical field observed for CSH(gel) P - 2, the paste hydration product of  $C_3S$ , after dispersion with the non-aqueous technique described earlier which does not involve ultrasonic treatment. Some of the particles can be described as fibers, the rest being more or less equant in shape; the latter may actually be bundles of undispersed fibers, but this is not at





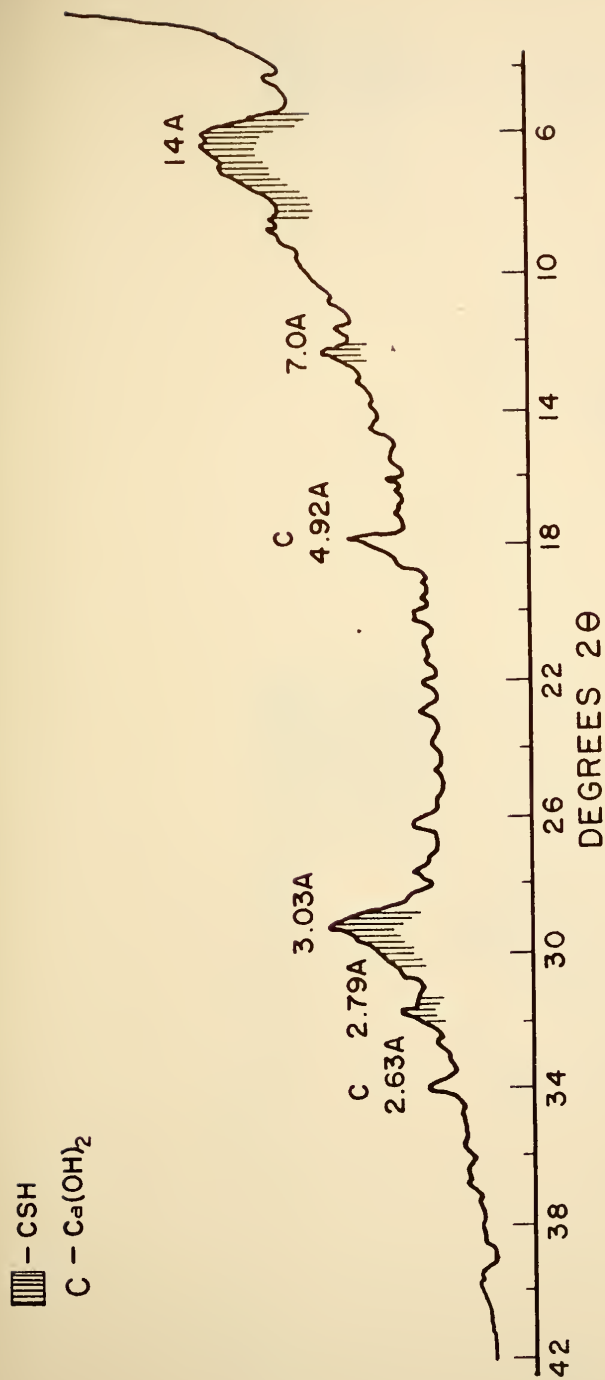
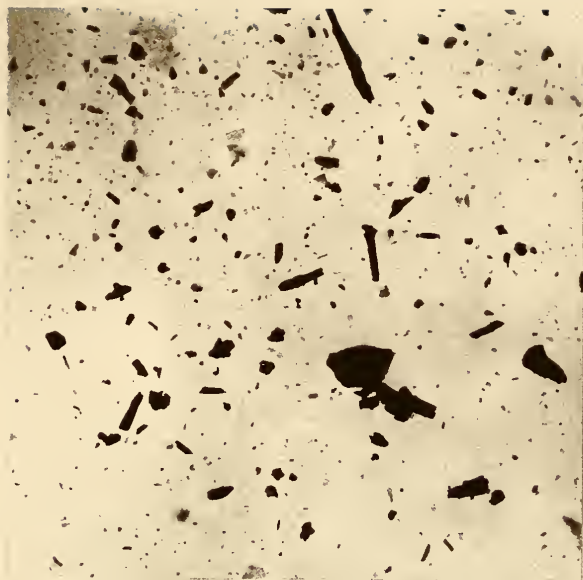


Figure 22. X-ray Diffractometer Trace for Moist CSH(gel) B - 2 Prepared as an Oriented Aggregate on a Porous Tile Mount.



(A)



(B)



Figure 23. Electron Micrographs of Paste and Bottle Hydration Products of  $C_3S$ . (A) Paste Product, CSH(gel) P - 2. (B) Bottle Product, CSH(gel) B - 2.



all evident. In addition, there are a number of very thin, flat, sheet-like particles in the field which show no apparent tendency to roll up into tubes or fibers.

Figure 23B shows the morphology of CSH(gel) B - 2, the bottle-hydration product of  $C_3S$ . These particles seem to be completely fibrous, with a few bundles of undispersed fibers clearly visible. Nothing comparable to the relatively large proportion of equant particles found in Figure 22A is evident.

Figure 24 shows the product designated CSH(gel) B - 1, a product of the bottle-hydration of  $\beta$ - $C_2S$ . Here the fibrous morphology is more evident, most of the particles apparently being aggregates of fibers. According to Copeland and Schulz (1962), Brunauer and Greenberg (1962) and others, such a preparation should yield CSH(II), with a distinctive cigar-shaped fiber bundle morphology and a slightly different x-ray diffraction pattern than CSH(gel). Neither of these criteria are met by the present sample; both morphologic and x-ray evidence indicates CSH(gel) and not CSH(II) has been formed.

#### Differential Thermal Analysis

The DTA results for the CSH(gel) products secured on the Eberbach portable instrument are given in Figure 25. The patterns are very much alike; all have a low-temperature endotherm, a  $Ca(OH)_2$  dehydroxylation endotherm at about  $570^\circ C$  (greater for the  $C_3S$  products than for the  $C_2S$  products) and a small high temperature exotherm at about  $860^\circ C$ . This exotherm is greater than that produced by unsubstituted tobermorite,



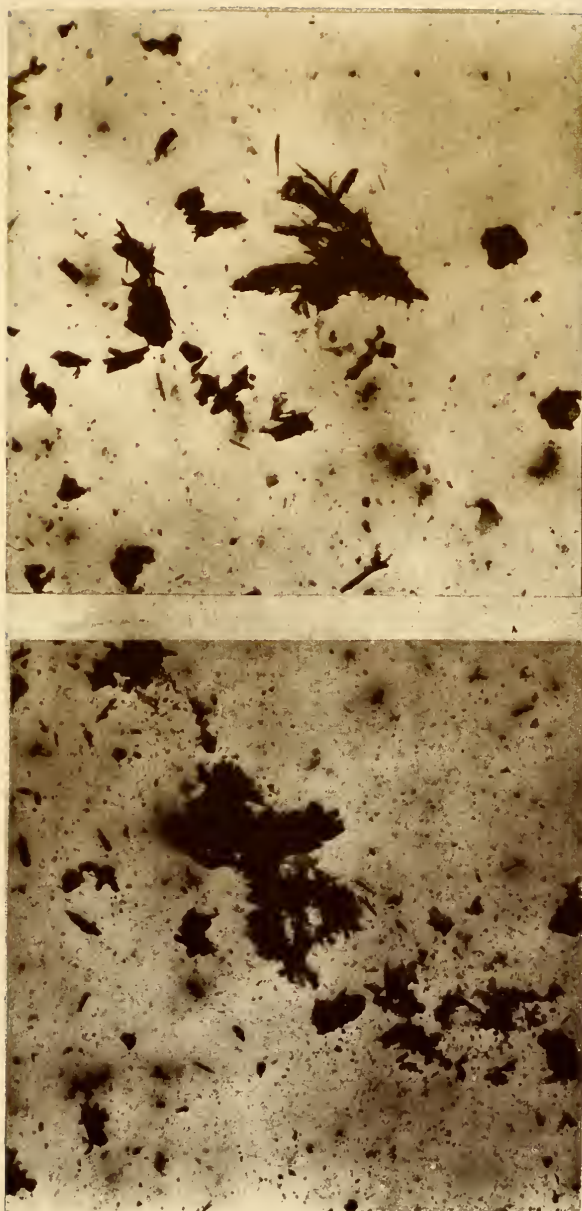


Figure 24. Electron Micrographs of Bottle-Hydrated  $\beta$ -C<sub>2</sub>S,  
CSH(gel) B - 1.





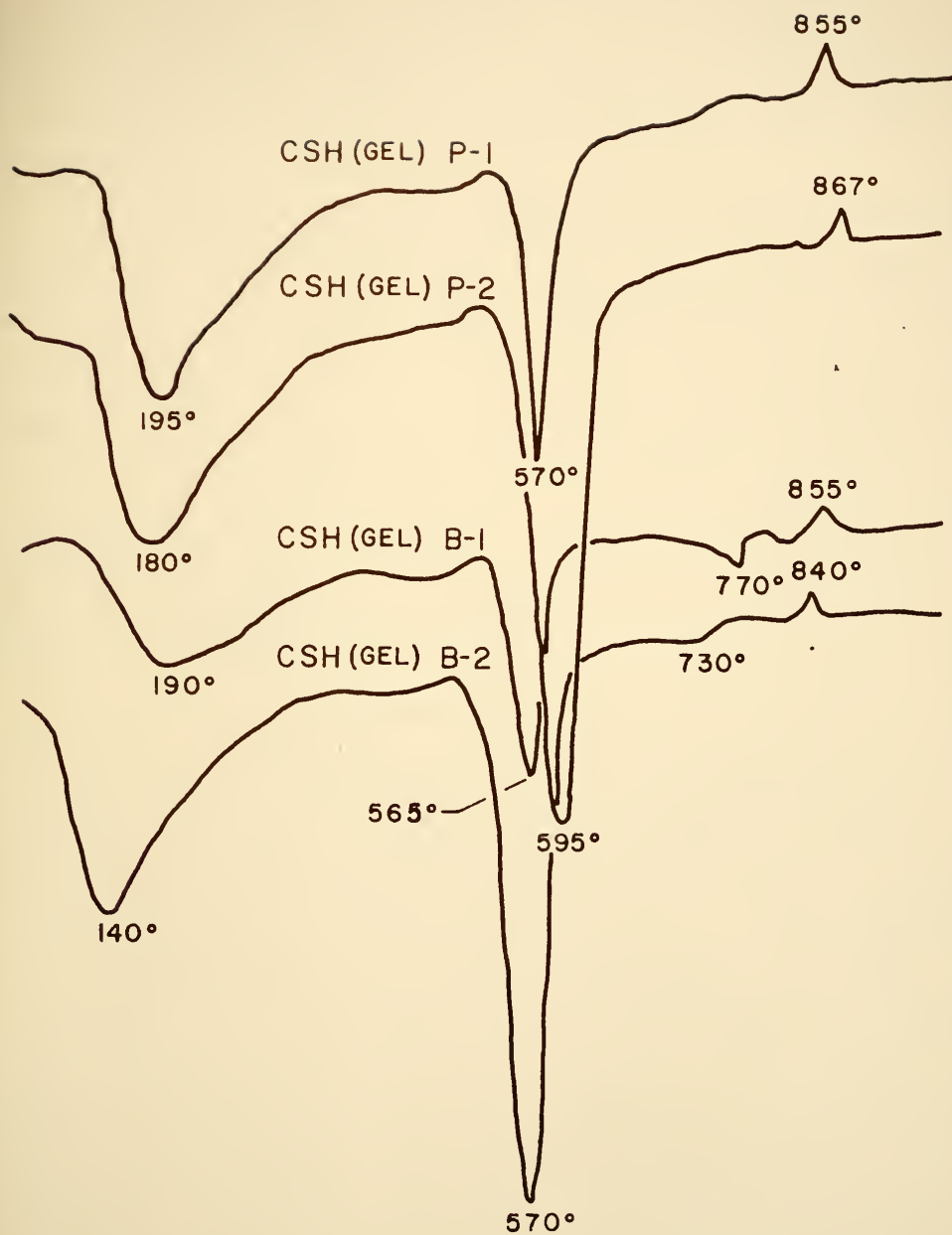


Figure 25. Differential Thermal Analysis of CSH(gel) Products. Heating Rate Varies from 58°C to 5°C per Minute.



but not as large as that for CSH(I). In most of the curves there is a small endothermic break at about 730°C which may result from a trace of calcium carbonate due to atmospheric carbonation.

The patterns for the alite products (CSH(gel) B - 3 and 4, not shown in the figure) resemble closely those from products prepared from unsubstituted  $C_3S$ . The amount of water lost at low temperature by CSH(gel) B - 3 was less than the others; this sample was also shown by x-ray diffraction to have reacted to a lesser extent than the other  $C_3S$  type samples. The basic similarity of all these patterns (except for the extent of the lime peak) offers support for the concept of CSH(gel) as a phase distinct from CSH(I) or CSH(II).

#### Infrared Absorption

The infrared absorption spectra for the CSH(gel) samples are given in Figure 26. The procedure involved in specimen preparation was exactly the same as that used earlier, but due to equipment difficulties, it was necessary to run the samples on a different instrument, a Perkin-Elmer Model 221. This instrument has a readout that is linear with respect to wavelength rather than with respect to frequency, which has the effect of stretching out the infrared pattern at the low frequency end of the chart. One of the samples (CSH(gel) B - 3) was run on both the 421 and the 221 instruments; the recorded positions and intensities of the bands were in good agreement, although the apparent sharpness of the low-frequency peaks is much reduced with the present instrument.



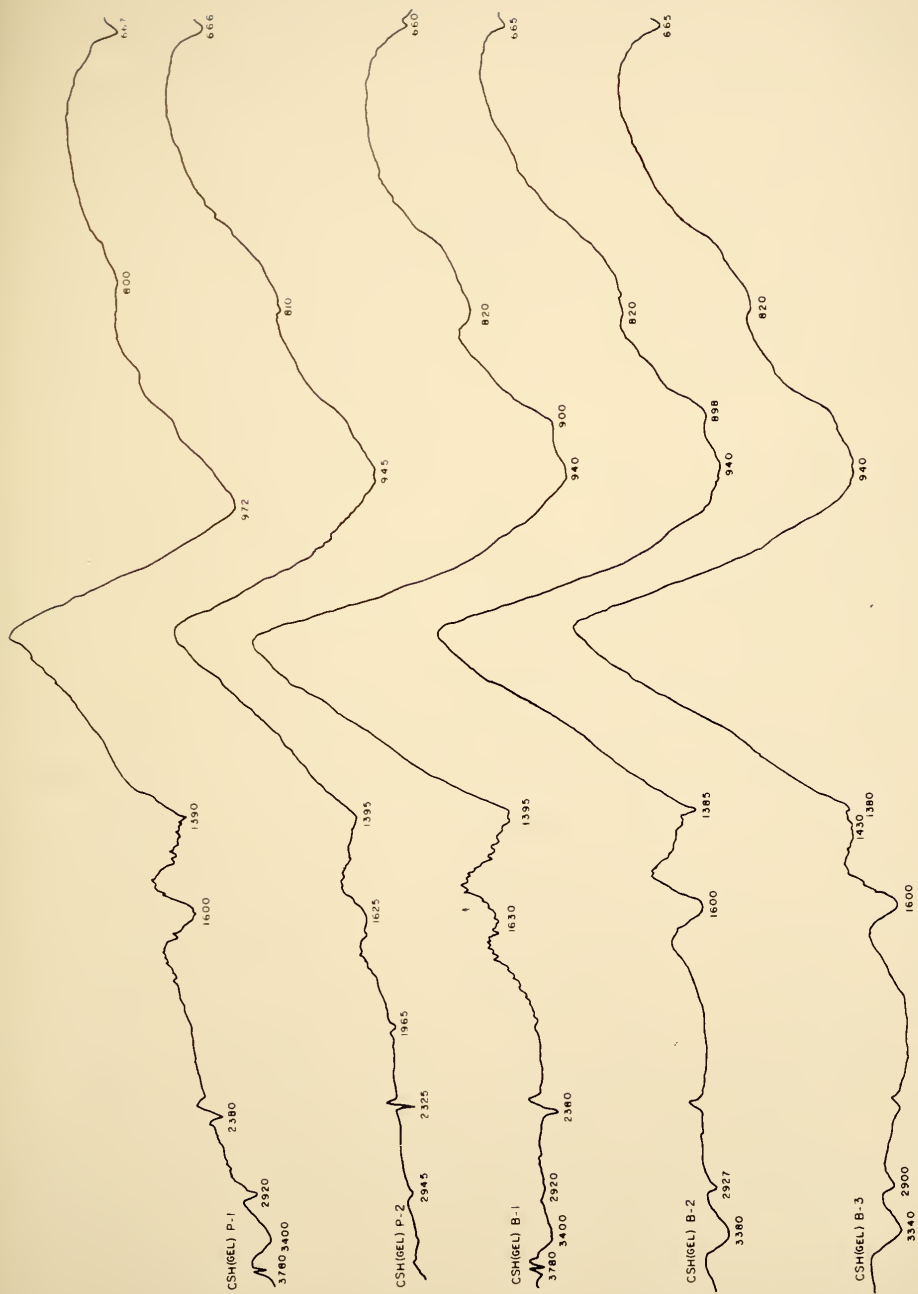


Figure 26. Infrared Absorption Spectra for CSH(gel) Products.



The spectra for all the CSH(gel) samples are similar. The most prominent feature is the pronounced minimum in absorption that occurs at about  $1100\text{ cm}^{-1}$  ( $9.0\ \mu$ ), as compared with much smaller minima in absorption at approximately this position for other CSH products. This feature may be an artifact of specimen preparation, since it is not observed in infrared spectra of corresponding minerals by Lehmann and Dutz (1959) or by Hunt (1959), who used the KBr pellet procedure involving sample disseminated throughout the KBr disc.

The main Si-O lattice vibration band is extremely broad and occurs at about  $940\text{ cm}^{-1}$  for all samples except the  $\beta\text{-C}_2\text{S}$  paste hydration product, where the position of the maximum is about  $970\text{ cm}^{-1}$ . Except for this specimen, the position of the maximum is distinctly lower in frequency than those of tobermorites ( $970\text{ cm}^{-1}$ ) and those of CSH(I) preparations ( $950\text{-}980\text{ cm}^{-1}$ ). Lehmann and Dutz (1959) have interpreted the low frequency position of this maximum for cement hydration products as being indicative of the degree of polymerization of the silica tetrahedra, the theoretical value for completely independent  $\text{SiO}_4$  tetrahedra being  $935\text{ cm}^{-1}$ . These results thus support the idea that the tetrahedra in CSH(gel) are largely unpolymerized.

Secondary broad absorption features are observed at about  $900\text{ cm}^{-1}$  and at about  $820\text{ cm}^{-1}$  in most of the samples. These are also presumably associated with the silicate lattice structure.

The next most prominent features are the bands at  $1600\text{-}1630\text{ cm}^{-1}$  and  $1380\text{-}1395\text{ cm}^{-1}$ . The former are attributed to the





water deformation vibration and the latter to the asymmetrical in-plane vibration of  $\text{CO}_3^{=}$  as suggested by Hunt (1959). It is noteworthy that the position of this band is distinctly lower in frequency than the corresponding bands in CSH(I) and in tobermorite, suggesting that the carbonate combined as a result of incidental carbonation of the samples in the atmosphere is rather more tightly held in these high-surface area materials.

Small spectral features of unknown origin are observed at about  $2380 \text{ cm}^{-1}$  and again at about  $2920 \text{ cm}^{-1}$ . A small stretching vibration for bonded OH is observed at about  $3400 \text{ cm}^{-1}$  and for two of the samples a small sharp vibration at  $3780 \text{ cm}^{-1}$ , which may be one of a complex set of OH stretching vibrations characteristic for  $\text{Ca(OH)}_2$ . However, it was observed only for the CSH(gel) derived from  $\beta\text{-C}_2\text{S}$  and thus may have some other explanation. The comments previously made about the small size of the bonded OH band in the present spectra compared to those published by other workers who used KBr pellets are applicable here.

#### Surface Area

In view of the many water vapor surface area measurements of CSH(gel) products by the Portland Cement Association workers, and the experimental difficulties involved in correcting for the effects of other phases that are present, surface area determinations for these CSH(gel) samples were not attempted.

#### Cation Exchange Capacity

Cation exchange capacity determinations were made on the



CSH(gel) samples by a procedure which involved removal of the replaced potassium ions with ammonium acetate solution. A gel set up in some of the samples but mechanical agitation broke up most of the gel structure before the potassium-containing suspension was centrifuged and decanted. Because of the uncertainty that must be attached to their significance the values obtained are not tabulated. However, it is of interest to note that the two paste products (CSH(gel) P - 1 and P - 2) had values close to 15 and 20 meq/100 g respectively. Of the bottle-hydrated products, no measurement was obtained for the  $\beta$ -C<sub>2</sub>S product, but the C<sub>3</sub>S product yielded a value of about 7 meq/100 g. The two bottle-hydrated alites both yielded values of about 18 meq/100 g.

Separate measurements were made of the apparent cation exchange capacities on the other constituents present in the products in addition to the calcium silicate hydrate; i.e. Ca(OH)<sub>2</sub> and the  $\beta$ -C<sub>2</sub>S, C<sub>3</sub>S, and alite unhydrated phases. The lime had no exchange capacity, as expected, and all of the anhydrous calcium silicate starting materials showed very similar small values of about 3 meq/100 g. Thus, as expected, essentially all of the CEC of the CSH(gel) products is attributable to the CSH(gel) phase itself.

#### Zeta Potential and Surface Charge

Attempts to measure the zeta potential of the CSH(gel) materials were even less successful than those with CSH(I); dispersions adequate for the purpose could not be obtained.



However, it was determined that CSH(gel) particles are similar to other calcium silicate hydrates with respect to reversal of the sign of the surface charge. Samples dispersed in saturated  $\text{Ca(OH)}_2$  were strongly positive, but if the products were dispersed and washed repeatedly in distilled water to remove the accompanying  $\text{Ca(OH)}_2$  their positive charge was visibly decreased, and at a pH of about 10 the particles were converted to negatively-charged ones.

### Summary

CSH(gel) samples were prepared by paste and by bottle hydration of  $\beta\text{-C}_2\text{S}$ ,  $\text{C}_3\text{S}$  and alite. The materials exhibit only several very weak and broadened x-ray lines for the CSH(gel) phase; lines for  $\text{Ca(OH)}_2$  and in some samples, for unreacted starting material were observed. A basal spacing of 14Å was found on a specially-prepared mount of one sample (a bottle-hydrated  $\text{C}_3\text{S}$  product). The specimens of paste-hydrated  $\text{C}_3\text{S}$  examined by electron microscopy appear to be only partially fibrous or lath-like; equant-shaped particles are also observed. The bottle-hydrated  $\text{C}_2\text{S}$  product produced in this experiment is CSH(gel), not CSH(II). DTA results for all phases are similar, showing a large amount of water removed at low temperatures, a strong endotherm at about  $570^\circ\text{C}$  for dehydroxylation of  $\text{Ca(OH)}_2$ , a small endothermic break at about  $730^\circ\text{C}$ , possibly due to carbonation, and a fairly definite but relatively weak exotherm at about  $860^\circ\text{C}$ . Infrared absorption disclosed that the main SiO band was broadened and occurred at about  $940\text{ cm}^{-1}$ ; secondary broadened maximum occurrence at about  $900\text{ cm}^{-1}$  and



820  $\text{cm}^{-1}$ , and the band attributable to  $\text{CO}_3^{=}$  asymmetrical stretching mode occurred at a lower frequency than previously observed, 1390  $\text{cm}^{-1}$ .

Surface areas and zeta potentials were not measured, but it was shown that the CSH(gel) particles, normally positive in view of the  $\text{Ca}(\text{OH})_2$  present, are converted to negatively-charged ones on extended washing in distilled water. Cation exchange measurements yielded values ranging from 7 to about 20 milli-equivalents per hundred grams, but the reliability of these measurements is somewhat uncertain.

#### Products of Chemical Reaction Between $\text{Ca}(\text{OH})_2$ and Silicate Minerals At or Near Room Temperature

##### Reaction of Compacted Mixtures at 60°C

Starting Materials, Reaction Conditions, and Methods of Examination of Products. This mode of reaction was designed to simulate to some degree the conditions under which lime and soil minerals might react in soil stabilization practice. The materials were mixed, moistened, compacted and left to cure in a manner more or less analagous to that which would occur in the field. To facilitate identification of the products of the reaction a larger proportion of lime was used (40% by weight of the silicate) than could be considered in practice and to speed up the reaction a temperature (60°C) higher than would be reached in the field was used. The details of the procedure and of the nature of the starting materials are given in the section on Materials and Procedures.





The resulting products were examined principally by x-ray diffraction, DTA and electron microscopy; water-vapor sorption measurements were also performed on them. The DTA of these materials was run on the Bureau of Public Roads apparatus.

Reaction Product of Quartz. The material examined after the two month reaction period had obviously undergone cementation; apparently it was dry and cemented strongly enough so that it rang when struck; a hammer and chisel had to be employed to remove some of it from the container. Nevertheless, despite the apparent dry state of the material the moisture content as determined by oven drying at  $110^{\circ}\text{C}$  was almost 50% by weight of solids. Figure 27 shows x-ray diffractometer traces for the reacting mixture and for the powdered product. The peaks for  $\text{Ca}(\text{OH})_2$  have been reduced greatly in intensity, and new peaks attributed to a CSH phase are shown at 3.03A, 2.93A and approximately 2.84A. A strong quartz peak at 1.81A (not shown) interferes with the observation of any possible CSH peak at this position. The pattern for the initial mixture shows a small peak at 3.03A suggesting a slight contamination of the  $\text{Ca}(\text{OH})_2$  with  $\text{CaCO}_3$ , but it is evident that no additional carbonation has occurred during the course of the reaction. The DTA pattern of the product (Figure 28) failed to reveal any low-temperature endothermic response, but showed a small peak for residual  $\text{Ca}(\text{OH})_2$  at  $520^{\circ}\text{C}$ , the residual quartz peak, a small peak at  $765^{\circ}\text{C}$  possibly due to carbonation and, significantly, a relatively small, but definite, high temperature exotherm at  $885^{\circ}\text{C}$ , suggesting the formation of a CSH(gel) phase.



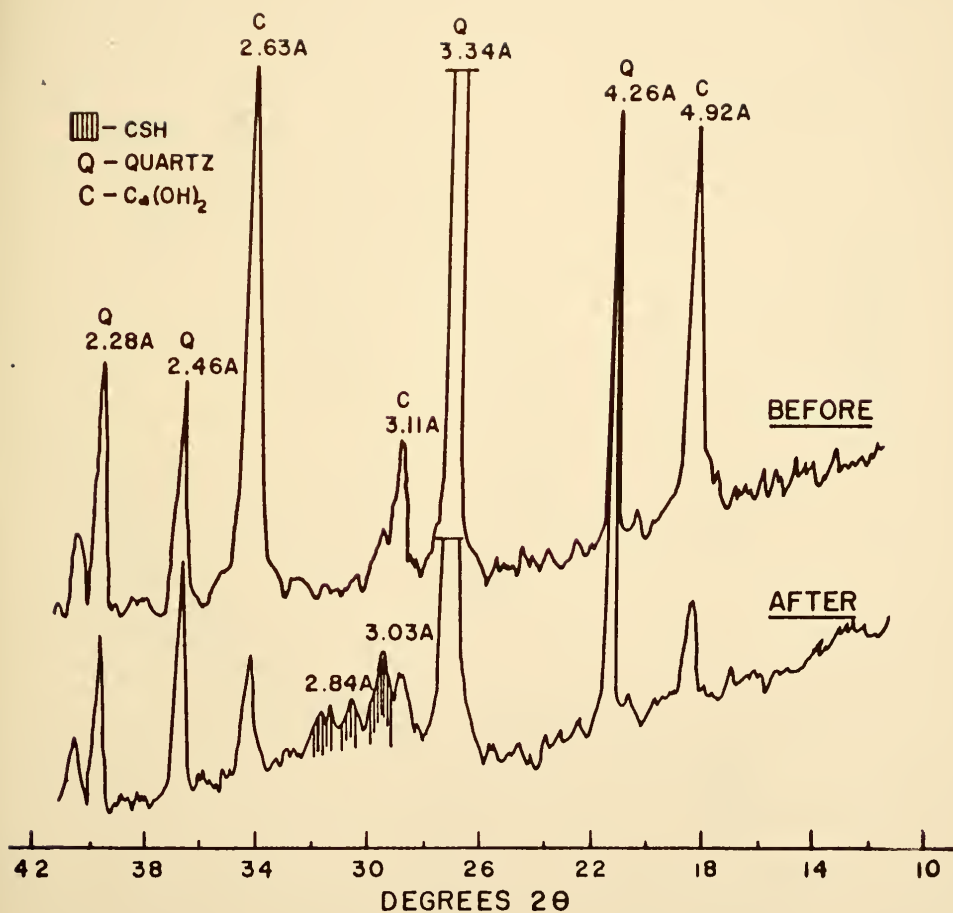


Figure 27. X-ray Diffractometer Traces of Quartz- $\text{Ca}(\text{OH})_2$  Mixture Before and After Reaction at  $60^\circ\text{C}$ .



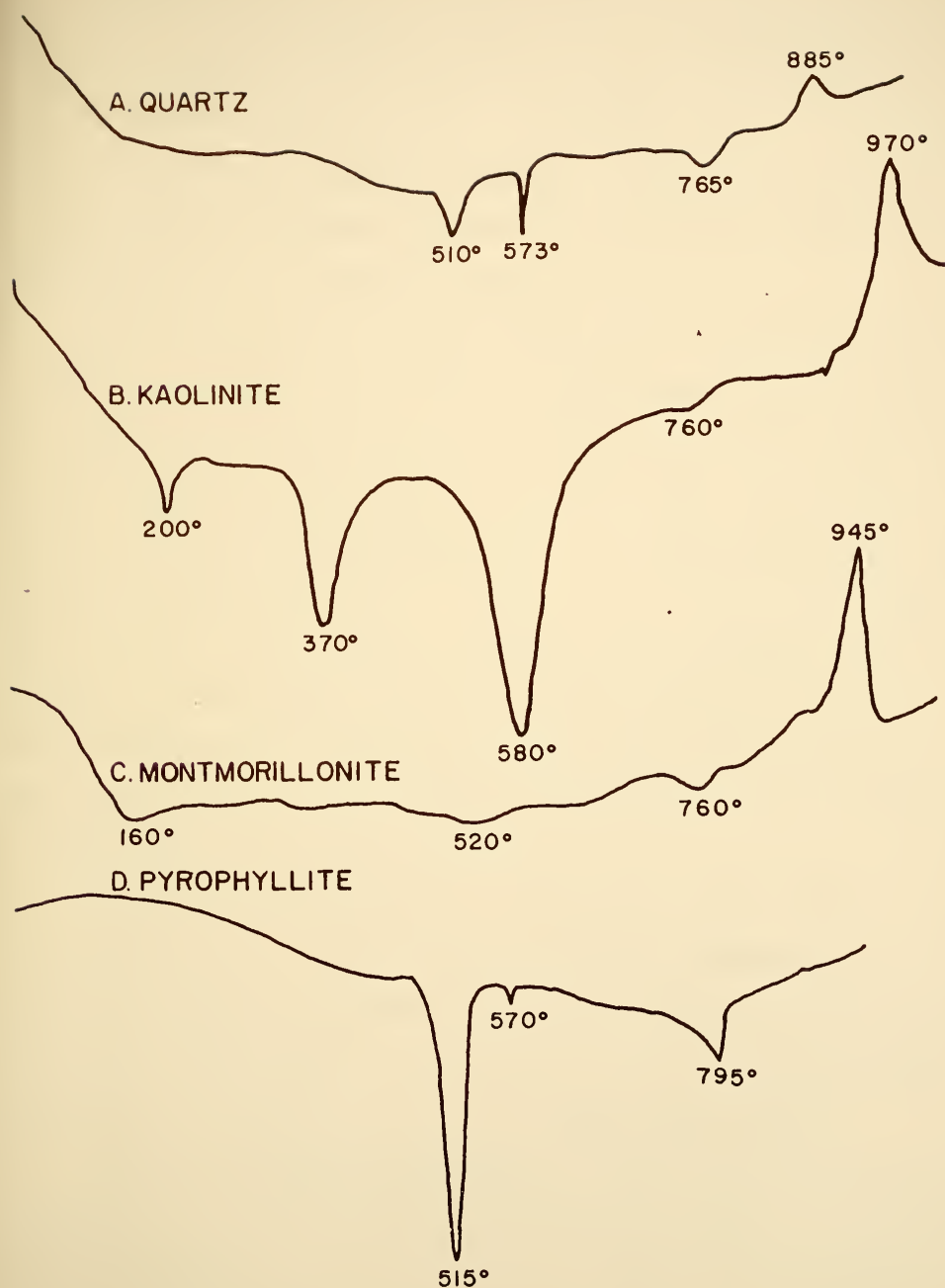


Figure 28. Differential Thermal Analysis of Products of  $\text{Ca}(\text{OH})_2$ -Silicate Reactions at  $60^\circ\text{C}$ . Heating Rate  $10^\circ\text{C}$  Per Minute.



Electron microscopy of the product (Figure 29A) was revealing. Evidently the dispersion procedure had segregated out the coarse residual quartz particles, which are not visible here. The reaction products consist entirely of well-shaped fibers which are obviously rolled up sheets--the "classical" morphology for the CSH(gel) phase.

The surface area of the  $\text{Ca}(\text{OH})_2$  used in preparing these mixtures was measured by water vapor adsorption and using an area per  $\text{H}_2\text{O}$  molecule of 10.3A on this surface (Brunauer, Kantro, and Weise, 1956) the value found was  $36 \text{ m}^2/\text{g}$ . The surface area of the quartz was so small it could not be measured; thus the calculated surface area of the initial mixture was less than  $23 \text{ m}^2/\text{g}$ . The measured surface of the material after reaction was more than twice this value, or  $53 \text{ m}^2/\text{g}$ . The reacted material still contained much of the original quartz and some lime; thus the surface area of the CSH(gel) formed is much higher than this value.

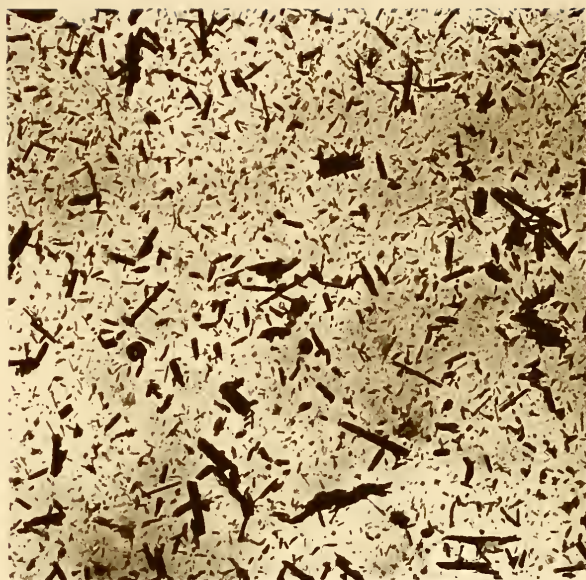
Thus despite the failure of Glenn and Handy (1963) to note any reaction of lime with quartz at room temperature for up to two years, under the present conditions quartz reacted strongly with lime in two months to produce a fibrous CSH(gel) product of excellent cementing ability and high surface area.

Reaction Product of Kaolinite. It was also obvious from the hardness of this material after reaction that a cementitious reaction product had been produced. A comparison of the x-ray diffractometer traces of the reaction mixture and of the products (Figure 30) provides striking evidence for this. The





(A)



(B)

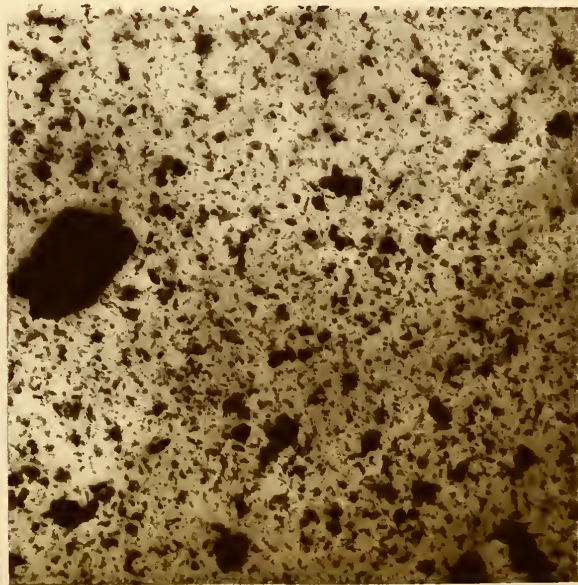


Figure 29. Electron Micrographs of  $\text{Ca}(\text{OH})_2$ -Silicate Reaction Products at  $60^\circ\text{C}$ . (A) Quartz. (B) Kaolinite.



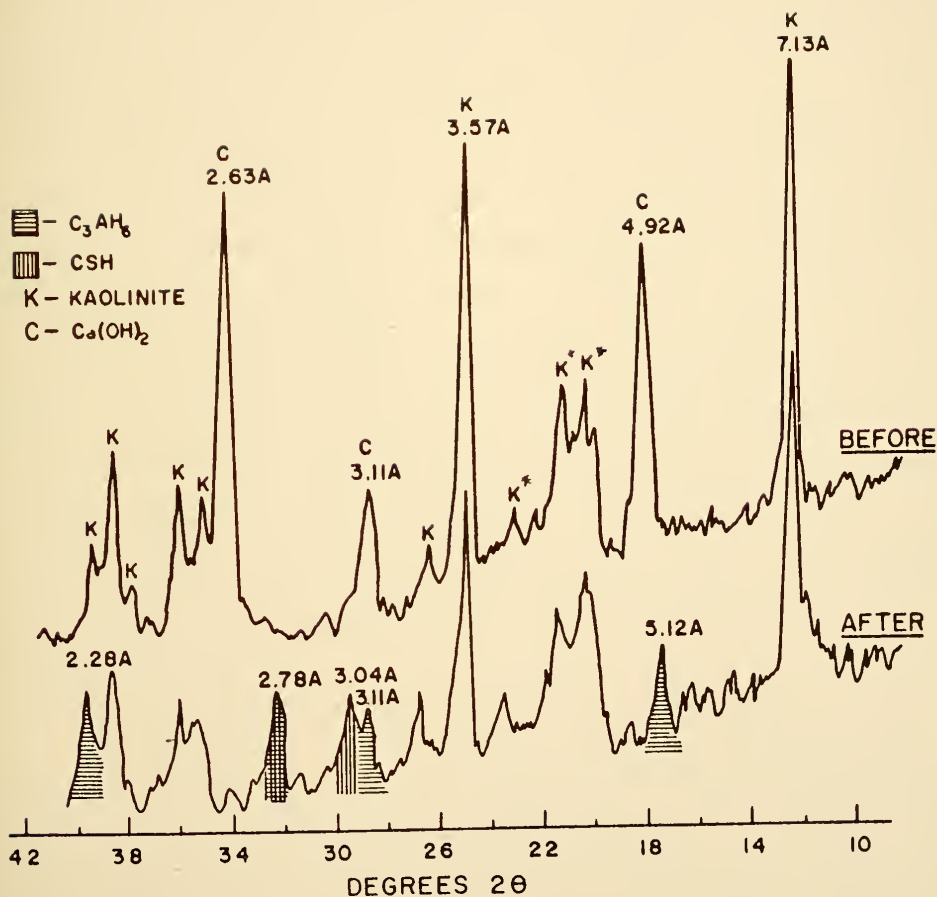


Figure 30. X-ray Diffractometer Traces of  $\text{Ca}(\text{OH})_2$ -Kaolinite Mixture Before and After Reaction at  $60^\circ\text{C}$ .



$\text{Ca(OH)}_2$  lines have completely disappeared from the pattern for the reacted material. The kaolinite lines have been reduced in intensity, particularly the (00 $\bar{1}$ ) lines. The integrated peak intensity of the basal peak at 7.13Å was measured in a special study involving duplicate integrated intensity determinations of five separate random powder mounts for both the "starting mixture" and the reacted product. The average integrated intensity of the kaolinite peak before reaction was 117 arbitrary units; that of the reacted product was 69 arbitrary units, suggesting that about 60% of the original kaolinite was left and about 40% had reacted with lime. Eades and Grim (1960) suggested that the prism or (hk0) reflections were initially broadened and their intensity reduced; the present pattern suggests that these reflections (marked with an asterisk) retained their sharpness and intensity and that it is primarily the basal spacings that are reduced. Inspection of the kaolinite (001) peak also reveals a degree of broadening on the low angle side, which suggests slight expansion of some of the layers.

The appearance of a number of new x-ray lines for the reaction products was noted. The pattern reveals definite peaks at 3.04Å and at 2.98Å corresponding to the CSH(gel) lines noted earlier for the quartz reaction product, and a smaller peak is also present at 1.79Å. In addition to these lines, a series of lines is present at 5.12Å, 3.11Å, 2.78Å and the peak at 2.28Å is grossly enlarged. These lines are all attributed to the cubic  $\text{C}_3\text{AH}_6$  calcium aluminate hydrate. This is the



stable calcium aluminate hydrate and the phase that one would expect to find at this relatively high temperature. Since the kaolinite releases just as many moles of alumina as it does silica on its decomposition, the appearance of this phase is not surprising.

The DTA pattern for the reaction product is given in Figure 28. The complete absence of any  $\text{Ca}(\text{OH})_2$  dehydroxylation peak confirms that all the lime has reacted. The prominent features are a relatively small low-temperature endotherm at  $200^\circ\text{C}$ , a second stronger one at  $370^\circ\text{C}$ , the kaolinite dehydroxylation peak at  $580^\circ\text{C}$ , and a broadened kaolinite recrystallization exotherm at  $980^\circ\text{C}$ . The latter peak actually appears to start at about  $900^\circ\text{C}$  and this first portion may be due to the CSH product. The first two endothermic peaks are difficult to interpret; presumably they should be attributable to CSH and  $\text{C}_3\text{AH}_6$ . The latter has two endotherms in this region according to Majumder and Roy (1956), but these authors found a strong endotherm at  $325^\circ\text{C}$  and a weaker one at  $480^\circ\text{C}$ .

The morphology of this material as revealed by electron microscopy is shown in Figure 29B. The material is apparently not the CSH(gel) found in the preceding material, but rather definitely a typical thin foil CSH(I) product. There are some darker, thicker particles of relatively small size that may be the  $\text{C}_3\text{AH}_6$  phase. There is one large particle in the field that is obviously a residual kaolinite particle; one can observe how the edges appear to have been frayed by chemical attack, and in the corner a small section appears to have







partially exfoliated.

Surface area measurement on the kaolinite gave poor results, but the order of magnitude was about  $20 \text{ m}^2/\text{g}$ , leading to an estimated average surface area for the reacting mixture of  $24 \text{ m}^2/\text{g}$ ; the surface area measured for the product was  $66 \text{ m}^2/\text{g}$ , again indicating that products of high surface area were formed.

Thus the results for the kaolinite-lime reaction under these conditions reveal that the  $\text{Ca}(\text{OH})_2$  has reacted with about 40% of the kaolinite to produce two reaction products; a calcium silicate hydrate that is apparently CSH(I) and the cubic calcium aluminate hydrate,  $\text{C}_3\text{AH}_6$ .

Reaction Products of Montmorillonite. It was obvious from the hardness of the sample after reaction that cementitious reaction products had been produced; although the moisture content removable on oven drying was 60%. Diffractometer traces for the reacting mixture and for the reaction product are given in Figure 31. The  $\text{Ca}(\text{OH})_2$  has completely reacted. The peaks of the residual montmorillonite, although lessened in intensity, have not been appreciably disordered. The position of the (060) peak (not visible in the chart) is unchanged at  $1.495\text{\AA}$ . There is a small amount of quartz present in the original bentonite, as can be seen from its main peak at  $3.34\text{\AA}$ ; it is possible some of this impurity phase has reacted also.

The reaction produced two broad peaks at  $3.06\text{\AA}$  and  $2.74\text{\AA}$  which are attributed to a CSH phase. No evidence of the  $\text{C}_3\text{AH}_6$  phase is present in this pattern. There is a noticeable peak at  $9.2\text{\AA}$  of unknown significance.



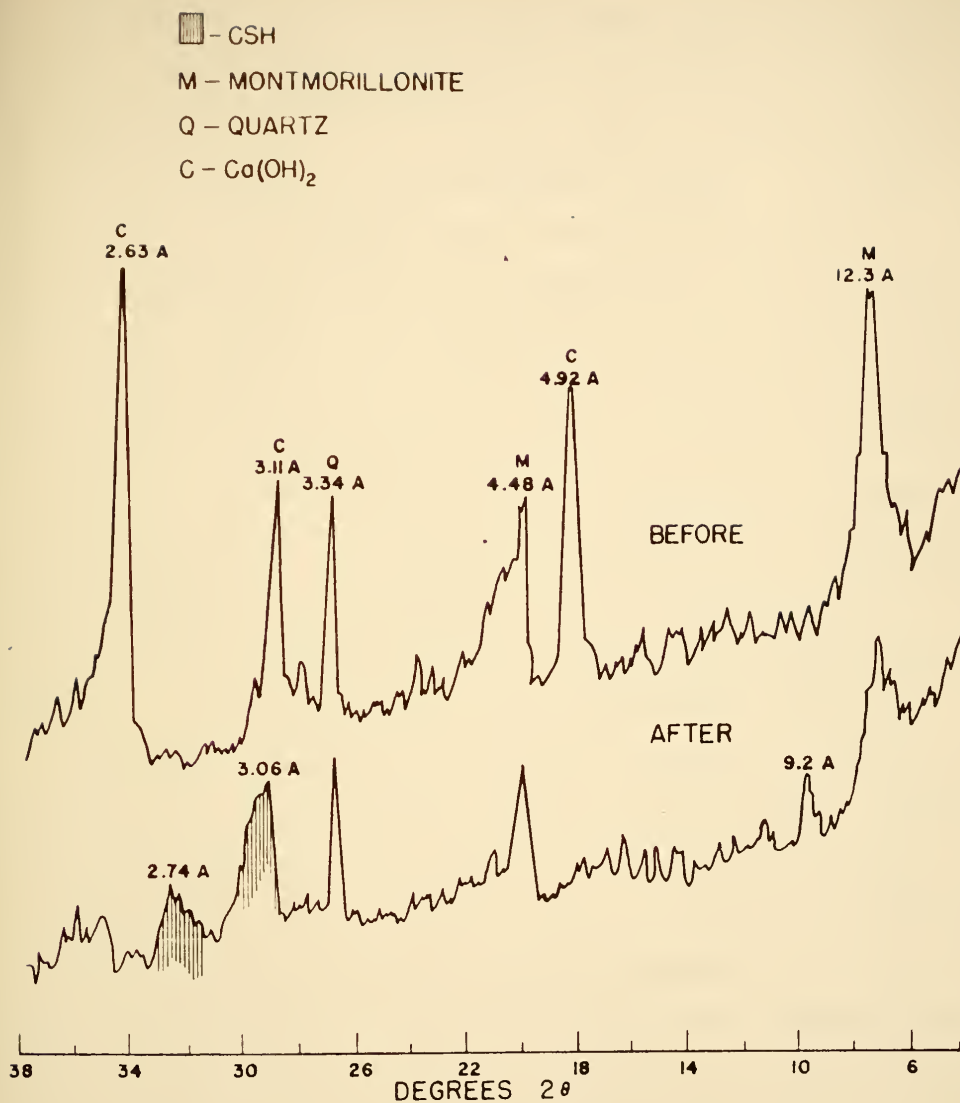


Figure 31. X-ray Diffractometer Traces of  $\text{Ca}(\text{OH})_2$  Montmorillonite Mixtures Before and After Reaction at  $60^\circ\text{C}$ .



The DTA result for this phase (Figure 28) is a peculiar pattern, showing a weak low-temperature endotherm at 160°C, weak endothermic bulges at 520°C and 760°C; a weak endotherm at 810°C and finally a strong exotherm at 940°C. A similar pattern for a corresponding reaction product of lime and Wyoming bentonite was given by Eades and Grim (1960) as their Figure 8D. The 520°C break may be due to early dehydroxylation of partially reacted montmorillonite. It is thought that the higher temperature features may be associated with the formation of a CSH(I) product, which characteristically gives a strong exothermic reaction on conversion to wollastonite. The apparent lack of formation of any separate calcium aluminate hydrate phase probably implies that much of the alumina released by the montmorillonite has substituted in the CSH(I) lattice.

Electron microscopy of the product (Figure 32) confirms that the main product formed is the foil-shaped CSH(I) and not fibrous CSH(gel), although a few fibrous particles may be distinguished on careful examination. A study of the effect of the non-aqueous dispersion technique employed on the appearance of unreacted montmorillonite under the electron microscope suggests that the coarser, darker particles seen in the figure are undispersed aggregates of montmorillonite. The characteristic "fleecy cloud" morphology usually associated with montmorillonite after dispersion in water is not observed following this type of pre-treatment.

The surface area of montmorillonite is generally conceded to be in the neighborhood of 800 m<sup>2</sup>/g; that of the present



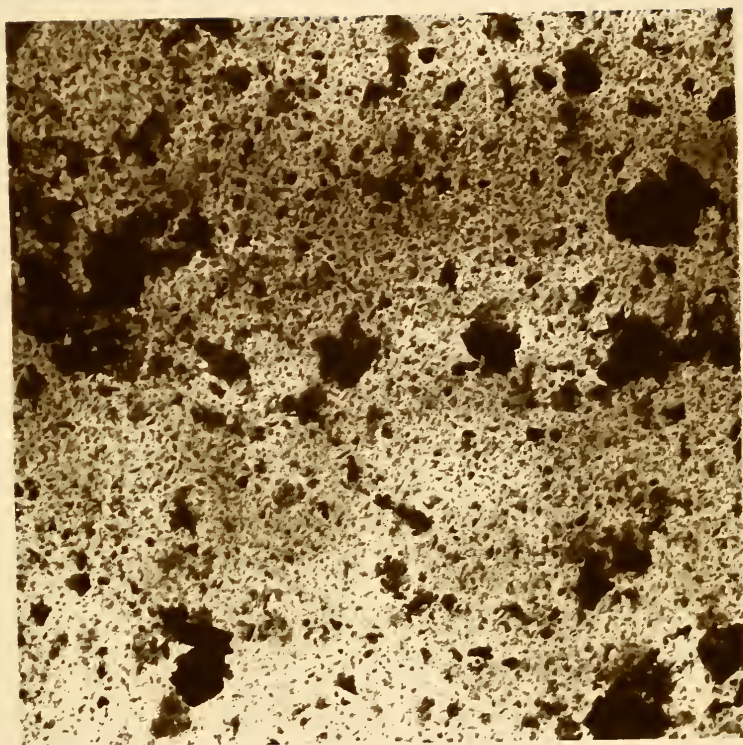


Figure 32. Electron Micrograph of  $C.(OH)_2$ -Montmorillonite  
Reaction Product at  $60^{\circ}C$ .







impure bentonite is undoubtedly slightly less than this. However, the measured surface area of the reaction product was  $160 \text{ m}^2/\text{g}$ . This is approximately in the range for CSH(I) products, but is rather lower than expected, considering the substantial amount of montmorillonite remaining after the reaction.

The effect of the presence of the cementing agent on the ability of the montmorillonite lattice to expand was investigated by treating samples of unreacted bentonite, bentonite- $\text{Ca}(\text{OH})_2$  mixture, the undried reaction product, and reaction product after drying at  $100^\circ\text{C}$ , with glycerol. As expected, the bentonite and bentonite- $\text{Ca}(\text{OH})_2$  mixture both immediately yielded strong peaks at  $17.7\text{\AA}$  indicative of lattice expansion; no expansion was noted for the reacted products. Re-examination of the reacted products after a twenty-four hour waiting period showed that both samples expanded at least partially; however, both had considerable material still diffracting at  $12\text{-}13\text{\AA}$ ., indicating that the process of expansion was far from complete. Apparently the CSH(I) in some unknown way interferes with the adsorption and lattice expansion process. Thus montmorillonite has been shown to react with  $\text{Ca}(\text{OH})_2$  under the conditions of this experiment to yield a CSH(I) product; without production of detectable amounts of calcium aluminate hydrate.

Failure of Pyrophyllite to React. The pyrophyllite- $\text{Ca}(\text{OH})_2$  "reaction product" appeared as wet as it was before the reaction period and it was quite apparent that no particular cementation had occurred. This was confirmed on examination by x-ray diffraction, the  $\text{Ca}(\text{OH})_2$  peaks being as strong after



as before the treatment. For all practical purposes the x-ray diffractometer trace for the "reaction product" was identical to that for the reacting mixture, and it was concluded that no appreciable reaction of any kind had occurred with pyrophyllite under these conditions.

#### Effect of Immersion on Cementation of Reacted Products.

To check the ability of the products of the lime-clay reaction to retain their strength and integrity against water saturation, portions of the quartz, kaolinite, and montmorillonite products were cut with a hacksaw and immersed in water for several weeks. No slaking occurred and no change in the appearance or hardness of the samples were detected.

#### Summary of Reaction Products of Compacted Mixtures at 60°C.

Under these conditions (40%  $\text{Ca(OH)}_2$  by weight of silicate mineral, approximately 50-60% initial moisture content by weight of solids, compaction, and storage under conditions free from  $\text{CO}_2$  contamination), quartz reacted to produce CSH(gel) of high surface area, exhibiting characteristic DTA pattern and typical fiber or rod morphology for this material. Kaolinite reacted with all of the lime present to yield CSH(I) of high surface area and foil or "snowflake" morphology, and a cubic hydrated calcium aluminate,  $\text{C}_3\text{AH}_6$ . Montmorillonite (Wyoming bentonite) also reacted with all of the lime added and produced a CSH(I) product having morphology similar to that of the kaolinite product, but no evidence for any hydrated calcium aluminate was found. It was suggested that the alumina may be present substituting for silicon in the CSH phase. Pyrophyllite did not appear to react with lime under these conditions. Despite



the cementation, all of the samples had high moisture contents removable on oven drying.

One item of importance disclosed in this experiment is that the CSH phase with foil morphology (CSH(I)) is apparently just as good a cementing agent as the fibrous CSH(gel) normally produced on the hydration of cement compounds. Thus any potential explanation of cementitious behavior that depends on a model involving the special characteristics of fibrous rolled up sheets, such as that advanced by Brunauer (1961), may be inadequate.

#### Reaction of Slurry Mixtures at 45°C

Starting Materials, Reaction Conditions, and Methods of Examination of Products. This mode of reaction was designed to promote as complete a reaction as possible between the  $\text{Ca(OH)}_2$  and the silicate at a comparatively low temperature. Details of the starting materials and procedures are given in the chapter on Materials and Procedures; briefly the procedure involved reaction of a large excess of lime with  $\sim 2\mu$  fractions of the silicates, with sufficient water added to produce a wet slurry, which was shaken continuously for two months at 45°C. The wet products were examined initially by x-ray diffraction using the "slurry mount" technique previously described. The large excess of lime which remained unreacted was then removed by washing in water; the washings were repeated until the pH of the suspension dropped below that of a saturated lime solution (pH 10-11). The products of this washing procedure were then examined using the slurry mount procedure, then finally



oven dried and again x-rayed, this time using the standard powder mount procedure. The dried samples were subsequently examined by DTA (using the Eberbach portable instrument); and several of them were studied by electron microscopy.

Reaction Products of Quartz. Initial examination of the slurry by x-ray diffraction disclosed definite peaks for a CSH product at 3.04A and 2.79A. A quartz peak overlaps the 1.82A position; thus, the possible presence of a peak here for the CSH could not be confirmed. Much of the quartz seemed to have reacted, but there was considerable  $\text{Ca}(\text{OH})_2$  remaining. No evidence of carbonation was detected. A small broad peak at about 8A of unknown significance was observed. After removal of the lime by washing, x-ray examination of a dried powder mount revealed some evidence of carbonation, the peak at 3.04A was sharpened and other very weak calcite lines were observed. The 8A peak was no longer-present. There was broad general diffraction effects observed between 2.8A and 3A, suggesting that much of the material in the reaction product was disordered CSH. The height of the residual quartz peak at 3.34A was only 66 cps compared to a peak height of several thousand cps for pure quartz under these conditions, suggesting that almost all of the quartz had been consumed in the reaction with lime.

The DTA of this material (Figure 33A) confirmed the virtually complete reaction of the quartz, the characteristic sharp endotherm for the transition at  $573^\circ\text{C}$  being unobserved. There was a broad low-temperature endotherm between  $130^\circ\text{C}$  and







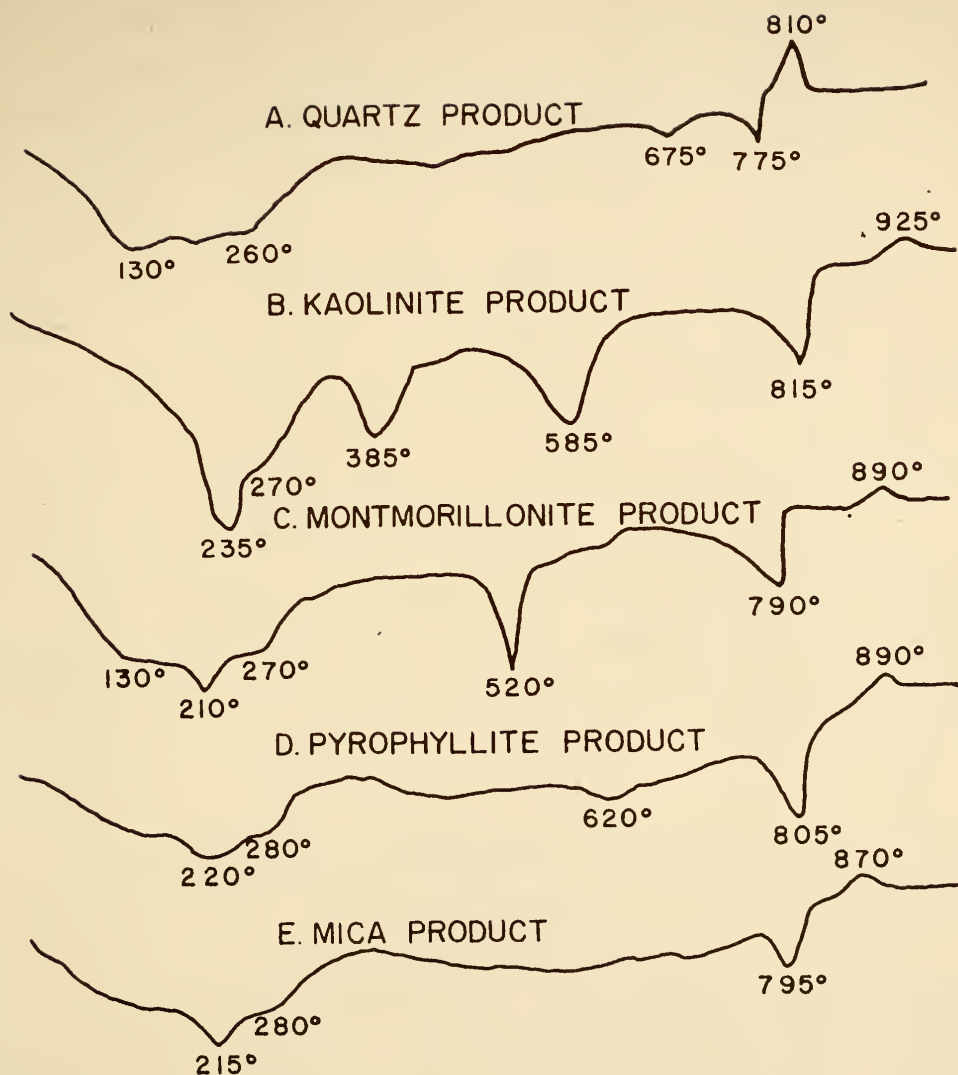


Figure 33. Differential Thermal Analysis of  $\text{Ca}(\text{OH})_2$ -Silicate Reaction Products at  $45^\circ\text{C}$ . Heating Rate Varies from  $58^\circ\text{C}$  to  $5^\circ$  Per Minute.



260°C, a small endotherm at 675°C, a sharp endothermic peak at 775°C indicating the presence of  $\text{CaCO}_3$ , and finally a moderately sharp exotherm for the CSH phase at 810°C.

Electron microscopy (Figure 34) revealed a fibrous morphology similar to that shown in Figure 29A for the quartz reaction product of the previous experiment. In the present sample the fibers seemed to be associated into laths or even sheets, some of them having a characteristic tapered appearance. One residual quartz particle can be noted at the top portion of the right-hand side of the photograph; the edges seem to be frayed and eaten away by chemical attack.

These results indicate that under appropriate conditions, including a reaction temperature near room temperature, finely divided quartz may be readily attacked by  $\text{Ca(OH)}_2$  to produce a CSH(gel) hydrate, and that the reaction can go almost to completion within a few months.

Reaction Products of Kaolinite. Examination of the slurry after the reaction period disclosed that it was not homogeneous but consisted of a white smooth gel portion and a number of hard, yellowish cemented granules which were dispersed through the smooth white portion. The smooth, white portion proved to be mostly  $\text{Ca(OH)}_2$  and contained no residual kaolinite. There were peaks for a 7.6A phase to be discussed later, and for CSH at 3.05A and 2.84A. A separate examination of the yellow, granular portion showed a very small peak for residual kaolinite, a strong one for the 7.6A product, and the peaks for CSH with no  $\text{Ca(OH)}_2$  lines present. After removal of the  $\text{Ca(OH)}_2$  by



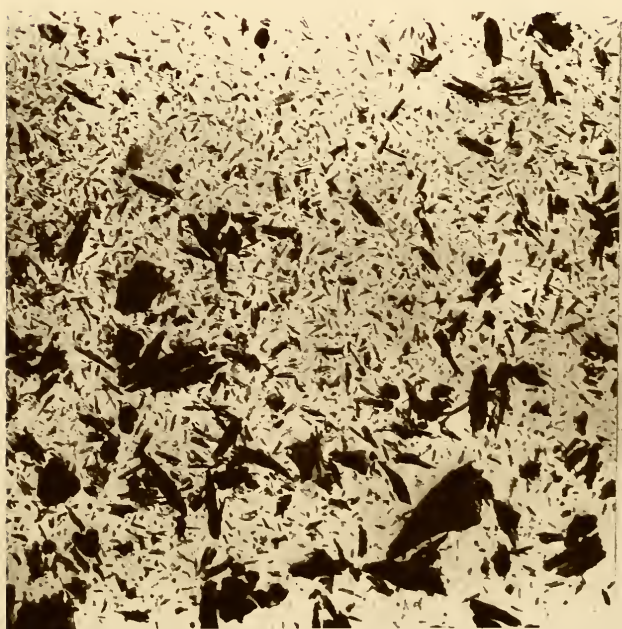
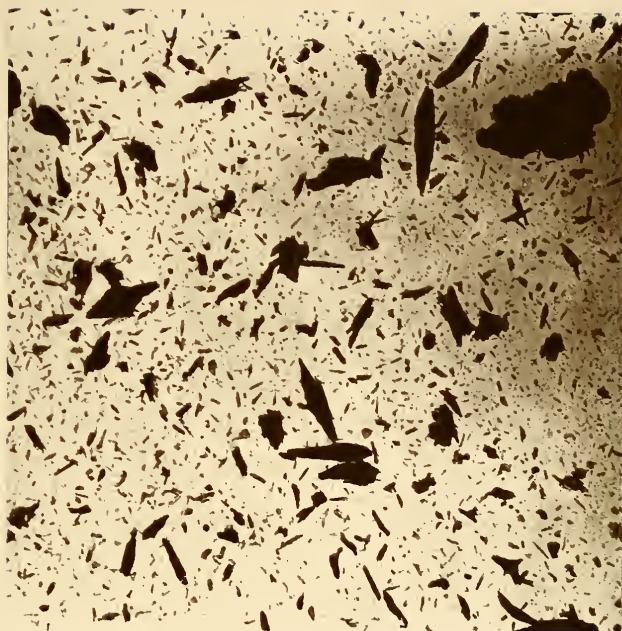


Figure 34. Electron Micrographs of  $\text{Ca}(\text{OH})_2$ -Quartz Reaction Products at  $45^\circ\text{C}$ .



repeated washing with water, a slurry-mount pattern made for the combined portions showed a strong peak for the 7.6A phase, a small residual kaolinite peak at 7.15A and distinct evidences of the formation of calcium carbonate by carbonation of  $\text{Ca(OH)}_2$ . The sample was then dried and a powder mount prepared and x-rayed. The phases produced, particularly the aluminum compound, seem to be extremely well crystallized, a total of over 35 individual x-ray reflections being observed on the original trace, which was carried out to  $60^\circ 2\theta$ . It is clear that most of the kaolinite has reacted; the basal peak for this compound was reduced to 35 cps from an initial value of over 250 cps for the pure kaolinite. The reaction products are a CSH phase and a 7.6A hydrated hexagonal calcium aluminate similar to  $\text{C}_4\text{AH}_{13}$ .

Because of the complexity of the hydrated calcium aluminates as discussed in the literature review, some additional work was done in an attempt to characterize the 7.6A aluminum-bearing phase more fully. The x-ray spacings attributed to it do not exactly match the pattern of Buttler, Dert Glasser, and Taylor (1959), but are close to a perfect match with the powder pattern of Hilt and Davidson (1961) for their lime-montmorillonite product. The basal spacings cited in the literature for  $\text{C}_4\text{AH}_{13}$  without drying are 7.9A or 8.2A, depending on which polymorphic variety is present. On oven-drying at  $110^\circ\text{C}$  both of these varieties show a partially dehydrated spacing of 7.4A, which may later partially rehydrate and expand to 7.6 or 7.7A, according to Buttler et al. However, in the present material the wet slurry pattern and the pattern for the oven-dried material







both gave identical spacings of approximately 7.6A, as do most of the patterns in the literature for lime-clay reaction products in which this phase is present (see for example Glenn and Handy, 1963; Benton, 1959). It was thought that perhaps this stability to dehydration by oven-drying is conferred by the presence of  $\text{CO}_2$  in the lattice. In a heating experiment undertaken to determine the extent of this thermal stability, the sharp basal spacing was found to disappear on heating to  $150^\circ\text{C}$ , and a 6.1A dehydrated spacing was observed. Such behavior occurs for  $\text{C}_4\text{AH}_{13}$ , but hydrocalumite, the phase isostructural with  $\text{C}_4\text{AH}_{13}$  that has a small degree of  $\text{CO}_2$  substitution does not dehydrate to this extent on heating to  $150^\circ\text{C}$ ; rather its basal spacing only shrinks from 7.9A to 7.3A (Buttler, Dent Glasser, and Taylor, 1959). The other known  $\text{CO}_2$  substituted phase is the calcium monocarboaluminate which has a considerable degree of  $\text{CO}_2$  substitutions, but this is unlikely to have formed in the sealed containers, since there was no evidence of carbonation converting any of the large excess of  $\text{Ca}(\text{OH})_2$  to  $\text{CaCO}_3$  prior to the processing involved in washing out the excess lime. Furthermore, the monocarboaluminate has a DTA diagram different from that of the present sample, a distinct exotherm at about  $550^\circ\text{C}$  being characteristic (Turriziani and Schippa, 1956). Hence the present phase is neither of these recognized compounds, and pending further clarification will simply be referred to as  $\text{C}_4\text{AH}_{13}$ .

The DTA of this reaction product is given in Figure 33. The features displayed include four successive endotherms at  $235^\circ$ ,  $385^\circ$ ,  $585^\circ$ , and  $815^\circ\text{C}$ , respectively, and a small exotherm



at 925°C. The first endotherm is apparently complex, and is presumed to be caused by the simultaneous dehydration of the CSH and the  $C_4AH_{13}$  products. The second endotherm is not easily explained; a possible explanation is that this may be due to poorly crystallized gibbsite formed from some of the alumina released by the highly aluminous clay. The third endotherm is due to dehydroxylation of unreacted kaolinite, and the fourth is due to decomposition of the  $CaCO_3$  contaminant formed in processing the original reaction product. The final exotherm is that of the CSH phase and its small size indicates CSH(gel) rather than CSH(I).

The electron micrographs of this reaction product (Figure 35) are interesting. There are a number of individual rod-shaped or fibrous particles, and some aggregates of such particles somewhat similar to those found in the previous specimen and in hydrated  $C_3S$  and  $\beta$ - $C_2S$  phases. This morphology confirms that the CSH produced in this reaction is CSH(gel) and not the CSH(I) foil material produced by kaolinite in the preceding experiment. Several comparatively coarse particles with ragged edges visible in the figure are most likely residual kaolinite particles. There are a number of thin sheets present in the figure most of which are irregular. Several sheets which have definite hexagonal outlines may be the calcium aluminate hydrate phase. In addition there are a number of particles of nondescript appearance.

Reaction Product of Montmorillonite. The appearance of this product was like that of kaolinite, in that the reaction



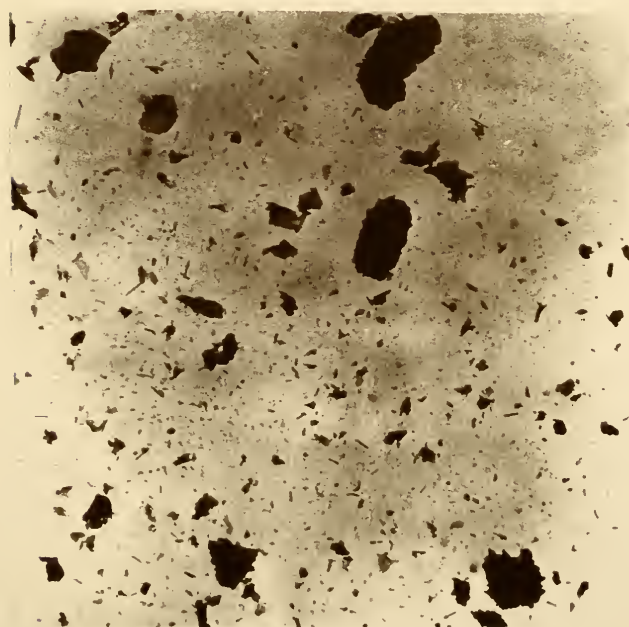
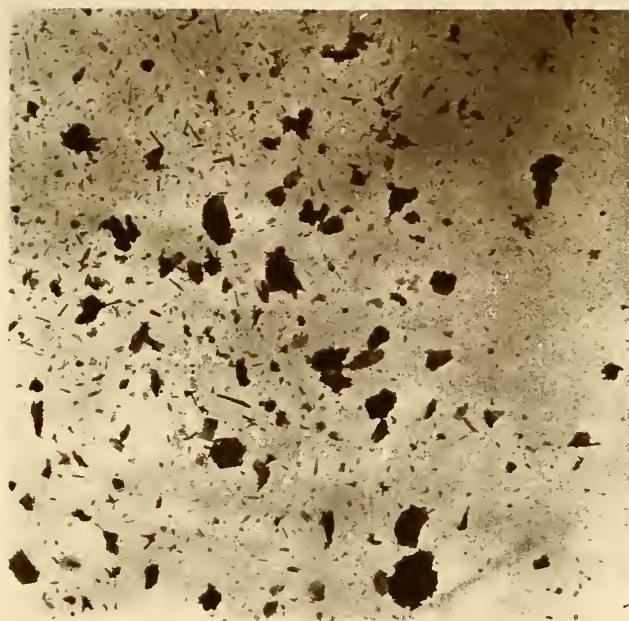


Figure 35. Electron Micrographs of  $\text{Ca}(\text{OH})_2$ -Kaolinite Reaction Products at  $45^\circ\text{C}$ .





product was not homogeneous. A solid, hard, yellowish cemented portion was attached to one end of the reaction tube, the remainder of the material being a smooth white slurry. On x-ray examination in the wet state, it was found that most of the residual  $\text{Ca}(\text{OH})_2$  was in the slurry, only a very small portion of lime being present in the cemented material. The latter yielded a CSH peak at 3.02A, and a number of peaks for the same 7.6A calcium aluminate hydrate phase found with kaolinite. In addition, there was a very broad peak at around 9A. The slurry portion gave smaller peaks for both these ingredients and a large one for the lime. There is no distinct peak for residual montmorillonite in either pattern. Unfortunately, on washing the  $\text{Ca}(\text{OH})_2$  out of this material considerable calcite was formed. The powder pattern revealed the presence of some residual montmorillonite with a broad peak at about 14A; peaks for both a CSH phase and the calcium aluminate hydrate found previously are present. The intensity of the peaks for the latter is significantly less than in the kaolinite product, which is not surprising since montmorillonite has less aluminum in its structure.

The DTA pattern for this product (Figure 33) confirms the incomplete removal of  $\text{Ca}(\text{OH})_2$  on washing by a fairly substantial endotherm at 520°C for lime; also the degree of formation of calcite due to accidental carbonation is obvious from the endotherm at 790°C. The CSH phase would be considered a CSH(gel) from the very small exotherm visible at 890°C. There is no endotherm in the 385°C region such as that attributed to





gibbsite in the preceding pattern; however endothermic response at lower temperatures is apparently a complex reaction. There is no particular indication of residual montmorillonite, but this is not surprising in view of the smallness of the amount that remains in the sample and the weakness of the overall DTA response to montmorillonite in general.

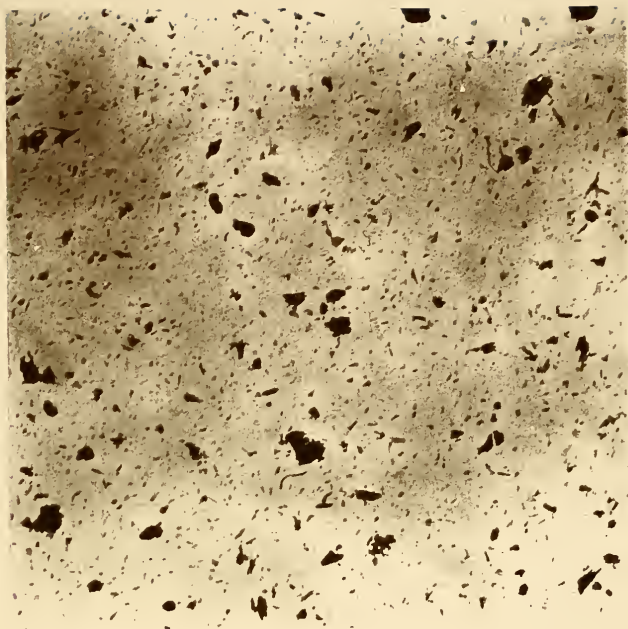
The morphology of the constituents as revealed by electron microscopy is indicated in Figure 36A. The CSH(gel) phase occurs in unusually small fibers or rods, or in aggregations of them. There are a few thin sheet-like particles present, some of which appear to have rods associated with them. No particles having a hexagonal outline seem to occur in any of the fields examined. The  $\text{Ca}(\text{OH})_2$  that remained in the system is probably coarsely crystalline in nature and thus segregated from the remaining products.

Thus, montmorillonite is attacked at  $45^\circ\text{C}$  under these conditions to yield a CSH(gel) phase of very fine particle size and a hydrated calcium aluminate with an x-ray pattern similar to the product produced by kaolinite.

Reaction Product of Pyrophyllite. This material gave an apparently homogeneous white slurry. Initial examination of the slurry mount disclosed a large peak at 10.5A along with a smaller basal peak for residual pyrophyllite at 9.2A, a peak for the hydrated calcium aluminate at 7.6A and a fairly strong peak for a CSH product at 3.07A. Residual  $\text{Ca}(\text{OH})_2$  was present in large quantity. After washing out the lime, all but the 10.5A peak were confirmed, and a broad general diffraction



(A)



(B)

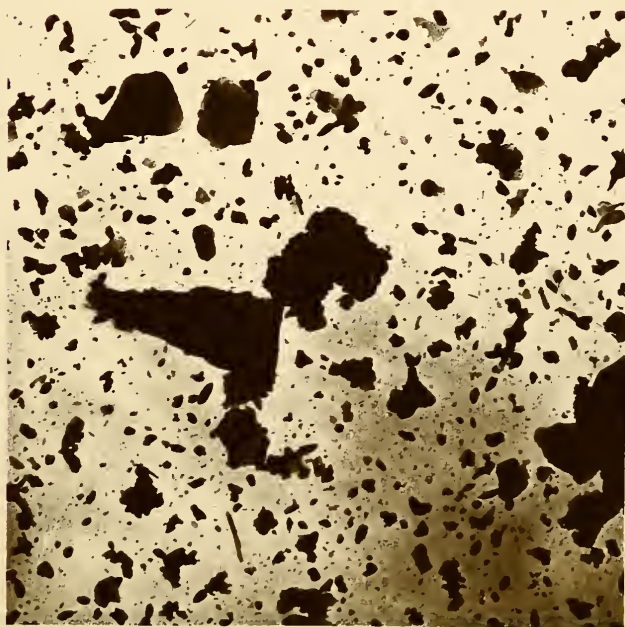


Figure 36. Electron Micrographs of  $\text{Ca}(\text{OH})_2$ -Silicate Reaction Products at  $45^\circ\text{C}$ . (A) Montmorillonite.



near 3A was found, attesting to the presence of disordered CSH. Some carbonation had apparently occurred. After drying, a powder pattern confirmed these results in detail. The percentage of the pyrophyllite that appeared to have reacted was not as high as that of the samples previously discussed, but it was apparently substantial.

DTA of the product (Figure 33) is similar to that of the montmorillonite except that in this case all the lime was successfully washed out of the preparation. No electron microscopy was undertaken for this material but in view of the similarity to the other materials it is likely that the CSH produced is also a CSH(gel) phase of fibrous morphology, and the hydrated calcium aluminate is  $C_4AH_{13}$ . The nature of the phase giving the initial 10.5A peak is unknown.

Reaction Product of Mica. This reaction product was reasonably homogeneous; and initial x-ray diffraction examination of the slurry suggested that a considerable amount of reaction had occurred, yielding the same products as observed for the previous aluminosilicates, a CSH product, probably CSH(gel), and  $C_4AH_{13}$ . On removal of the lime and drying this was confirmed by the powder pattern. A noteworthy observation was that while the basal peak for residual mica had an intensity of only about one-fourth that of the initial mica before reaction, nevertheless, all the lines characteristic of the  $2M_1$  polymorph were present and retained their sharpness.

The DTA of the reaction product (Figure 27) is similar to that of the preceding sample; the weak exotherm characteristic of CSH(gel) is observed at  $870^{\circ}C$ . The morphology of this





sample however was quite distinctive. Figure 36B shows a typical field; although there are a few fibrous or rod shaped particles, almost all of the particles visible are of a distinctive morphology not heretofore observed, which can be best described as ovoid or "football shaped". The large particles are obviously residual mica flakes. Some of them appear to have very ragged outlines as a result of chemical attack. Certain of the mica particles appear delaminated. It may very well be that the reaction proceeds both by attack inward from the edges, and by delamination or splitting off of the individual mica sheets.

Mica has thus been shown to react with lime to produce  $C_4AH_{13}$  and a CSH(gel)? phase of unusual ovoid morphology.

Reaction Products of Illite. The mixture after reaction for this phase was an apparently homogeneous yellow slurry; x-ray diffraction disclosed that a substantial portion of the illite had reacted to produce relatively weak indications of  $C_4AH_{13}$  and a CSH phase. Unfortunately, considerable formation of calcite occurred during the processing. It was observed that this  $2M_1$  polymorph retained its crystallinity apparently intact, with little weakening of the distinguishing lines for this polymorph.

The DTA of this phase (not shown) is essentially identical to that of the mica sample. No electron microscopy of this sample was undertaken.

Failure of Talc to React. Examination of this homogeneous-appearing product by x-ray diffraction suggested that essentially





no reaction had occurred, except that some of the  $\text{Ca}(\text{OH})_2$  had carbonated. The powder mount prepared after washing out the  $\text{Ca}(\text{OH})_2$  revealed that the talc peaks were essentially as strong as those for the pure mineral. In view of this no further investigation of this product was undertaken.

Summary of the Reaction Products of Slurry Mixes at 45°C.

Under these reaction conditions (a large excess of lime, excess water, continuous shaking at 45°C) all of the clay-sized fractions of the various silicates reacted appreciably with lime except talc. All produced a CSH product showing a weak DTA exotherm and all the products that were examined except that of mica showed the fibrous morphology characteristic of CSH(gel). The mica produced particles having a distinctive ovoid morphology. All the alumina-bearing phases that reacted produced a  $\text{C}_4\text{AH}_{13}$  hexagonal hydrated calcium aluminate phase at this temperature. In addition, kaolinite, the clay with the large aluminum content, may have produced some gibbsite, but this has not been definitely shown. The CSH(gel) apparently tended to be cementing in most of the phases, even though there was a large excess of water present. It is clear that the quartz and some of the aluminum-bearing silicates have been almost completely decomposed by the reaction process, only a relatively small content of the original minerals being left. Others, materials, notably mica, illite, and pyrophyllite, were not quite so completely decomposed by the reaction.



Reaction of  $\text{Ca}(\text{OH})_2$  and Kaolinite  
in Suspension at  $23^\circ\text{C}$

This reaction took place in a sealed plastic bottle mounted on a rotating wheel device, in the same manner as that employed for the hydration of  $\beta\text{-C}_2\text{S}$  and  $\text{C}_3\text{S}$ . Five grams of the same clay-size fraction of kaolinite from Bath, South Carolina, were reacted with an equal weight of lime in 150 ml of suspension. The reaction was allowed to proceed for six months.

The resulting suspension was too thin to examine by the slurry mount technique. A porous tile mount was prepared from one portion of the material; the remainder was dried over  $\text{P}_2\text{O}_5$  in vacuo at room temperature, to avoid carbonation of any excess lime, and a powder mount prepared. Both specimens were x-rayed in a nitrogen atmosphere. The resulting patterns are shown in Figure 37. The reaction was obviously incomplete, a fair amount of  $\text{Ca}(\text{OH})_2$  and considerable kaolinite being left unreacted. The products were similar to those found in the previous experiment, a  $\text{CSH}$  phase and  $\text{C}_4\text{AH}_{13}$ .

The lack of cementing action in this dilute suspension is quite clear from the excellent orientation displayed in the very much enhanced basal spacings of both the kaolinite and the  $\text{C}_4\text{AH}_{13}$  in the tile mount. The  $\text{Ca}(\text{OH})_2$  apparently did not orient preferentially.

The DTA of the  $\text{P}_2\text{O}_5$  dried material is given in Figure 38. The complex low-temperature endotherm found in the slurry samples ranging from about  $130^\circ\text{C}$  to about  $300^\circ\text{C}$  is here replaced by two well-resolved endotherms with individual maxima



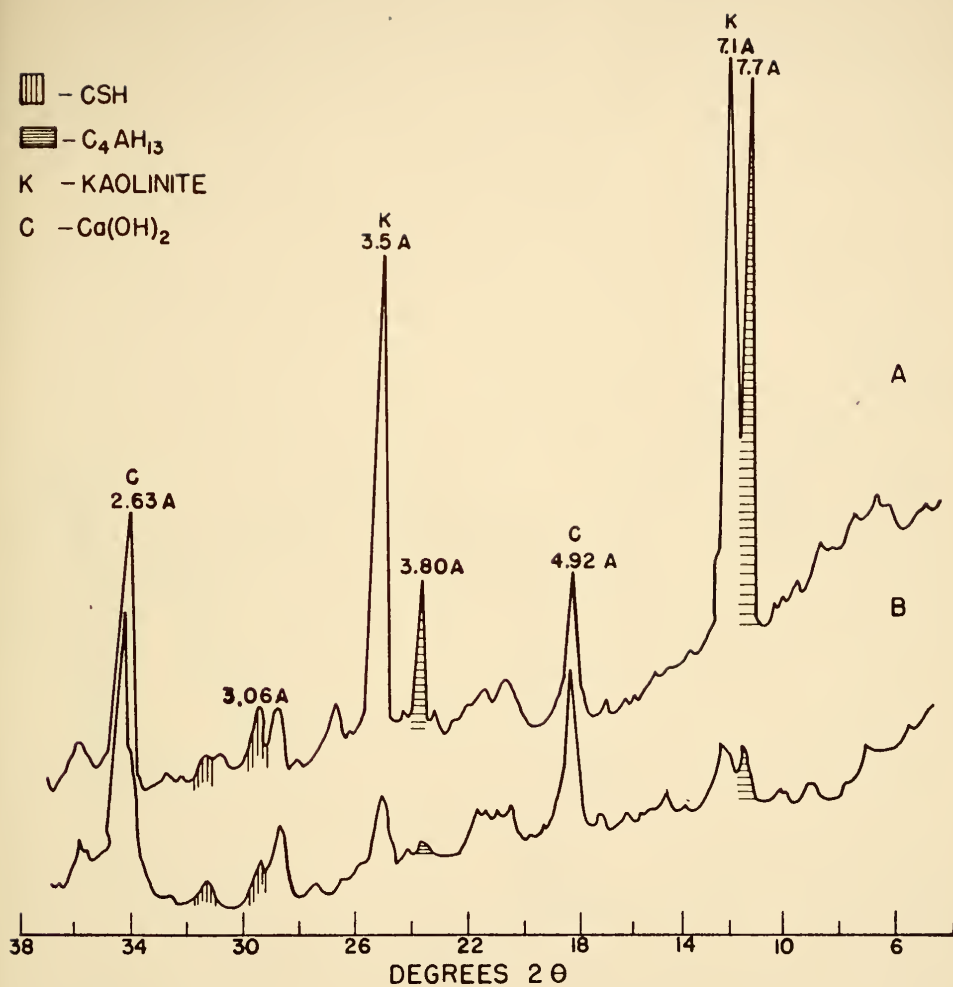


Figure 37. X-ray Diffractometer Traces of the Reaction Products of  $Ca(OH)_2$  and Kaolinite at  $23^\circ C$ .



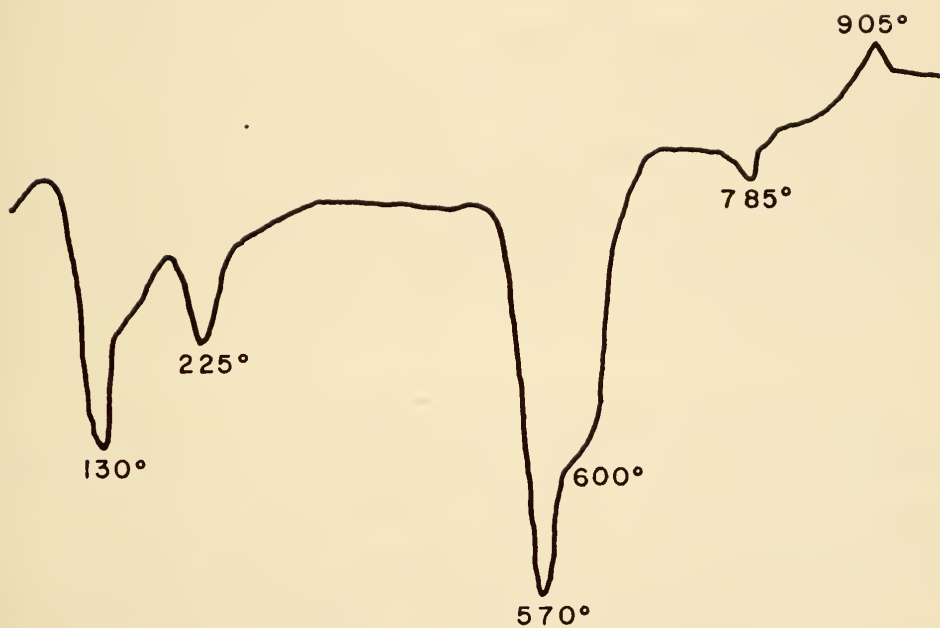


Figure 38. Differential Thermal Analysis of  $\text{Ca}(\text{OH})_2$ -  
Kaolinite Reaction Product at  $23^\circ\text{C}$ . Heating  
Rate Varies from  $58^\circ\text{C}$  to  $5^\circ\text{C}$  Per Minute.





at 130°C and 225°C. There is a large complex endotherm in the 600°C region which is due to separate dehydroxylation reactions of  $\text{Ca}(\text{OH})_2$  and of kaolinite; a small endotherm at 785°C due to calcite contamination, and a small exotherm at 905°C suggestive of CSH(gel).

The electron micrographs of this product are unusually descriptive (Figure 39). The CSH(gel) appears as individual fibers or rods; the  $\text{C}_4\text{AH}_{13}$  as very well-formed hexagonal crystals with well-formed crystalline outlines. A few kaolinite particles recognizable by their large size and more or less hexagonal morphology are present; these exhibit badly deformed and eroded edges. The coarsely crystalline  $\text{Ca}(\text{OH})_2$  particles are apparently segregated out in the electron microscope preparation procedure.

Thus one may generalize the conclusions of the last section; apparently in wet systems (slurries or suspensions) near or at room temperatures, lime and aluminosilicate clays react to form CSH(gel) and  $\text{C}_4\text{AH}_{13}$ . This very likely holds for comparatively dry systems at lower temperatures as well.

#### The Reaction Between $\text{Ca}(\text{OH})_2$ and Hydrous Alumina

Since  $\text{Ca}(\text{OH})_2$  reacts readily with aluminosilicates to produce comparatively well-crystallized calcium aluminate hydrate phases, it was thought worthwhile to investigate the possible reaction between lime and a more available form of alumina in the form of the "amorphous" hydrous alumina gel  $\text{AlO}(\text{OH})$  or  $\text{Al}_2\text{O}_3 \cdot \text{H}_2\text{O}$ . Such a phase is readily prepared by



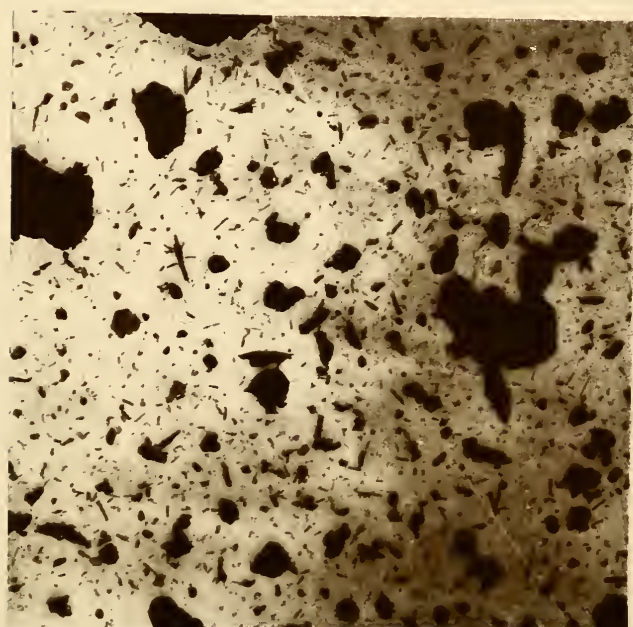
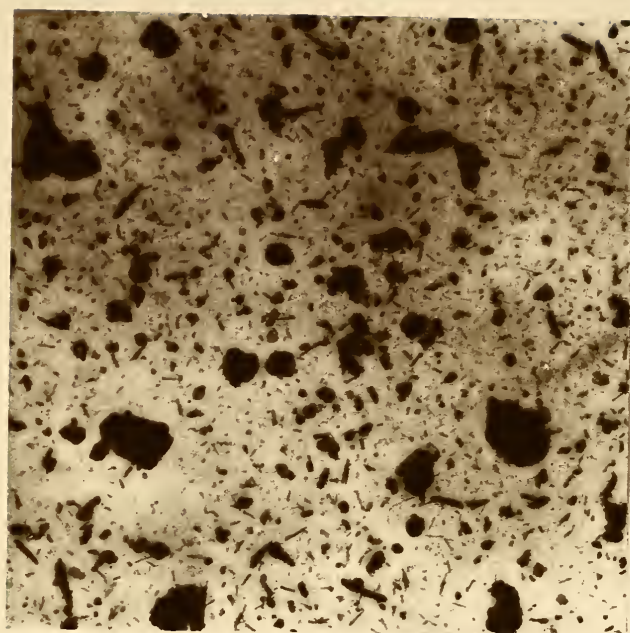


Figure 39. Electron Micrographs of  $\text{Ca}(\text{OH})_2$ -Kaolinite Reaction Products at  $23^\circ\text{C}$ .



reactions such as that of sodium hydroxide on an aluminum chloride solution. The precipitated gel so produced is actually a disordered form of boehmite (Rooksby, 1961).

A 1N solution of  $\text{AlCl}_3$  was titrated to neutrality with a solution of  $\text{NaOH}$  and the white precipitated gel washed repeatedly with distilled water until free of  $\text{Cl}^-$  ions as indicated by lack of reaction with silver nitrate. The x-ray pattern for the resulting hydrous alumina phase (Figure 40A) gave five broad diffraction maxima corresponding to the strong peaks of boehmite. Surface area measurements by the water-vapor BET technique yielded a value of  $270 \text{ m}^2/\text{g}$ .

One gram of this material was mixed with 0.25 grams of reagent grade  $\text{Ca(OH)}_2$ , wetted to a plastic condition with distilled water, compacted in a mold, sealed and allowed to cure at  $60^\circ\text{C}$  for 3 days. The x-ray pattern for the dry mixture is given in Figure 40B. Examination of the product by x-ray diffraction (Figure 40C) revealed a complete disappearance of the lime peaks, and the appearance of a very strong pattern for  $\beta\text{-C}_4\text{AH}_{13}$  (basal spacing 7.9A); peaks indicating a small content of the cubic  $\text{C}_3\text{AH}_6$  phase were also observed. The high background in the regions of the spacings of the hydrous alumina suggested that a considerable excess of this phase remained unreacted.

The reaction was repeated for a longer time using a large excess of  $\text{Ca(OH)}_2$  in an attempt to get all of the alumina-bearing phase to react. After 6 days at  $60^\circ\text{C}$  it was found that the same products had formed, excess  $\text{Ca(OH)}_2$  was present, and



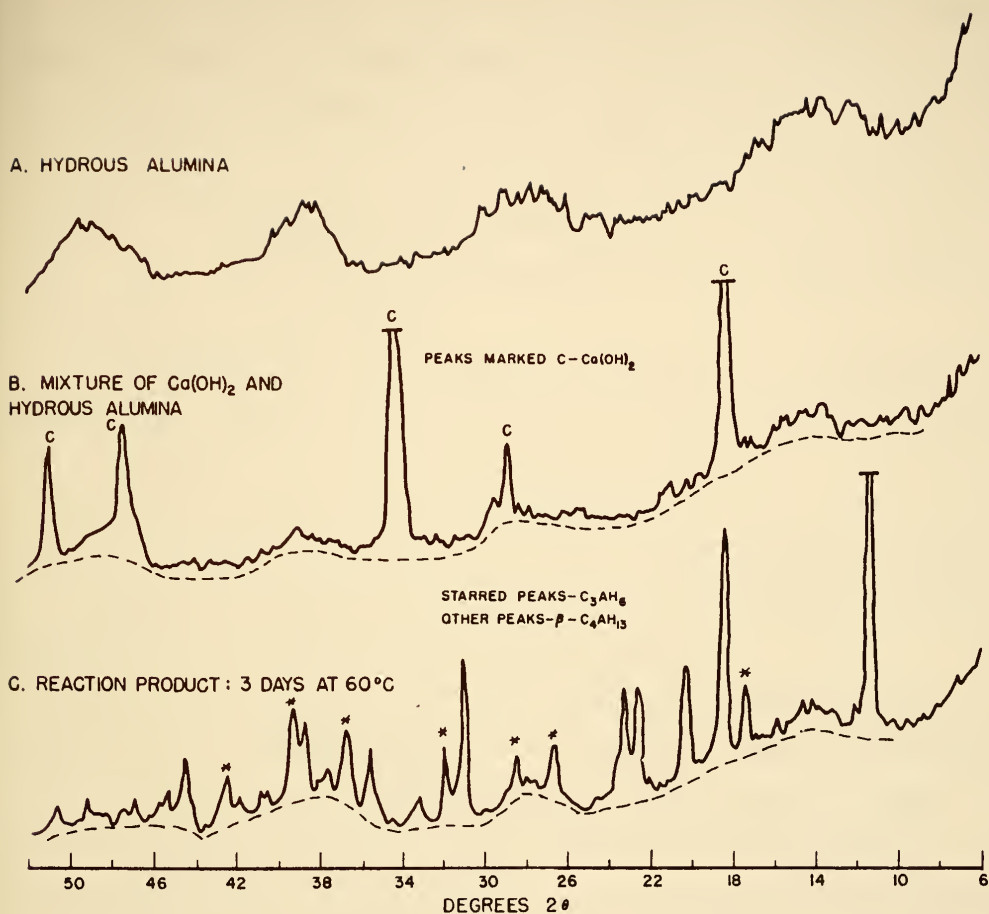


Figure 40. X-ray Diffractometer Traces of (A) Hydrous Alumina, (B) Dry Mixture of 4 Parts Hydrous Alumina and 1 Part  $\text{Ca}(\text{OH})_2$  by Weight, and (C) Reaction Product of this Mixture, 3 Days at  $60^\circ$ .







apparently all of the alumina-bearing phase had reacted. The reacted material was washed twice with water to remove the excess  $\text{Ca}(\text{OH})_2$ , dried rigorously in a vacuum desiccator over  $\text{P}_2\text{O}_5$  at a temperature of  $110^\circ\text{C}$ . The resulting dehydration caused almost complete collapse of the 7.9Å basal peak to about 6.2Å. Considering the known lack of thermal stability of  $\text{C}_4\text{AH}_{13}$ , these results were not surprising.

The reaction of lime on hydrous alumina did not appear to be a truly cementing reaction; however, some mechanical strength was developed by the compacted product.

Further trials of the reaction at room temperature suggested that the  $60^\circ\text{C}$  heating was not required, and that the reaction would proceed rapidly at room temperature.

Confirmation that the major product was actually  $\text{C}_4\text{AH}_{13}$  was sought by chemical analysis. It was also deemed desirable to demonstrate that atmospheric  $\text{CO}_2$  was not a necessary constituent of the alumina reaction product. A trial run was made in which the hydrous alumina and lime were reacted under nitrogen in a dry bag and x-rayed under nitrogen; this showed that a product identical to that produced in the atmosphere resulted. An excess of  $\text{Ca}(\text{OH})_2$  was used to avoid the possibility of having unreacted hydrous alumina which would influence the chemical analysis found. The reaction was allowed to proceed under nitrogen for 6 hours and yielded a pattern for  $\beta\text{-C}_4\text{AH}_{13}$  and residual  $\text{Ca}(\text{OH})_2$  (Figure 41A). The reaction product was washed repeatedly in distilled water, the intensity of the peak for the remaining lime being checked after each wash. Three



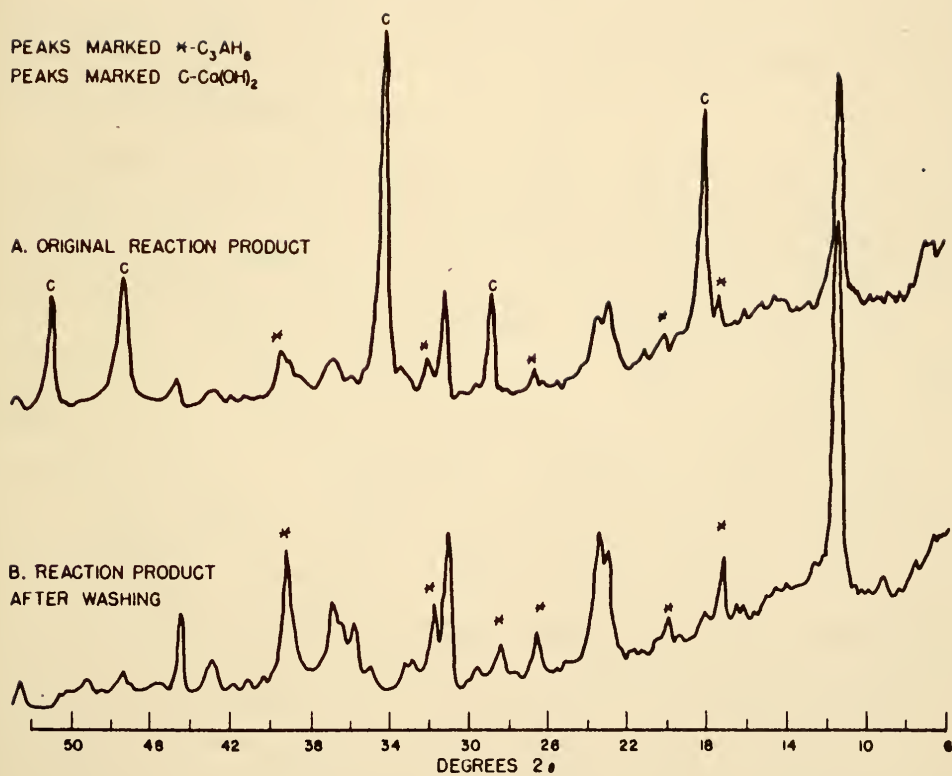
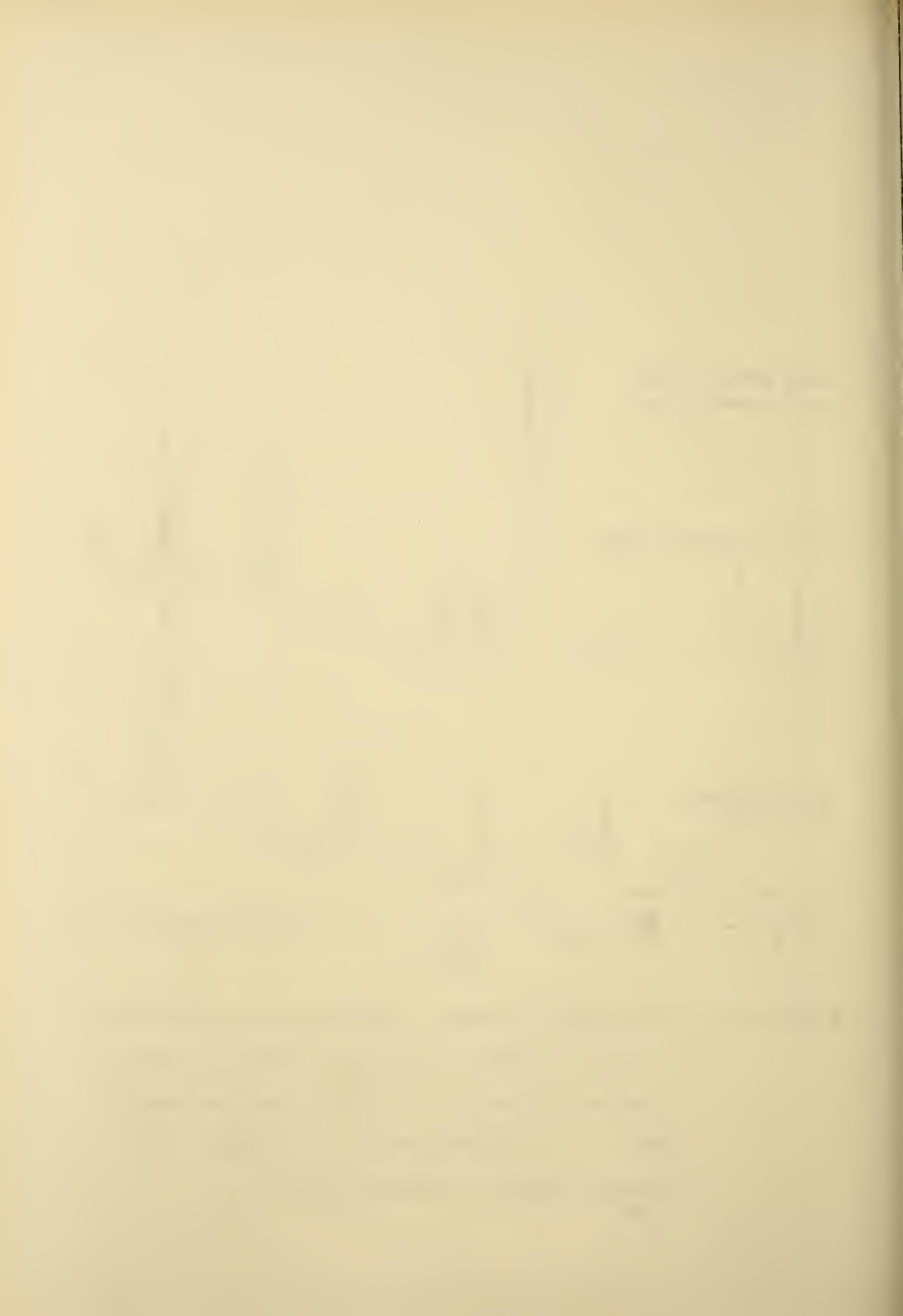


Figure 41. X-ray Diffractometer Traces of Reaction Product of 1 Part Hydrous Alumina and 3 Parts  $\text{Ca}(\text{OH})_2$  by Weight, 6 Hours at  $22^\circ\text{C}$  in Nitrogen Atmosphere. (A) Original Reaction Product. (B) Reaction Product After Washing.



1 liter washes sufficed to completely remove the excess lime from the 10 gram sample. The sample was then dried briefly ( $\frac{1}{2}$  hour) at  $110^{\circ}\text{C}$ , powdered, and x-rayed. The resulting pattern (Figure 41B) confirms the complete removal of  $\text{Ca}(\text{OH})_2$ , the apparent absence of residual hydrous alumina, and the dominant hydrated calcium aluminate pattern with a 7.8A basal spacing. A small amount of the cubic  $\text{C}_3\text{AH}_6$  was also apparently formed; the peaks attributed to this phase are marked with an asterisk in the pattern.

Chemical analysis of the washed product, however, gave a composition of almost exactly  $\text{C}_2\text{AH}_{7.5}$  rather than  $\text{C}_4\text{AH}_{13}$ . A check of the diffraction pattern with that given by Midgley (1959) for  $\text{C}_2\text{AH}_8$  gave good agreement, except that the basal spacing given by that author was 10.7A. However, Roberts (1959) showed that on oven drying  $\text{C}_2\text{AH}_8$  collapsed to the same 7.4A spacing as  $\text{C}_4\text{AH}_{13}$ . A comparison of spacings other than the basal peaks given by Midgley for  $\text{C}_2\text{AH}_8$  and  $\text{C}_4\text{AH}_{13}$  showed them to be virtually identical. Considering the variability inherent in patterns for both of these phases due to stacking disorder, it is apparent that they cannot be distinguished by x-ray diffraction in any reliable manner after drying.

The conversion of  $\text{C}_4\text{AH}_{13}$  to  $\text{C}_2\text{AH}_8$  in samples washed free of excess lime has been reported previously; Bessey (1938) quotes an earlier work by Lafuma to this effect.

A check was made on the response to further heating of both the  $\text{C}_4\text{AH}_{13}$  phase with the extra  $\text{Ca}(\text{OH})_2$  present, and the  $\text{C}_2\text{AH}_8$  phase resulting from its removal. Samples of both heated



to  $110^{\circ}\text{C}$  and x-rayed immediately under dry nitrogen showed excellent basal spacing peaks at 7.6A for the former and 7.5A for the latter. However, brief heating (1 hour) at  $150^{\circ}\text{C}$  destroyed this peak in both cases, the  $\text{C}_4\text{AH}_{13}$  product yielding a small peak at 9.4A and a dehydrated basal spacing at 6.0A, and the washed product only the latter peak. Thus both phases behave essentially like the  $\text{C}_4\text{AH}_{13}$  of Buttler, Dent Glasser, and Taylor (1959).

An electron micrograph of the washed product is given in Figure 42. The material consists of distinct well-crystallized hexagonal plates. It is noteworthy that despite the lability and ready changes undergone by these phases they are well-crystallized from the standpoint of crystal outline as well as from the standpoint of regular internal structure as revealed by x-ray diffraction.

Infrared spectra of both the unwashed product ( $\text{C}_4\text{AH}_{13}$ ) and of the  $\text{Ca}(\text{OH})_2$ -free washed material (analyzed as  $\text{C}_2\text{AH}_{7.5}$ ) were obtained using the Perkin-Elmer Model 221 instrument and are given in Figure 43. The spectra are almost exactly alike and closely resemble that of Midgley (1962) for  $\text{C}_4\text{AH}_{13}$ . Midgley attempted no assignment of the bands of his spectrum, but the following assignments appear reasonable:

1625  $\text{cm}^{-1}$  : water deformation band

1390  $\text{cm}^{-1}$  : carbonate asymmetrical stretching mode ( $\text{V}_3$ )

858-865  $\text{cm}^{-1}$  : carbonate out of plane bending mode ( $\text{V}_2$ )

This leaves the strong bands at about 1065  $\text{cm}^{-1}$ , 775  $\text{cm}^{-1}$  and the weaker one at 950-980  $\text{cm}^{-1}$  to be assigned to the  $\text{C}_4\text{AH}_{13}$







Figure 42. Electron Micrograph of Washed Product of the Reaction Between Hydrous Alumina and  $\text{Ca}(\text{OH})_2$ .



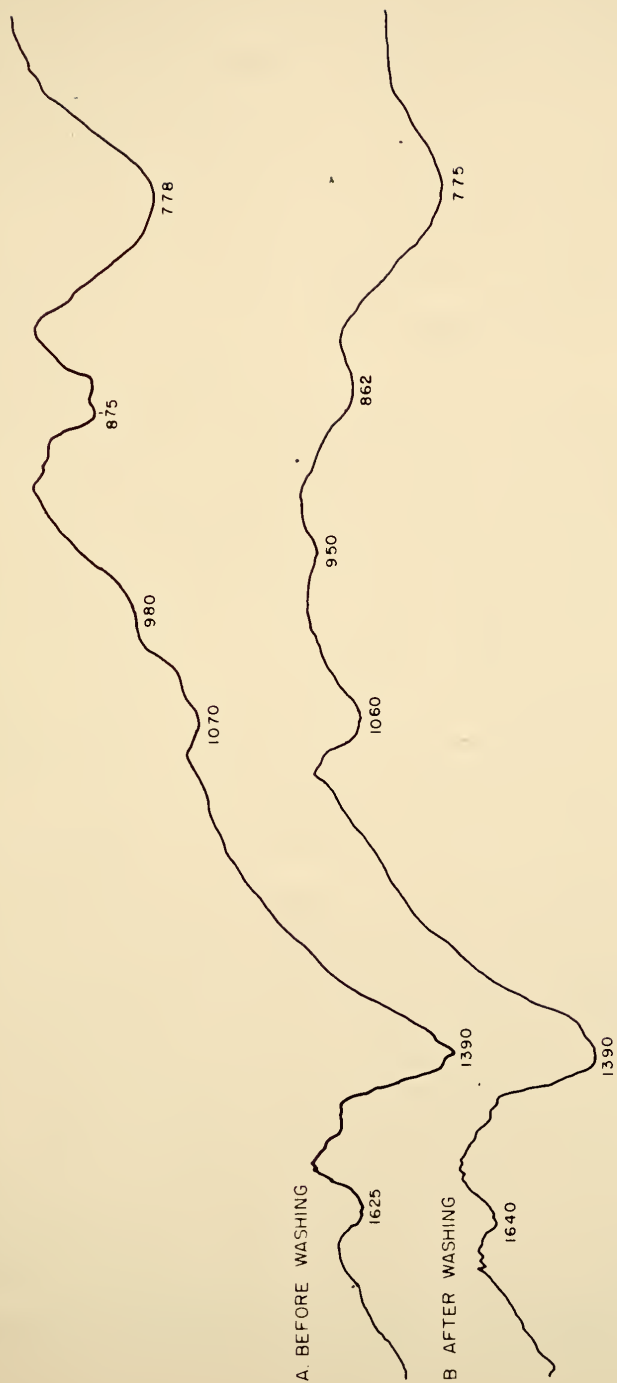


Figure 43. Infrared Spectra of the Product of the Reaction Between Hydrous Alumina and  $\text{Ca(OH)}_2$ . (A) Before Washing. (B) After Washing.



proper. Evidently considerable carbonation occurred subsequent to the removal of the sample from the nitrogen atmosphere, or more likely, the  $\text{Ca}(\text{OH})_2$  used to prepare the sample had a small percentage of  $\text{CaCO}_3$  impurity.

High frequency portions of both spectra, not shown in the figure, have a comparatively weak absorption band at about  $3450\text{ cm}^{-1}$  for bonded OH groups, and smaller features at  $3760\text{ cm}^{-1}$ ,  $2940\text{ cm}^{-1}$ , and  $2380\text{ cm}^{-1}$ , similar to those found in some of the CSH(gel) patterns of Figure 26.

Since the reaction between  $\text{Ca}(\text{OH})_2$  and the hydrous alumina seemed to be unusually rapid, even at room temperature, it was decided to attempt to evaluate its speed quantitatively. A dry mixture was prepared containing four parts of alumina phase by weight for each part of  $\text{Ca}(\text{OH})_2$  and a small amount of  $\text{MgO}$  as an internal standard. A portion of the mixture was wetted to a moisture content of about 60% and compacted into a plastic container. The reacted mixture was extruded from the container after only 15 minutes of reaction, dried rapidly in the oven, and x-rayed. The result (Figure 44) indicated that essentially all of the lime had reacted in this short 15 minute interval and a strong pattern for the  $\text{C}_4\text{AH}_{13}$  product was obtained. The DTA of this reaction product is also given in Figure 44; it shows endothermic peaks at  $215^\circ\text{C}$ ,  $320^\circ\text{C}$  and  $385^\circ\text{C}$ , the latter presumably due to the unreacted hydrous alumina.

A small portion of the same dry mix used in the preceding experiment was prepared as an x-ray diffraction powder mount, in a conventional McCreery-type holder. The sample was x-rayed,



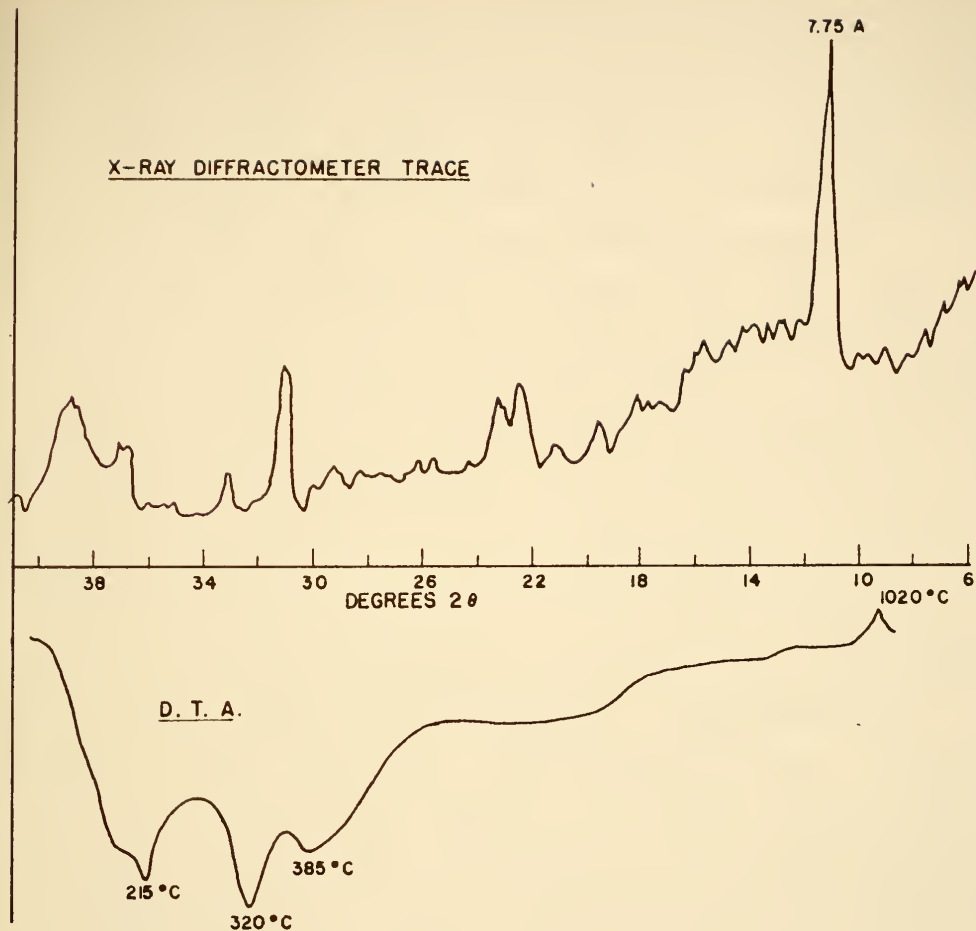


Figure 44. X-ray Diffractometer Trace and Differential Thermal Analysis (Heating Rate 10° Per Minute) for Hydrous Alumina- $\text{Ca}(\text{OH})_2$  Product Reacted for 15 Minutes at 22°C.





and after the scan the intensity of diffraction at several positions were determined by stationary counting with the goniometer fixed. The positions measured were that of the strongest  $\text{Ca}(\text{OH})_2$  line ( $34.05^\circ \pm 2^\circ$ ), the main peak for the  $\text{MgO}$  internal standard ( $42.85^\circ \pm 2^\circ$ ), a convenient background position ( $41.50^\circ \pm 2^\circ$ ), and the expected position of the  $\text{C}_4\text{AH}_{13}$  basal peak ( $11.25^\circ \pm 2^\circ$ ). After several repetitions of these counts the sample mount was removed from the diffractometer and several drops (0.2 ml.) of water carefully added to the exposed face of the powder. The water was absorbed rapidly and little distortion of the geometry of the face of the sample occurred. The mount was immediately replaced on the diffractometer and the intensities of diffraction at the several fixed positions again counted. These counts were repeated sequentially for a period of about a half hour. The results are shown in Figure 45, in which the net peak heights of the  $\text{Ca}(\text{OH})_2$  reactant and of the  $\text{C}_4\text{AH}_{13}$  product relative to those of the internal standard are plotted versus time. It is apparent from the data that most of the reaction occurred almost immediately following the addition of the water, certainly within a few minutes.

This is an unusually rapid rate of reaction for an essentially dry system, the amount of water present being several orders of magnitude smaller than that necessary to dissolve the  $\text{Ca}(\text{OH})_2$  present.

It appears that this exceedingly rapid reaction is confined to the hydrous alumina type of material; a trial with a soil clay containing a large proportion of gibbsite (B horizon of



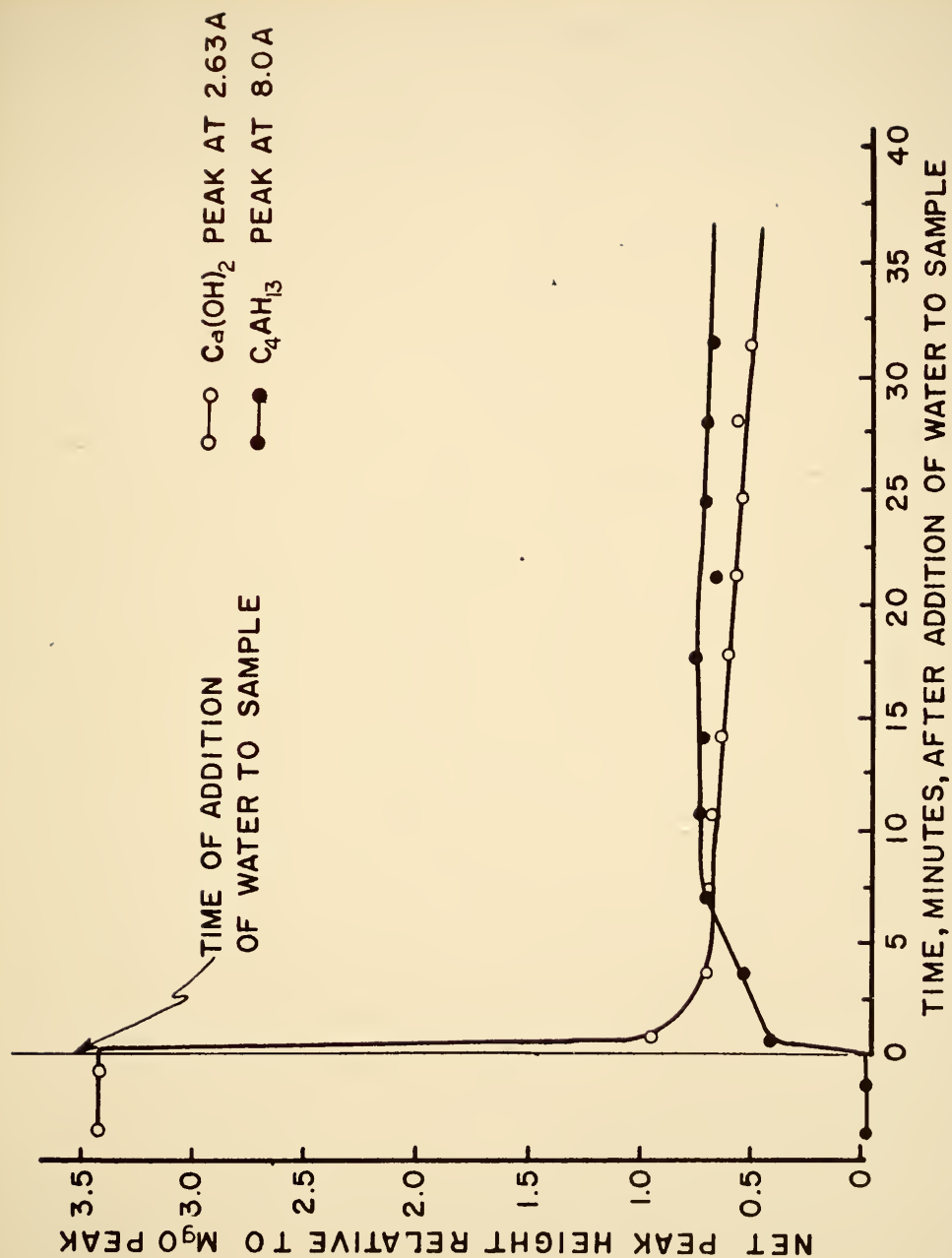


Figure 45. Relative Intensities of Peaks for  $\text{Ca}(\text{OH})_2$  and  $\text{C}_4\text{AH}_{13}$  Compared to Internal Standard as Functions of Time after Addition of Water to Dry Specimen.



Ruston fine sandy loam, Dale County, Alabama, kindly supplied by Mr. Earl Kinter) indicated that no appreciable reaction with lime took place at room temperature even after overnight treatment.



## DISCUSSION

### Classification of the Tobermorite-like Calcium Silicate Hydrates

All the data assembled here support the concept that the tobermorite-like calcium silicate hydrates form not a continuous series of phases varying only in degree of crystallinity, but rather a group of distinct phases, each of which has certain characteristic properties that distinguish it from the others:

The phases treated in this work are tobermorite (and substituted tobermorites), CSH(I) and CSH(gel). Efforts to prepare CSH(II) were unsuccessful.

A summary of the characteristic properties of the various phases, as determined in this work and also from the literature is given below:

**Tobermorite:** This is a well-crystallized compound exhibiting a distinct basal spacing near 11Å, strong x-ray peaks at 9.07Å, 2.97Å, 2.82Å and 1.82Å, and weaker peaks at a large number of characteristic positions. DTA yields only a small and indistinct exothermic response in the high temperature region, unless the material is aluminum-substituted. The infrared spectra show a strong, comparatively sharp Si-O lattice vibration at  $970\text{ cm}^{-1}$  and the samples studied here show a distinct band near  $1200\text{ cm}^{-1}$  not previously reported. A number of other characteristic bands are observed. The particles are platy in shape, and the material





disperses readily in water to yield individual crystallites that can be oriented on a surface as they settle out. The Ca:Si ratio is close to 1.

CSH(I): This is a much less well-crystallized compound showing only spacings at about 3.03A, 2.82A, and 1.81A, with sometimes weak additional lines at 1.66A and 3.25A. Basal spacings are observed with difficulty or not at all. DTA yields a very sharp exotherm in the high-temperature region. The infrared pattern is less distinct than that of tobermorite; there is no band in the  $1200\text{ cm}^{-1}$  region and often strong absorption on the low-frequency side of the Si-O band. The particles are foil-shaped, usually very fine, and may be twisted or crinkled; sometimes spherical aggregates of crinkled foils are present. The ultimate particles, though small, are well-cemented together, and the material cannot readily be dispersed in aqueous systems. The Ca:Si ratio is variable between wide limits, probably 0.8 to 1.6.

CSH(II): This is a generally poorly crystalline compound showing x-ray spacings at about 3.3A, 2.82A, 1.81A, and several additional lines. The line at 1.56A is probably distinctive for this phase (Heller and Taylor, 1956). The DTA behavior of this phase is regarded as "variable". The infrared peak found at  $840\text{ cm}^{-1}$  in some preparations may be characteristic. The morphology is fibrous and sometimes the fibers are arranged in cigar-shaped bundles. The nature of the surface properties and the degree of cementing between ultimate particles is unknown. The Ca:Si ratio is high, probably 1.5-1.7.



CSH(gel): This is a very poorly crystalline phase exhibiting a single strong x-ray peak at 3.03Å, accompanied only by two weak additional peaks at 2.82Å and 1.82Å. DTA yields only a small, comparatively weak high-temperature exotherm. The morphology is mostly fibrous, but platy or equant particles are also found. Infrared spectra presented here show a strong absorption minimum at about  $1100\text{ cm}^{-1}$ . A broad Si-O maximum is found at  $940\text{ cm}^{-1}$ , distinctly lower in wave number than that of most CSH(I) specimens. The material is said to consist of very fine particles, probably only two or three unit layers thick, rolled into fibers and well-cemented; it is almost impossible to disperse into individual particles in aqueous systems. The Ca:Si ratio is high, probably near 1.5.

The calcium silicate hydrate phases produced on reaction of clay and other silicate minerals with lime under various conditions are definitely related to one or another of these phases, and have the typical morphology and other properties characteristic of the phase concerned.

### Structural and Cation-Exchange

#### Properties of Tobermorite

The Megaw and Kelsey (1956) model of the tobermorite structure is admittedly incomplete. Not only are the positions of hydroxyls and water molecules unspecified, but approximately one-fifth of the calcium necessary to make up the minimum calcium content of the phase (Ca:Si ratio 0.8) has not been located. The calcium ions are believed to be in the grooves



or channels between the silica chains. Presumably, any additional calcium, such as would be found in tobermorites of higher Ca:Si ratio would also be so located. The state of the calcium is unspecified; presumably it occurs as free  $\text{Ca}^{++}$  ions,  $\text{CaO}$  molecules, or both. It may be that the overall situation is similar to that of the minerals loughlinite and sepiolite, which are chain-structure magnesium silicates. Loughlinite has sodium ions located in the channels running the length of the particle between silica chains, analagous to the tobermorite channels. When loughlinite is leached with  $\text{MgCl}_2$ , these sodium ions are readily exchanged for magnesium ions and the mineral sepiolite, of identical structure but bearing magnesium ions, is produced (Fahey, Ross and Axelrod, 1960; Freisinger, 1962).

It is reasonable to speculate that the exchangeable cations whose existence has been demonstrated in this study are some of the calcium ions located within the tobermorite channels. If this is so, the measured cation exchange capacity, as determined in short-time experiments such as the present measurements, should be considered as a minimum value only. The channels are only a few Å wide and presumably run the full length of the particle, which in these well-crystallized materials is of the order of a micron. Diffusion through such long, narrow channels is likely to be a slow process as it is in zeolites, and thus the full extent of the possible exchange of cations may not be realized during relatively short periods.

The exchangeable cation (sodium) in loughlinite does not arise from isomorphous substitution of ions of lower valency



for ions of higher valency in the structure of the material and the resultant charge effect, as do most exchangeable cations in clays. Rather, according to Preisinger (1962), two sodium ions proxy for a magnesium ion at the end of an octahedral row facing an internal channel; one of the sodiums occupies the physical site in the octahedral row, but the other remains in the channel itself, coordinated only to water molecules, and, is thus readily exchangeable. The present data suggest that some such situation may also be responsible for the observed exchange capacity of tobermorite and related phases, since isomorphous substitution such as that of iron or aluminum for silicon does not give rise to additional exchange sites over those possessed by the unsubstituted tobermorite. The charge deficiency introduced by such substitution must be compensated in some manner, however, perhaps in one of the ways suggested by Kalousek (1957).

The status of the hydroxyl groups in tobermorite is of some interest. The structure of tobermorite, according to Megaw and Kelsey, includes the feature that every third silica tetrahedron along each chain is elevated above the general level of the chain and can share corner oxygens at only two, rather than all four of its corners. To maintain electrical neutrality the two corners that do not share oxygens must contain hydroxyl groups rather than oxygen ions. These hydroxyl groups are probably too far separated to form hydrogen bonds with each other either across or along the chains. Any hydrogen bonding that occurs should be with water molecules or with other groups





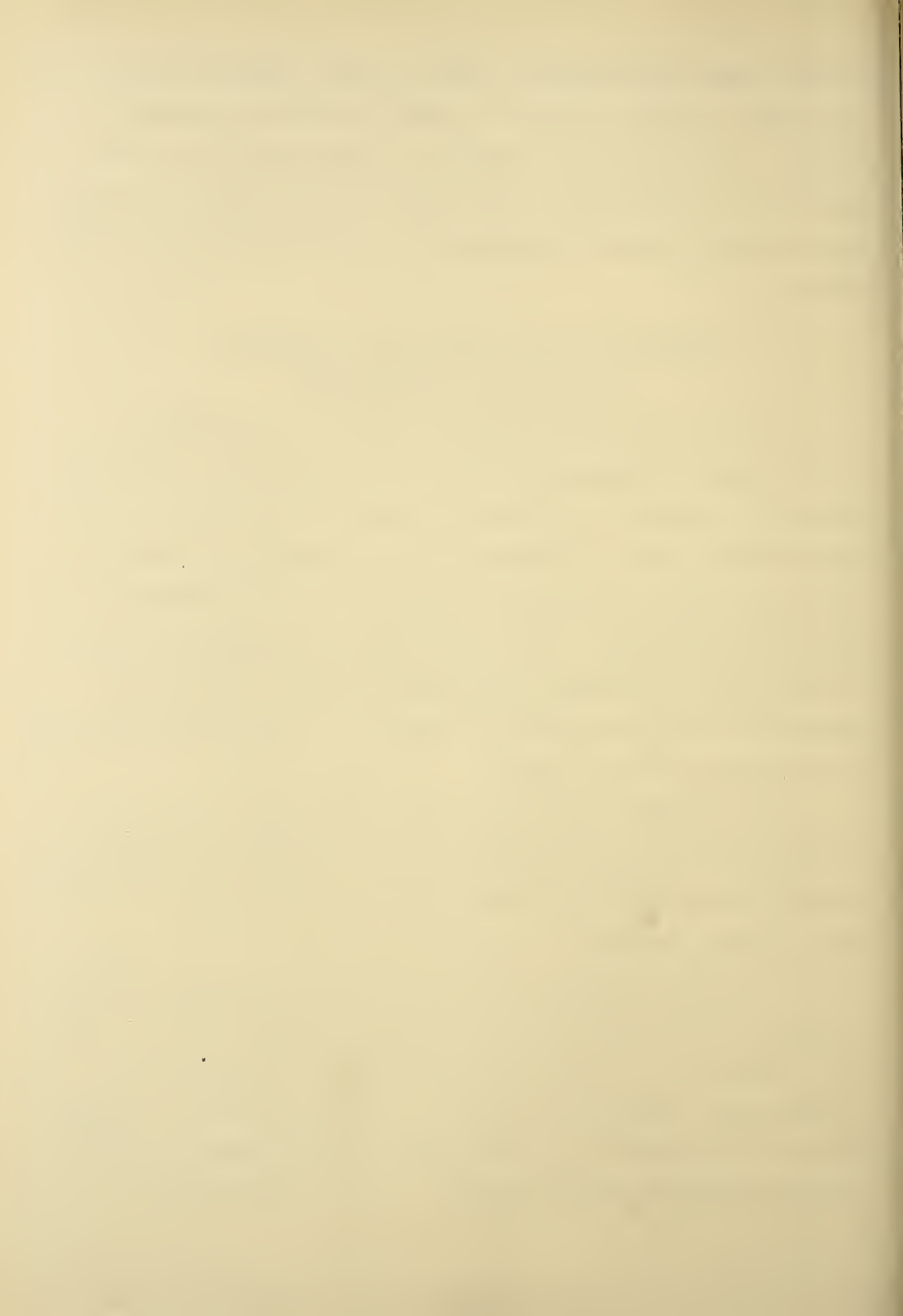
located within the adjacent channel spaces. The failure of the present infrared studies, as well as those of previous workers, to disclose any absorption at the position for free hydroxyl stretching vibrations seems to imply that the hydroxyl groups associated with the chains are in fact strongly hydrogen bonded.

### Effects of Lattice Substitution on the Properties of Tobermorite

It appears that the effects of lattice substitution on the properties of tobermorite are definite but small, involving only a few changes in position and intensity of certain x-ray peaks, minor shifts in frequency of some secondary infrared absorption bands and a slight reduction in the affinity of the surface for water. The major change in properties observed is the effect of aluminum substitution on the nature of the reaction at high temperatures by which the dehydrated tobermorite is converted to wollastonite.

The interpretation of this feature is complicated by the discovery that in at least one of the Al-substituted tobermorite preparations CSH(I) was formed along with the tobermorite during the original synthesis.

It has been observed in all samples of aluminum-substituted tobermorite that the exothermic reaction between 800°C and 900°C was accompanied by marked shrinkage and the formation of a strong, hard, dense fired product. The material was so strong that it was necessary to crush with pliers in order to remove it from around the thermocouples. The only phase found on



subsequent x-ray diffraction was wollastonite. In contrast to this behavior, unsubstituted or iron- and magnesium-substituted tobermorites produced only an insignificant DTA exotherm, did not shrink, and remained soft and friable after firing. They too yielded x-ray peaks indicative of wollastonite. CSH(I) without any lattice substitution also gave a sharp, strong exotherm at the high-temperature transition to wollastonite. There is some shrinkage accompanying this process, but it is not nearly as pronounced as that for Al-substituted tobermorite. The fired product is soft and crumbly and resembles that of unsubstituted tobermorite.

Taylor (1959) pointed out that since the wollastonite produced on the firing of tobermorite probably has its normal Ca:Si ratio of 1, while the tobermorite itself normally has a Ca:Si ratio of about 0.83, some of the excess silica must be segregated out of the lattice and be present as a separate amorphous constituent of the fired material. One explanation of the behavior of the aluminum-substituted tobermorite may be that free silica is thus available to react with some or all of the alumina present to produce an amorphous aluminosilicate (mullite, ?) which is then chiefly responsible for the strength properties of the fired product. Mullite is the product whose formation in heated kaolinite is associated with the strong exothermic reaction found at about  $980^{\circ}\text{C}$  in this material (Holdridge and Vaughn, 1957), and is usually formed in DTA runs in a poorly crystalline or amorphous condition.

The observed exotherm in CSH(I) free of any alumina substitution must be due to a different cause. It may be the

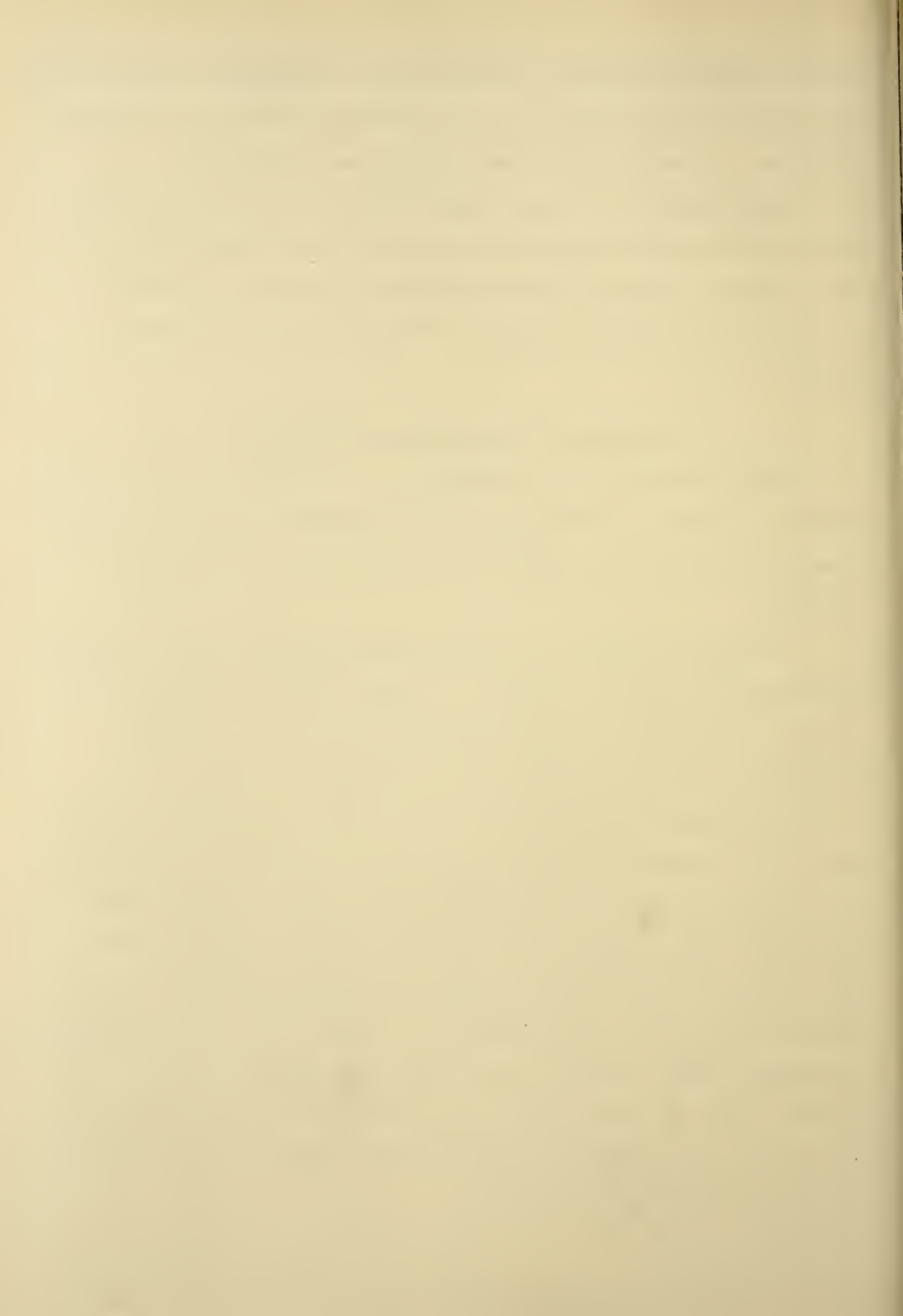


result of some structural transformation involved in the formation of wollastonite from CSH(I), and hence may point to a structural difference of some kind between CSH(I) and tobermorite. It is thought that the observed transition in the DTA results of the present aluminum-substituted samples are primarily due to the aluminum content of the tobermorite, but may also be influenced by the CSH(I) impurity found in at least one of the samples.

#### Variation in Composition of CSH(I)

The variation in the composition of the CSH(I) preparations (Table 4) seems to cover essentially the whole span of possible compositions for this phase. The relationships involved are complex.

The initial product of precipitation between mixed calcium salt-sodium silicate solutions, as represented by preparations CSH(I) - 2 through - 4, seems to have virtually a constant composition of about  $C_{1.0}Si_{1.0}H_{1.6}$ , regardless of the molar ratios of the solutions mixed. This composition approximates that of a tobermorite with excess water. CSH(I) - 5, prepared by mixing solutions of a high molar proportion of lime without significant aging, give a Ca:Si ratio only a little higher than those of the previous samples (1.18), but a water content much closer to that of tobermorite (1.00). Direct room-temperature synthesis from lime and silica gave a composition not much different than the latter when a 1:1 mole ratio of reactants was used, but much richer in both lime and water ( $C_{1.58}Si_{1.00}H_{1.80}$ ) when a 2:1 mole ratio was used.



Taylor and Howison (1956) suggested that the various CSH(I) compositions could be explained on the basis of a structure differing from that of tobermorite by successive replacements of  $\text{Si}(\text{OH})_2$  of the bridging tetrahedra by additional  $\text{Ca}^{++}$  in the channels between the silica chains. On the basis of such a hypothesis one would not expect to find any consistent relationship between the Ca:Si ratio and the  $\text{H}_2\text{O}$  ratio of CSH(I) compounds, and Taylor and Howison found no such overall relationship for their products. The present data, taken collectively, are in agreement with this expectation; no overall relationship between these quantities exists.

On the other hand, Brunauer and Greenberg (1962) modified this suggestion to the effect that the replacement be of the nature of a  $\text{Ca}^{++}$  ion plus a water molecule for each  $\text{Si}(\text{OH})_2$  group removed. This change would result in a direct correspondence between Ca:Si ratio and  $\text{H}_2\text{O}$ :Si ratio for members of such a hypothetical replacement series, and Brunauer and Greenberg gave data for a series of samples in which the fractional increase in Ca between successive members was just matched by the fractional increase in  $\text{H}_2\text{O}$ . In the present data, this hypothesis would account for the data for the two products prepared by direction reaction of lime and silica sol, CSH(I) - 6 and - 7, of compositions  $\text{C}_{0.91}\text{S}_{1.00}\text{H}_{1.08}$  and  $\text{C}_{1.58}\text{S}_{1.00}\text{H}_{1.80}$ . These were prepared in an identical manner using 1:1 and 2:1 mole ratios of the starting materials. The fractional difference in CaO is 0.67 moles per  $\text{SiO}_2$ ; the corresponding water difference is 0.72 moles.





It appears that the relationship postulated by Brunauer and Greenberg may hold good within a series of preparations of the same kind; however, considering the CSH(I) group as a whole such a relationship is not evident. The actual structures of the individual samples must vary from that of tobermorite in a variety of ways, depending on the specific mode and details of the preparation. Nevertheless, the characteristics of the CSH(I) phase in the matter of x-ray diffraction, DTA, infrared pattern, morphology, etc. appear to be remarkably uniform, and the phase is well-defined by these characteristic properties.

#### Surface Properties and Plasticity of Tobermorite and CSH(I)

The discovery that tobermorite particles interact with water to produce a decidedly plastic system analagous to that of a wet clay is of considerable interest.

The peculiar plastic properties of wet clay are usually explained on the basis of fine particle size, platy morphology and strong attraction of the surface of the solid for a restricted number of layers of water; when the thickness of the water film surrounding the particles becomes greater than the number of layers that are strongly held, the extra water acts as a lubricant, and the particles can slip past each other easily in response to a shearing force. A more complete treatment of the plasticity of clays along these lines is given by Grim (1953, p. 173) and by Iler (1955, p. 217). It should be noted that the strength with which the firmly bound water is



held and the amount of water that is so bound are partially a function of the exchangeable cation present.

The platy shape and fine particle size of tobermorite are appropriate for the development of plasticity according to this picture. The suggestion was made earlier that the tobermorite surface interacts strongly with the first layer of adsorbed water (high  $E_1$  value), but only weakly with succeeding layers. Such behavior is compatible with the ideas underlying these explanations of the plasticity of the clays, and hence the presence of the phenomenon of plasticity in the tobermorite-water system is not surprising.

The most striking difference between the rheological properties of tobermorite phases and those of the CSH(I) materials appears to be the cementation that ties the aggregates of the latter phase together and makes dispersion into primary particles in aqueous systems difficult or impossible. This property does not seem to depend on the calcium content of the phase, since CSH(I) preparations relatively low in calcium (CSH(I) - 1, 2, and 6, for example) appear to be just as strongly resistant to dispersive efforts as the others. This cementing action is entirely absent from tobermorite, which disperses spontaneously in water.

In consequence of the cementation of the primary particles of CSH(I) into aggregates, the plastic properties that become evident in a wetted tobermorite system are not found in CSH(I)-water mixes. Rather, despite their very small ultimate particle size, the particles behave as silt particles; there is a distinct



silty feel to the moist material when rubbed, and there is a critical, very narrow moisture range in which the material is almost, but not quite, plastic. In accord with the usual behavior of silty systems, a slight increase in the moisture content results in a dilatent suspension and a slight decrease in moisture produces a dry, definitely non-plastic feel.

The surface properties of CSH(I) with respect to sign of surface charge in various chemical environments were shown to be substantially similar to those of tobermorite. Furthermore the BET  $E_1$  values were only moderately lower, suggesting nearly as strong an attraction for the first layer of water in CSH(I) as in tobermorite. This was true except for the nearly amorphous member of the CSH(I) group, which showed a very low heat of adsorption of the first layer. The major differences between the surface properties of tobermorite and CSH(I) appear to be that on one hand, the attraction of tobermorite for water layers in excess of the first is for some reason low, and that, on the other hand, CSH(I) primary particles are cemented together effectively. Whether these two phenomena are related to each other is not known, but it does not seem to be likely.

### Reactions Between Lime and Silicates

#### Near Room Temperature

The results of the study of the reaction products of lime and the various silicate materials has shown, first, the reactivity of the several phases is much greater than previously imagined. In the experiments involving large excesses of lime at 45°C, nearly all of the clay minerals were almost



completely destroyed and even minerals commonly thought of as resistant to chemical attack, such as muscovite mica and pyrophyllite, reacted extensively. It seems likely that if a continuous leaching system were set up to remove the products of attack, most of the minerals could be completely dissolved by prolonged leaching in saturated  $\text{Ca}(\text{OH})_2$ .

The nature of the attack has not been studied in detail. Eades, in an unpublished communication, has suggested that the factor mainly responsible for the attack is the high pH (12.4) maintained by the saturated  $\text{Ca}(\text{OH})_2$  solution. Eades and Grim (1960) have interpreted some of their x-ray data as suggesting that attack on some kinds of particles, notably kaolinite, is from the prism or edge surfaces. The prevalence of attack from the edges was confirmed by the present electron micrographs in which the raggedness of the edges of the decomposing particles was quite apparent. However, several of the photos suggested that delamination as well as edge attack was taking place, and undue emphasis should not be placed on any specific mode of decomposition of the silicate particles.

One important result of this study is that the exact nature of the products of the attack are for the first time clearly indicated.  $\text{Ca}(\text{OH})_2$  reacts with quartz to produce CSH(gel), and the identity of this phase with the CSH(gel) produced by hydrating cement minerals is made apparent. The aluminosilicate clays almost always produced separate CSH and calcium aluminate hydrate phases, the latter always being quite well-crystallized in comparison with the former. The clays reacted at  $60^\circ\text{C}$  in





relatively dry environments produced CSH(I) rather than CSH(gel); the hydrated calcium aluminate found was the cubic phase  $C_3AH_6$ . No alumina-bearing product of the montmorillonite reaction under this condition was identified. At temperatures closer to room temperature ( $45^{\circ}C$  or  $23^{\circ}C$ ) and in wetter systems, the CSH phase found in all the aluminosilicate reactions was CSH(gel) rather than CSH(I), and the hydrated calcium aluminate phase was  $C_4AH_{13}$ , possibly containing some substituted silica. The possibility of substituted alumina in the CSH phases also exists. Nevertheless, there is some indirect evidence against it. Aluminum substitution in tobermorite results in a changed exothermic response at high temperature from a modest and weak peak to a strong, sharp one, and changes occur in the nature of the fired product. CSH(gel) prepared from pure calcium silicate phases has an exotherm that is normally almost as weak as that of unsubstituted tobermorite; the corresponding exotherms for the various reacted clay systems that give rise to CSH(gel) show no significant increase in the extent and sharpness of this thermal feature, nor was there any unusual shrinkage noted. Consequently, in the absence of demonstration to the contrary, it can be assumed that in these systems little if any substitution occurs.

#### Characteristics of the $C_4AH_{13}$ Phase

The nature of the  $C_4AH_{13}$  phase produced in these reactions may be somewhat different from that produced by most previous investigators, who generally prepared the phase by the reaction



of calcium aluminate with lime in dilute solution. Such phases actually have a composition of  $C_4AH_{19}$  according to Roberts (1959), and it is only on removal from the water system and partial dehydration that the  $C_4AH_{13}$  composition and characteristic 7.9A-8.2A basal spacings are formed. Further dehydration below that of oven-drying lowers both the basal spacing and the water content, but these effects are at least partially reversible.

In contrast to this, the  $C_4AH_{13}$ -type phases formed in reacting clay-lime systems, where the water content is much less, are formed with a 7.5-7.7A basal spacing and are, as it were, partially dehydrated already at the time of their formation. However, heating at 150°C produces further collapse and rearrangement of these materials as it does in the corresponding  $C_4AH_{13}$  phases made in dilute solution.

The possibility of the incorporation of either silica,  $CO_3^{=}$ , or both, remains open. Since it is difficult to get reagent  $Ca(OH)_2$  entirely free from carbonate, a certain amount of carbonate is usually incorporated into the product from this source. The question of the possibility of silica substitution is more vexing. The high silica and very low alumina content of the sample of single-crystal material reported by Hilt and Davidson to give a  $C_4AH_{13}$  x-ray pattern would argue for a high degree of possible solid solution; however it is possible that this analysis was in error.

Substitution of silica in the  $C_4AH_{13}$  lattice would in effect produce a quaternary phase containing lime, alumina, silica and water. There are several well-known phases which fall into this



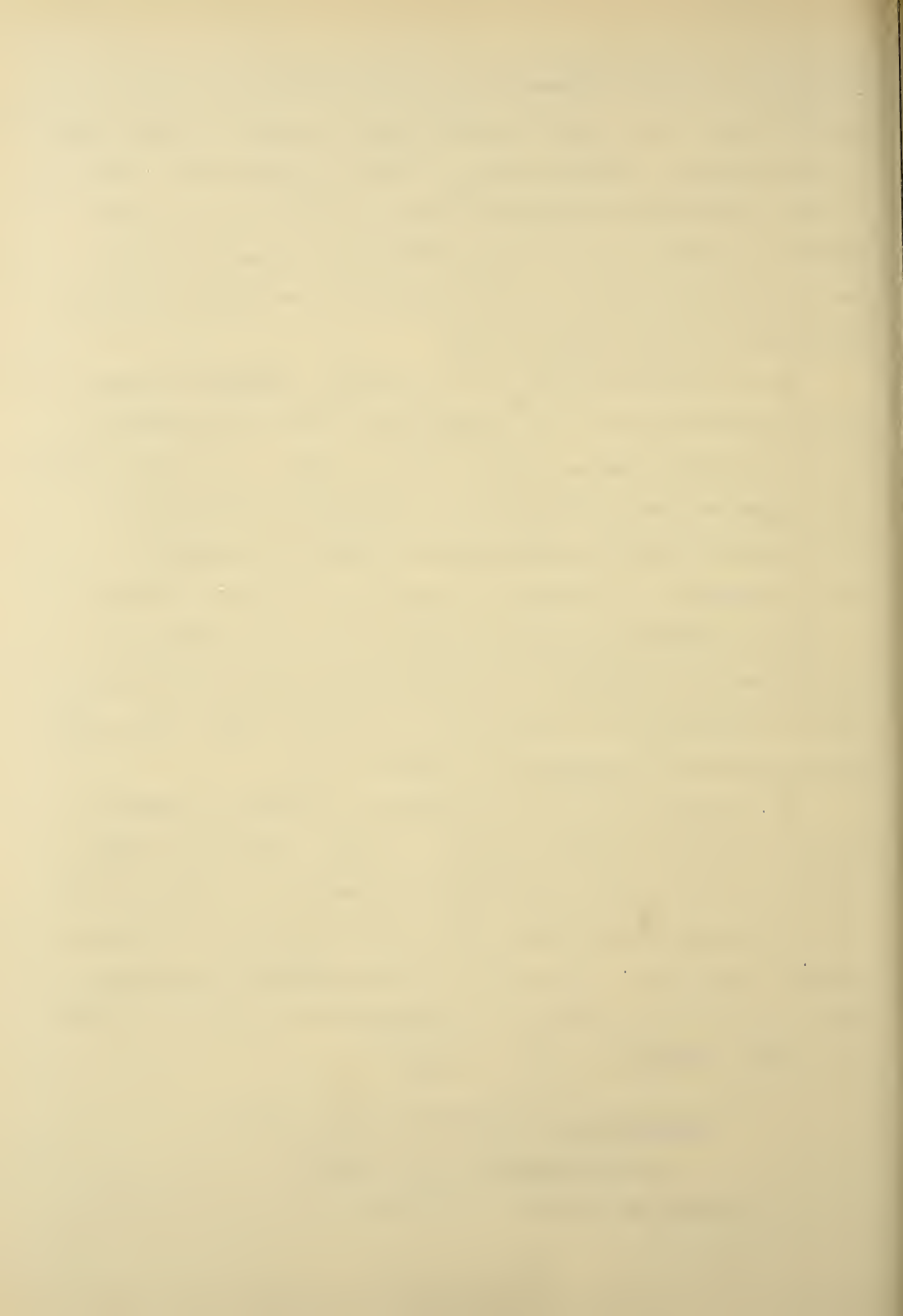
category, e.g. the hydrogarnet solid-solution series that is isostructural with  $C_3AH_6$ , and Stratling's compound  $C_2ASH_8$ , which is isostructural with the  $C_4AH_{13}$ . It is definite that neither of these recognized quaternary phases is formed in lime-clay reacting systems in this work, although Stratling's compound has been reported to form in reactions of lime with previously calcined kaolinite (Benton, 1959).

The structure of  $C_4AH_{13}$  was originally considered to involve alternating layers of  $Ca(OH)_2$  and  $Al(OH)_3$  (Brandenberger, 1933), but more recently Buttler, Dent Glasser, and Taylor (1959) have suggested the possibility of a more complex structure. This proposed structure consists of a structural element a single octahedral layer thick containing two calcium ions and a single aluminum ion in ordered positions in the layer surrounded by six OH groups. A seventh OH group and the associated water molecules were said to occur in a second layer that alternates regularly with one of the first variety.

The present work was not designed to provide information on the structure of this compound. However, the demonstrated lability of the  $C_4AH_{13}$  with respect to removal of half its lime by water washing without any particular damage to the infrared pattern, the x-ray diffraction diagram, or the appearance of the crystallites is difficult to understand on the basis of the structure proposed by Buttler, et al.

#### Implications of the Present Work on the Understanding of Cementation

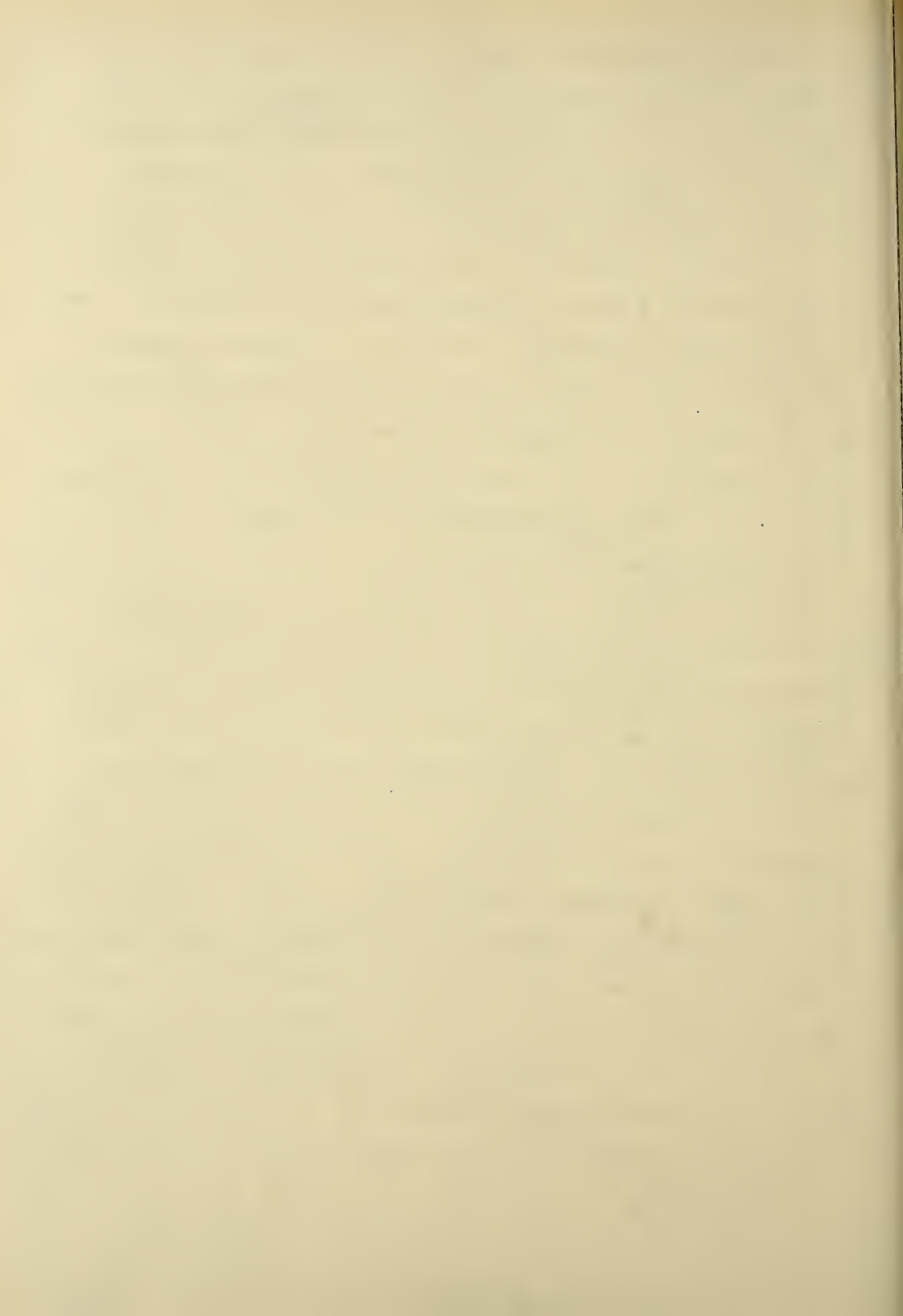
The present work shows clearly that the cementing product





of lime-clay reactions is usually CSH(gel), identical in all identifiable respects with the CSH(gel) that has been picturesquely described as the "heart of concrete". Thus the explanation of the degree of hardening, strength and permanence attained in lime-soil stabilization is readily understandable.

On the other hand, the cementing phase formed in the reactions between lime and kaolinite and lime and montmorillonite at 60°C was not CSH(gel) but CSH(I) of a distinctly different DTA behavior, and more important, distinctly different morphology. These cementing particles are not fibers but definitely thin, wrinkled foils or "snowflakes" as was made plain in the electron micrographs. The lime-kaolinite and lime-montmorillonite reaction products at 60°C, cemented by thin CSH(I) foils, are every bit as strong, well-cemented, and resistant to weakening by immersion in water, as the corresponding lime-quartz reaction product, which is cemented with what are obviously fibers of CSH(gel). The importance of this observation is that efforts to explain the unique strength and cementative properties of hydrates of Portland cement or of CSH(gel) on the basis of its particular fibrous or rod-shaped morphology appear to be inadequate, since apparently the identical strength and the degree of cementation are obtained with particles of entirely different morphology. It seems that emphasis needs to be placed rather on the chemical or physical-chemical features responsible for the adhesion of CSH(gel) or CSH(I) particles to each other so firmly that no appreciable dispersion in water systems can be obtained, even when the surface charge is reduced or even reversed in sign.





## SUMMARY AND CONCLUSIONS

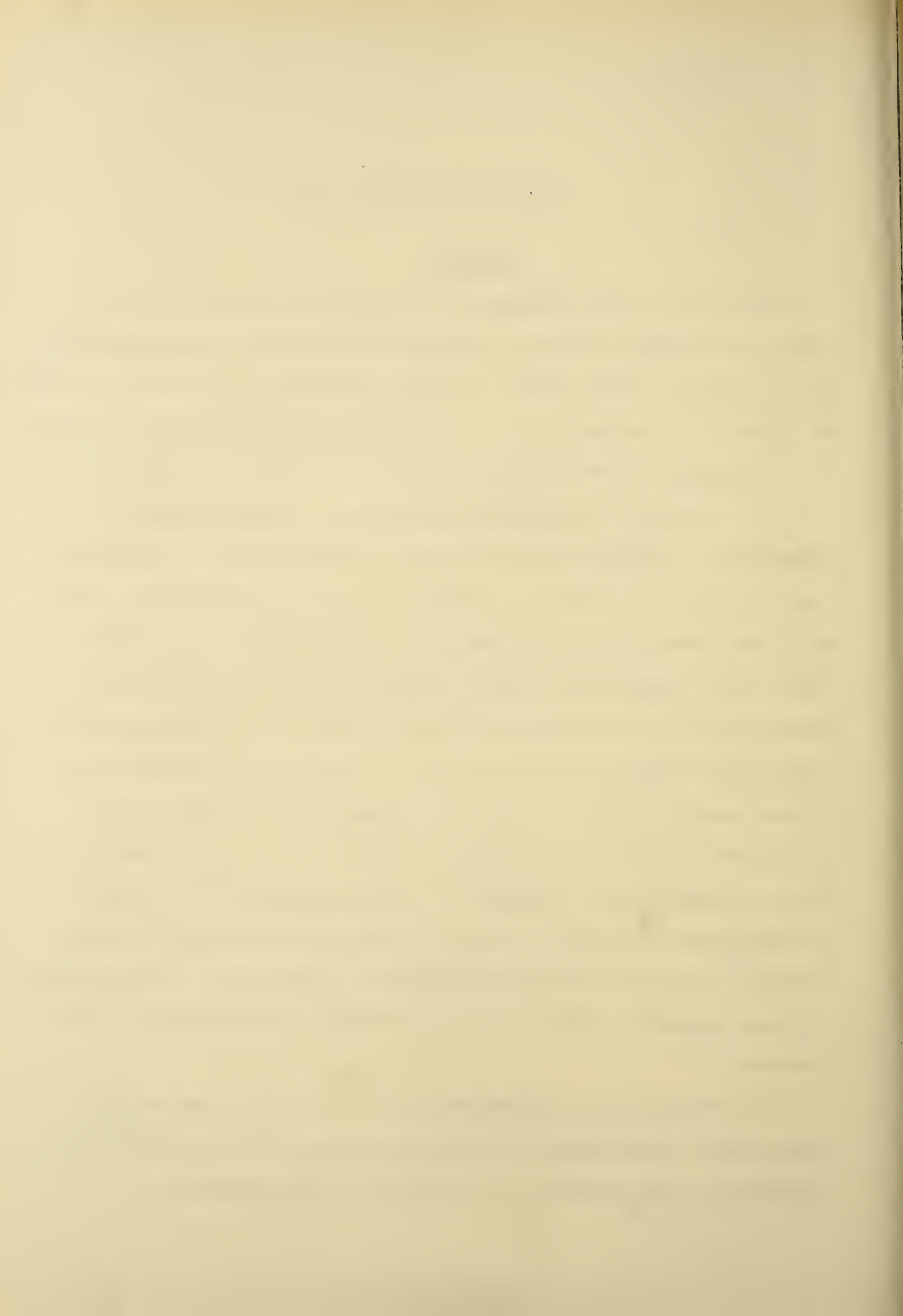
### Summary

Because of the large amount of detailed information presented, individual summaries have been appended to each portion of the results. The reader is directed to the individual sections for appropriate summaries of the properties of individual phases.

In general, the findings of this study were as follows:

(1) The x-ray diffraction pattern of tobermorite was changed only slightly as a result of substitution of aluminum, iron, or magnesium into the lattice. Iron and magnesium substitution considerably reduced the intensities of the (002) and (222) peaks, suggesting c-axis disorder may arise from these replacements. The x-ray diffraction patterns of CSH(I) samples showed less detail and consisted of a line at 3.03Å and three or four weaker lines; no basal spacings were observed. One sample was amorphous to x-rays, despite its having other properties characteristic of CSH(I). CSH(gel) preparations prepared by hydration of cement minerals yielded x-ray patterns similar to those of CSH(I) but the presence of  $\text{Ca(OH)}_2$  and incompletely hydrated cement minerals complicated the interpretation of the patterns.

(2) DTA curves of tobermorite and iron- and magnesium-substituted tobermorites exhibited very weak high-temperature exotherms on conversion of the minerals to wollastonite.



Aluminum substitution caused a strong, sharp exotherm accompanied by marked shrinkage and cementation of the sample which may have been due to mullite formation. All CSH(I) samples yielded intense high-temperature exotherms, but the samples did not shrink as much, and the product was friable and different in appearance from those formed by aluminum-substituted tobermorites. CSH(gel) produced from the different calcium silicate phases all exhibited weak but sharp high-temperature exotherms, distinguishable from those of both CSH(gel) and tobermorite.

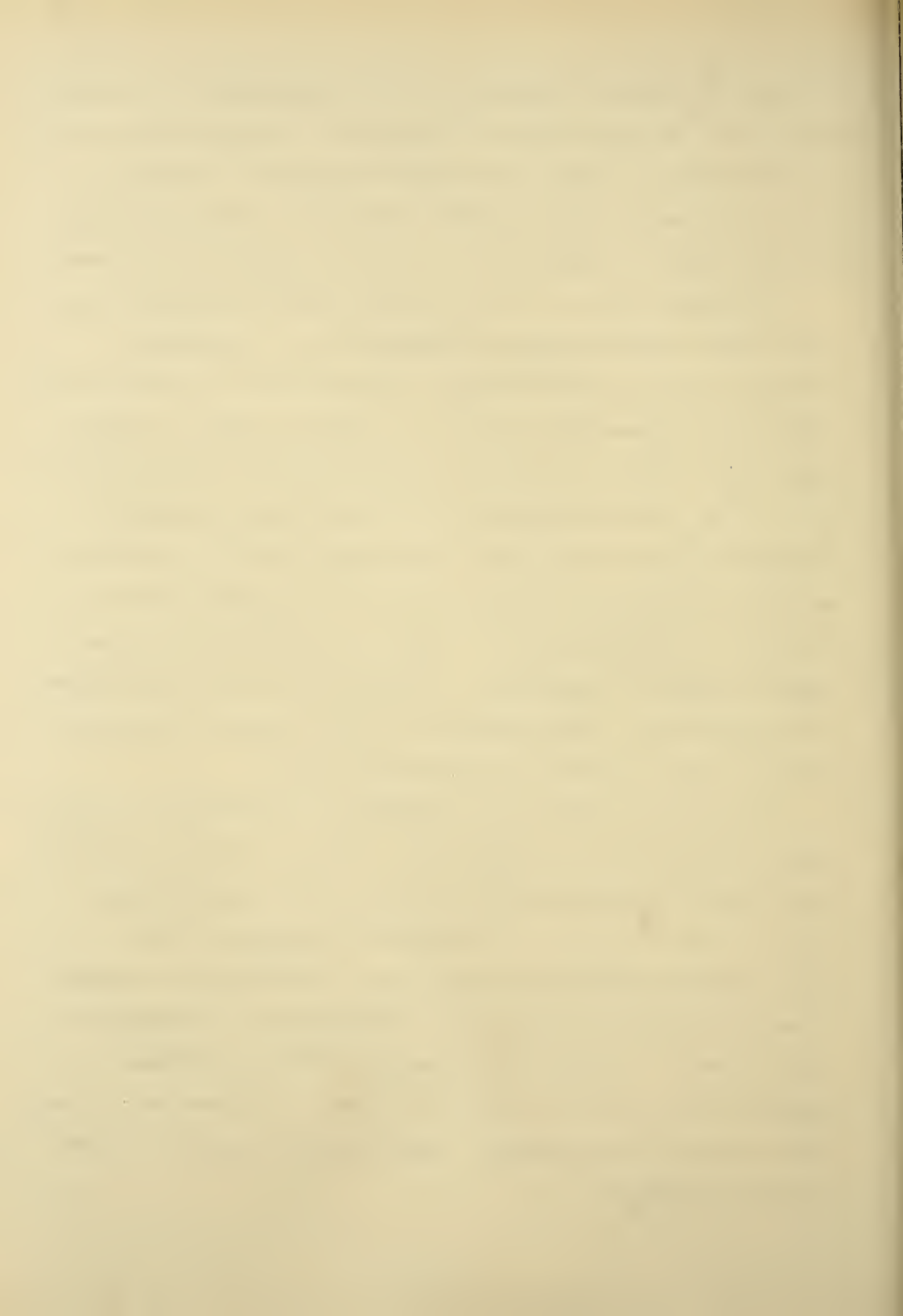
(3) Infrared spectra of tobermorite and substituted tobermorites were characterized by the strong Si-O band at  $970\text{ cm}^{-1}$ ; a number of additional bands, not previously reported, were found for these phases. Lattice substitution produced only small changes in the infrared spectra. CSH(I) samples of varying composition had quite similar spectra. Strong general absorption was observed on the low-frequency side of the Si-O band, particularly with samples of high calcium content. The spectra of CSH(gel) were dominated by a pronounced minimum in absorption, which may be an artifact due to specimen preparation, since it has not been reported previously. The Si-O band is considerably broadened and its position is shifted to about  $940\text{ cm}^{-1}$ , suggesting that this phase contains almost completely depolymerized silica tetrahedra. The bands attributed to the stretching vibration of bonded OH groups and to the bending vibration of water are considerably weaker in these patterns than in previously published results obtained from samples incorporated into KBr



pellets. The feature attributed to the asymmetrical stretching mode of  $\text{CO}_3^{=}$  at about  $1430 \text{ cm}^{-1}$  was present in all samples, but was particularly strong in the CSH(I) patterns. The band in CSH(gel) actually occurs at about  $1390 \text{ cm}^{-1}$ , perhaps due to a different mode of incorporation of the carbonate in this phase.

(4) Surface areas of the various phases were measured by water vapor adsorption at room temperature. Tobermorite yielded a value of about  $80 \text{ m}^2/\text{g}$ , and the values for the various substituted tobermorites were only slightly greater. In contrast, the surface areas of the CSH(I) samples ranged from 150 to  $350 \text{ m}^2/\text{g}$ . Heats of adsorption of water vapor calculated from the BET theory were about 13,500 cal/mole for the tobermorite and substituted tobermorites, but distinctly less for the CSH(I) specimens and only about 11,700 cal/mole for the amorphous CSH(I) preparation. Adsorption in tobermorites seems to be restricted to two molecular layers, but this restriction does not appear to hold for the CSH(I) phase.

(5) Electron microscopic observations confirmed the platy shape characteristic of tobermorite. Aluminum substitution did not affect the particle morphology but iron substitution resulted in the formation of lath-shaped particles. CSH(I) particles were dominantly fine foils or "snowflakes", although a few platy particles and massive "crinkled foil aggregates" were observed. CSH(gel) particles are definitely fibrous in nature although cemented sheets of fibers and occasionally platy particles were also observed. Cigar-shaped bundles of fibers were not observed.





(6) Zeta potential measurements carried out with tobermorite and substituted tobermorites revealed that the particles are negatively charged when dispersed in distilled water but become positively charged in solutions containing appropriate concentrations of calcium or aluminum cations. Similar behavior was found for CSH(I) and CSH(gel) materials except that the latter is formed initially as a positively charged material due to the presence of  $\text{Ca}(\text{OH})_2$  as a byproduct of its formation. When the  $\text{Ca}(\text{OH})_2$  is leached out by repeated washing in water the CSH(gel) particles assume a negative surface charge.

(7) Tobermorite and substituted tobermorites disperse readily in water to yield primary particles that orient readily on deposition. CSH(I) and CSH(gel) particles were cemented into aggregates which do not disperse in water suspension, despite ultrasonic treatment and attempts at chemical dispersion. Tobermorite-water systems of appropriate moisture content exhibit plasticity analogous to that of clay, but the CSH phases act rheologically as silt-size particles.

(8) Cation exchange capacity measurements made in alcoholic solution indicate a CEC for tobermorite of 34 meq/100 g. Substitution decreased rather than increased this value. The measured CEC values of the CSH(I) and CSH(gel) phases varied somewhat, but all were distinctly less than that of tobermorite.

(9)  $\text{Ca}(\text{OH})_2$  reacted with quartz in compacted mixtures at  $60^\circ\text{C}$  to produce a strongly cemented CSH(gel) product of distinct fibrous morphology and high surface area. Under the same conditions  $\text{Ca}(\text{OH})_2$  reacted with kaolinite and montmorillonite to





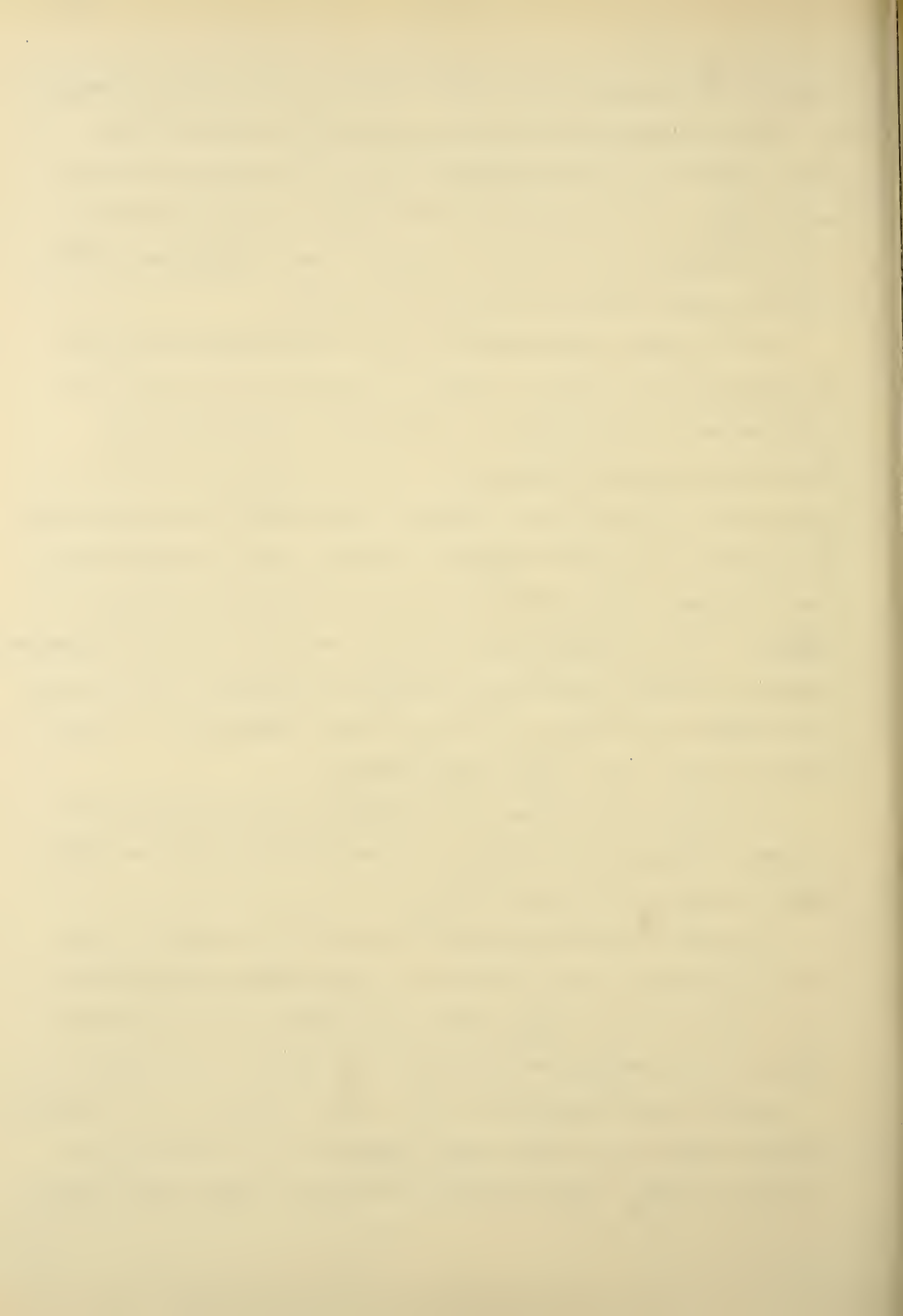
produce a high-surface area CSH(I) phase of foil-shaped morphology, but the cementation achieved was as good as that of the quartz reaction. With kaolinite a separate calcium aluminate phase,  $C_3AH_6$ , is produced, but this phase was not identified in the montmorillonite product. Under these conditions  $Ca(OH)_2$  does not react appreciably with pyrophyllite.

(10) At lower temperatures ( $45^{\circ}C$ ) and reaction conditions involving the presence of  $Ca(OH)_2$  in large excess and the reaction mixture in the form of a constantly agitated slurry, the attack of calcium hydroxide virtually destroyed certain clay mineral phases; even resistant phases such as pyrophyllite and muscovite mica were severely attacked. The CSH product was always CSH(gel) under these conditions. Quartz yielded only CSH(gel). The aluminum-bearing phases-kaolinite, montmorillonite, pyrophyllite, mica, and illite-yielded a hexagonal calcium aluminate hydrate identified as  $C_4AH_{13}$ . Talc, a magnesium silicate, did not react to any significant degree.

(11) Kaolinite reacted with  $Ca(OH)_2$  in dilute suspension at room temperature to produce the same products, fibrous CSH(gel) and platy, hexagonal  $C_4AH_{13}$ .

(12) These reactions appear to result from attack of the silicate particles from the edges, as postulated by Eades and Grim (1960); in this study some visual evidence of the delamination of clay particles during the reaction was also found.

(13) It was found that  $Ca(OH)_2$  reacts readily with synthetic hydrous alumina to produce  $C_4AH_{13}$  together with a small proportion of  $C_3AH_6$ . The reaction is extremely rapid, the  $Ca(OH)_2$



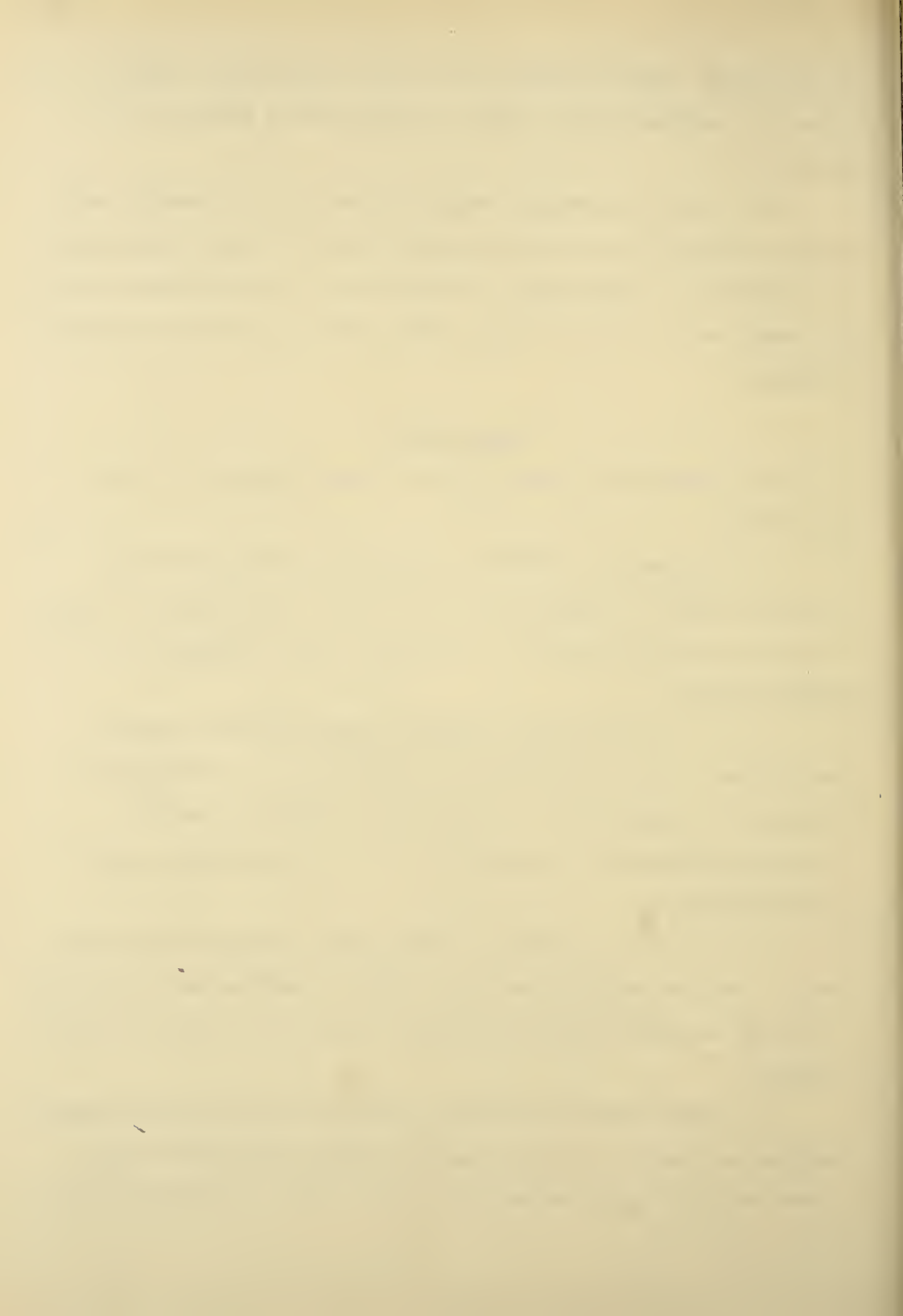
disappearing almost instantly and well-crystallized  $C_4AH_{13}$  appearing within minutes after the addition of water to dry mixtures.

(14)  $C_4AH_{13}$  is readily converted to  $C_2AH_8$  on washing with water to remove accompanying excess lime. The resulting product is identical in morphology and behavior on heating to the  $C_4AH_{13}$ , and very similar in its x-ray diffraction pattern and infrared spectrum.

### Conclusions

The major generalizations drawn from this study are the following:

1. Tobermorite, CSH(I) and CSH(gel) are separate and distinct phases having distinctive physical and chemical properties, and are not part of a continuous series varying only in crystallinity.
2. All of the phases examined possess cation exchange properties. The cation exchange capacity must be measured in solutions in which these materials are insoluble, but the phenomenon of cation exchange is not necessarily restricted to such conditions.
3. All of the phases are negatively charged in distilled water, but the negative surface charge is reduced and eventually reversed in concentrated solutions containing calcium or aluminum ions.
4. Substitution of various ions into the lattice of tobermorite may readily be accomplished, and appears to have only minor effects on the properties of the resulting tobermorites.



5.  $\text{Ca(OH)}_2$  readily attacks clay and other silicate minerals to a much greater extent than previously considered. The products of the various reactions can usually be identified as known calcium silicate hydrate and calcium aluminate hydrate phases. Observations of particle morphology are particularly helpful in this regard.

6. Both CSH(I) and CSH(gel) possess cementing qualities, and when produced in identical circumstances seem to be about equally effective in producing strong, water-resistant cemented products. Thus, explanations of the cementing action of calcium silicate hydrates that rest on the particular morphology of the CSH(gel) phase may be misleading.



## BIBLIOGRAPHY





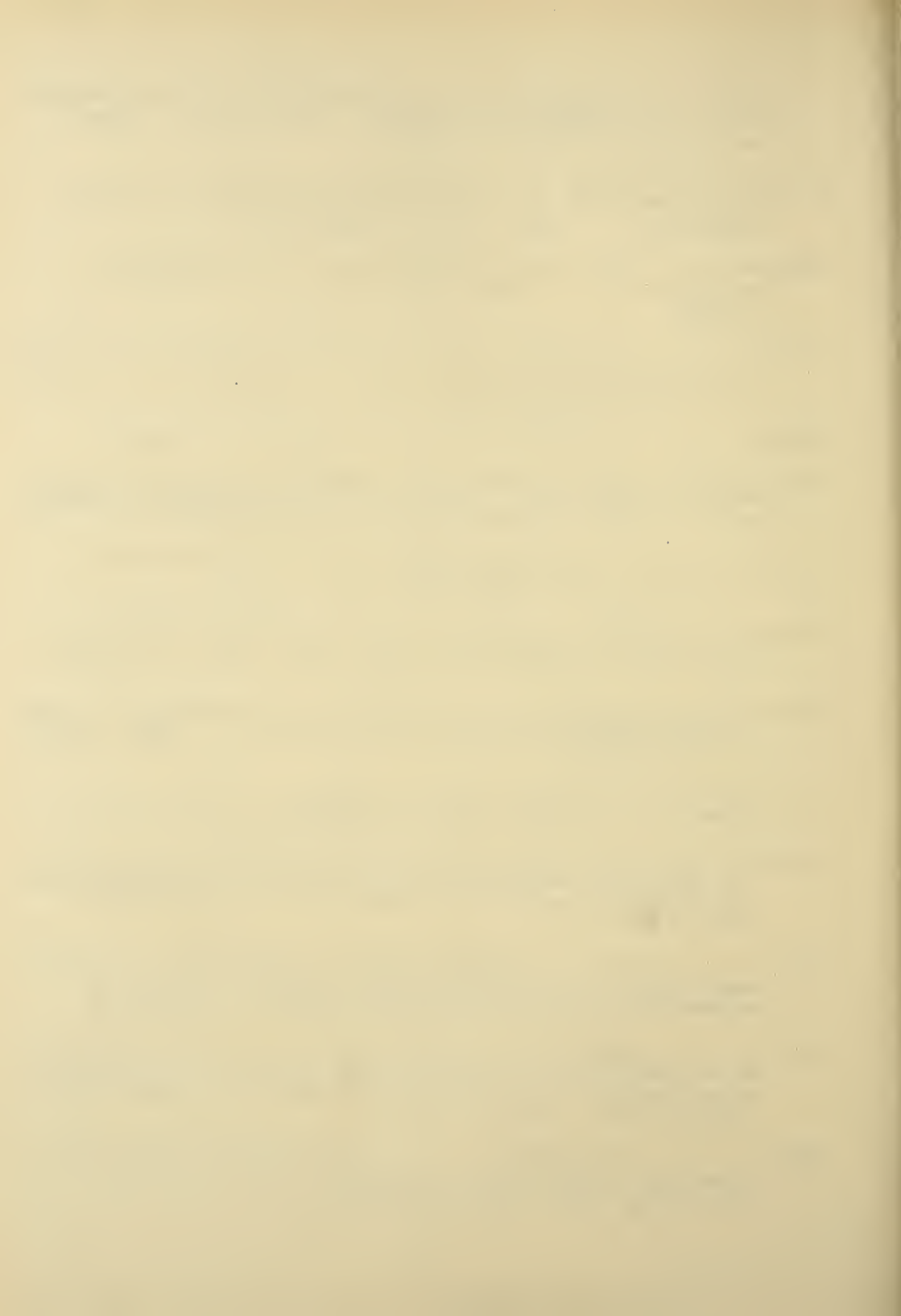
## BIBLIOGRAPHY

- Abramson, H. A., Moyer, L. S. and Gorin, M. H. (1942). Electro-phoresis of Proteins. Reinhold Publ. Corp., New York.
- Aitken, A. and Taylor, H. F. W. (1960). Reactions in lime-quartz pastes. *J. Applied Chem.* 10 7-15.
- American Society for Testing and Materials (1961) Book of ASTM Standards, Part 4. A.S.T.M., Philadelphia.
- Benton, E. (1959) Cement-pozzolan reactions. Highway Research Board Bul. 239 (NAS-NRC Publ. 725) pp. 56-65.
- Bessey, G. E. (1938). The calcium aluminate and silicate hydrates in Proc. Symp. on Chemistry of Cements, Stockholm, 1938. pp. 178-214.
- Bogue, R. H. (1953) A note on the nomenclature of the calcium silicate hydrates. *Mag. Concrete Res.* 3 87.
- Bogue, R. H. (1954) The calcium silicate hydrates. Paper No. 69; Portland Cement Fellowship at the National Bureau of Standards, Washington, D. C.
- Brandenberger, E. (1933) Investigations on the Crystal Structures of Calcium Aluminate Hydrates. *Schweiz. Mineral. Petrog. Mitt.* 13 569-570 (in German).
- Brandenberger, E. (1936) Intercrystalline Structure and the Chemistry of Cement. *Schweiz. Arch. angew. Wiss. u. Tech.* 2 45-48. (in German).
- Brunauer, S. (1943) The Adsorption of Gases and Vapors. Princeton University Press, Princeton, N. J.
- Brunauer, S. (1962) Tobermorite gel - the heart of concrete. *American Scientist* 50 210-229.
- Brunauer, S., Deming, L. S., Deming, W. E., and Teller, E. (1940) On a theory of the van der Waals adsorption of gases. *J. Amer. Chem. Soc.* 62 1723-1732.
- Brunauer, S., Emmett, P. H., and Teller, E. (1938) Adsorption of gases in multimolecular layers. *J. Amer. Chem. Soc.* 60 309-319.
- Brunauer, S. and Greenberg, S. A. (1962) The hydration of

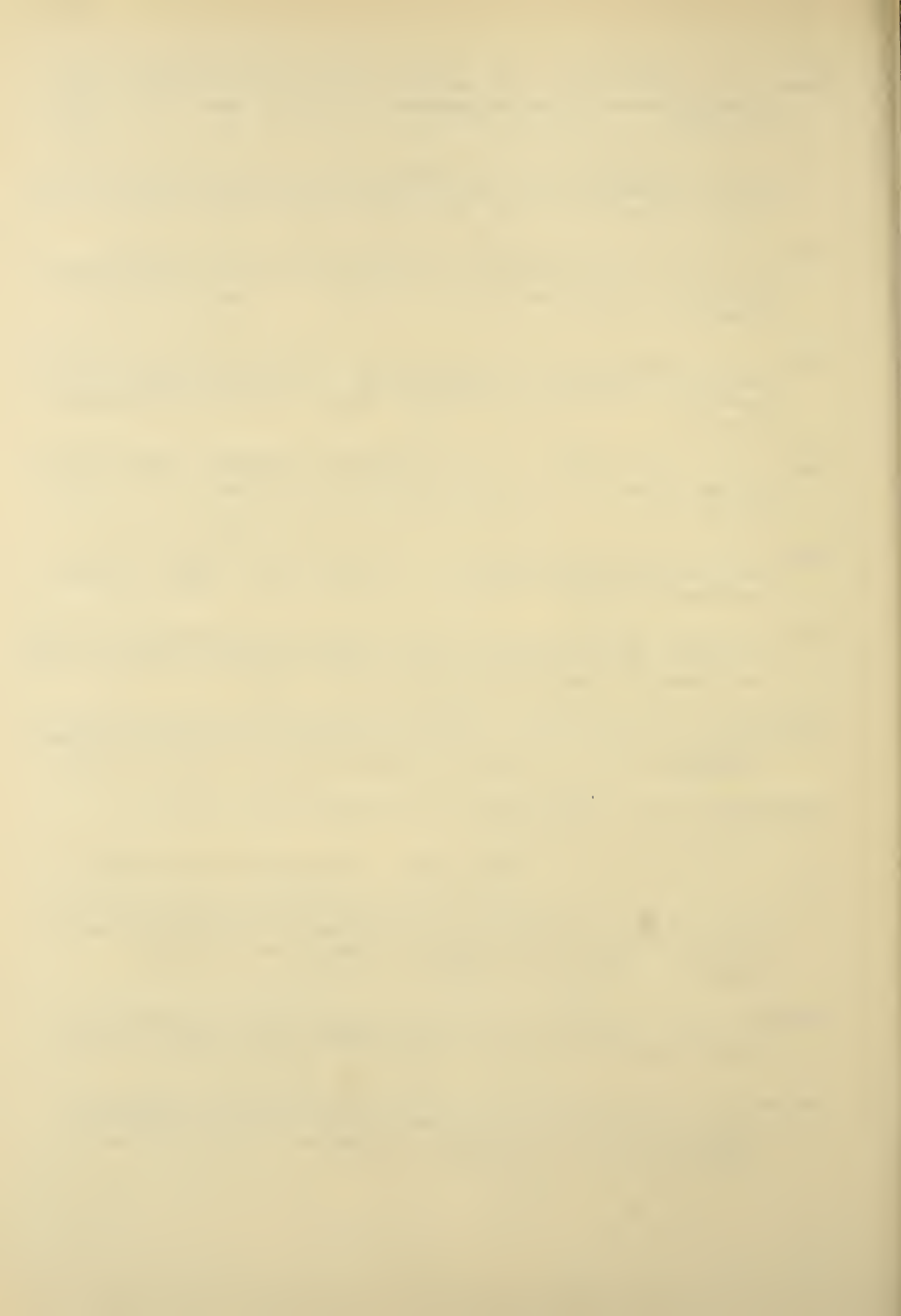


tricalcium silicate and dicalcium silicate at room temperature. In "Chemistry of Cement", (Proc. 4th Int. Conf., Washington, 1960) pp. 135-165.

- Brunauer, S., Kantro, D. L., and Copeland, L. E. (1958) The stoichiometry of the hydration of  $\beta$ -C<sub>2</sub>S and C<sub>3</sub>S at room temperature. J. Amer. Chem. Soc. 80 761-776.
- Brunauer, S., Kantro, D. L., and Weise, C. H. (1959) The surface energy of tobermorite. Canadian J. of Chem. 37 714-724.
- Buckle, E. R., and Taylor, H. F. W. (1959). The hydration of C<sub>3</sub>S and  $\beta$ -C<sub>2</sub>S in pastes under normal and steam-curing conditions. J. Applied Chem. 9 163-172.
- Buttler, F. G. (1958) Ph.D. Thesis, University of Aberdeen.
- Buttler, F. G., Dent Glasser, L. S. and Taylor, H. F. W. (1959) Studies on 4CaO·Al<sub>2</sub>O<sub>3</sub>·13H<sub>2</sub>O and the related natural mineral hydrocalumite. J. Amer. Ceram. Soc. 42 121-126.
- Carlson, E. T. (1958) The system lime-alumina-water at 1°C. J. Res. Nat. Bur. Stand. 61 1-11.
- Chang, K. L., Kurtz, T., and Bray, P. H. (1952) Determination of calcium and magnesium in limestone. Anal. Chem. 24 1640
- Chatterji, S. and Jeffery, J. W. (1962) Studies of early stages of paste hydration of cement compounds. I. J. Amer. Ceram. Soc. 45 536-543.
- Claringbull, G. F. and Hey, M. H. (1952). A re-examination of tobermorite. Mineral. Mag. 29 960-963.
- Copeland, L. E. and Schulz, E. G. (1962) Electron-optical investigation of the hydration products of calcium silicates and portland cement. J. of the P.C.A. Res. and Devel. Labs. 4 2-12.
- Eades, J., and Grim, R. (1960) Reactions of hydrated lime with pure clay minerals in soil stabilization. Highway Research Board Bulletin 262(NAS-NRC Publ. 771) pp 51-63.
- Eades, J. L., Nichols, F. P., and Grim, R. E. (1962) Formation of new minerals with lime stabilization as proved by field experiments in Virginia. Highway Research Board Bul. 335 (NAS-NRC Publ. 1017) pp 32-39.
- Eakle, A. S. (1917) Minerals associated with the crystalline limestone at Crestmore, Riverside County, Calif. Univ. of Calif. Bul. Dept. Geol. 10 327-350

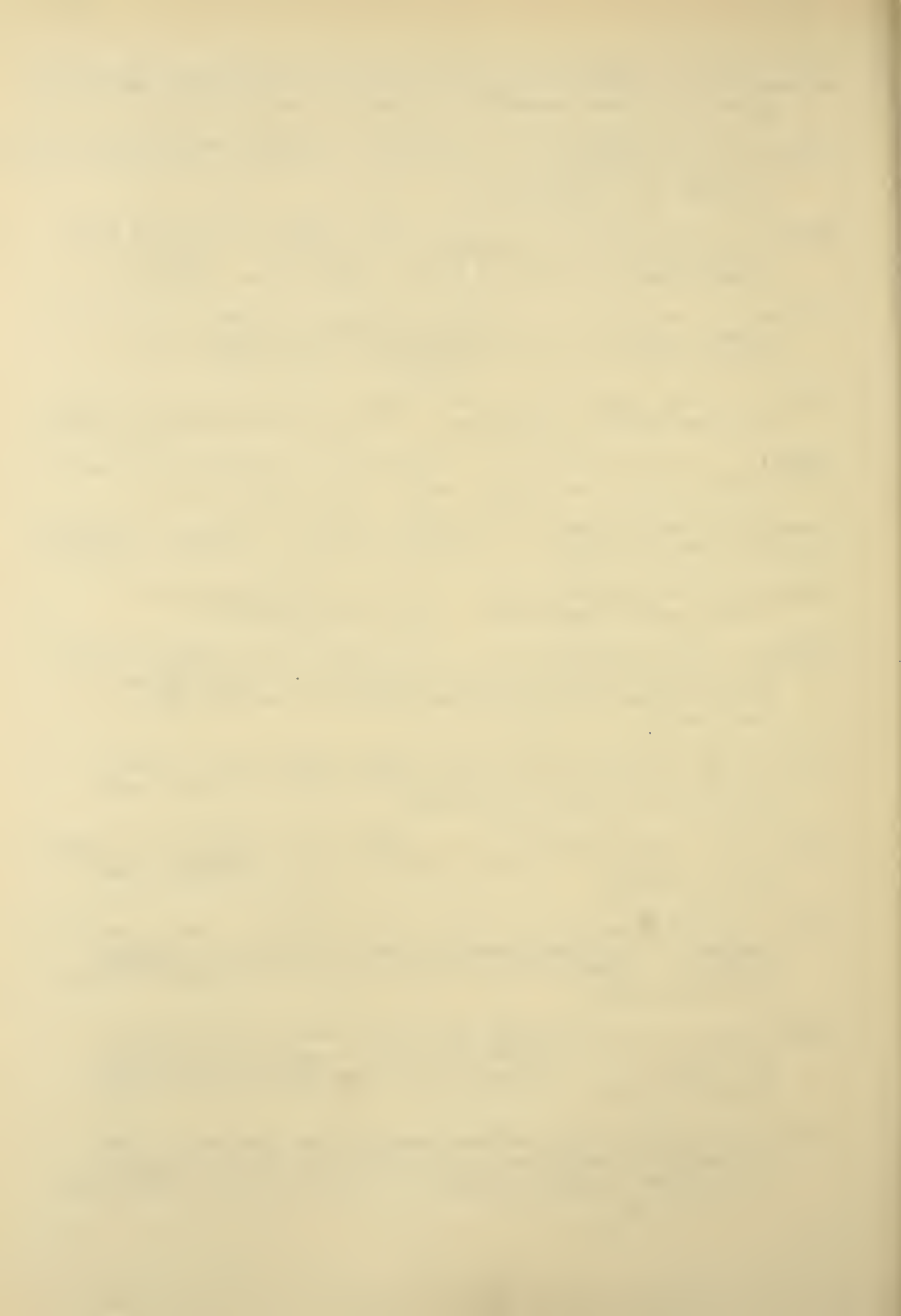


- Fahey, J. J., Ross, M., and Axelrod, J. M. (1960) Loughlinite, a new hydrous sodium magnesium silicate. *Amer. Min.* 45 270-281.
- Flint, E. P., MacMurdie, H. F., and Wells, L. S. (1938) Formation of hydrated calcium silicates at elevated temperatures and pressures. *J. Res. Nat. Bur. Stand.* 21 617-638.
- Flint, E. P., and Wells, L. S. (1944) Analogy of hydrated calcium silicoaluminates and hexagonal calcium aluminates to hydrated calcium sulfoaluminates. *J. Res. Nat. Bur. Stand.* 30 367-403.
- Gard, J. A., Howison, J. W. and Taylor, H. F. W. (1959) Synthetic compounds related to tobermorite: an electron microscope, x-ray, and dehydration study. *Mag. Concrete Research* 11 151-158.
- Gard, J. A. and Taylor, H. F. W. (1957) A further investigation of the tobermorite from Loch Eynort, Scotland. *Min. Mag.* 31 361-370.
- Gaze, R. and Robertson, R. H. S. (1956) Some observations on calcium silicate hydrate (I)-tobermorite. *Mag. Concrete Research* 8 7-12.
- Glenn, G. R., and Handy, R. L. (1963) Lime-clay mineral reaction products. Paper given at Forty-second Annual Meeting, Highway Research Board, Washington, Jan. 1963.
- Goldberg, I., and Klein, A. (1952) Some effects of treating expansive clays with calcium hydroxide in Symp. on Exchange Phenomena in Soils, ASTM Special Publ. No. 142 pp 53-71.
- Greenberg, S. A. (1954) Calcium silicate hydrate (I). *J. Phys. Chem.* 58 362-367.
- Grim, R. E. (1953) *Clay Mineralogy*. McGraw-Hill, New York.
- Grudemo, A. (1955) An electronographic study of the morphology and crystallization properties of calcium silicate hydrates. *Proceedings, Swedish Cement and Concrete Research Institute, Stockholm*, No. 26.
- Harned, H. S. and Hamer, W. J. (1935) The thermodynamics of aqueous sulfuric acid solution from electromotive force measurements. *J. Amer. Chem. Soc.* 57 27-33.
- Harvey, R. D. and Beck, C. W. (1962) Hydrothermal regularly interstratified chlorite-vermiculite and tobermorite in alteration zones at Goldfield, Nevada. In *Clays and Clay Minerals*, 2 343-353.



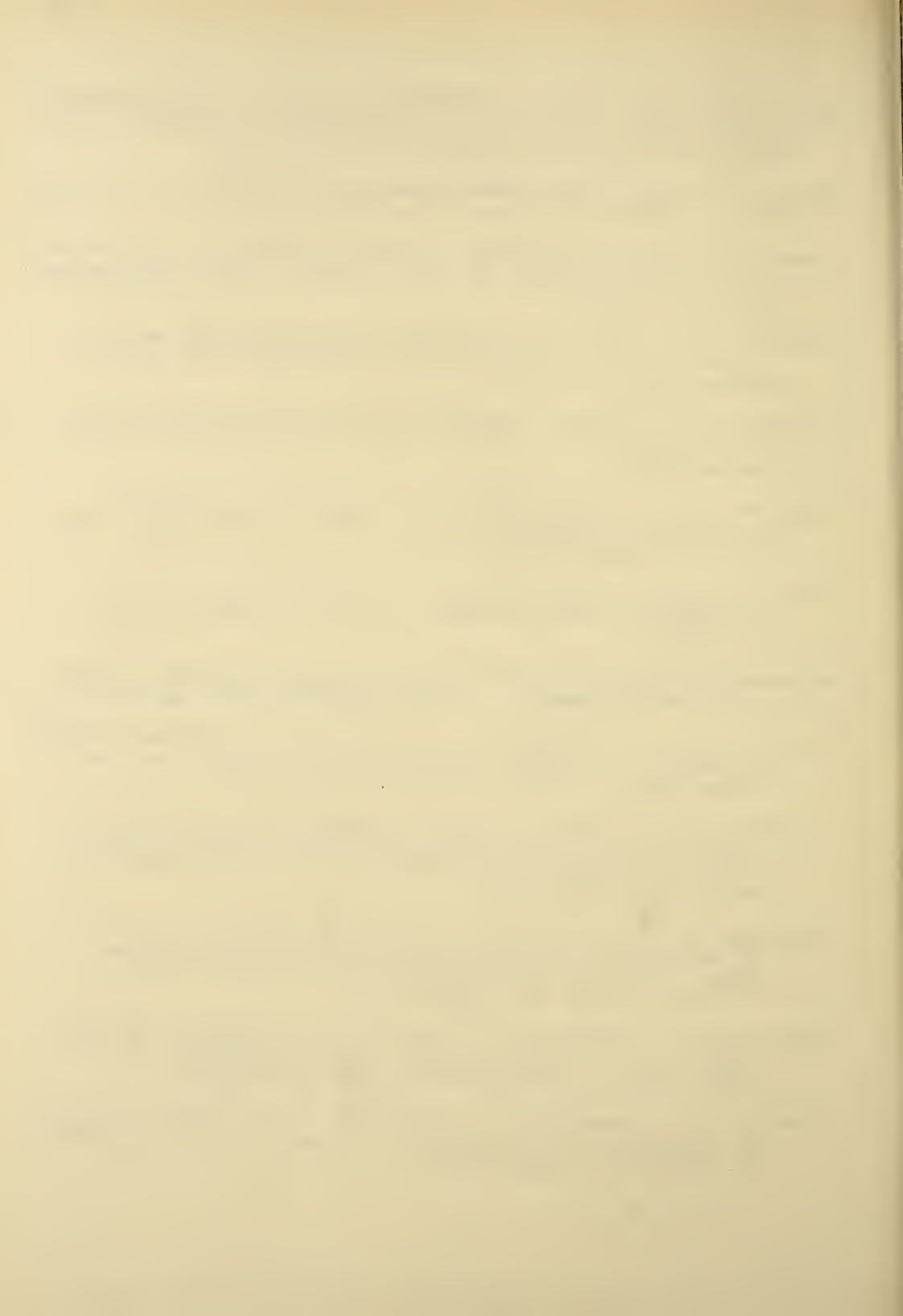


- Heddle, M. F. (1880) Preliminary notice of substances which may prove to be new minerals. *Mineral. Mag.* 4 117-123.
- Heller, L. and Taylor, H. F. W. (1951) Hydrated calcium silicates: Part II: Hydrothermal reactions; lime-silica ratio 1:1. *J. Chem. Soc.* 2397-2401.
- Heller, L. and Taylor, H. F. W. (1952) Hydrated calcium silicates. Part III. Hydrothermal reactions of mixtures of lime:silica molar ratio 3:2. *J. Chem. Soc.* 1018-1020.
- Heller, L., and Taylor, H. F. W. (1952a) Hydrated calcium silicates. Part IV. Hydrothermal reactions: lime:silica ratios 2:1 and 3:1. *J. Chem. Soc.* 2535-2541.
- Heller, L. and Taylor, H. F. W. (1956) Crystallographic data for the calcium silicates. H.M. Stationery Office, London.
- Hemwall, J. B. and Low, P. F. (1956) The hydrostatic repulsive force in clay swelling. *Soil Science* 82 135-145.
- Herrin, M. and Mitchell, H. (1961) Lime-soil mixtures. Highway Research Board Bul. 304 (NAS-NRC Publ. 932) pp. 99-138.
- Herzog, A. and Mitchell, J. K. (1962) X-ray evidence for cement-clay interaction. *Nature* 195 989-990.
- Herzog, A. and Mitchell, J. K. (1963) Reactions accompanying the stabilization of clay with cement. Paper given at Forty-second Annual Meeting Highway Research Board, Washington, Jan. 1963.
- Hilt, G. H. (1961) Isolation and investigation of a lime-montmorillonite reaction product. Ph.D. Thesis, Iowa State Univ. of Sci. and Tech.
- Hilt, G. H. and Davidson, D. T. (1960) Lime fixation in clayey soils. Highway Research Board Bul. 262 (NAS-NRC Publ. 771) pp 20-32.
- Hilt, G. H. and Davidson, D. T. (1961) Isolation and investigation of a lime-montmorillonite crystalline reaction product. Highway Research Board Bul. 304 (NAS-NRC Publ. 932) pp 51-64.
- Holdridge, D. A. and Vaughn, F. (1957) The Kaolin Minerals (Kandites), in "The Differential Thermal Investigation of Clays", B. C. Mackenzie, ed., Mineralogical Society, London 98-140.
- Hunt, C. M. (1959) The infrared absorption spectra of some silicates, aluminates, and other compounds of interest in portland cement chemistry. Thesis, Univ. of Maryland.

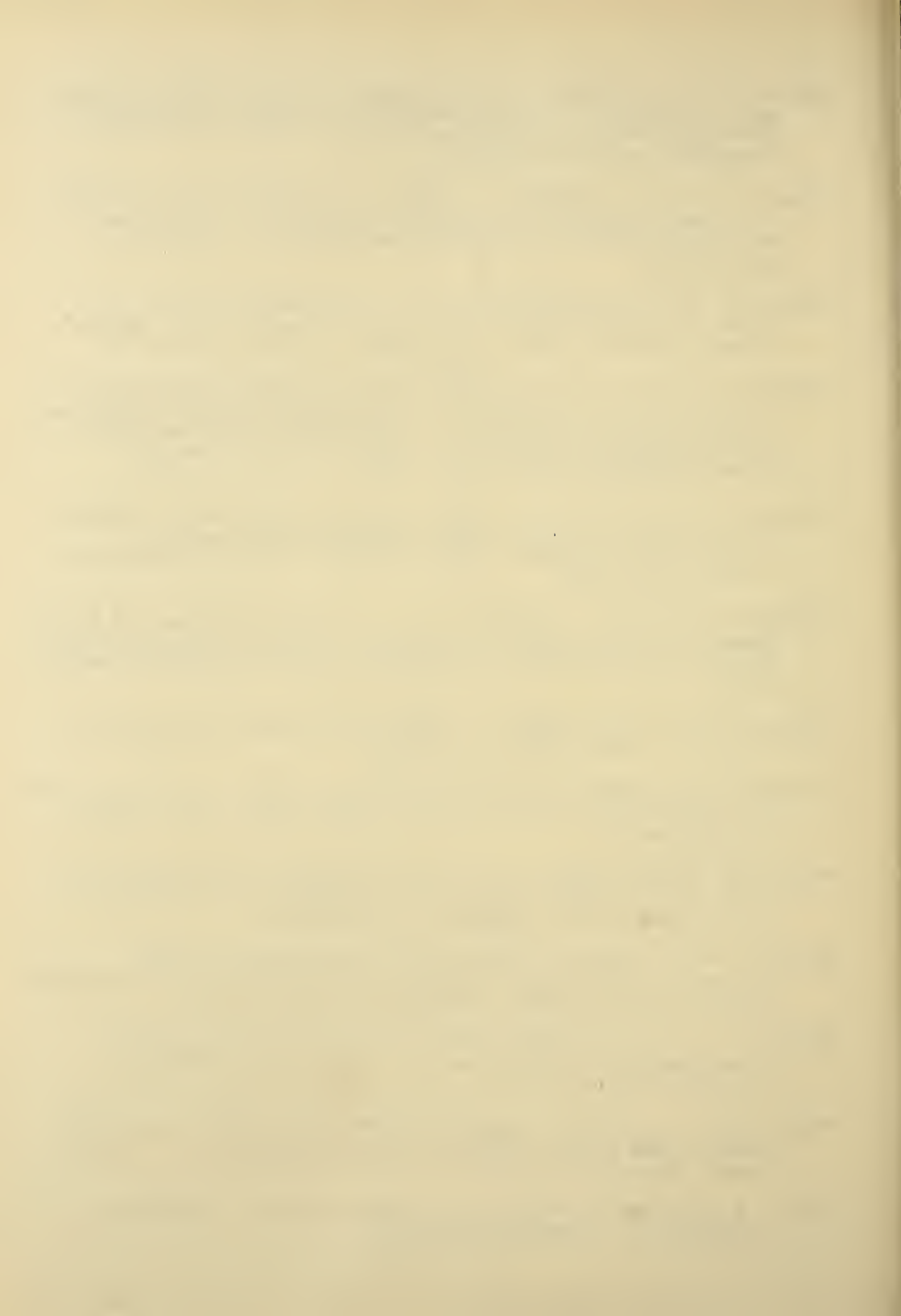




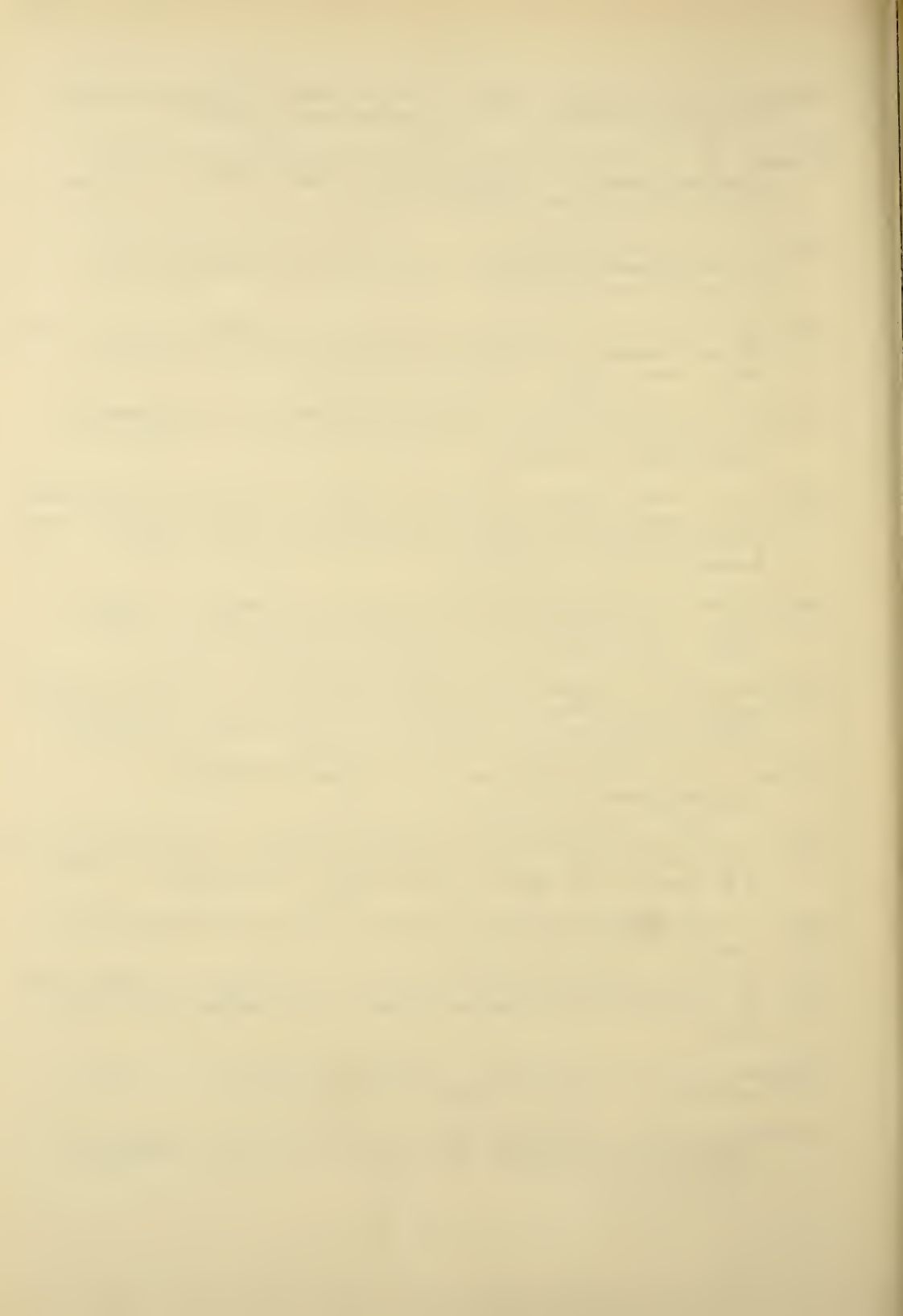
- Hunt, C. M. (1962) Infrared absorption spectra of some compounds in the  $\text{CaO-SiO}_2\text{-H}_2\text{O}$  system, in "Chemistry of Cement" (Proc. 4th Int. Conf., Washington, 1960) pp 297-305.
- Iler, R. K. (1955) The Colloid Chemistry of Silica and Silicates Cornell University Press, Ithaca, New York.
- Jones, F. E. (1962) Hydration of calcium aluminates and ferrites in "Chemistry of Cement" (Proc. 4th Int. Symp., Washington 1960) pp 205-246.
- Kalousek, G. L. (1954) Hydrous calcium silicates and methods of preparation. U.S. Patent No. 2,665,996 assigned to Owens-Illinois Glass Co.
- Kalousek, G. L. (1954a) Reactions of cement hydration at elevated temperatures. Proc. 3rd Int. Symp. Chem. Cements London 334-355.
- Kalousek, G. L. (1954b) Applications of DTA in a study of the system lime-silica-water. Proc. 3rd Int. Symp. Chem. Cements, London 296-311.
- Kalousek, G. L. (1954c) Fundamental factors in the drying-shrinkage of concrete block. J. Amer. Concrete Inst. 26 233-248.
- Kalousek, G. L. (1955) Tobermorite and related phases in the system  $\text{CaO-SiO}_2\text{-H}_2\text{O}$ . J. Amer. Concrete Inst. 26 989-1011.
- Kalousek, G. L. (1957) Crystal chemistry of the hydrous calcium silicates: I, Substitution of aluminum in the lattice of tobermorite. J. Amer. Ceramic Soc. 40 74-80.
- Kalousek, G. L., Davis, C. W., and Schmertz, W. E. (1949) An investigation of hydrating cements and related hydrous solids by differential thermal analysis. J. Amer. Concrete Inst. 20 693-713.
- Kalousek, G. L., and Prebus, A. F. (1958) Crystal chemistry of the hydrous calcium silicates: III, Morphology and other properties of tobermorite and related phases. J. Amer. Ceramic Soc. 41 124-132.
- Kalousek, G. L. and Roy, R. (1957) Crystal chemistry of the hydrous calcium silicates: II. Characterization of inter-layer water. J. Amer. Ceram. Soc. 40 236-239.
- Kantro, D. L., Brunauer, S., and Weise, C. H. (1959) The ball-mill hydration of tricalcium silicate at room temperature. J. Colloid Sci. 14 363-376.



- Kantro, D. L., Brunauer, S., and Weise, C. H. (1961) Development of surface in the hydration of calcium silicates, In Solid Surfaces and the Gas-Solid Interface, Advances in Chemistry Series 33 199-219.
- Kinter, E. B. and Diamond, S. (1955) A new method for preparation and treatment of oriented aggregate specimens of soil clays for x-ray diffraction analysis. Soil Science 81 111-120.
- Kurczyk, H. G. and Schwiete, H. E. (1962) Concerning the hydration products of  $C_3S$  and  $C_2S$  in "Chemistry of Cement" (Proc. 4th Int. Conf., Washington, 1960) pp 349-358.
- Lehmann, H., and Dutz, H. (1959) Infrared spectroscopy as a tool for determining mineral composition and the formation of new minerals and raw and intermediate minerals used in the mineral industries. Tonind. Ztg. U. Keram. Rundschau 83 219-238. (In German).
- Lehmann, H., and Dutz, H. (1962) Infrared spectroscopy studies on the hydration of clinker minerals and cements in "Chemistry of Cement" (Proc. 4th Int. Conf., Washington, 1960) pp 513-518.
- MacKenzie, R. E. and Mitchell, B. D. (1957) Apparatus and Technique for DTA in the Differential Thermal Investigation of Clays, R. C. MacKenzie, ed. Mineralogical Society, London 23-64.
- Majumder, A. J., and Roy, R. (1956) The system  $CaO-Al_2O_3-H_2O$  J. Amer. Ceram. Soc. 39 434-442.
- Mamedov, K. S., and Belov, N. V. (1958) On the crystal structure of tobermorites. Doklady Akad. Nauk. SSSR 123 163-164 (In Russian).
- Mankin, C. J. and Dodd, C. G. (1963) Proposed reference illite from the Ouachita Mountains of southeastern Oklahoma. In "Clays and Clay Minerals" 10 372-379.
- McCaleb, S. B. (1962) Hydrothermal products formed from montmorillonite-clay systems. In "Clays and Clay Minerals" Proc. 9th Nat. Conf., Lafayette, Ind. 276-294.
- McConnell, J. D. C. (1954) The hydrated calcium silicates riversideite, tobermorite, and plombierite. Mineral. Mag. 30 293-305.
- McCreary, G. L. (1949) Improved mount for powdered specimens used in the Geiger-counter x-ray spectrometer. J. Amer. Ceram. Soc. 32 141-146.
- Megaw, H. D., and Kelsey, C. H. (1956) Crystal structure of tobermorite. Nature 177 390-391.



- Midgley, H. G. (1957) A compilation of x-ray diffraction data of cement minerals. *Mag. Concrete Res.* 17-24.
- Midgley, H. G. (1962) The mineralogical examination of set portland cement in "Chemistry of Cement" (Proc. 4th Int. Conf., Washington, 1960) 479-490.
- Midgley, H. G. and Chopra, S. K. (1960) Hydrothermal reactions in the lime-rich part of the system  $\text{CaO-SiO}_2\text{-H}_2\text{O}$ . *Mag. Concrete Res.* 12 19-26.
- Midgley, H. G. and Rosaman, D. (1962) The composition of ettringite in set cement in "Chemistry of Cement" (Proc. 4th Int. Conf., Washington, 1960) pp. 259-262.
- Ormsby, C. W. and Shartsis, (1960) Surface area and exchange capacity relation in a Florida kaolinite. *J. Amer. Ceramic Soc.* 43 44-47.
- Pike, R. G. and Hubbard, D. (1958) Source of the non-migratable ionic charges developed by portland and high-alumina cements during hydration. Proc. 37th Annual Meeting, Highway Research Board, 256-270.
- Preisinger, A. (1962) Sepiolite and related compounds: its stability and application in "Clays and Clay Minerals" (Proc. 10th Nat. Conf., Austin, 1961) 365-371.
- Pressler, E. E., Brunauer, S., and Kantro, D. L. (1956) Investigation of the Franke method of determining free calcium hydroxide and free calcium oxide. *Anal. Chem.* 28 896-901.
- Roberts, M. H. (1957) New calcium aluminate hydrates. *J. Applied Chem.* 543-546.
- Ross, C. S. and Hendricks, S. (1945) Minerals of the montmorillonite group, their origin and relation to soils and clays. *U.S. Geol. Surv. Prof. Paper* 205-B, pp 151-180.
- Roy, R. (1956) Discussion on paper by Gaze and Robertson, *Mag. Concrete Research* 24 167.
- Roy, R. (1962) Discussion of paper by C. M. Hunt, in "Chemistry of Cement" (Proc. 4th Int. Conf., Washington, 1960) 304-305.
- Rutgers, A. J., and deSmet, M. (1945) Researches in electro-endosmosis. *Trans. Faraday Soc.* 41 758-771.
- Schmitt, C. H. (1962) Discussion of paper by F. E. Jones, in "Chemistry of Cement" (Proc. 4th Int. Conf., Washington, 1960)p. 244.



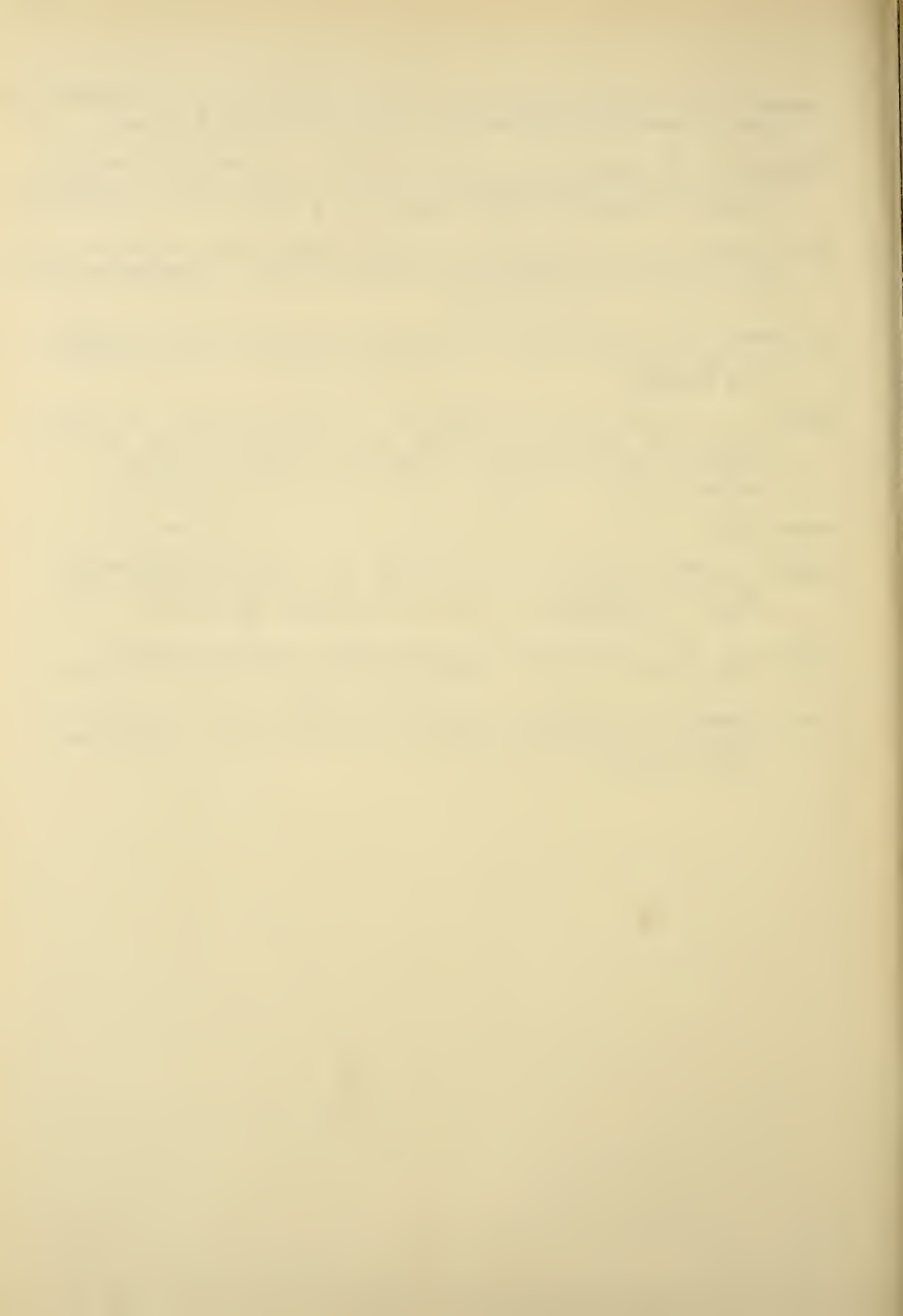


- Schuit, G. C. A. and Wyatt, R. (1962) Written discussion on Paper III-2, in "Chemistry of Cement" (Proc. 4th Int. Symp., Washington, 1960) pp. 201-202.
- Serratosa, J. and Bradley, W. F. (1958) Determination of the orientation of OH bond axes in layer silicates by infrared absorption. *J. Phys. Chem.* 62 1164-1167.
- Stein, H. N. (1960) The zero point of charge of tobermorite. *J. Colloid Sci.* 15 578-584.
- Stubican, V. and Roy, R. (1961) Isomorphous substitution and infrared spectra of the layer lattice silicates. *Amer. Mineralogist* 46 32-51.
- Stubican, V., and Roy, R. (1961a) New approach to assignment of infrared absorption bands in layer structure silicates *Zeit. Krist.* 115 200-214.
- Sudo, G. and Mori, H. (1961) Influence of KOH solution in the formation of tobermorite phase at room temperature. *Yogyo Kyohai Shi* 62 367-72 (in Japanese) *Chem. Abstr.* 1963, 3189c.
- Swerdlow, M., McMurdie, H. F., and Heckman, F. A. (1957) Hydration of tricalcium silicate. *Proc. Int. Conf. Electron Microscopy*, London, 1954 500-503.
- Taylor, H. F. W. (1950) Hydrated calcium silicates: Part I: Compound formation at ordinary temperatures. *J. Chem Soc.* 3682-3690.
- Taylor, H. F. W. (1953) Hydrated calcium silicates: Part V: The water content of calcium silicate hydrate (I). *J. Chem Soc.* 163-171.
- Taylor, H. F. W. (1959) The dehydration of tobermorite in "Clays and Clay Minerals" (Proc. 6th Nat. Conf., Berkeley 1957) Ada Swineford, ed. Pergamon Press pp 101-109.
- Taylor, H. F. W. (1961) The chemistry of cement hydration, in *Progress in Ceramic Science*, Vol I, J. E. Burke, ed., Pergamon Press, New York.
- Taylor, H. F. W. (1962) Hydrothermal reactions in the system  $\text{CaO-SiO}_2\text{-H}_2\text{O}$  and the steam curing of cement and cement-silica products. *Chemistry of Cement* (Proc. 4th Int. Symp., Washington, 1960), pp. 167-190.
- Taylor, H. F. W. and Howison, J. W. (1956) Relationships between calcium silicate hydrates and clay minerals. *Clay Minerals Bulletin* 3 98-111.





- Toropov, N. A., Borisenko, A. I., and Shirokova, P. V. (1953) *Izv. Akad. Nauk SSSR, Otdel Khim. Nauk* 65-69. (In Russian).
- Trooper, E. B., and Worth, L. F. (1956). Ion exchange resins in "Ion Exchange Technology", F. C. Nachod and J. Schubert, editors, Academic Press, New York, p. 13.
- Turriziani, R., and Schippa, G. (1956) Concerning the existence of a hydrated calcium monocarboaluminate. *Ricerca Scientifica* 26 2792-2797. (In Italian).
- Van Bemst, A. (1957) Contribution to the study of the hydration of calcium silicates. *Silicates Industriels* 22 213-218 (in French).
- Wade, W. H., Cole, H. D., Meyer, D. E. and Hackerman, N. (1961) Adsorptive behavior of fused quartz powders. In "Solid Surfaces and the Gas-Solid Interface" Adv. in Chem Series No. 33. American Chem. Soc., Washington 35-41.
- Washington, (1930) Rock analysis. John Wiley & Sons, Inc.
- Wells, L. S., Clarke, W. F. and McMurdie, H. F. (1943) Study of the system  $\text{CaO-Al}_2\text{O}_3\text{-H}_2\text{O}$  at temperatures of  $21^\circ\text{C}$  and  $90^\circ\text{C}$ . *J. Research of Nat. Bur. Stand.* 30 367-406.
- White, J. L. (1956) Reactions of molten salts with layer-lattice silicates in "Clays and Clay Minerals" 4 133-146.
- zur Strassen, H. (1962) Discussion on paper by F. E. Jones in "Chemistry of Cement" (Proc. 4th Int. Conf., Washington, 1960) 244-245.



## APPENDIX



## APPENDIX

Table 1. Chemical Analysis of Calcium Silicate Samples.

Sample Designation	C <sub>2</sub> S* PCA B-91	C <sub>3</sub> S* PCA B-94	Alite* PCA B-93	Alite** A. Klein, "Sept"
SiO <sub>2</sub>	33.74	25.97	25.02	25.57
CaO	65.51	73.74	73.63	72.78
R <sub>2</sub> O <sub>3</sub>	0.09	0.06	0.88	0.65
MgO	0.05	0.00	0.27	1.00
B <sub>2</sub> O <sub>3</sub>	0.47	--	--	--
Free CaO	0.20	1.15	2.20	0.41

\* Analyses courtesy Dr. D. L. Kantro, Portland Cement Association

\*\* Analysis courtesy Mr. A. Klein, University of California, Berkeley



## APPENDIX

Table 2. Chemical Analysis of CSH(I)  
Preparations.

	SiO <sub>2</sub>	CaO	H <sub>2</sub> O
CSH(I) - 1	36.4	32.9	29.9
CSH(I) - 2	41.0	36.6	19.6
CSH(I) - 3	39.6	36.3	19.2
CSH(I) - 4	41.2	39.0	20.2
CSH(I) - 5	41.2	44.7	12.4
CSH(I) - 6	45.9	38.7	14.8
CSH(I) - 7	32.4	47.9	17.5





VITA



## VITA

Sidney Diamond, son of Julius and Ethel Diamond, was born in New York City on November 10, 1929. He graduated from the Bronx High School of Science in 1946. He was awarded a New York State Regent's Competitive Scholarship, and attended Syracuse University, where he received a B.S. degree in 1950, majoring in forestry. He then enrolled in the graduate School of Forestry at Duke University, and in 1951 was awarded the degree of Master of Forestry, with a major in forest soils.

He entered the U.S. Army in September, 1951, and served two years as an enlisted research specialist at the Engineer Research and Development Laboratories, Fort Belvoir. After completion of his military service he joined the staff of the Materials Research Division, U.S. Bureau of Public Roads, and was engaged in research on soil clay minerals for a number of years.

In 1961 he entered the Graduate School of Purdue University, majoring in soil chemistry and minoring in highway materials and physical chemistry. He was a Graduate Assistant on the staff of the Joint Highway Research Project, School of Civil Engineering.

Mr. Diamond is senior author and co-author of a number of papers in the fields of clay mineralogy and its engineering applications. He is a member of Sigma Xi, the American Chemical Society and a number of other professional societies, and is



listed in "American Men of Science".

In 1953, he married the former Harriet Urish; they have two children, Florence Ruth, born in 1956, and Julia Beth, born in 1958.

On completion of his graduate program Mr. Diamond will return to his position with the Bureau of Public Roads.





